LBNL/PUB-5498

Report on
Ernest Orlando Lawrence
Berkeley National Laboratory

Laboratory Directed Research and Development Program

FY 2003

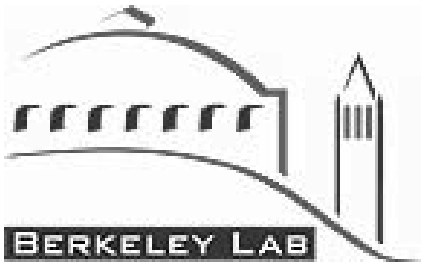

Ernest Orlando Lawrence
Berkeley National Laboratory
Berkeley, CA 94720

Prepared for the U.S. Department of Energy under Contract No. DE-AC-76SF00098

Table of Contents

Introduction

The Ernest Orlando Lawrence Berkeley National Laboratory (Berkeley Lab or LBNL) is a multi-program national research facility operated by the University of California for the Department of Energy (DOE). As an integral element of DOE's National Laboratory System, Berkeley Lab supports DOE's missions in fundamental science, energy resources, and environmental quality. Berkeley Lab programs advance four distinct goals for DOE and the nation:

- To perform leading multidisciplinary research in the computing sciences, physical sciences, energy sciences, biosciences, and general sciences in a manner that ensures employee and public safety and protection of the environment.
- To develop and operate unique national experimental facilities for qualified investigators.
- To educate and train future generations of scientists and engineers to promote national science and education goals.
- To transfer knowledge and technological innovations and to foster productive relationships among Berkeley Lab's research programs, universities, and industry in order to promote national economic competitiveness.

Berkeley Lab's research and the Laboratory Directed Research and Development (LDRD) program support DOE's Strategic Goals that are codified in DOE's September 2003 Strategic Plan, with a primary focus on Advancing Scientific Understanding. For that goal, the Fiscal Year (FY) 2003 LDRD projects support every one of the eight strategies described in the plan. In addition, LDRD efforts support the goals of Investing in America's Energy Future (six of the fourteen strategies), Resolving the Environmental Legacy (four of the eight strategies), and Meeting National Security Challenges (unclassified fundamental research that supports stockpile safety and nonproliferation programs). The LDRD supports Office of Science strategic plans, including the 20 year Scientific Facilities Plan and the draft Office of Science Strategic Plan. The research also supports the strategic directions periodically under review by the Office of Science Program Offices, such as strategic LDRD projects germane to new research facility concepts and new fundamental science directions.

The *Berkeley Lab Laboratory Directed Research and Development Program FY 2003* report is compiled from annual reports submitted by principal investigators following the close of the fiscal year. This report describes the supported projects and summarizes their accomplishments. It constitutes a part of the LDRD program planning and documentation process that includes an annual planning cycle, project selection, implementation, and review.

The Berkeley Lab LDRD program is a critical tool for directing the Laboratory's forefront scientific research capabilities toward vital, excellent, and emerging scientific challenges. The program provides the resources for Berkeley Lab scientists to make rapid and significant contributions to critical national science and technology problems. The LDRD program also advances Berkeley Lab's core competencies, foundations, and scientific capability, and permits exploration of exciting new opportunities. All projects are work in forefront areas of science and technology. Areas eligible for support include the following:

- Advanced study of hypotheses, concepts, or innovative approaches to scientific or technical problems;
- Experiments and analyses directed toward "proof of principle" or early determination of the utility of new scientific ideas, technical concepts, or devices; and
- Conception and preliminary technical analyses of experimental facilities or devices.

The LDRD program supports Berkeley Lab's mission in many ways. First, because LDRD funds can be allocated within a relatively short time frame, Berkeley Lab researchers can support the mission of the Department of Energy (DOE) and serve the needs of the nation by quickly responding to forefront scientific problems. Second, LDRD enables Berkeley Lab to attract and retain highly qualified scientists and to support their efforts to carry out world-leading research. In addition, the LDRD program also supports new projects that involve graduate students and postdoctoral fellows, thus contributing to the education mission of Berkeley Lab.

Berkeley Lab has a formal process for allocating funds for the LDRD program. The process relies on individual scientific investigators and the scientific leadership of Berkeley Lab to identify opportunities that will contribute to scientific and institutional goals. The process is also designed to maintain compliance with DOE Orders, in particular DOE Order 413.2A, dated January 8, 2001. From year to year, the distribution of funds among the scientific program areas changes. This flexibility optimizes Berkeley Lab's ability to respond to opportunities.

Berkeley Lab LDRD policy and program decisions are the responsibility of the Laboratory Director. The Director has assigned general programmatic oversight responsibility to the Deputy Director. Administration and reporting on the LDRD program is supported by the Directorate's Office for Planning and Strategic Development. LDRD accounting procedures and financial management are consistent with the Laboratory's accounting principles and stipulations under the contract between the University of California and the Department of Energy, with accounting maintained through the Laboratory's Chief Financial Officer.

In FY03, Berkeley Lab was authorized by DOE to establish a funding ceiling for the LDRD program of $15.0 M, which equates to about 3.2% of Berkeley Lab's FY03 projected operating and capital equipment budgets. This funding level was provided to develop new scientific ideas and opportunities and allow the Berkeley Lab Director an opportunity to initiate new directions. Budget constraints limited available resources, however, so only $10.1 M was expended for operating and $0.6 M for capital equipment (2.4% of actual Berkeley Lab FY03 costs).

In FY03, scientists submitted 168 proposals, requesting over $24.2 M in operating funding. Eighty-two projects were funded, with awards ranging from $45 K to $500 K. These projects are summarized in Table 1.

Accelerator and Fusion Research Division

Ultra-fast X-ray Source for fsec Dynamics

Principal Investigators: John Corlett, Kem Robinson, Alexander Zholents, Russell Wells, Howard Padmore, Philip Heimann, Robert Schoenlein, and Steve Leone

Project No.: 01003

Project Description

Ultra-short pulses of visible light produced by femtosecond laser techniques have revolutionized many areas of physical, chemical and biological science. These techniques are limited in not being able to directly probe atomic motion. X-ray techniques, through x-ray diffraction and spectroscopy, are capable of exquisite sensitivity to atomic motion. Combining x-ray techniques with short pulses is being pioneered at the Advanced Light Source (ALS), but it is already clear that although of huge potential, we need to plan for a much more intense source to attack the most exciting areas of science.

We have identified a method of producing ultra-short x-ray pulses with an intensity of up to 10^7 photons per pulse, 0.1% bandwidth, at 10 keV—10^6 times higher than currently used at the ALS; use of this source would revolutionize the study of ultra-fast dynamics across a broad range of scientific areas.

The purpose of this project is to develop critical aspects of the proposed technique in continuation of the prior two years' work.

The design of a new type of x-ray light source, based on a superconducting linear accelerator, will be intensively studied. The machine will produce very short, intense x-ray pulses from an electron beam accelerated from a photocathode gun through a linear accelerator. The bunches will be compressed and rotated to enable further optical compression to a bunch length of 50 femtoseconds full width at half maximum. X-rays will be generated by wiggler or undulator magnets, as in the ALS. This project will look at pre-conceptual design and research and development on critical components and systems. Initial work has verified the tremendous scientific potential of a national facility, and the practicality of all aspects of the project.

Accomplishments

We have developed design concepts for a novel synchrotron radiation facility for x-ray science of ultrafast dynamic processes. A recirculating superconducting linac is used for acceleration of electrons, which radiate x-rays in both coherent and spontaneous processes; various techniques have been developed to produce intense ultra-short time duration x-ray pulses.

A technique for production of intense soft x-rays by cascaded harmonic generation has been studied. This scheme involves a laser-seeded process in a cascaded series of free-electron lasers, each operating at a shorter-wavelength harmonic than the previous free-electron laser. The coherent soft x-rays can be tuned over a range of tens of eV to one keV, and ultrashort seed laser pulses produce pulse durations of 10 to 200 femtoseconds. Techniques for short-pulse hard x-ray generation have been further developed, using a novel bunch tilting process followed by optical compression of the incoherent emission from insertion devices.

We have developed design concepts for high-brightness radio frequency photocathode guns, operating at high gradient and high repetition rate, and producing low-emittance bunches. Techniques for production of a "flat" beam with x/y emittance ratio 50/1 and small vertical normalized emittance of 0.4 mm-mrad have been further developed with analytical studies and simulations, and we continue to collaborate in experiments in generating beams with low emittance in one plane at the Fermilab-NICADD Photoinjector Laboratory facility.

In the recirculating linac, a choice of superconducting radio frequency provides beam energy stability and reduced wakefield effects, improving beam quality above that expected for a conventional conducting structure. For operations in continuous mode, a requirement for the proposed facility, engineering modifications to existing cryomodule designs have been developed to accommodate the increased thermal load in the liquid helium.

The lattice concept has been designed to allow control and preservation of electron beam transverse and longitudinal emittances. Longitudinal and transverse dynamics have been modeled from the radio-frequency gun through the injector linac and all passes of the main

linac. In the injector, a harmonic cavity to control the longitudinal phase-space following the injector linac has been modeled. Coherent synchrotron radiation emission has been studied, and the vacuum chamber geometry has been designed to minimize this effect by shielding against lower-frequency radiation. Particle tracking studies have included the effects of cavity wakefields, resistive wall impedance, magnet errors, and misalignments; the studies show only modest emittance growth, with negligible impact on machine performance. We have developed a preliminary design for a seven-cell superconducting deflecting cavity, which imparts a transverse momentum to the electrons—required for optical compression of the hard x-ray pulses.

A laser-seeded cascaded harmonic-generation scheme has been developed to produce high-flux, short-pulse, coherent photons over an energy range of tens of electrovolts to one kilo-electrovolt. Two chains of cascaded harmonic generation are proposed, providing exceptional flexibility in producing EUV and soft x-ray pulses.

Sophisticated laser systems will be an integral part of the facility, and concepts for multiple tuneable lasers covering a range of 267 to 3000 nanometers and pulse durations of $\leq$ 50 femtoseconds have been identified. Concepts have been developed for timing distribution systems using fiber-optic transmission lines providing optical seed pulses to each beamline, with path lengths stabilized by feedback based on optical interferometric measurements. To provide maximum stability, we have investigated the use of a mode-locked laser oscillator as the facility master oscillator.

Scientific applications have been developed through interactions with Berkeley Laboratory staff across multiple divisions, with UC Berkeley faculty, and others. The proposed facility has been designed with a view toward solving problems in ultrafast science; applications have been identified across all fields of science, from biology, chemistry, and physics, to novel areas such as quantum computing, spintronics, and highly nonlinear phenomena. These studies have indicated facility performance requirements, and have driven the design for a facility combining capabilities of both diffraction to explore nuclear positions in real time, and spectroscopy to interrogate electronic and atomic states and their structural parameters and chemical environments.

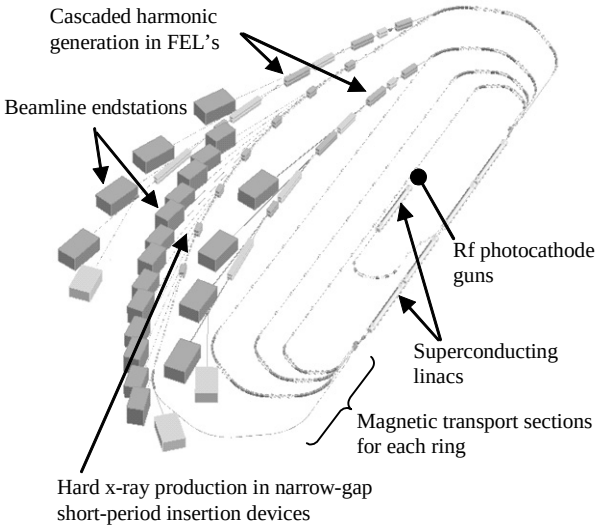

Figure 1: Machine layout. The bright electron beams generated at the radio frequency (rf) photocathode guns travel through the injector linac, main linac, transport arcs, and either hard x-ray production section or a cascaded harmonic generation section, to the beam dump. Multiple beamline endstations serve a large community with a broadly flexible range of x-ray pulses. Machine footprint is approximately 150x50 meters.

Publications

J. N. Corlett, S. R. Leone, and A. Zholents, "Faster, brighter, shorter," CERN Courier, October 2003. http://www.cerncourier.com/main/article/43/8/10

J. N. Corlett, W. A. Barletta, S. DeSantis, et al., "LUX—A recirculating linac-based ultrafast x-ray source," SRI03 San Francisco, (August 2003). Accepted for publication. http://www.sri2003.lbl.gov/

J.N. Corlett, W.A. Barletta, S. De Santis, et al., "A recirculating linac-based facility for ultrafast x-ray science," 2003 Particle Accelerator Conference, Portland, Oregon, May 12–16, 2003, submitted. http://www-conf.slac.stanford.edu/pac03/

J.N. Corlett, L. Doolittle, R. Schoenlein, J. Staples, R. Wilcox, and A. Zholents, "Techniques for synchronization of x-ray pulses to the pump laser in an ultrafast x-ray facility," 2003 Particle Accelerator Conference, Portland, Oregon, May 12–16, 2003, submitted. http://www-conf.slac.stanford.edu/pac03/

S. De Santis, J.N. Corlett, A. Wolski, and A. Zholents, "Collective effects analysis for the Berkeley Femtosource," 2003 Particle Accelerator Conference,

Portland, Oregon, May 12–16, 2003, submitted. http://www-conf.slac.stanford.edu/pac03/

W. Fawley, W.A. Barletta, J. Corlett, and A. Zholents, "Simulation studies of an XUV/soft x-ray harmonic-cascade FEL for the proposed LBNL recirculating linac," 2003 Particle Accelerator Conference, Portland, Oregon, May 12–16, 2003, submitted. http://www-conf.slac.stanford.edu/pac03/

D. Li and J.N. Corlett, "Deflecting radio frequency cavity design for a recirculating linac based facility for ultrafast x-ray science," 2003 Particle Accelerator Conference, Portland, Oregon, May 12–16, 2003, submitted. http://www-conf.slac.stanford.edu/pac03/

S. Lidia, J.N. Corlett, J. Pusina, J. Staples, A. Zholents, S. Wang, "An injector for the proposed Berkeley Ultrafast X-ray Light Source," 2003 Particle Accelerator Conference, Portland, Oregon, May 12–16, 2003, submitted. http://www-conf.slac.stanford.edu/pac03/

J. Staples, S. Lidia, S.P. Virostek, and R. Rimmer, "The LBNL femtosource (LUX) 10 kHz photoinjector," 2003 Particle Accelerator Conference, Portland, Oregon, May 12–16, 2003, submitted. http://www-conf.slac.stanford.edu/pac03/

S.-H Wang, J. Corlett, S. Lidia, J. Staples, A. Zholents, "Flat beam production in low energy injectors," 2003 Particle Accelerator Conference, Portland, Oregon, May 12–16, 2003, submitted. http://www-conf.slac.stanford.edu/pac03/

R.P. Wells, J.N. Corlett, and A. Zholents, "Re-circulating linac vacuum system," 2003 Particle Accelerator Conference, Portland, Oregon, May 12–16, 2003, submitted. http://www-conf.slac.stanford.edu/pac03/

A. Zholents, "Longitudinal phase space control in the Berkeley Femtosecond X-Ray Light Source LUX," 2003 Particle Accelerator Conference, Portland, Oregon, May 12–16, 2003, submitted. http://www-conf.slac.stanford.edu/pac03/

W. Barry, W. A. Barletta, J. Byrd, J. et al., "Feasibility study for a recirculating linac-based facility for femtosecond dynamics," LBNL report 51766, December 2002, posted. http://www-library.lbl.gov/lbnl_reports/sf

D. Li and J. Corlett, "Preliminary coupler design for a seven-cell SC deflecting cavity," Workshop on High-Power Couplers for Superconducting Accelerators, Jefferson Lab, Newport News, Virginia October 30–November 1, 2002, Presented.

J. N. Corlett, S. Lidia, R. Schoenlein, A. Zholents, "An radio frequency Photocathode for a recirculating linac-based ultrafast dynamics facility," Workshop on Laser Issues for Electron Radio Frequency Photoinjectors, October 2002, posted. http://www-conf.slac.stanford.edu/li-erp/

Short Period Superconducting Undulator Development

Principal Investigators: Daniel Dietderich and Soren Prestemon

Project No.: 03009

Project Description

The purpose of this research is: (1) investigate the undulator performance that may be attained through the use of NbTi and Nb_3Sn superconductors, (2) determine and evaluate the feasibility of candidate superconductors and coil designs, and (3) build and test a prototype superconducting undulator (SCU). SCUs have the potential to yield higher brightness and, perhaps, more importantly, to extend the spectral range that can be accessed for a given electron energy.

Optimal performance of superconducting magnet systems depends on a number of engineering choices that range from superconductor material and cable design to cryogenic system and overall system protection. This research is intended to develop the basic technology for fabricating SCUs and determining performance limitations.

The choice of superconductor and strand/cable design impacts all other aspects of the system, from support structure design to cryogenics and quench protection. Similarly, the cable design and winding techniques need to be matched for optimal magnet performance. Short-period, high field SCUs can benefit from novel windings and custom strand/cable designs that result in high packing factors and minimal potential for coil motion. Strand and/or cable design must minimize AC losses sufficiently to allow for ramp rates acceptable by the application.

We propose to investigate the optimal design of SCUs using NbTi and Nb_3Sn superconductors. A key thrust of the investigation concerns the optimal strand/cable design—superconductor filament size, packing methodology, and stabilizer design—and the optimal stabilizer copper (Cu) to superconductor ratio (Cu/SC).

The latter is a critical parameter in superconducting magnet design; as the Cu/SC ratio decreases, the overall superconductor cross section increases, resulting in increased average current density.

Accomplishments

The theoretical performance that can be attained using SCUs has been derived for gaps of 4 to 16 millimeters (mm) and periods from 10 to 35 mm. Due to geometric constraints, SCU performance is severely affected by limits to the average current density. We show that for these devices, advances in the J_c performance of superconducting materials can only result in performance enhancement if the protection system is able to handle the imposed copper current density during a quench. We have designed, constructed, and tested a six-period, 30 mm period prototype undulator using Nb_3Sn conductor, a six-strand cable fabricated in-house using 0.48 mm diameter jelly-roll strand. The winding design is applicable for a range of periods and minimizes hard-way bends for conductors with large aspect ratios. A passive protection method was applied using diodes to absorb a large fraction of the stored energy during a quench. The magnet was heat-treated, potted, assembled, and tested at Berkeley Lab by the Accelerator and Fusion Research Division (AFRD) Supercon group, see Figure 2.

Detailed performance curves have been developed for SCUs that indicate significant improvements in performance can be achieved for short period devices over existing permanent and hybrid magnet undulator technologies, see Figure 3. We have demonstrated that passive protection systems can allow for magnet operation with copper current densities significantly higher than currently in use in high-field superconducting magnets. Furthermore, we have obtained fields significantly higher than can be achieved using traditional permanent magnet technology, as well as with NbTi SCUs. We expect additional field increases after correcting the end splice design. The use of Nb_3Sn is of particular interest due to its high critical temperature, which will allow for operation at temperatures of 5° to 10° K where cryocoolers have sufficient capacity to remove the image current heat loads expected in many synchrotron ring applications.

The results provide a sound foundation for the development of this important technology for a Linac/Laser-based Ultrafast X-Ray Facility (LUX) and future synchrotron applications. The technology will also increase the intensity and spectral range capability of existing facilities, thereby maintaining their competitiveness.

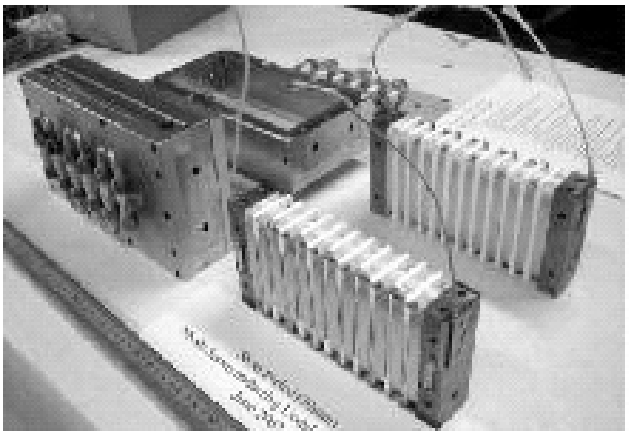

Figure 2. On the right are the two halves of the prototype undulator with 30 mm period before assembly in the reaction tooling on the left. The coil form at the top right shows the uniform cable windings on the beam side while the lower coil form shows the coil pack to coil pack transitions. The Nb_3Sn leads are extending out of each coil form prior to reaction. After reaction ductile NbTi leads are spliced to these leads and supported by an internal structure.

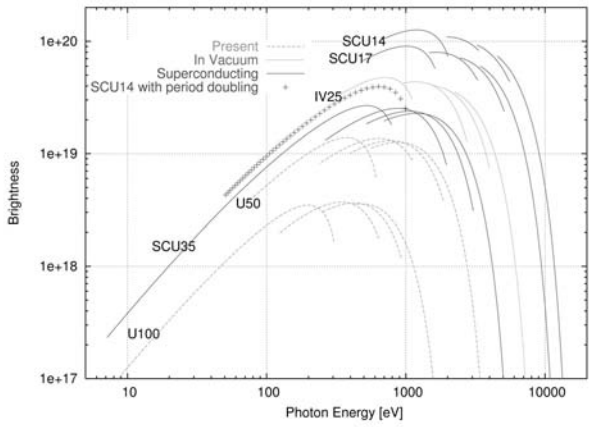

Figure 3. Spectral performance of existing undulators U50 and U10, 50 and 100mm period, respectively, compared with two 5mm period permanent magnet in-vacuum devices (IV25) and Nb_3Sn superconducting devices, (SC14, SC17 and SC35, with 14, 17, and three 5mm periods, respectively. Period doubling via electrical switching would allow the SCU14 device to extend to energies from ~70eV to more than 10keV. Brightness is based on existing ALS parameters and a 4.5m device length. The IV and SC designs assume a 5mm vacuum gap.

Publications

S. Prestemon, D.R. Dietderich, S.A. Gourlay, P. Heimann, S. Marks, G.L. Sabbi, R.M. Scanlan,

R. Schlueter, B. Wang, and B. Wahrer, "Design and evaluation of a short period Nb_3Sn superconducting undulator prototype," Particle Accelerator Conference 2003, Portland, May 12-16, 2003.

S. Prestemon, D. Dietderich, S. Marks, and R. Schlueter, "NbTi and Nb_3Sn Superconducting undulator designs," Synchrotron Radiation Instrumentation 2003, San Francisco, August 25-29, 2003.

Novel Coherent THz and IR Source Using a Laser Wakefield Accelerator and Applications

Principal Investigators: Wim Leemans

Project No.: 02001

Project Description

This proposal is aimed at (1) developing a source of high peak flux, coherent, ultra-short pulse, single cycle, infrared (IR) and terrahertz (THz) radiation from a laser-driven accelerator and (2) investigating the interaction of this radiation with atomic media, which includes gaseous and condensed media. Source development will comprise the design and implementation of the THz radiator, collection optics and diagnostics, calibration of figures of merit–flux, temporal, spatial and spectral properties, and systematic characterization of the source response to electron beam and laser parameters. Detailed theoretical calculations in support of these measurements will be performed. Coherent THz pulses with peak source strengths several orders of magnitude beyond current technology should be obtainable, thus allowing for applications to be performed in new nonlinear regimes. Practical application of the THz source will be demonstrated through nonlinear and time-resolved experiments such as high field transport in semiconductors.

Accomplishments

Coherent far-infrared and THz radiation has been generated from ultra-short electron bunches produced by a laser driven plasma based accelerator operating in the self-modulated regime. The electron bunches contained charge ranging between 0.1 to 10 nC charge.

Coherent emission of radiation from bunched electron beams can occur for wavelengths comparable to the bunch length. For such wavelengths, the emitted power is quadratically dependent on the charge in the bunch and can exceed radiation levels produced with conventional sources by several orders of magnitude. The duration of an electron bunch exiting from a conventional radiofrequency based accelerator structure can be 10 to 100 times smaller than the wavelength of the accelerating field used in the structure, resulting in millimeter-long bunches. Shorter bunches have been produced using external magnetic compression of energy chirped electron beams or using free electron based microbunching. The amount of charge however for such sub-picosecond bunches emerging from accelerators with energy ranging in the few tens of MeVs is limited to a few pC due to space charge effects. Space charge forces can cause longitudinal bunch lengthening as well as transverse emittance increase thereby diluting both the longitudinal and transverse phase space density.

In our experiments, electron bunches were generated by focusing laser pulses from a $Ti:Al_2O_3$ laser operating at 800 nanometers (nm) onto a supersonic helium gas jet with a length of 2 mm, mounted inside an evacuated vacuum chamber. The laser pulses were focused to a size w = 6 mm with a 30 cm focal length (F/4) off-axis parabola (OAP), had a full-width-half-maximum duration t_{FWHM} = 55 fs and contained up to 400 microjoules of energy, resulting in peak power levels P = 8 TW and intensities I = 1.5 10^{19} W/cm^2. The total charge per bunch and spatial profile of the electron beam were measured using an integrating current transformer (ICT) and phosphor screen imaged onto a 16 bit charge-coupled devices (CCD) camera, respectively. The ICT and phosphor screen were located 30 and 75 centimeters downstream, respectively.

During the past year we have continued to study the detailed properties of the source and have developed methods to collect the radiation and direct it onto detection systems capable of measuring the amount of energy per pulse (bolometer system) with some spectral sensitivity.

A silicone-based bolometer, which was manufactured by Infrared Laboratories, cooled at 4.2° K with a 100 cm^{-1} cut-on filter was used to measure radiation in the 0.015 to 1 mm range. Quadratic dependence of the bolometer signal with charge per bunch was observed and, through calibration of all optical elements in the path of the beam we have been able to quantify the amount of radiated energy per pulse, within the collection solid angle. We also have obtained preliminary spectral measurements in two energy ranges. The result of these measurements was found to be in good agreement with theoretical calculations. The maximum energy collected to date for a collection angle of about 150 to 200 milliradians, is on the order of 100 nanoJoules, in

excellent agreement with theory. This is several orders of magnitude larger than obtained from optical rectification but smaller than what has been achieved using switched Ga-As antennas and from synchrotron radiation using ultra-short electron bunches at Jefferson Laboratory. The experiments planned for this year will study practical implementation of methods aimed at producing two to three orders of magnitude larger energy per pulse than those devices. This includes increasing the collection efficiency, the electron beam energy and the transverse size of the plasma.

We have also carried out polarization measurements of the radiation. Transition radiation is radially polarized. Using a wire mesh polarizer placed in front of the bolometer, the transmitted energy was measured as a function of rotation angle of the polarizer. No dependence was found, consistent with radial polarization of the radiation.

The preliminary spectral measurements carried out using the bolometer and two infrared filters have allowed us to estimate the electron bunch length. From the theoretical model, the radiated spectrum is affected on the long wavelength end by diffraction effects arising from the finite transverse size of the plasma, and on the short wavelength end by the bunch duration. By measuring the energy content in two different frequency bands and comparing this with our theoretical model, bunch lengths on the order of 30 to 50 femtoseconds were calculated to best fit the experimental results. At the present time, an infrared spectrometer has been installed to measure the detailed radiated spectrum and to confirm the preliminary results. The expected results will be the first measurements of the duration of laser accelerated electron bunches.

The first results of the work that has been carried out to date as part of this LDRD has been published in *Physical Review Letters*. The theoretical background has been accepted for publication in *Physical Review E* and an overview paper has been submitted to *Physics of Plasmas.* The work also forms the basis of the doctoral dissertation of Mr. Jeroen van Tilborg who is a graduate student in the l'OASIS group.

Publications

W.P. Leemans et al., "Observation of terrahertz emission from a laser-plasma accelerated electron bunch crossing a plasma-vacuum boundary," *Physical Review Letters* **91** (August 2003).

C.B. Schroeder et al., "Theory of coherent transition radiation generated at a plasma-vacuum interface," *Physical Review E* (December 2003).

W.P. Leemans et al., "Terrahertz radiation from laser accelerated electron bunches," submitted to *Physics of Plasmas,* (November 2003).

J. van Tilborg et al., "Coherent radiation in the far IR and mm-wave regime from laser wakefield accelerated ultrashort electron bunches," submitted to Particle Accelerator Conference 2003, May 2003.

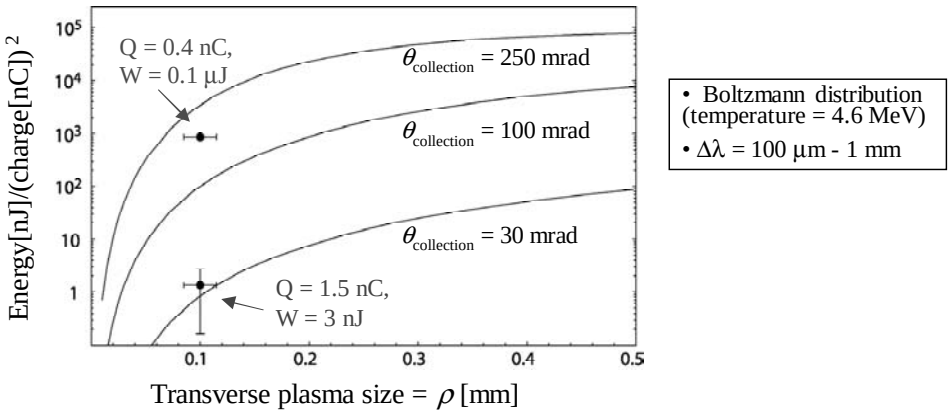

Figure 4. Radiated energy, in nJ, normalized to bunch charge, in nC, as a function of transverse plasma size, for three different collection angles—30 mrad, 100 mrad, and 250 mrad. The measured energy per pulse for a transverse plasma size of 0.1 mm is shown for two different collection angles. Increasing the collection angle and transverse size is expected to result in the collection of 10's of microJoules which is several orders of magnitude larger than for conventional sources.

Advanced Simulation of Complex Beam Systems

Principal Investigators: Phillip Colella, Eric Esarey, Alex Friedman, Robert Ryne, and Jean-Luc Vay

Project No.: 01002

Project Description

This work has two important strategic goals:

- First, to provide a computational foundation for the two key scientific areas critical to the development of the next generation of particle and laser-beam based accelerators: (1) wave-particle interaction in the full six-dimensional phase-space of multi-particle, multi-mode particle-wave systems; and (2) coulomb and electromagnetic space-charge-dominated transport of high-intensity, charged particle beams. These will have immediate applications in the studies of laser-plasma acceleration, acceleration and transport of heavy ions for fusion, and simulations of intense bunches in circular accelerators including three dimensional space-charge effects.

- Second, to build a capability that combines accelerator physics with applied mathematics, numerical algorithms, and advanced computing, in order to address the nation's next-generation programs in accelerator science and technology.

This project brings together theoretical and experimental beam physicists, computational scientists, and computer scientists to address some of the most critical problems in beam science. Although all the accelerator/beam systems have unique features that require special techniques for simulation, there are many computational tools and techniques that are common to all these systems and to many others. Our approach is to identify and develop tools that can be adopted to meet the needs of a broad spectrum of particle beam simulation projects. The primary focus will be on tools that significantly enhance code performance, permit codes to be readily ported to the highest performance machines at the National Energy Research Scientific Computing (NERSC) Center and elsewhere, and allow accelerator scientists to use advanced visualization techniques to understand complex beam systems. These tools will be turned into components that can be used by a number of simulation projects. Some of the techniques to be developed are general, and will have applicability to a broad range of emerging research areas at Berkeley Lab and elsewhere.

Accomplishments

Development of an AMR-based modeling capability for intense beams in accelerators

A set of routines to pass particle information to Chombo was implemented in WARP and tested using a prototype branch of Chombo, called ChomboPIC. Using the Chombo field solver, single particle tests were continued, in order to assess the dependence of the spurious self-force on the operating mode of the solver, single pass versus multi-pass, and on the order of the interpolation at the parent/child grid patch interface. Measures of the global error on the patch, including the average error over the patch and the degree of violation of the integral Gauss' Law around it, were also computed. This revealed a strong correlation between the average error and violation of Gauss' Law when the solver is used in the multi-pass mode.

Using the prototype axisymmetric (r,z) AMR solver implemented in WARPrz, further simulations of an ion beam source were conducted. These simulations showed the importance of refining both the beam edge and the emitted region, emphasizing the need to refine in the neighborhood of steep gradients, rather than simply in high-density regions. The experimentally observed time dependence of the resulting beam current was compared with the WARP prediction, and the effectiveness of mesh refinement was demonstrated.

Combining high order optical effects and space-charge effects in rings

This year we completed the development of an advanced simulation capability to model particle beams in the presence of high order optical effects in rings and space-charge effects. Our approach makes use of symplectic split-operator methods. This approach is very efficient, because it allows one to separate the rapid variation of the externally applied electromagnetic fields from the more slowly varying space-charge fields. For improved accuracy, we implemented new Poisson solvers that are based on a novel integrated-green function (IGF) approach. We used a symbolic algebra program to produce the highly complex equations associated with the three-dimensional IGF approach. The use of a symbolic algebra program ensures that the resulting equations are correct and free of calculational errors.

To test the accuracy of our advanced simulation capability we developed a series of benchmark problems. One such problem involved the innovative use of Vlasov theory to find stationary solutions of the Vlasov/Poisson equations for a self-consistent

bi-thermal distribution. Such a distribution provides an excellent test case because it has nonlinear space-charge fields and a pronounced beam halo, while the stationary nature of the distribution makes it easy to compare the numerical solution with the exact solution. In addition to this benchmark, which is spherically symmetric, we also developed a benchmark for a stationary distribution that is not spherically symmetric, through this inclusion of an angular momentum term in the Hamiltonian.

Development of fluid models for modeling laser/plasma accelerators

We have continued the development of fluid codes for the modeling of intense laser-plasma interactions with applications to advanced accelerators [e.g., laser wakefield accelerators, in support of on going experiments in the laser Optics and Acceleration Systems Integrated Studies (l'OASIS) laboratory]. Progress has been made in three areas: (1) the development of time-averaged envelope models, (2) the development of higher-order methods, and (3) the development of a warm fluid model. The previous fluid code developed under this program solved the full cold plasma fluid-Maxwell equations, including the fast scale of the laser oscillation, with a second-order algorithm. New codes developed are being used to study problems of interest to the l'OASIS experimental program, e.g., the effect of laser chirp and pulse shape on the forward Raman instability, pump depletion of the drive laser pulse as it propagates through the plasma and the effect of temperature on the structure of nonlinear wakefields.

Publications

J.-L. Vay, P. Colella, A. Friedman, D.P. Grote, P. McCorquodale, and D.B. Serafini, "Implementations of mesh refinement schemes for Particle-In-Cell plasma simulations," submitted to Computer Physics Communication, *Proceedings of the 18th International Conference on Numerical Simulation of Plasmas*, Cape Cod, 2003.

J.-L. Vay, P. Colella, J.W. Kwan, P. McCorquodale, D.B. Serafini, A. Friedman, D.P. Grote, G. Westenskow, J.-C. Adam, A. Héron, and I. Haber, "Application of adaptive mesh refinement to particle-in-cell simulations of plasmas and beams," *Physics of Plasmas*, Proceedings of invited papers at the 45th Annual Meeting of the Division of Plasma Physics, Albuquerque, 2003.

R. D. Ryne et al, "Non-equipartitioned quasi-thermal equilibria for intense bunched beams in uniform focusing channels," in preparation.

C.B. Schroeder, E. Esarey, B.A. Shadwick, and W.P.Leemans, "Raman forward scattering of chirped laser pulses," *Physics of Plasmas* **10** (1), 285-295 (2003), also published in *Virtual Journal of Ultrafast Science* (January 2003) LBNL-50729.

G.M. Tarkenton, B.A. Shadwick, and C.B. Schroeder, "Higher-order differencing schemes for modeling intense laser-plasma interactions," *Bulletin American Physical Society* **48**, 108 (2003).

B.A. Shadwick, C.B. Schroeder, G.M. Tarkenton, and E. Esarey, "Comparing envelope and full-fluid models of intense laser-plasma interactions," *Bulletin American Physical Society*. **48**, 108 (2003).

B.A. Shadwick, G.M. Tarkenton, E. Esarey et al., "A warm fluid model of intense laser-plasma interactions," in preparation.

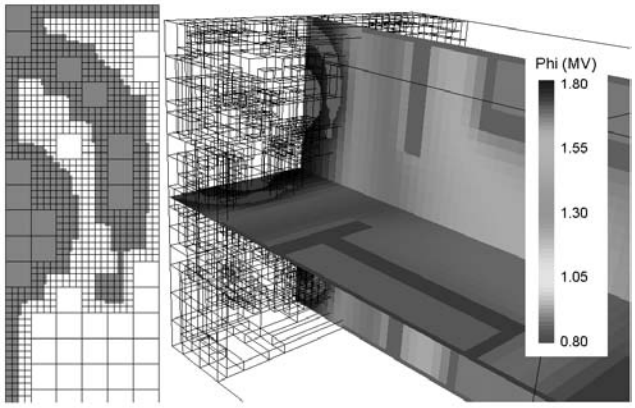

Figure 5. Three-dimensional solution of the field potential in the front end of an accelerator, as given by Chombo. A slice with the actual meshing (left) shows that the regions close to the boundaries of conductors (grey) are described with a fine mesh, while the interiors of conductors and regions of vacuum, less critical with regard to fine detail, are covered with coarser meshes. The picture on the right shows a three-dimensional rendering that includes two orthogonal slices of the solution and the edges of the different domains containing finer mesh spacing (in this case, mesh refinement covered the conductor edges only in the area surrounding the source).

Optimal Solvers for Infinite Dimensional Hamiltonian Systems

Principal Investigators: Robert Ryne and Esmond Ng

Project No.: 03021

Project Description

We will develop optimal discrete models for infinite-dimensional Hamiltonian systems, and to develop time-domain and eigenmode algorithms and solvers for these models. This work is motivated in part by the great success of symplectic integrators for classical finite-dimensional Hamiltonian systems. These have become indispensable for studying long-term behavior including the dynamics of charged particles in plasmas, the dynamics of stars in gravitational systems, and the dynamics of atoms and molecules in materials. Under this project we will develop new methods that can be applied to infinite dimensional systems governed by equations such as Maxwell's equations, the Schrodinger equation, and the nonlinear Schrodinger equation.

We will take a dual approach to develop discrete models of infinite-dimensional Hamiltonian systems. First, we will discretize the Lagrangian density using finite elements and use it to obtain the corresponding Hamiltonian. Second, we will prescribe properties that we want the model to have (e.g., a specific dispersion relation, a certain maximal bandwidth, etc.), and use optimization techniques to obtain the coefficients for a discrete Hamiltonian system leading to these properties. In both cases, the discrete Hamiltonian will be the basis for the development of solvers involving split-operator techniques and symplectic eigensolvers.

Accomplishments

Our approach is based on using finite element and related basis functions to obtain discrete Lagrangians and Hamiltonians from the corresponding Lagrangian and Hamiltonian densities. The resulting equations are solved using symplectic integration methods in the time domain.

To date, progress has been made in three areas. First, we tested and compared several approximation and discretization techniques for solving partial differential equations representative of the infinite-dimensional systems under study. This led us to identify the finite element and wavelet-based discretization schemes as most promising, and the technique to adopt for further analysis. An important advantage of these schemes is that they result in discrete models involving sparse matrices, a feature that allows for highly efficient implementations of the models on parallel supercomputers.

Second, the work completed so far has resulted in an improved understanding of the role of dual and orthonormal bases in the formulation of discretization algorithms for generating finite-dimensional approximating systems that have a correct continuum limit and inherit, in a consistent and well-defined way, the symplectic structure of the original infinite-dimensional system.

Third, we have developed and implemented a prototype solver for one-dimensional hyperbolic partial differential equations (PDEs) based on a fourth-order-in-time split-operator symplectic integrator combined with an expansion in a basis of finite element functions of position variables. This solver was used to compare the performance of algorithms and solvers based on first- and second-order local element bases; the solver will be built upon in the near future as we move onto modeling systems that are either nonlinear, or involve three spatial dimensions, or both.

Work currently in progress is focused on comparing different approaches to discretization and identifying to what extent the resulting finite-dimensional approximations are dynamically equivalent. Other areas of concentration are developing and testing a solver for two-dimensional and three-dimensional linear and one-dimensional nonlinear problems, developing tools for dealing with irregularly shaped domain boundaries, and studying the possibilities presented by the use of other bases.

Publications

I. Pogorelov, J. Qiang, R. D. Ryne, and R. Gluckstern, "Symplectic discretization of infinite-dimensional Hamiltonian systems," in preparation.

Superconducting Magnets for Ex Situ *Nuclear Magnetic Resonance Spectroscopy*

Principal Investigators: GianLuca Sabbi
Project No.: 03022

Project Description

Magnet systems capable of producing a volume with sufficient field strength and homogeneity are required to recover nuclear magnetic resonance (NMR) information from samples placed outside the instrument. The goal of this project is to develop a prototype superconducting magnet system for *ex situ* NMR applications, providing substantially higher and better field quality than can be achieved using either permanent magnets or normal conducting coils.

The basic approach is to create a saddle point outside the magnet where the gradients of all field components vanish. A superconducting system can achieve a ten-fold increase of the magnetic field strength at the sample location with respect to a system based on permanent magnets. The main design objectives are optimization of the field strength and homogeneity, compactness and robustness of the structure, and simplicity and economy of fabrication.

Accomplishments

The original proposal was based on three racetrack coils arranged side by side. Several alternative coil geometries were investigated; a racetrack configuration with vertical layout was selected. This arrangement is magnetically less efficient, but has a potential for higher field quality due to fewer geometrical constraints, and results in faster field decay outside the region of interest. Mechanical support is also improved, due to a more favorable aspect ratio and winding orientation. The coil features a straight section with translational symmetry along the z axis, allowing to approach the field analysis and optimization in a two-dimensional cross-section and to extend the good field volume along the z axis by simply increasing the coil length.

Mechanical support to the coil package is provided by a 19 millimeter thick aluminum shell, tensioned to 250 megapascals by a system of bladders and keys. This method was developed at Berkeley Laboratory for use in high field accelerator dipoles. The configuration has demonstrated the capability of generating large forces with accurate control of the stress, and facilitates magnet assembly and disassembly. For the present application, the mechanical structure was modified to allow open access to the NMR analysis volume. A challenging requirement of the new configuration is to minimize the support structure on the magnet side where the analysis is performed. This problem can be mitigated by optimizing the magnetic design to reduce or eliminate the outward component of the Lorentz force.

It was realized at the proposal stage that the design concepts and fabrication techniques developed for Berkeley Lab Nb_3Sn "sub-scale" prototype series are well matched to this problem. Further analysis showed that Nb_3Sn coils of this design could be used with minimal modifications. The first prototype features four modules: two existing baseline coils and two new ones fabricated using standard parts, reaction, and impregnation tooling. The prototype was assembled in May 2003 and tested in July 2003. The maximum magnetic field obtained in the NMR analysis volume was 1600 Gauss, to be compared with an initial target of 2000 Gauss. Unfortunately, premature quenching in one of the coils prevented the realization of the full potential of this prototype. Field measurements were performed to verify the field intensity and shape as function of current; good agreement with design calculations was found.

The goal of the first prototype was to demonstrate the *ex-situ* magnet design concept, in particular the coil configuration and support structure that will allow full access to the analysis volume. However, the use of existing coil modules resulted in some practical limitations affecting the field homogeneity. Design studies of optimized geometries with high field quality were completed in FY03. The new coil designs maintain a similar layout but feature narrower conductor blocks (5 to 8 mm vs 16 mm), larger separation between lead and return currents (15 to 20 cm vs 4 cm) and increased coil length (60 to 80 cm vs 30 cm). The fabrication and test of a field quality optimized prototype will be pursued in FY04.

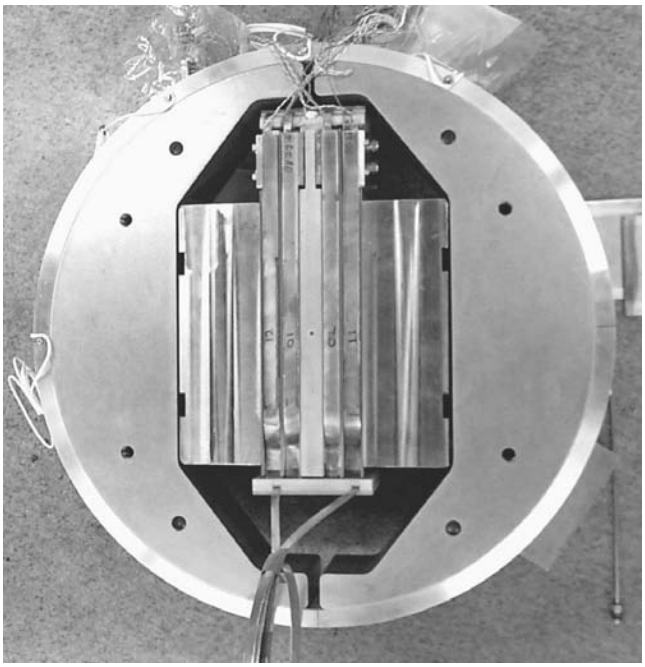

Figure 6. Prototype assembly

Solid State Quantum Computer Development with Single Ion Implantation

Principal Investigators: Thomas Schenkel and Jeffrey Bokor

Project No.: 02002

Project Description

This project focuses on experimental studies of fundamental device physics, which is critical for the development of a prototype solid state quantum computer (SQC). Several promising schemes for the realization of scalable SQCs are based on arrays of single donor atoms (e.g. ^{31}P, or ^{125}Te) embedded in a solid matrix (e. g., Si, or Si_xGe_y hetero-structures). To date, theoretical studies by far outnumber experimental programs in solid state quantum computing. Our approach is based on the formation of qubit arrays by single ion implantation. The development of integrated qubit arrays is aimed at gaining experimental data that enable the leap from device proposals to the design and testing of prototype solid state quantum computers.

Arrays of qubits are formed by single ion implantation of $^{31}P^{15+}$ ions at the Electron Beam Ion Trap facility. Using highly charged ions for implantation allows the detection of single ion impacts with 100% efficiency. This enables the formation of non-Poissonian array structures, where exactly one, rather than on average one ion is implanted into a given device area. A combination of focused beam and mask technology is used for pattern definition at the 100 nanometer level. Through detailed characterization of the electrical properties of qubit arrays, we determine defect levels and optimize processing steps in relation to requirements for functional device elements. These studies provide data for the design of a processing scheme for the integration of qubit arrays into functional, prototype solid state quantum computer test structures. Here, pairs of single electron transistors will be formed in silicon on insulator substrates and integrated with control gates and pairs of ^{31}P atoms.

Accomplishments

In the second year of our project we succeeded in forming pairs of single electron transistors (SETs) in silicon on insulator (SOI). SET development in silicon is crucial for an all silicon integration of quantum bit structures complementary metal oxide semiconductor (CMOS). The use of an all-silicon, compatible process, is highly desirable since it allows use of the most advanced processing infrastructure for quantum computer development. Access to this infrastructure significantly increases the chances for success in light of the extreme demands for precision and control posed by quantum computer processing. Additionally, charging energies in silicon based SETs are orders of magnitude larger than charging energies in metal oxide based SETs. This allows SET characterization and optimization at LHe temperatures, and can also enable SET operation at the quantum shot noise limit of sensitivity (10^{-6} $e^-/Hz^{1/2}$). The electron beam lithography and dry etch technology at Berkeley Lab allowed us to form SET pairs with silicon nanowire line widths of just 10 nanometers, see Figure 7. Coulomb blockade of electron transport across the silicon island was observed at 4.2^{o}K and charging energies of SETs were determined to be 5 to 10 milli-electronvolts.

In parallel to silicon SET development, we further characterized the electrical properties of the low energy (<20 kilo-electrovolts), extremely low dose ($<10^{11}$ cm^{-2}) ^{31}P implants that form qubit arrays. In these studies we found a strong effect of dopant segregation to the SiO_2/Si interface. Dopants move to the interface during rapid thermal annealing. This segregation is detrimental to single atom qubit integration, since ^{31}P arrays are

dissolved, ^{31}P atoms are not electrically active when they are bound at the interface, and their electrons do not exhibit the quasi hydrogenic wave function that is crucial for coherent control of spin states at low temperatures. The segregation effect can be controlled by use of silicon nitride barrier layers instead of SiO_2. Silicon nitride injects vacancies that retard dopant segregation, while SiO_2 injects silicon interstitials that enhance it. These crucial findings were fed back into process development and led us to refine the SET-qubit integration process.

Having developed silicon SETs and having gained a detailed understanding of extremely low dose P implants in silicon we have began to integrate single ^{31}P atoms into SET structures through scanning probe aligned single ion implantation and to design experiments were the SETs are used to sense individual dopant atoms.

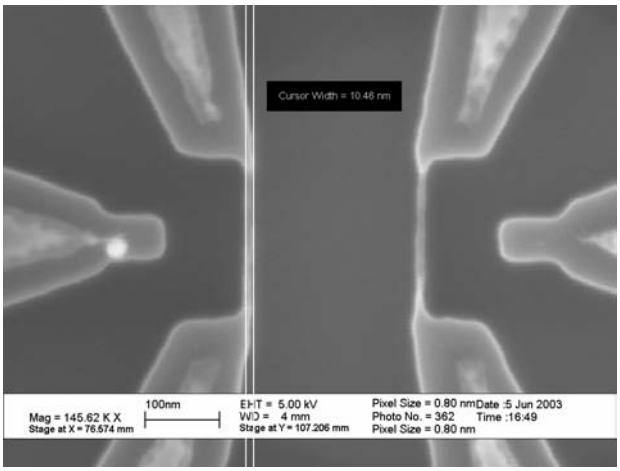

Figure 7. A pair of single electron transistors in silicon on insulator (SOI). The width of the silicon nanowire is about 10 nanometers. Electrical measurements of devices at 4.2^o K showed Coulomb blockade with charging energies of 5 to 10 meV. SETs are sensitive electrometers that will be used for single spin measurements through spin dependent charge transfer.

Publications

T. Schenkel, I. W. Rangelow, R. Keller, S. J. Park, J. Nilsson, A. Persaud, V. R. Radmilovic, P. Grabiec, D. H. Schneider, J. A. Liddle, and J. Bokor, "Open questions in electronic sputtering of solids by slow highly charged ions with respect to applications in single ion implantation," *Nuclear Instruments and Methods in Physics Research B*, in press (for 2004).

T. Schenkel, V. Radmilovic, E.A. Stach, S.-J. Park and A. Persaud, "Formation of a few nanometer wide holes in membranes with a dual beam focused ion beam system," *The Journal of Science and Technology B*, in press (December 2003).

T. Schenkel, A. Persaud, S. J. Park, J. Nilsson, J. Bokor, J. A. Liddle, R. Keller, D. H. Schneider, D. W. Cheng, and D. E. Humphries, "Solid state quantum computer development in silicon with single ion implantation", *Journal of Applied Physics*, (*Applied Physics Review*), **94,** 7017 (2003).

S.-J. Park, A. Persaud, J. A. Liddle, J. Nilsson, J. Bokor, D. H. Schneider, I. Rangelow, and T. Schenkel "Processing issues in top-down approaches to quantum computer development in Silicon," submitted for 2004, *Microelectronic Engineering*, also: cond-mat/0310195.

Synchrotron and Wiggler Radiation Measurement of the Longitudinal Bunch Distribution in Hadron Colliders

Principal Investigators: Stefano De Santis and William Turner

Project No.: 02003

Project Description

The project's purpose is to develop a concept for the measurement of the longitudinal bunch distribution of protons and heavy ions in hadron colliders. Emphasis will be placed on developing a concept that can operate over a wide range of operating conditions that include: (1) injection to top energy, (2) commissioning to full luminosity, and (3) protons and heavy ions. Such a device would find a wide-range of applications that provide essential information for machine operation including the following measurements: (1) untrapped beam fraction, (2) intensity of ghost bunches, (3) fraction of particles in the beam abort gap, (4) longitudinal bunch shape, and (5) coherent multi-bunch modes. The information provided by such a device is necessary in order to protect the collider from extensive damage by the large stored energy of the circulating beam [360 megajoules per proton beam in the case of the Large Hadron Collider (LHC) under construction at the European Laboratory for Particle Physics near Geneva, Switzerland (CERN)].

The approach that will be investigated has two parts: (1) utilization of the synchrotron and wiggler radiation emitted by highly relativistic proton and heavy ion

bunches in strong magnetic fields and (2) cross-correlation of the synchrotron and wiggler radiation with a laser pulse that is phase locked to the storage ring radio frequency system. A prototype system will be assembled and tested at the Advanced Light Source (ALS) electron storage ring at Berkeley Lab.

Accomplishments

The method of longitudinal density measurement uses the non-linear mixing of synchrotron radiation from the bunched beam of the ALS with a mode-locked, solid-state laser oscillator and detection of the up-converted radiation with a photo-multiplier tube. Specifications are given in last year's report for this project.

In FY03, we continued development of the electronic hardware and software for the laser mixing experiment at the ALS. The signal-to-noise ratio of the optical line was increased by improving the rejection of unwanted frequencies after the non-linear mixing. We also improved our understanding of the dynamic range observed at the ALS and are close to the 10^4 target value. Since the experiment at the ALS operates exclusively in single photon counting mode, a discriminator was inserted after the photomultiplier tube for signal detection. The analog front-end was also modified to maintain synchronization with other parts of the system. Following several experimental sessions at the ALS, a plan for changing the board-timing signal from the laser pulse detected on a photodiode, to direct synchronization to the orbit clock was developed. This would also allow for storing beam data in a consistent way, even after repeatedly restarting the instrument, effectively synchronizing the board to the beam rather than to the laser/photodiode. The analog-to-digital amplifier was also replaced, improving its slew rate characteristics. A standardized board has been identified as the best candidate for a new version of the instrument with better data integrity and radio frequency noise characteristics.

We began the investigation of a dedicated technique for monitoring of the abort gap using simple highly reliable hardware (e.g., gated photomultiplier) suitable to be included in the safety interlock chain of future accelerators. This is important because future hadron colliders (beginning with LHC) will have stored beam energies that could easily damage equipment, particularly superconducting magnets. We conducted an experiment at the ALS, detecting the synchrotron light out of a bending dipole with a gated microchannel plate photomultiplier. The first results show that it is possible to detect low-intensity parasitic bunches near the much larger camshaft bunch, after it has been gated out. Figure 8 shows an image of the ALS gap with camshaft, obtained on Beamline 3.1. We can zoom on the camshaft pulse and time the microchannel plate gate signal as the camshaft pulse is gated out, at which point the trailing parasitic bunch, having an intensity 10^3 times lower, becomes apparent. Further tests to assess the saturation properties of the front stage will be performed using a pockel cell switch. Numerical analysis of the data is also required to compare it to the LHC specification, which requires the ability to detect proton densities as low as 60 protons per picosecond over a time span of at least 100 nanoseconds. From a qualitative analysis of Figure 8 we can expect the photomultiplier tube instrument to be as sensitive as the laser-mixing based one.

Finally, an accurate analysis of the performance required by the different applications of the instrument, using LHC parameters, was performed. We identified three working modes of the instruments—ultra-high sensitivity, high sensitivity, and standard sensitivity—corresponding to a wide range of measurements of various longitudinal beam parameters relevant to the LHC accelerator physics. Given the presently expected photon flux, the results showed that our instrument, in its 40 megahertz LHC-dedicated version, is suitable for monitoring the abort gap, ghost bunches, bunch tails, and is suitable for measuring bunch core longitudinal parameters in a time that is short compared to the synchrotron frequency.

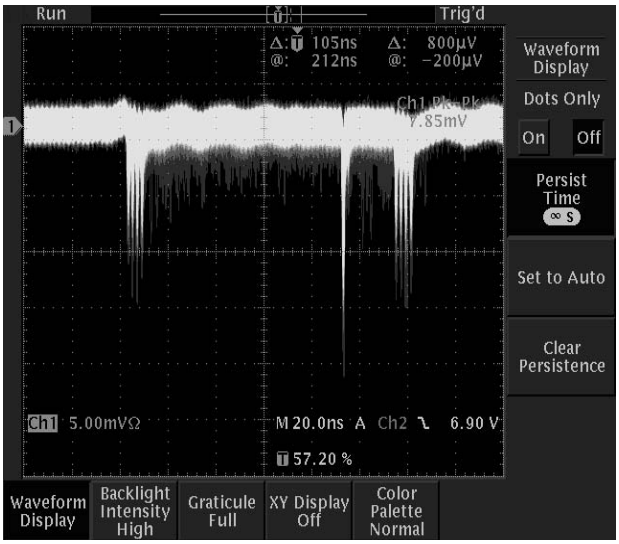

Figure 8. Photomultiplier image of the ALS gap with camshaft bunch. Four bunches at the beginning and the end of the bunch train are also visible.

Publications

M. Zolotorev, J.-F. Beche, J.M. Byrd, P. Datte, S. De Santis, P. Denes, M. Placidi, A. Ratti, V. Riot, R. Schoenlein, and W.C. Turner, "Measurement of longitudinal beam density via the non-linear mixing of synchrotron radiation with a mode locked laser oscillator," 2003 Particle Accelerator Conference, May 12-16, 2003. http://www-conf.slac.stanford.edu/pac03/

M. Placidi, W.C. Turner, and M. Zolotorev, "Notes on the measurements of longitudinal beam density in LHC using optical methods," *CBP Tech Note* **307**, January 2003.

M. Zolotorev, J.-F. Beche, J.M. Byrd, S. De Santis, P. Denes, M. Placidi, A. Ratti, V. Riot, R. Schoenlein, and W.C. Turner, "An optical sampling technique for measuring longitudinal beam density in a storage ring," *Physical Review Special Topics–Accelerators and Beams*, in preparation.

Electron Production and Collective Field Generation in Intense Particle Beams

Principal Investigators: Jean-Luc Vay and Miguel Furman

Project No.: 03028

Project Description

Electron cloud effects (ECEs) are increasingly recognized as important, but incompletely understood, dynamical phenomena. ECEs can severely limit the performance of present electron colliders—the next generation of high-intensity rings, such as PEP-II upgrade, or future high-intensity heavy ion accelerators. Deleterious effects include ion-electron instabilities, emittance growth, particle loss, increase in vacuum pressure, added heat load at the vacuum chamber walls, and interference with certain beam diagnostics. A comprehensive research and development program including experiments, theory, and simulations is needed to better understand the phenomena, establish the essential parameters, and develop mitigating mechanisms. This project will address the technical questions on which to focus future directions.

We will develop insights into the essential processes, models of the relevant physics, and implement these models in computational production tools that can be used for self-consistent study of the effect on ion beams. We will validate the models and tools through comparison with experimental data, including data from new diagnostics to be developed as part of this work and validated on the High-Current Experiment (HCX) presently beginning operations at Berkeley Lab for studies of beam physics relevant for heavy ion fusion (HIF). We will apply these models and diagnostic techniques to High-Energy Physics (HEP) and other advanced accelerators.

Accomplishments

During FY03, we improved our particle-wall interaction modeling capabilities, which rely on subroutines developed in the code POSINST. We enhanced the input ability of POSINST to accept more standard variables for primary electron generation. The tracking module in a magnetic field and the electron-wall collision description were modified for greater efficiency. The structure of POSINST was remodeled toward a higher modularity, which eases the maintenance and the portability of routines to other codes. Comparisons between POSINST simulations and measurements at the Proton Storage Ring (PSR) at Los Alamos National Laboratory are ongoing, particularly following beam extraction. This process is sensitive to the low-energy value of the secondary emission yield, which is important in the dissipation rate of the electron cloud. Owing to the simpler physics of the dissipation process, the code prediction is expected to be more reliable for this case than in steady state, hence this comparison offers a good calibration test.

We formulated a conceptual framework for self-consistently simulating electron and neutral gas effects code and also initiated the development of modules to describe the various effects, which include electron generation from the walls and from gas ionization, gyro-averaged (drift-kinetic) electron transport, and neutrals generation and transport. We formulated options for gyro-averaged (drift-kinetic) and bounce-averaged electron movers and started the coding of a prototype drift-kinetic mover. We also participated in the design of an algorithm for efficient treatment of particle collisions with complicated vacuum chamber structures in WARP. We ran the existing code in slice (XY) mode using an input deck modeling the HCX beam through 100 quadrupoles. We found that randomly varying electron densities of greater than several percent of the ion density are required to cause significant growth of the ion beam halo in 200 quadrupoles, see Figure 9.

On the HCX beam, we measured electron emission and gas desorption from one MeV K^+ impinging on a target near grazing incidence and developed models for these processes based on the above-mentioned electron-wall collision models, properly taking into account the energy loss of the ions in matter. Mitigation techniques will be applied to second generation diagnostics to reduce secondary electron emission and ion scattering in order to gain improved diagnostics and reduced electron effects on the beam.

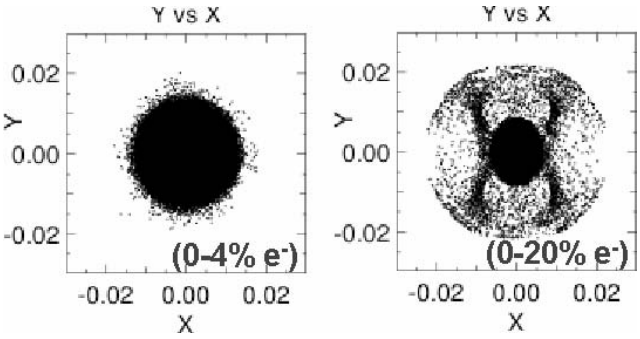

Figure 9. WARP simulations of an ion beam with prescribed electron density variations as a percentage of the ion beam density. These results show that electron density variations greater than several percent of the ion density are required to cause significant halo growth in 200 quadrupoles.

Publications

A.W. Molvik, F.M. Bieniosek, R.H. Cohen, A. Friedman, M.A. Furman, E.P. Lee, S.M. Lund, L. Prost, P.A. Seidl, and J.-L. Vay, "Initial experimental studies of electron accumulation in a heavy-ion beam," Particle Accelerator Conference, 2003, LBNL-52532.

R. H. Cohen, A. Friedman, M.A. Furman, S.M. Lund, A.W. Molvik, P. Stoltz, and J.-L. Vay, "Stray-electron accumulation and effects in HIF accelerators," Particle Accelerator Conference, 2003, LBNL-53100.

A.W. Molvik, R.H. Cohen, A. Friedman, M. Kireef-Covo, S.M. Lund, F.M. Bieniosek, E.P. Lee, L. Prost, P.A. Seidl, J-L. Vay, and M.A Furman, "Progress in Measuring Electron Cloud Effects in HIF Accelerators," *Bulletin American Physical Society* **48,** 315 (2003) Abstract. LBNL-53550.

R.H. Cohen, A. Friedman, A.W. Molvik, A. Azevedo, J-L. Vay, M.A. Furman, and P.H. Stoltz, "Progress in Modeling Electron Cloud Effects in HIF Accelerators," *Bulletin American Physical Society* **48**, 315 (2003) Abstract.

P.H. Stoltz, R.H. Cohen, A.W. Molvik, M.A. Furman, J.-L. Vay, and A. Adelmann, "The CMEE Library for Numerical Modeling of Electron Effects," *Bulletin American Physical Society* **48**, 315 (2003) Abstract.

P.H. Stoltz, M.A. Furman, J.-L. Vay, A.W. Molvik, and R.H. Cohen, "Numerical simulation of the generation of secondary electrons in the High Current Experiment," *Physical Review Special Topics* **6** (2003).

Advanced Light Source Division

A Novel Ultra-high Resolution (< = 10meV) Inelastic Scattering Spectrograph to Study Coupled Electron-Phonon-Orbiton Interactions in Degenerate Quantum Systems

Principal Investigators: Zahid Hussain, Eric Gullikson, and M. Zahid Hasan

Project No.: 03013

Project Description

We will use resonant inelastic (frequency resolved) x-ray scattering near the 3p-edges of transition metals to study interactions of orbitons, phonons, polarons and magnons in highly correlated electron systems, such as colossal magnetoresistive (CMR) oxides and high-temperature superconducting cuprates. Our goal is to develop the photon-in photon-out facility that enables us to study electron-orbiton-phonon interaction as a function of doping around the CMR transition. This will also allow us to study high-temperature superconductors. We would also like to develop the experimental capability to allow us to study manganites and cuprates in the presence of a tunable magnetic field, up to 5T, which is the key aspect to elucidate the physics of CMR manganites and high Tc superconductors.

We will build an ultra-high resolution, <=10 meV, inelastic scattering spectrograph at the Advanced Light Source, which is an ideal location for the spectrograph's high brilliance at the soft x-ray energies, near 3p excitation energies of transition metals, and where there is a staff with the expertise in developing such an emission spectrograph. This novel design will incorporate a variable line spacing grating, a high quantum efficiency, a high spatial resolution back-illuminated CCD detector, and a small photon spot, approximately = 5 microns, at the sample to deliver high throughput–one to two order of magnitude increase as compared with spectrograph based on spherical grating design–and significantly high energy resolution, better by a factor of 10, as compared to what is presently available.

Accomplishments

Optical design of the ultra-high energy resolution emission spectrograph is completed. This unit has similar optics to our previous design of the soft x-ray emission spectrograph. It consists of two elements: (1) a spherical mirror focusing the light onto a CCD detector and (2) a variable line spacing (VLS) plane grating dispersing the light. The overall length of the spectrograph is two meters. The goal is to achieve resolving power of 10,000 at manganese 3p edge, 47eV, with 4 microns, vertical, source size and 13.5 microns detector pixel. With such energy resolution, we hope to study interplay of electron-phonon-orbiton in degenerate quantum systems.

The optical design of the VLS grating based spectrograph has been completed and the ray-tracing results are shown in Figure 1. The source height used in ray-tracing is four microns and the energies of incoming photons are 49eV +/- 5meV. These images are well separated from each other, demonstrating the unsurpassed energy resolution from the design. The mechanical design of the spectrograph is also completed and the orders for optics have been placed. During the first year of this effort, a research proposal based on this design concept was submitted to the Department of Energy (DOE), Basic Energy Sciences. DOE has funded the DOE proposal at a level of $3.5 million, which is allocated to build a dedicated beamline named MERLIN at the ALS. The ultra-high resolution spectrograph will be the main part of the experimental endstation.

In parallel, further characterization of the moderate resolution soft x-ray emission spectrograph has been done. The spectrograph has been tested at BL 6.3.2, with direct synchrotron beam passing though a 15 micron slit as the source. The energy resolution of the spectrograph is determined by observing different image positions with respect to different incoming photon energies. At 700eV, the resolution is determined to be around 1eV, which gives the resolving power of 700 at this energy. When going to second order in spectrograph, the resolving power is doubled. Theoretical calculation predicts that the source size limitation on energy resolution, with a 5 micron source, is approximately 2,300 at 700eV photon energies and it scales linearly with source size. Thus, our test indicates that the spectrograph is well aligned and does deliver the designed energy resolution. These results further confirm soundness of our design concepts.

An endstation housing this soft x-ray emission spectrograph has been built and commissioned for carrying out some early experiments. The endstation has the capability of rotating the spectrograph by 30 degrees. We are able to

perform momentum-resolved soft x-ray scattering experiments by mounting emission spectrograph at different ports and rotating the chamber to cover 30 degrees angular range with five identical ports separated by 30 degrees. The accessible scattering angle ranges from 5 degrees to 155 degrees, relative to the incoming beam, and the corresponding momentum transfer **q** covers nearly the full Brillouin zone. This endstation will serve as a prototype of the system that houses this high-resolution spectrograph in the newly funded MERLIN beamline.

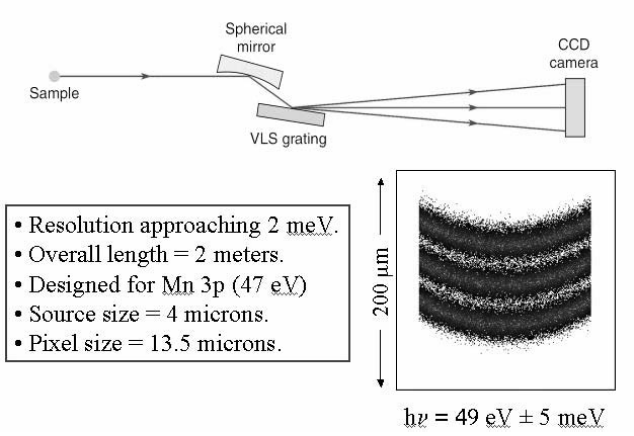

Figure 1. Ray-tracing results on ultra-high resolution spectrograph. The source size is 4 microns. Three photon energies are used: 48.995 eV, 49 eV, and 49.005 eV.

Development of a Coherent Far-infrared Synchrotron Source at the ALS

Principal Investigators: Michael Martin, John Byrd, Fernando Sannibale, Wayne McKinney, and David Robin

Project No.: 02004

Project Description

The purpose of this project is twofold: (1) to further our understanding of the generation of coherent synchrotron radiation through experiments at the ALS using unique modes of operation of the ring, and (2) to consider a pre-conceptual design of a dedicated infrared storage ring to be located at the ALS. A source in the far IR that is much brighter than what is available at present will open up new possibilities for research in this traditionally difficult energy range. We intend to characterize super-radiant far-IR radiation from various novel modes of ring operations, including further experiments with femtosecond laser slicing. This research will be carried out with the goal of understanding how to create stable, coherent far-IR radiation from a storage ring. This will also lead to generation of a pre-conceptual design for a possible future infrared storage ring.

Accomplishments

This year's research has resulted in a number of significant accomplishments and publications. We have made extensive measurements of far-IR bursts caused by micro-modulations of the electron bunch distribution. We showed that the beam current threshold for the onset of these bursts agrees very well with a model of self-amplified spontaneous bunch dynamics driven by the coherent synchrotron radiation (CSR) itself. The experimental data agrees very well with the theoretical model results with no adjustable parameters. This model also fits very well with bursting instabilities measured at Berliner Elektronenspeicherring–Gesellschaft für Synchrotronstrahlung m.b.H. (BESSY). Therefore, the model is quite robust to different synchrotrons and we can now use it to set an upper limit to the amount of current per bunch that can be stored in a future ring optimized for stable CSR.

We collaborated with researchers at Jefferson Lab in Virginia and Brookhaven National Lab in New York to make measurements of the CSR power and spectrum from a new energy recovery linac (ERL) located at Jefferson Lab. This source produces ~500-femtoseconds of electron bunches at a repetition rate of 75 megahertz which are normally used for a high-power mid-IR free electron laser (FEL). We measured the CSR from a bend magnet just before the FEL and showed that 20 watts of average power in the sub-terrahertz frequency range was being emitted. This is about four orders of magnitude greater power than the previous world record for this frequency regime. The fluctuations inherent to a single-pass accelerator such as this ERL may make it a problematic source for spectroscopy where keeping noise to a minimum is crucial.

Stable CSR from a storage ring was demonstrated at the BESSY synchrotron facility in Berlin; we collaborated on the analysis and understanding of the results. In the past few months we have developed a detailed model for how CSR can self-induce a static deformation of the electron bunch profile thus generating CSR to higher frequencies than the nominal bunch length would allow. This model qualitatively predicts the observed spectra measured at BESSY and allows us to carefully plan how a dedicated ring can be designed to maximize the CSR output while remaining below the bursting threshold.

The source at BESSY has also provided us the opportunity to begin demonstration measurements of science that is made possible by high-power CSR. We used two dedicated

machine shifts at BESSY to make the first measurements of the Josephson plasma resonance (JPR) in the high-temperature superconductor $Bi_2Sr_2CaCu_2O_8$. Shown in Figure 2 is the measured c-axis reflectivity as a function of temperature, shown in the upper panel, with a simple model shown in the lower panel. The JPR is clearly observed and can now be used to deduce important parameters about the superfluid such as the c-axis penetration depth, $\lambda_c = 21$ μm. Further analysis of the data reveals that the simple model does not quite fit the data; a distribution of resonances works better. This may be a direct indication of the inhomogeneity in the superfluid density throughout these complex samples.

We have also completed a preliminary design of the Coherent InfraRed CEnter (CIRCE) source. The location of the CIRCE ring is on top of the existing ALS booster shielding. The ring design allows for numerous CSR beamlines located directly next to the shield walls and the parasitic use of the ALS injector for full-energy beam injection into CIRCE. The unusually large dipole photon beam extraction chamber has been tested for trapped radio frequency (RF) modes via simulations and a mock chamber built. The preliminary conceptual design is completed including lattice, magnets, collection optics, RF, injection, shielding, and facilities; there are no technical showstoppers.

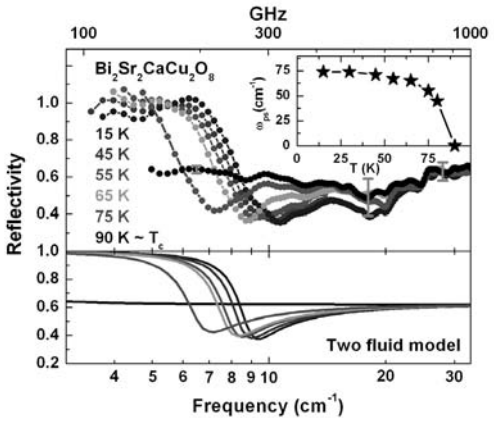

Figure 2. Measured c-axis polarized near-normal reflectivity of $Bi_2Sr_2CaCu_2O_8$, upper panel, for various representative temperatures at or below the superconducting transition temperature, T_c. A resonance that shifts with temperature and disappears above T_c is clearly observed. The lower panel shows the calculated reflectivity of a superconductor with a shifting Josephson plasma resonance. The inset of the top panel shows the temperature dependence of the unscreened superfluid plasma frequency as determined from fits to the data.

Publications

F. Sannibale, J.M. Byrd, A. Loftsdottir, M. Venturini, M. Abo Bakr, J Feikes, K. Holldack, P. Kuske, G. Wustefeld, H-W Hubers, and R. Warnock, "A model for describing powerful, stable, broadband terahertz coherent synchrotron radiation in storage rings," submitted to *Physical Review Letters*.

E.J. Singley, M. Abo-Bakr, D.N. Basov, J. Feikes, K. Holldack, H.W. Hübers, P. Kuske, M.C. Martin, W.B. Peatman, U. Schade, and G. Wüstefeld, "New scientific opportunities using intense coherent THz synchrotron radiation: measuring the Josephson plasma resonance in $Bi_2Sr_2CaCu_2O_8$," submitted to *Physical Review Letters*.

J.M. Byrd, Michael C. Martin, W.R. McKinney, D.V. Munson, H. Nishimura, D.S. Robin, F. Sannibale, R.D. Schlueter, W.G. Thur, J.Y. Jung, and W. Wan, "CIRCE: A dedicated storage ring for coherent THz synchrotron radiation," *Infrared Physics and Technology*, in press. LBNL-53699

W.P. Leemans, C.G.R. Geddes, J. Faure, C.S. Toth, J. van Tilborg, C.B. Schroeder, E. Esarey, G. Fubiani, D. Auerbach, B. Marcelis, M. A. Carnahan, R. A. Kaindl, J. Byrd, and M. C. Martin, "Observation of coherent terahertz emission from ultrashort laser accelerated electron bunches at a plasma boundary," *Physical Review Letters* **91**, 074802 (2003). LBNL-52554.

F. Sannibale, J.M. Byrd, A. Loftsdottir, M.C. Martin, and M. Venturini, "A model for producing stable, broadband terahertz coherent synchrotron radiation in storage rings," Particle Accelerator Conference, 2003.

G.R. Neil, G.L. Carr, J.F. Gubeli III, K. Jordan, M.C. Martin, W.R. McKinney, M .Shinn, M. Tani, G.P. Williams, and X.-C. Zhang, "Production of high power femtosecond terahertz radiation," *Nuclear Instruments and Methods in Physics Research A* **507**, 537-540 (2003), LBNL-52358

E.J. Singley, M. Abo-Bakr, D.N. Basov, J. Feikes, K. Holldack, H.-W. Hübers, P. Kuske, M.C. Martin, W.B. Peatman, U. Schade, and G. Wüstefeld, "Observations in the THz gap: The Josephson-plasma resonance of $Bi_2Sr_2CaCu_2O_8$," *BESSY Annual Report 2002*, 18–19.

J.M. Byrd, W. Leemans, A. Loftsdottir, B. Marcelis, M.C. Martin, W.R. McKinney, F. Sannibale, "Observation of broadband self-amplified spontaneous coherent terahertz synchrotron radiation in a storage ring," *Physical Review Letters* **89**, 224801 (2002) and selected for the *Virtual Journal of Ultrafast Science*, LBNL-50459.

G.L. Carr, Michael C. Martin, Wayne R. McKinney, K. Jordan, George R. Neil, and G.P. Williams, "High-power terahertz radiation from relativistic electrons," *Nature* **420,** 153–156 (November 14, 2002). LBNL-50417.

Aberration Correction of Electron Microscopes

Principal Investigators: Howard Padmore, David Robin, and Ulrich Dahmen

Project No.: 03019

Project Description

We will focus our efforts on establishing the next-generation aberration corrected electron microscopy, specifically photoemission electron microscopy (PEEM), and transmission electron microscopy (TEM). Aberration correction in PEEM can lead to resolution an order of magnitude better than today and a transmission two orders of magnitude better that today's systems at moderate spatial resolution. To surpass the 0.15 nanometer resolution of state-of-the-art TEMs presently requires electron holography or focal series restoration together with complex image processing. Aberration correction in TEM provides the opportunity to go well beyond current limitations. Corrected electron optics for PEEM and TEM will enable significant advances in nanometer and atomic-scale characterization of materials.

The ultimate resolution of electron microscopes is limited by aberrations as well as by electron diffraction. We propose to drive forward next generation designs for PEEM and TEM and in doing so, form the basis for continuing work in this area at Berkeley Lab and help lay the groundwork for proposals to funding agencies for new microscopes. The issues to be addressed are underlying assumptions relating to (1) static fields, (2) axially symmetric systems, (3) no space charge, and (4) no change of sign for the axial ray velocity.

Similar techniques can be applied in many areas of electron imaging; for example, we are starting a study of correction of the temporal spreading in streak cameras caused by the chromatic nature of x-ray photocathodes. By eliminating this temporal spread caused by differing flight times of electrons of different initial energy, the temporal resolution should improve from the picosecond to sub 100 femtosecond level and enable a new generation of ultrafast experiments.

Accomplishments

Dr. Schmid joined the laboratory as a post doctoral fellow in November, 2002. Dr. Schmid is a theoretical physicist whose expertise has been in designing and analyzing schemes for aberration correction in electron microscopes and electron lithography devices. Following the arrival of Dr. Schmid, effort has been focused on building tools for the analysis of aberrations in X-PEEM. In particular, Dr. Schmid has collaborated with several scientists at Berkeley Lab, as well as Duke University and High Energy Accelerator Research Organization (KEK) in Japan, to develop differential algebra mapping tools for studying the impact of construction and modeling errors on aberrations and subsequent correction schemes. Differential algebra (DA) is a semi-analytic tool for performing sensitivity analysis and is frequently used in the design and analysis of particle accelerators. DA can compute aberration coefficients and the dependence of the aberration coefficients on various parameters, such as misalignments or field errors. DA maps are very powerful tools that can be used to quickly perform sensitivity analysis.

In electron microscopes the front-end optics are mostly responsible for generating the spherical and chromatic aberrations. To compensate for the aberrations requires that one or more of Scherzer's assumptions be broken. In aberration corrected X-PEEMs, one technique is to bend the electron trajectories with a separator and then reflect the electrons in an electron mirror. This violates the axial symmetry and unidirectional assumptions of Scherzer. The addition of the corrector greatly increases the sensitivity to errors and the complexity of tuning the microscope. As a result, it is important to understand the effect of errors and how to practically compensate for them. DA maps were developed and employed to study these issues.

Below is an example of the use of DA maps in studying the effect of errors in the separator on the resolution of the microscope. The top panel of Figure 3 shows the resolution in the case of an ideal microscope. The resolution of the ideal separator is 0.54 nm x 2.1 nm. When machining errors are introduced, the resolution is largely spoiled and increases to 26 nm x 5.9 nm. The method for compensating the aberrations was determined through the analysis of the DA maps. Using tuning coils in the corrector the resolution is almost fully restored to 0.57 nm x 2.1 nm.

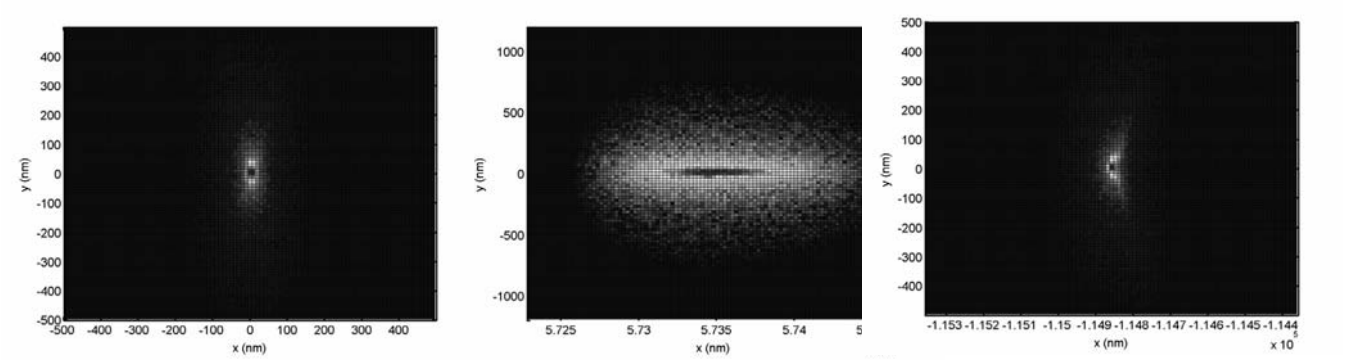

Figure 3. Increase in spot size for a microscope: no errors (left), with errors (center), with errors and correction (right).

Simulations of Femtosecond X-ray Spectra of Photoexcited Molecules

Principal Investigators: Shaul Mukamel (University of Rochester), Robert Schoenlein, and Thornton Glover

Project No.: 02006

Project Description

The goal of this project is to develop a theoretical framework for simulating and interpreting ultrafast x-ray absorption spectra on the 100-femtosecond time scale. This theoretical work is driven by new experimental capability for generating ultrashort x-ray pulses from the Advanced Light Source (ALS). Time-resolved spectroscopy with femtosecond x-ray pulses will open new areas of research in physics, chemistry, and biology by allowing the motion of atoms in materials to be directly probed on the time scale of a vibrational period, which is the fundamental time scale for structural dynamics. At present, there is a strong need for theoretical support to interpret time-resolved x-ray absorption spectra.

Nonlinear spectroscopy in the visible regime is successfully described using the well developed machinery of nonlinear response functions (NRF), which are expressed as combinations of multiple-time correlation functions of the dipole operator and provide the most compact and general formulation of optical signals. The research will focus on extending this approach to coherent nonlinear ultrafast x-ray spectroscopies. The various signals in terms of the NRF will be represented as combinations of multiple-time correlation functions of the current and the charge-density. X-ray techniques thus probe the dynamics of charge and current densities rather than of the dipole. Since charge distributions are directly related to chemical bonding and structure, the creation and breaking of bonds and other electronic and nuclear motions can be monitored with femtosecond time resolution.

Accomplishments

In ultrafast x-ray absorption spectroscopy (XAS), the transient molecular states will generally be in the electronic excited state. In this regime, the XAS spectrum can be influenced by the moving charges in the excited state as well as by the changing positions of the atoms. Existing codes, such as FEFF, for predicting x-ray absorption spectra find a self-consistent electronic structure that converges to the ground state. This makes conventional XAS modeling codes of limited use for ultrafast XAS experiments.

During the past year, Dr. Luke Campbell has developed a new computer code, XSNAP, for assisting in the simulation of x-ray absorption spectra of molecules in the excited state. XSNAP uses the quantum chemistry code Gaussian to determine the excited-state electron distribution. This distribution is then introduced to the x-ray absorption code FEFF. The FEFF algorithm calculates the XAS in several independent steps using the excited-state charge distribution and associate scattering potentials around the atoms determined from Gaussian.

Several tests have been conducted to verify the validity of the XSNAP code. Starting with zero change in the electron density, XSNAP was able to reproduce the ground-state potentials for the test molecule ruthenium bipyridine. The second test relied on a system with a known difference in charge distribution, hexaamine ruthenium, that closely approximates the charge distribution of ruthenium bipyridine in the excited state. The conventional FEFF code was used to calculate charge distributions for both molecules. From this, the differential charge distribution, excited state minus ground state, was derived and compared with the charge distribution calculated by XSNAP of ruthenium bipyridine in the excited state. There was very good agreement in the electron densities, indicating that the

XSNAP code is working properly. Presently, XSNAP is being tested against recent experimental measurements of the x-ray absorption near edge structure (XANES) spectrum of ruthenium tris-bipyridine in the photoexcited state.

Publications

L. Campbell and S. Mukamel, "Simulation of time resolved EXAFS and XANES spectra of photoexcited molecules," to be submitted to *Chemical Physics Letters.*

P-sec Time-resolved Photo-electron Emission Microscopy on Magnetic Nano-structures

Principal Investigators: Andreas Scholl, Sug-Bong Choe, Yves Acremann, Aaron Lindenberg, Howard A. Padmore, and Joachim Stöhr

Project No.: 02007

Project Description

The purpose of this work is to pioneer the study of ultra-fast magnetic processes with a combination of temporal and spatial resolution hitherto inaccessible to the magnetic materials research community. Understanding the dynamics of the magnetization process is one of the fundamental issues in magnetism research and it is of great importance for technological applications. Of key interest is the dynamics of magnetization-precession and magnetization-damping which govern the speed of magnetization reversal in magneto-electronic devices.

This work will also provide a foundation for next-generation microscopes such as PEEM3. We will use an existing photoelectron microscope, PEEM2, for imaging, and use a combination of the native bunch structure of the Advanced Light Source (ALS) (50-picosecond x-ray pulses) and a picosecond rise-time magnetic pulse system for pump-probe magnetization studies. The fast magnetic pulse for the pump will be generated by the interaction of a picosecond laser with a semiconductor photo-switch; this will provide current to a lithographically defined micro-coil to provide the field. The system will also be deposited on the semiconductor surface, at the center of the micro-coil. The laser system will be locked to the revolution frequency of the ALS, and a programmable delay between magnetic field pump and x-ray probe will allow us to map out the spatially resolved dynamics of the system.

Accomplishments

In the second year of this project we have focused on optimizing the sample design and conducting demonstration experiments that illustrates the capabilities of the new technique. The sample design has been optimized to: (a) provide higher currents and thereby magnetic fields, (b) reduce the risk of accidental high-voltage discharges, and (c) improve the pulse shape to a clean exponential. These goals have been achieved. We have also improved the laser setup, in particular the beam transmission through an optical fiber into the x-ray microscope.

In a demonstration experiment, we studied the dynamics of magnetic vortices in response to fast field pulses. The vortices were trapped in micron-size structures that were patterned by focused ion-beam milling on top of a wave guide. Magnetic vortices are of possible significance in magnetic data storage because of the high stability of the vortex structure and its low stray field, allowing high integration density. The current pulse, triggered by the pump laser and running trough the wave guide, produced an in-plane field pulse that started the dynamics. We observed the domain dynamics for various pattern sizes and shapes at high spatial resolution using an x-ray photoemission electron microscope. Images of the magnetic structure at two selected times after the initial field pulse show the motion of the vortex center in three rectangular pattern of different aspect ratio, see Figure 4 below. In addition to the domain images the core trajectories are shown, illustrating the gyrotopic vortex mode. From this data we were able to deduce important physical quantities such as the material dependent damping constant, the magnetic field strength, and the torque near the core and the resulting speed of the vortex core in response to this torque.

We have also explored the possibility of directly driving the dynamics of the system using the optical laser pulse. The laser pulse heats the material on the time scale of the laser pulse length. The heating then results in a reduction of the moment and, potentially, in a change of the magnetic anisotropy and magnetic coupling. These experiments have been hindered by the very low pulse energy and the high repetition rate of the pump laser. Still we have been able to determine the demagnetization of thin nickel films with a time resolution of 70 picoseconds and as function of the time after the heating pulse. For future experiment we will need to improve the time resolution significantly to be able to clearly resolve the demagnetization process. More intense laser sources will also be needed.

As result of this project, we have been able to attract users from SLAC, Argonne, University of Maryland and University of California, Berkeley, and Berlin, Germany, who wish to use the setup for the investigation of domain dynamics in ferromagnetic and ferroelectric materials. We

plan to transfer the setup to a new Photoemission Electron Microscope and Scanning Transmission X-ray Microscope facility, which will allow time-resolved measurements with higher spatial resolution, higher temporal resolution, and higher sensitivity. The research enabled by this proposal has been rewarded by invitations to several international conferences and has initiated similar research and development efforts at other synchrotron radiation facilities.

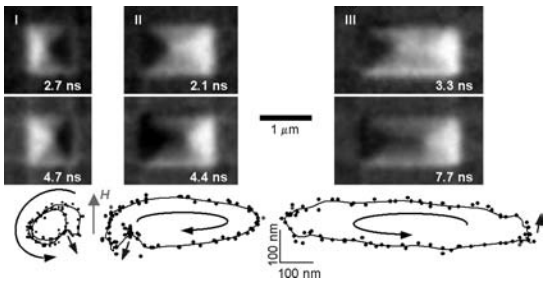

Figure 4. Time-resolved magnetic domain images of rectangular vortex patterns. The vortex trajectories are shown below.

Publications

S.-B. Choe, Y. Acremann, A. Scholl, A. Bauer, A. Doran, J. Stöhr, and H.A. Padmore, "Hidden parameter in magnetic vortex dynamics," in preparation.

Choe, S.-B., et al., "P-sec time-resolved microscopy of magnetic structures using X-PEEM," accepted for publication in *Review of Scientific Instruments.*

X-ray Diffraction for the Study of Strongly Correlated Materials

Principal Investigators: John Spence, Simon Clark, Howard Padmore, S.W. Cheong, J.M. Zuo, and B. Jiang

Project No.: 03025

Project Description

The Advanced Light Source (ALS) is establishing itself as a center for the study of electronic properties of strongly correlated materials through its state of the art facilities for high resolution angle resolved photoemission and infrared spectroscopy. However, these techniques only give partial information on the electronic structure and much has to be inferred. Charge density mapping, i.e., ultra-high resolution x-ray diffraction that can reveal not only atom core positions but bonding information is a powerful new tool in the study of these materials. The aim of this project is to demonstrate this technique in application to colossal magnetoresistive (CMR) materials.

The useful electronic properties (magnetoresistance, superconductivity) of strongly correlated materials are known to depend on a subtle temperature and doping-dependant competition between charge, spin, and orbital ordering (OO). We have recently demonstrated a new method for real space imaging of orbital holes (charge densities) and electron transfer. Our aim is to use this to observe OO in LaMnO3 in real space, to measure one-electron d-orbital hybridization coefficients, electron transfer, and covalency.

ALS beamline 11.3.1 will be used for this work. It is a new system for small molecule x-ray diffraction, and is equipped with a state of the art x-ray detector, cryo-cooler, and the necessary hardware and software for structure determination. The beamline will be applied first to the solution of some simple small molecule systems, and ultimately we will attempt initial charge density mapping work on LaMnO3.

Accomplishments

We achieved a number of landmarks in this year of funding:

- Commissioned beamline 11.3 for small molecule x-ray diffraction.
- Commissioned an optical viewing system for microcrystal alignment.
- Established data collection on a range of challenging small molecule systems.
- The above study revealed unforeseen problems with the x-ray area detector that precluded studies in which very accurate structure factors were needed, e.g., for charge density mapping. The problems related to non-normalizable background variations and spot-splitting at high angle.
- Embarked on a series of detector tests with the manufacturer, ultimately involving three changes of the detector which resulted in more optimum versions.
- Tested a fourth detector with good initial results.
- Proved that we can take data on very small crystals at high photon energies; the latter is needed to avoid as much as possible the problems of extinction caused by crystalline imperfections and absorption. Small beams are needed to avoid as much as possible crystallographically twinned regions.
- Commissioned a cryocooler for low temperature sample cooling.
- Grew LaMnO3 crystals (Cheong) with twin free-areas bigger than the focused beam.
- Undertook Complementary Electron Diffraction studies.

Publications

B. Jiang et al., "Orbital ordering in LaMnO3 and its effect on structure factors," *Acta Crystallographica* **A58,** 4 (2002).

B. Jiang et al., "On the consistency of QCBED structure factor measurements for TiO2 (Rutile)," *Microscopy and Microanalysis* **9,** 1 (2003).

Bonding in Low-dimensional Structures: Theory and Computation

Principal Investigators: Michel Van Hove, Andrew Canning, and Lin-Wang Wang

Project No.: 02008

Project Description

This theoretical and computational project will interpret and analyze data to understand the bonding between atoms in low-dimensional structures. The results, based on experiment, will be fundamental to the design and exploitation of novel nanoscale structures and processes. In its first year, the work will focus on three state-of-the-art experiments: (1) quantum-well states relevant to magnetism at metallic interfaces; (2) structural studies of nanoparticle-molecule interactions that control nanoparticle growth mechanisms. The long-term benefit will be theoretical and computational capabilities that greatly enhance the value of a broad range of nanoscale studies aimed at designing new devices.

The project joins theoretical and computational expertise in the Materials Sciences Division and the National Energy Research Scientific Computing Center with experimental programs in several Berkeley Lab divisions. Large-scale, first-principles calculations will be applied to complex structures to model and understand their bonding and properties. Advanced multiple-scattering calculations will be used to extract bonding and related electronic and magnetic information from experiments conducted at the Advanced Light Source (ALS), primarily with photoemission and x-ray absorption. The two sets of calculations will feed into each other at the fundamental level of quantum wavefunctions, forming a closely coherent program.

Accomplishments

During the second year of this project, we expanded our studies of the systems described in the first year report. Our focus was on quantum-well states that are localized within the copper film, whose energies were accurately measured as a function of both copper and cobalt film thickness.

We also included the local interface structures, such as relaxations in atomic positions at the interfaces from their ideal bulk locations, as well as the surface potential barrier at the solid-vacuum interface. The difference between these and the bulk characteristics of thicker samples can have important consequences on the physical properties of these films. We have also modeled the possible interdiffusion of atoms across the interface between cobalt and copper, since this can easily occur in real samples, and have shown that the quantum-well states are quite tolerant to such interdiffusion.

In parallel, we have conducted exploratory studies that have been very valuable in examining the potential of the theoretical modeling of structure determination with extended x-ray absorption fine structure (EXAFS) for nanoparticles, and in suggesting optimum experimental conditions. This work addressed experimental data measured at the ALS by D.M. Aruguete, a student of A.P. Alivisatos, and M. Marcus for a system of oriented cadmium selenide nanorods. The purpose was to investigate to what extent EXAFS data could indicate structural details of the surface of this type of nanostructure. Through modeling with the FEFF and IFEFFIT codes (based on methods by J.J. Rehr et al.), we could evaluate the size and character of the experimental dataset that would be needed to extract faceting behavior and bonding information at the multiple facets. New ALS experiments along those lines are being performed at this time.

Publications

J.M. An, D. Raczkowski, Y.Z. Wu, C.Y. Won, L.-W. Wang, A. Canning, M.A. Van Hove, E. Rotenberg, and Z.Q. Qiu, "The quantization condition of quantum-well states in Cu/Co(100)," *Physical Review B* **68**, 045419 (2003).

J.M. An, Y.Z. Wu, C.Y. Won, L.-W. Wang, A. Canning, M.A. Van Hove, E. Rotenberg, and Z.Q. Qiu, "The interaction of quantum-well states in Cu/Co(100) with Co ultra-thin-film states," draft.

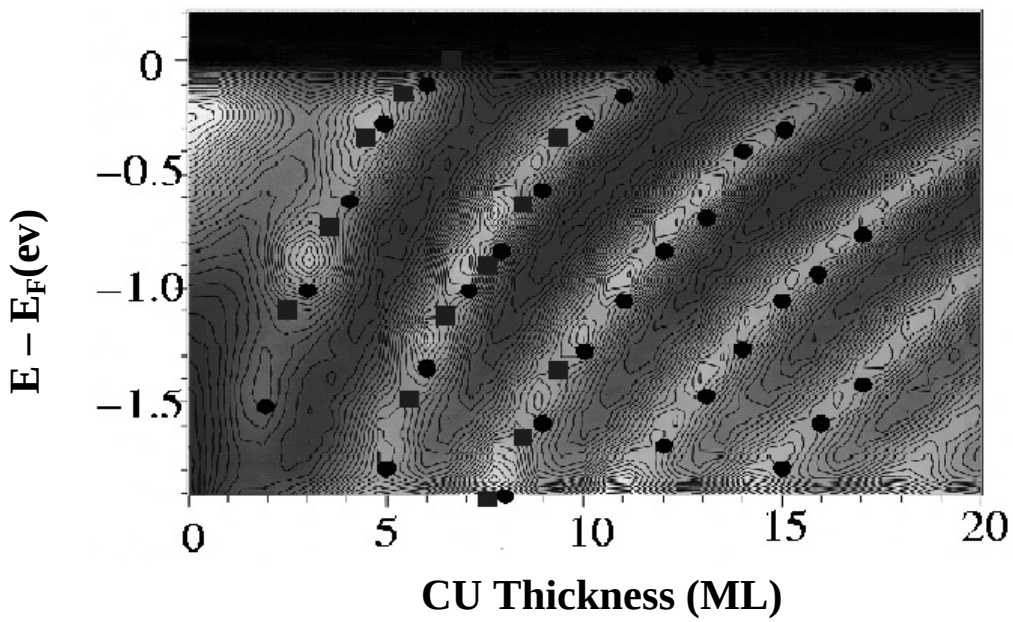

Figure 5. Shading with contour lines shows the experimental photoemission yield as a function of electron energy below the Fermi level (ordinate) and thickness (abscissa) of a copper film deposited on a cobalt layer, deposited in turn on a Cu (100) substrate. Light shades correspond to quantum well states. The theoretically calculated quantum well states are shown as circles for integer-monolayer thicknesses of copper, matching peaks in photoemission yield. The squares show calculated quantum well states for a simple model of interdiffusion between cobalt and copper at the interface: they help explain the smearing out of the experimental peaks along the ridges of high photoemission yield. The good agreement between measured and calculated quantum well state energies enables our methods to reliably predict the properties of such states in a variety of nanomaterials.

Chemical Sciences Division

Disorder and Multiple Length Scales in Non-Fermi Liquid F*-electron Intermetallics*

Principal Investigators: Corwin Booth

Project No.: 02009

Project Description

The main motivation behind this project is to better understand non-Fermi liquid (NFL) behavior. Such behavior has broad implications not only for *f*-electron intermetallic systems, but also for the high-temperature superconductors. Our goal is to determine the role that lattice disorder plays in *f*-electron NFLs. In systems that appear to be disorder free, we will simply make an exhaustive search for lattice disorder at all length scales in selected materials. Other systems that are known to be disordered, theoretically, may have clusters with long-range magnetic interactions. Here we will characterize the disorder at all length scales in order to relate to current theories of NFL behavior in disordered systems.

To accomplish local (0.2 to 0.5 nm) structure will be measured using the x-ray absorption fine structure (XAFS) technique. Results will be used to better characterize pair-distribution function (PDF) analysis of powder diffraction data at the shortest length scales. Long-range order will be measured with powder diffraction using Rietveld analysis. Deviations from the short- and long-range order should then be observable in the 0.5 to 2 nanometer range in the PDF. Measurements will be made at the Stanford Synchrotron Radiation Laboratory (SSRL), Advanced Photon Source (APS), Intense Pulsed Neutron Source (IPNS) and Los Alamos Neutron Science Center (LANSCE). Some supposedly disorder-free NFLs require applied pressure or a magnetic field. These measurements will be made in a diamond anvil at HPCAT at the APS, and on the 13 T magnet at SSRL.

Accomplishments

Our effort in FY03 focused on several areas: (1) completing a study of $Tb_2Ti_2O_7$, (2) continuing basic PDF analysis of $CeRhRuSi_2$ data, (3) performing work toward measuring the difference-PDF around the Pd *K*-edge of UCu_4Pd, and (4) performing experiments on the $CeAl_2$ and $CePt_{2+x}$ nanoparticle systems.

Addressing the first area, although materials that exhibit nearest-neighbor-only antiferromagnetic interactions and geometrical frustration, theoretically, should not magnetically order in the absence of disorder, few such systems have been observed experimentally. One such system appears to be the pyrochlore $Tb_2Ti_2O_7$. However, previous structural studies indicated that $Tb_2Ti_2O_7$ is an imperfect pyrochlore. To clarify the situation, we performed neutron powder diffraction (NPD) and XAFS measurements on samples that were prepared identically to those that show no magnetic order. The NPD measurements show that the long-range structure of $Tb_2Ti_2O_7$ is well ordered with no structural transitions between 4.5 and 600~K. We conclude that $Tb_2Ti_2O_7$ has, within experimental error, an ideal, disorder-free pyrochlore lattice, thereby allowing the system to remain in a dynamic, frustrated spin state to the lowest observed temperatures.

Second, the atomic local structural properties of NFL system $CeRhRuSi_2$ were studied with temperature dependent XAFS measurements at the Ce L_{m-}, Ru *K*-, Rh *K*-edges, and with PDF analysis of powder x-ray diffraction data. Although XAFS is unable to directly address whether Rh-rich regions exist, Ce L_m-edge XAFS data indicated no special disorder in the Ru/Rh site. Data collected at the Ru and Rh *K*- edges are nearly identical in all respects, suggesting that they are randomly distributed in the Ru/Rh site. In fact, fits with a Debye model to the measured disorder parameters show that very little intrinsic disorder could exist on all atomic sites, and in particular, not enough disorder could be present to explain the NFL behavior in the system with the Kondo lattice disorder model. This lack of disorder is also observed at intermediate length scales from the PDF analysis. Annealing the system from one to five weeks produced, at most, a very small ordering of the crystal, in contrast to the effect on UCu_4Pd.

Third, in order to obtain better measurements of the local environment around a Pd-on-16*e* sites in UCu_4Pd, we collected below and near the peak in *f'* of the Pd*K* edge, both on beam line 7-2 at SSRL, and again on beamline 11-ID-B of BESSRC of the APS. Data were also collected around the Ag *K* edge of $YbCu_4Ag$ as a control. By subtracting PDF data from below and above the Pd *K* edge, only those peaks in the PDF that involve Pd should remain. Such "difference-PDF" data should clarify the Pd/Cu site-interchange, and possibly allow the determination of important details about the environment around the Pd atoms on the 16*e* sites. Progress in understanding this data has been slow, and we plan a trip in FY04 to visit our

collaborators at Michigan State University, Professor Simon Billinge, to discuss these matters further.

Fourth, the most exciting development in FY03 came from measuring and analyzing the XAFS from nanoparticles of $CeAl_2$ and $CePt_{2+x}$. Bulk samples of $CeAl_2$, $CePt_2$ and $CePt_{2.5}$ exhibit both antiferromagnetism (AF) and Kondo behavior with low energy scales ($T_N \sim T_K \sim 4$ K). When the particle size is reduced to ~80 Å, AF is suppressed and Kondo behavior dominates. Although not originally considered, lattice disorder, may also play an important role. Our XAFS studies of the local Ce and Pt environments show that large distortions and other disorder are present on all atomic sites (Figure 1). These and other observations indicate that, in addition to size and surface effects, structural distortions and disorder play a role in determining the Kondo behavior in these nanoparticles.

In summary, we have made progress in all of the major areas of this proposal, namely applying new experimental techniques to relevant materials. Further analyses of these data, complementary measurements to better elucidate the intermediate length scales, and our first measurements of *f*-electron intermetallics under applied pressure, will be the target of FY04.

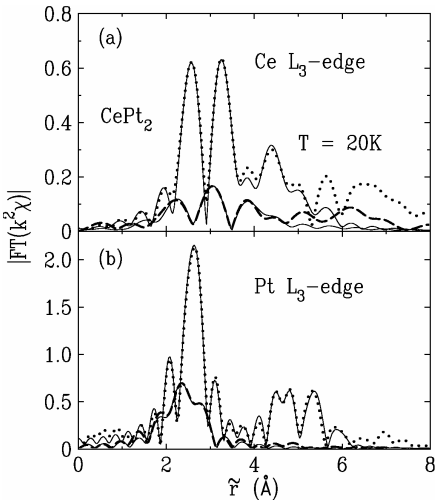

Figure 1. Magnitude of Fourier transformed XAFS data from a bulk (dotted line) and a nanocrystal (thick-dashed line) of $CePt_2$ as a function of distance from the absorbing atoms, Ce (a) and Pt (b). Solid lines are best fits. Ce L_m-edge data are transformed between 2.7 to 7.5 $Å^{-1}$ (nanocrystals) or 2.5 to 9.5 $Å^{-1}$ (bulk). Pt data are transformed between 2.5 to 14.5 $Å^{-1}$ (bulk) or 2.5 to 11.5 $Å^{-1}$ (nanocrystals). A Hanning window of width 0.5 $Å^{-1}$ was applied to all transforms. Data indicate the local environment around both Ce and Pt sites in the nanoparticles is severely distorted/disordered compared to the bulk samples.

Publications

S.-W. Han, C.H. Booth, E.D. Bauer, and M.B. Maple, "Temperature-dependent x-ray diffraction study of Pd/Cu site interchange in non-Fermi liquid UCu_4Pd," *Proceedings of the Strongly Correlated Electron Systems Conference,* Krakow, Poland, July 10–13, 2002, *Acta Physica Polonica B* **34**,403-6 (2003), LBNL-50908.

S.-W. Han, J.S. Gardner, and C.H. Booth, "Structural properties of the geometrically frustrated pyrochlore $Tb_2Ti_2O_7$," *Physical Review B,* in press, LBNL-54103.

S.-W. Han, C.H. Booth, E.D. Bauer, J.M. Lawrence, P.H. Huang, and Y.Y. Chen, "Disorder-induced Kondo behavior in nanoparticle $CeAl_2$." In *International Conference on Magnetism;* Rome, Italy; July 22–August 1, 2003. submitted to *Journal of Magnetism and Magnetic Materials*, LBNL-52531.

S.-W. Han, C.H. Booth, E.D. Bauer, J.M. Lawrence, P.H. Huang, and Y.Y. Chen, "Lattice Disorder and Size-Induced Kondo Behavior in $CeAl_2$ and $CePt_{2+x}$," manuscript in preparation to be submitted to *Physical Review Letters.*

S.-W. Han, C.H. Booth, J.L. Sarrao, and J.D Thompson, "Local order and disorder in non-Fermi liquid $CeRhRuSi_2$," manuscript in preparation to be submitted to *Physical Review B.*

S.-W. Han, C.H. Booth, E.D. Bauer, and M.B. Maple, "X-ray scattering studies of the local Pd-on-Cu environment in non-Fermi liquid UCu_4Pd," draft in preparation to be submitted to *Physical Review B.*

M. Daniel, S.-W. Han, C.H. Booth, E.D. Bauer, J.D. Thompson, and J.L. Sarrao, "Local structure and Sn-site order in $CeCoIn_{5-x}Sn_x$," draft in preparation to be submitted to *Physical Review B.*

Coherent Control and Quantum Information in Polyatomic Molecules

Principal Investigators: Stephen Leone

Project No.: 02043

Project Description

The advent of ultrafast femtosecond lasers as a tool for controlling processes such as branching ratios in chemical reactions and manipulating the evolution of vibrational

wavepackets with tailored femtosecond laser pulses has provided significant insight into the complex interplay between the electronic, vibrational, and rotational degrees of freedom both in diatomic and simple polyatomic systems. The present study involves stimulated Raman pumping of multimode wavepackets in the ground state of polyatomic molecules. The impulsive nature of these excitations eliminates the need for accessing resonances and as a result will prove a general and powerful technique for looking at vibrational coherences in the ground state. Previous collaborative work has addressed the issue of multimode vibrational wavepackets in simple polyatomic systems. Two key goals can be identified in the present chemical physics effort. The first is aimed at extending the work on polyatomic Raman wavepackets with a more refined set of experiments under jet-cooled conditions. By exciting better-defined multimode vibrational wavepackets, the specific goal of optimizing one motion over another using tailored femtosecond laser pulses will allow us to extend the work on quantum information from simple diatomics to more complex polyatomics with multiple degrees of freedom. The second goal focuses on the development of high harmonic generation as an ultrafast photoionization source. This will play a key role as a probe for tracking the dynamics of such multimode Raman wavepackets by direct single photon ionization from the ground state. In addition, coherent control experiments aimed at manipulating particular branching ratios in polyatomic photodissociation will also utilize the high harmonics as a time-delayed probe of the neutral photofragments.

Accomplishments

A custom modified regenerative amplifier system capable of producing sub 50 femtosecond pulses with a bandwidth of 30 nanometers has been installed in the principal investigator's laboratory. The large bandwidth ensures significant excitation of multiple ground state vibrational modes, which can be manipulated using shaped femtosecond laser pulses. A cost effective approach to pulse manipulation based on a thin film deformable membrane mirror will be used. In addition, a pulsed molecular beam apparatus has been fabricated at the workshops of the University of California, Berkeley, and is currently being used in the studies described. The pulsed molecular beam uses a piezo-pulsed valve similar to ones widely used. The maximum jet cooling that results reduces significantly the number of rotational states in the impulsive excitation and therefore avoids effects such as rotational dephasing. The principal investigator's laboratory was the first to successfully implement high harmonics to perform ultrafast pump-probe vacuum ultraviolet photoelectron experiments. High order harmonic generation is being developed here using a simple approach based on a static cell arrangement. Preliminary data indicate that harmonics up to the 17^{th} have been generated and, at present, efforts are underway to implement these in the detection of both the Raman experiments and also coherent control photodissociation experiments.

Initial experiments under jet-cooled conditions on diatomics such as O_2, N_2, and H_2 have successfully shown that impulsive excitation of rotational states lead to Raman wavepackets exhibiting time dependent rotational alignment. The experiments utilize degenerate four wave mixing (DFWM) techniques to align and probe the Raman wavepacket. These experiments were primarily aimed at addressing issues relating to the laser intensities necessary to generate such Raman wavepackets while avoiding deleterious effects of multiphoton ionization, a common occurrence when using high peak powered lasers such as the system employed in the current setup. The next step currently underway aims to impulsively excite multiple vibrational states in a simple diatomic (Br_2) and to study the extent to which we can control the vibrational wavepacket dynamics using tailored femtosecond laser pulses. While at present the Raman wavepackets are generated and detected using DFWM techniques, we plan to carry out more conventional pump-probe experiments utilizing high harmonics to probe, firstly, the rotational Raman wavepackets and, eventually, the vibrational and multimode vibrational Raman wavepackets.

A novel experiment combining the laser system described in this report together with the synchrotron source was recently set up, aimed at investigating the photodissociation dynamics of CH_2ClBr. The collaborative effort involved Dr. Musa Ahmed and his coworkers at the chemical dynamics beamline, Advanced Light Source. The main focus of the experiments was on controlling the branching ratios of certain product channels in the dissociation by applying tailored femtosecond pump pulses. By probing the dissociated radicals using synchrotron radiation, information pertaining to the mechanistic pathways of the control was sought. Technical issues related to the absolute timing between the almost continuous synchrotron source (500 megahertz) and the femtosecond laser (1 kilohertz) led to difficulties in the data analysis. Measures are currently underway to address such complications and a return to the synchrotron is planned in the near future.

Publications

V.G. Stavros, A. Arrowsmith, and S.R. Leone, "Rotational Raman wavepacket dynamics: laser intensity effects on homodyne vs. heterodyne detection," in preparation (2003).

Photoionization and Photoelectron Spectroscopy of Helium Droplets

Principal Investigators: Daniel Neumark

Project No.: 01011

Project Description

This project will perform photoionization and photoelectron spectroscopy experiments on atoms and molecules adsorbed onto large helium droplets, ~10^4 atoms, in order to understand how these fundamental and well-understood gas phase processes are altered in the environment of a helium droplet. A helium droplet source will be constructed and used on Endstation 3 of the Chemical Dynamics Beamline at the Advanced Light Source (ALS). Photoionization mass spectrometry and photoelectron spectroscopy experiments will be performed using the high-throughput vacuum ultraviolet monochromator on this endstation.

Accomplishments

The photoionization and photoelectron spectroscopy of pure helium nanodroplets, composed of ~10^4 atoms, was measured on the Chemical Dynamics beamline at the ALS. Two types of measurements were performed. The total electron yield was measured as a function of photon energy from 21 to 5 eV. At selected photon energies below the helium ionization potential at 24.6 eV, the photoelectron kinetic energy and angular distribution was measured using photoelectron velocity-map imaging. The photoelectron spectra were remarkable. The average photoelectron kinetic energy was extremely low, on the order of 0.5 meV, and the photoelectron spectra showed no significant dependence on photon energy. These results show that photoionization of helium droplets occurs through a novel mechanism, one in which the photoelectrons are essentially thermalized prior to leaving the droplet.

Publications

D.S. Peterka, A. Lindinger, L. Poisson, M. Ahmed, and D.M. Neumark, "Photoelectron imaging of helium droplets," *Physical Review Letters* **91**, 043401 (2003).

Soft X-ray Spectroscopy of Liquid Surfaces

Principal Investigators: Richard Saykally and David Shuh

Project No.: 03023

Project Description

We propose to further develop and apply the technology of x-ray spectroscopy of liquid microjets for the study of liquid surface chemistry, specifically exploiting the capabilities of the new Molecular Environmental Science (MES) Beamline 11.0.2. Liquid microjets allow the detection and subsequent analysis of electrons and ions induced by core level excitation of a liquid interface which, if combined with the unique optical capabilities of the new MES Beamline, will allow the study of liquid surfaces in unprecedented detail. Our goal is to apply this technique to the study of complex systems encountered in many diverse fields such as heterogeneous chemistry, biology, and environmental chemistry.

X-ray absorption fine structure (XAFS) spectroscopy is a powerful tool for probing the electronic and geometric properties of interfaces. Until recently it has been prohibitive to apply this approach to the study of volatile liquid surfaces (e.g., water) due to the high equilibrium vapor pressure of these liquids (~20 torr), which is incompatible with the ultra high vacuum environment necessary for soft x-ray spectroscopy. By employing liquid microjet technology, we have been able to transcend this technical difficulty and achieve windowless coupling of volatile liquids to the soft x-ray beamlines of the Advanced Light Source. Liquid jets provide unique targets, affording the opportunity to examine liquid surface chemistry with near-edge XAFS and extended-XAFS techniques.

Accomplishments

The primary focus of recent work has been the design, construction, and implementation of a new endstation for spectroscopy on liquid microjets. This versatile endstation was specifically designed to fully exploit the capabilities of the new MES Beamline 11.0.2 while still allowing for windowless coupling to other beamlines such as 8.0.1 and 9.0.1. Very recent experiments using the new endstation have shown that set up and alignment time are dramatically reduced, permitting much more efficient use of allotted beam time.

Recent experimental work using the new endstation has been geared towards beginning to characterize aqueous salt

solutions. Preliminary studies have shown that the addition of a salt (e.g. NaI, NaCl) imparts a significant change in the oxygen *K*-edge near edge x-ray absorption fine structure spectrum (NEXAFS) of the bulk liquid indicating changes in the electronic structure of the water solvent. The degree of this perturbation is highly dependent on the concentration and the salt added, and is much less evident at the surface.

We have also begun to investigate the temperature dependence of the liquid water NEXAFS spectra. Thus far, over a range of ~0 to 20°C no obvious change has been observed in either the bulk or surface water spectrum. This is surprising given the relative sensitivity of the pre-edge feature (1s to 4a1 transition) to the local bonding environment, which is thought to change drastically with temperature. Further investigation too much colder, "supercooled," and warmer temperatures is clearly desirable

Publications

K.R. Wilson, B.S. Rude, J.D. Smith, C.D. Cappa, D.T. Co, R.D. Shaller, M. Larsson, T. Catalano, and R.J. Saykally, "Investigation of volatile liquid surfaces by synchrotron x-ray spectroscopy of liquid microjets," *Review of Scientific Instruments*, accepted for publication.

J.D. Smith, C.D. Cappa, K.R. Wilson, D.T. Co, R.C. Cohen, and R.J. Saykally, "Raman thermometry measurements of evaporation from liquid microjets," in preparation.

Scientific Investigations and Technique Development of Wet Spectroscopy, High Pressure Photoelectron Spectroscopy, and STXM for Molecular Environmental Science

Principal Investigators: David Shuh

Project No.: 02044

Project Description

Three endstations at the Advanced Light Source-Molecular Environmental Science (ALS-MES) beamline are the wet spectroscopy, high pressure photoelectron spectroscopy, and the scanning transmission x-ray microscope (STXM) systems. The external experimental chambers are the soft x-ray endstation for environmental research, the wet spectroscopy surface science system, and the microjet system for the investigation of liquid surfaces. One common experimental theme and capability of all the endstations that we will apply is the ability to perform investigations of interfacial systems in the presence of water or under high pressure gas environments.

Research topics to be investigated are broadly defined in a range of scientific areas that include surface science, materials chemistry, interaction of biomaterials and organics at interfaces, and catalysis. A new potential area for study is the investigation of the interfacial chemistry of manganese oxide materials with several contaminant and gas phase species. Investigation of this materials system will also have substantial impact in the catalysis field. Similarly, there are numerous opportunities to investigate the interfacial chemistry of several gas phase and liquid species, including water and small molecules, at the surfaces of metal oxides and sulfides.

Accomplishments

A key activity has been the development and utilization of the ALS-MES endstations for scientific investigations in conjunction with beamline commissioning. The electron energy analyzer for the wet spectrometer was characterized. A novel mu-metal shield concept was developed and designed for the wet spectroscopy endstation electron spectrometer, and was sent out for fabrication. Several preliminary scientific investigations utilized the capabilities of this endstation. In addition, several external endstations have been successfully interfaced to the ALS-MES beamline for first experiments. The experimental capabilities of the endstations and the beamline, have been developed to support the performance of specific user experiments. Several of the beamline systems have been commissioned and characterized at the same time as the activities with the endstations. This has included the monochromator and overall beamline systems. One special effort involved the detailed characterization and understanding of the performance of the ALS-MES beamline's novel Kirkpatrick-Baesz (K-B) mirror system that provides the micron size photon beam to the spectroscopy branch line endstations.

Investigations of liquids utilizing the existing microjet endstation were performed at beamline 8 of the ALS during two beam runs. The results of these experiments, some of which involved alcohols and ionic solutions, are being prepared for publication. One of the main objectives related to the investigation of liquids with the microjet endstation was to fully re-design the liquid microjet endstation to make it a state-of-the-art instrument with enhanced capabilities. The updated microjet endstation was designed, fabricated, and assembled during this period. Of particular importance was the incorporation of both a stable and adjustable stand framework. As the beam size is similar to the jet dimensions, it enables the endstation to mate to the ALS-

MES beamline where the microjet experiments can take advantage of the small beam size provided by the K-B optics for improved signal to background. Furthermore, the positioning stability and reproducibility have made set-up, as well as the experiments, much more efficient at all ALS beamlines.

There have been several developments, both technical and scientific, pertaining to the ALS-MES scanning transmission x-ray microscope (STXM). A long term technical objective of the community utilizing STXM has been the implementation of chemical reaction cells compatible with the spectromicroscopy technique. In collaboration with an ALS user group, a micro-manufactured STXM cell has been fabricated that has computer controlled gas flow and temperature capabilities. Preliminary tests with the reaction cell have been successful. Several variants of the prototype cell are also being designed for specific experimental applications with the STXM.

One of the fundamental components of atmospheric science that has become increasingly recognized as important is the aerosols and the chemistry of aerosol particles. This is particularly true from an MES perspective. ALS-MES STXM spectromicroscopy is ideally suited to address aerosol (and larger airborne particulates) science since the length scales are the same (spatial resolution) and spectroscopic information can be obtained, both in a manner frequently less intrusive than transmission electron microscopy. The requisite STXM experimental methodologies and procedures to handle aerosols in a non-perturbing manner are being developed and put into place. This is being done at the ALS-MES STXM in conjunction with beamline 5.3.2 polymer STXM so that the community investigating atmospheric aerosol science can utilize both STXMs. Although the establishment of experimental protocols dovetailing with those currently used and accepted in aerosol research is essential, the most critical aspect is the establishment of the scientific background and baselines for aerosol studies. The science of carbon aerosols were chosen as a starting point for STXM aerosol investigations because carbonaceous particles are of interest for several MES reasons and is an active field in aerosol research, plus there is fair knowledge of selected carbon species from polymer STXM investigations. Experiments have been initiated with carbon aerosols at the two ALS STXMs, as well as a systematic experimental cataloging of relevant carbon materials. An STXM reaction cell, as mentioned above, is being designed to examine gas phase chemical reactions with carbon aerosols.

Publications

T. Warwick, N. Andresen, J. Comins, A. Franck, M. Gilles, T. Tonnessen, and T. Tyliszczak, "Large aperture micro-focus KB mirrors for spectroscopy experiments at the Advanced Light Source," *Proceedings of Synchrotron Radiation Instrumentation 2003*, American Institute of Physics (August 2003) in press.

T. Warwick, H. Ade, A.L.D. Kilcoyne, S. Fakra, M.K. Gilles, A. Hitchcock, D. K. Shuh, and T. Tyliszczak, "Further development of soft x-ray scanning microscopy with an elliptical undulator at the Advanced Light Source," *Synchrotron Radiation News* **16**, 22-27 (2003).

Presentations

T. Warwick, N. Andresen, J. Comins, A Franck, M. Gilles, T. Tonnessen, and T. Tyliszczak, "Large aperture micro-focus KB mirrors for spectroscopy experiments at the Advanced Light Source," Synchrotron Radiation Instrumentation 2003, San Francisco, California, August 25–29, 2003.

N. Andresen, M. Coleman, J. Comins, M. Decool, S. Fakra, M. K. Gilles, E. Hebenstreit, D. Kilcoyne, S. Marks, D. MacGill, J. P. McKean, D. F. Ogletree, K. Rex, M. Salmeron, D. K. Shuh, T. Stevens, T. Tyliszczak, T. Warwick, and R. Wiedenbach, "First results from the Molecular Environmental Science Beamline 11.0.2 at the Advanced Light Source," American Chemical Society National Meeting, New Orleans, Louisiana, March 23–27, 2003.

N. Andresen, M. Coleman, J. Comins, M. Decool, S. Fakra, N. Hebenstreit, M. Gilles, S. Marks, D. MacGill, P. McKean, F. Ogletree, K. Rex, M. Salmeron, D. Shuh, T. Stevens, T. Tyliszczak, T. Warwick, and R. Weidenbach, "Advanced Light Source Molecular Environmental Science Beamline 11.0.2," Poster presentation, Advanced Light Source Users Meeting, Berkeley, California, October 10–12, 2002.

Computing Sciences

(National Energy Research Scientific Computing Center, Computational Research, and Information Technologies and Services Divisions)

Experimental Mathematician's Toolkit

Principal Investigators: David Bailey and Xiaoye Li

Project No.: 02012

Project Description

This project will develop a "toolkit" for doing experimental mathematics. This capability, which will be hosted at the National Energy Research Scientific Computing (NERSC) Center, will enable a much broader range of mathematicians, physicists, and other researchers to utilize these emerging tools. This toolkit will be developed in collaboration with researchers at Simon Fraser University in Canada. During the past years, numerous computer programs for computational mathematics have been developed by the principal investigator and others. These include facilities for high-precision arithmetic, integer relation detection, high-precision numerical quadrature, and automatic constant recognition. These programs however require specialized expertise to use, including expertise in Fortran-90, C++, message passing interface (MPI) parallel programming, and numerical analysis. We will polish some of the prototype software now available, so that they are much more robust and do not require highly technical adjustments to obtain meaningful results. We will then encapsulate these programs into a highly usable interface, hosted on NERSC Center computers, accessible via the world wide web.

Accomplishments

Several enhancements and bug fixes have been made to the Experimental Mathematician's Toolkit during the past year. Now the user can control not only the numeric precision level (from 30 to 1000 decimal digit accuracy) but also parameters such as the level parameter for "PSLQ" integer relation searches and the type of numeric quadrature. Real and complex polynomial roots can now be calculated, as well as combinatorial functions such as the factorial and binomial coefficients.

Numerical integration (i.e., quadrature) has been improved. Recently for example, the Toolkit was used to compute the integral of the function Log[t^2 + 1] * Log[(t^2+1)/2]/(t–1) from 0 to 1 (here * denotes multiplication and ^ denotes exponentiation). This led to the identification of this numerical value as a concise mathematical expression.

Last year we reported a significant mathematical breakthrough: The existence of "BBP-type" formulas, which have been discovered through earlier versions of the Experimental Mathematician's Toolkit, has deep implications for the age-old question of whether the binary digits of pi and some other mathematical constants are "normal" (i.e., random in a certain precise statistical sense). In particular, the question of whether pi is normal has been reduced to a simple conjecture regarding certain chaotic pseudorandom sequences that have been studied in computer science.

This year we published a paper that actually proved normality, not for pi, but for another mathematical constant given by a simple infinite series (in fact an infinite family of such constants). This result vastly extends the number of known "normal" constants, and, more importantly, validates our approach as a likely way to finally resolve questions such as the normality of pi. In a related study, the principal investigator, together with three other researchers (see publication list) established some results on the number of ones in the binary digits of "algebraic" numbers, namely those numbers (such as the square root of two or the golden ratio) that are roots of algebraic equations with integer coefficients.

The Experimental Mathematician's Toolkit (in particular the MPFUN-90 and ARPREC high-precision arithmetic packages) was also used by the principal investigator and Alexi Frolov of Queen's University in Canada to perform some key computations in four-body problems that arise in nuclear and atomic physics. These computations cannot be done using ordinary computer arithmetic, because the numerical errors that arise render the results meaningless. With our high-precision arithmetic, however, such calculations can be done to produce reliable results.

Perhaps the most notable achievement during the past year has been the completion of a two-volume work on experimental mathematics, the first of its kind, co-authored by the principal investigator. The first volume will be out by November 2003, and the second by February 2004:

- Volume 1: *Mathematics By Experiment: Plausible Reasoning in the 21st Century*. This book presents the

rationale and historical context of experimental mathematics, and includes a series of examples that best portray the experimental methodology, together with some of the numerical techniques used in this research. Numerous historical and biographical notes are also included.

- Volume 2: *Experimentation in Mathematics: Computational Paths to Discovery*. This book gives numerous additional case studies of experimental mathematics in action, ranging from sequences, series, products, integrals, Fourier series, zeta functions, partitions, primes, and polynomials. Some advanced numerical techniques are also presented.

A 75-page "reader's digest" condensation of these books is freely available at the following website, which has been established to support these two books: http://www.expmath.info. This website also includes numerous links to valuable web-based resources, both software and online tools, relevant to computer-based and experimental mathematics.

Publications

Books

J.M. Borwein and D.H. Bailey, *Mathematics by experiment: plausible reasoning in the 21st century*, AK Peters, Ltd., Natick, Massachusetts (November 2003).

J.M. Borwein, D.H Bailey and R. Girgensohn, *Experimentation in mathematics: computational paths to discovery*, AK Peters, Ltd., Natick, Massachusetts, (February 2004).

Articles

D.H. Bailey, Y. Hida, X.S. Li and B. Thompson, "ARPREC: An arbitrary precision computation package," manuscript (September 2002) LBNL-53651, available at http://crd.lbl.gov/~dhbailey/dhbpapers/arprec.pdf.

D.H. Bailey and X.S. Li, "A comparison of three high-precision quadrature schemes." *Proceedings of the Real Numbers and Computing Conference*, Lyon, France (September 2003) LBNL-53652, available at http://crd.lbl.gov/~dhbailey/dhbpapers/quadrature.pdf.

D.H. Bailey, J.M. Borwein, R.E. Crandall, and C. Pomerance, "On the binary expansions of algebraic numbers," to appear in *Journal of Number Theory Bordeaux* (2003) LBNL-53654, available at http://crd.lbl.gov/~dhbailey/dhbpapers/algebraic.pdf.

A.M. Frolov and D.H. Bailey, "Highly accurate evaluation of the few-body auxiliary functions and four-body integrals," *Journal of Physics B: Atomic, Molecular and Optical Physics*, vol. 36 (2003), pg. 1857–1867; LBNL-53657, available at http://crd.lbl.gov/~dhbailey/dhbpapers/frolov-dhb2.pdf.

D.H. Bailey, "A hot-spot proof of normality for the alpha constants," manuscript (March 2003) LBNL-53658, available at http://crd.lbl.gov/~dhbailey/dhbpapers/alpha-normal.pdf.

D.H. Bailey and D.J. Rudolph, "A strong hot spot theorem," manuscript (May 2003) LBNL-53656, available at http://crd.lbl.gov/~dhbailey/dhbpapers/hotspot.pdf.

Nonlinear Mathematical Models of Phenomena Related to Petroleum Mining and Geological Engineering

Principal Investigators: Grigory Barenblatt
Co-Investigators: Tadeusz Patzek, V.M. Prostokishin, and Dmitriy Silin

Project No.: 01012

Project Description

The purpose of this project is to study mathematical models of the flow of complex fluids in complicated collectors. This study can be of importance for evaluating the safety and reliability of proposed nuclear waste disposal schemes. More specifically, we will study of the fluid flows in diatomite rocks forming collectors of basic oil fields in California (Lost Hills, Belridge). A set of asymptotic and numerical methods will be used for solving the equations of non-equilibrium two-phase flows in porous and fissurized-porous media and damage accumulation in aggressive environments and fissurized rocks.

Accomplishments

First, we obtained the analytic solutions of the problem of diffusion of carbon dioxide in a gas-filled porous medium with immovable water. The solutions are of fundamental importance for the quantitative evaluation of subsurface sequestration of this greenhouse gas, for calculation of oil recovery by carbon dioxide flooding and underground gas storage. The obtained solutions can be of direct use, and can also be used as the etalons for complex numerical investigations of the processes under more complicated conditions. The paper was published in the journal *Transport in Porous Media*.

Second, we have presented a definitive formulation of the theory of non-equilibrium water-oil displacement, which is

of fundamental importance for the quantitative analysis for development projects of oil deposits. The nonequilibrium effects play a decisive role in the capillary imbibition and the formation of the water-oil displacement front, basic processes involved in the development of oil deposits. The paper will be published in the *Journal of the Society of Petroleum Engineers* in December 2003.

Third, we performed important steps in evaluating the effects related to saturation dependence of the time of displacement—the basic parameter characterizing the non-equilibrium water-oil displacement. The results are presented in the paper which is accepted for publication in the journal *Transport in Porous Media.*

Fourth, we investigated the applicability of the widely used Kardar-Parisi-Zhang (KPZ) equation for modeling the motion of the water-air interface, and came to the conclusion that this model is inadequate. A preliminary draft of the paper is now ready; we would like to perform some additional studies.

Fifth, we constructed the mathematical model of the fluid flows in the process of development of oil deposits in the diatomaceous rocks, which are characteristic of basic Californian oil deposits. This model led us to a fundamentally new free-boundary problem for a system of non-linear equations. This mathematical problem was investigated by Italian mathematicians M. Bertsch, University of Rome, and R. Dal Passo, Institute of Applied Analysis, who also took part in this study. A computational investigation of this system was also performed. The preliminary version of the paper was published, and now we are preparing more detailed papers; the Italian mathematicians will also participate in this investigation.

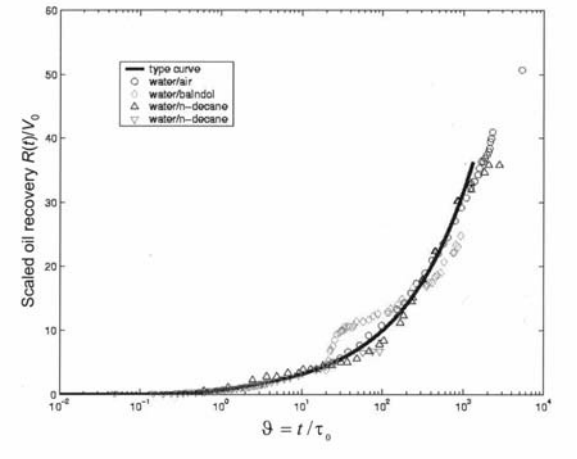

Figure 1. Matching countercurrent imbibition oil recovery. The time scale is t/τ, where τ is the estimated redistribution time.

Publications

T.W. Patzek, D.B. Silin, S.M. Benson, and G.I. Barenblatt, "On vertical diffusion of gases in a horizontal reservoir," *Transport in Porous Media*, **51** (2003), 141-156.

G.I. Barenblatt, T. Patzek, and D.B. Silin, "The mathematical model of non-equilibrium effects in water-oil displacement," *SPE Journal* (December 2003) LBNL-49484.

D.B. Silin and T.W. Patzek, "On the Barenblatt Model of spontaneous countercurrent imbibition," to appear in *Transport in Porous Media* (2004), LBNL-51373.

G.I. Barenblatt, T.W. Patzek, V.M. Prostokishin, and D.B. Silin, "Oil deposits in diatomites: a new challenge for subterranean mechanics," *SPE 75230, 13th Society of Petroleum Engineers/Department of Energy Symposium on Improved Oil Recovery*, Tulsa, Oklahoma April 2002, LBNL-49509.

T.W. Patzek, D.B. Silin, and G.I. Barenblatt, "Impact of rock micro- and macro-structure on the behavior of large waterfloods," *22nd Energy Information Agency Workshop*, Vienna, Austria, September 2001, LBNL-48859.

GI. Barenblatt, "A model of non-local damage accumulation," *Physical Mesomechanics,* **6** (2003), 79-84.

Infrastructure for Improving Protein Structure Prediction in Computational Biology

Principal Investigators: Silvia Crivelli and E. Wes Bethel

Project No.: 02013

Project Description

This project is to create a software-based environment for improving protein structure prediction in computational biology. The environment consists of high-performance protein structure optimization code coupled with discipline-centric visualization and human interface technology. We will enhance an existing computational code developed at Berkeley Lab by creating a visualization software tool that makes it possible to generate a better set of initial conditions for the optimization and solver code, as well as to better understand the results and analyze different energy functions. Successful completion of the proposed work will result in: (1) a high-performance code for computing the

tertiary structure of a protein; (2) a visual front end that can be used to create an initial condition for the optimization code with a graphical user interface (GUI) for human specification of biologically plausible initial configurations; (3) visual display of computed energy and locally minimized energy of a protein.

Our effort focuses on four primary areas: (1) making improvements to the computational engine that performs global energy optimization; (2) increasing the throughput of the local minimizations by parallelization of the local minimization algorithm and parallelization of the energy evaluation functions; (3) performing development of a visual front-end software tool that is used for display of geometry and energy of tertiary structures; (4) coupling these software components and deploying them in a way that promotes ease-of-use, and leveraging existing computational resources at the National Energy Research Scientific Computing (NERSC) Center.

Our first-year effort focused on the design of a software infrastructure for improving the efficiency of the setup phase and dealing with complex structures. We have created a visual tool to quickly generate and directly manipulate protein structures. The tool forms α-helices and β-strands, which are based on ideal geometric definitions of the two types of local secondary structure, and then manipulates those structures to form tertiary structure. Interactive display of the energy value associated with the structure guides the selection of the best configurations for the next phase.

Accomplishments

The stochastic perturbation method for protein structure prediction developed by a group of researchers at Berkeley Lab and the University of Colorado is a physics-based method that uses secondary but not tertiary structure information from known proteins to construct the predictions. It is composed of two phases. Phase 1 generates good starting structures, which are low-energy local minima. Phase 2 improves upon the starting structures using both global and local minimizations. Originally, Phase 1 generated the starting structures through local minimizations with soft constraints. Because a typical protein has thousands of atoms, these local minimizations took hours or even weeks to converge. During our first two years of this effort, we have developed ProteinShop, an interactive visualization tool for protein manipulation with the goal of streamlining the process of creating initial protein configurations. ProteinShop uses a combination of a buildup procedure that creates protein structures by adding one amino acid at a time and an inverse kinematics procedure that allows users to naturally manipulate those structures. ProteinShop allows us to generate a variety of configurations at a much greater rate than before. Most importantly, ProteinShop allows us to add human knowledge and intuition to the protein structure prediction process, bypassing those bad configurations that would otherwise be fruitless for optimization, thereby saving compute cycles and accelerating the process of finding a solution. Consequently, we can attempt to solve much larger problems than before. Structures created with ProteinShop still need to be minimized to be used as initial configurations for Phase 2. Because these configurations contained secondary structure already formed, and because the manipulations are guided by an energy function, the number of iterations needed to converge is significantly smaller. ProteinShop has been well received by the protein folding community. We released its binary code in May 2003 to academic and non-profit organizations. There have been hundreds of downloads from all over the world. Recently, our paper "Interactive Protein Manipulation," won the Best Application Award at the Institute of Electrical and Electronics Engineers (IEEE) Visualization 2003 Conference.

Although the stochastic perturbation method for protein structure prediction has the potential to find new folds, it is also extremely expensive. Therefore, we are developing a new knowledge-based method as a less expensive alternative when there are homologous proteins in the protein databases. Because in most cases only fragments of the proteins are similar, our new method combines the use of knowledge about secondary structure with the use of homologous fragments obtained from fold recognition servers and the stochastic perturbation method for those parts of the protein for which no homology is found. Unlike the original stochastic perturbation method, the new method creates initial configurations containing some correct tertiary structure. We have begun testing our new method on a target that is in the borderline between the fold recognition and new folds categories.

Phase 2 of our method improves the initial configurations through global minimizations in subspaces of the dihedral angles predicted to be coil according to the secondary structure predictions used in Phase 1. Thus, the large-scale global optimization problem is solved as a series of small-dimensional ones. The algorithm selects a set of local minimizers from a list of local minima and random subsets of dihedral angles and performs small-scale global optimizations in parallel on those subsets using the selected angles as variables while keeping the remaining ones temporarily fixed at their current values. These computations take weeks or even months to converge using hundreds of processors on Seaborg. Thus, an important goal is to reduce the computational cost associated with Phase 2. To that end, we have started using a ProteinShop feature that allows us to monitor and steer the protein structure prediction process. We are using this feature to evaluate new heuristics for selecting dihedral angles that will replace the current random selection.

Currently, we are in the process of coupling ProteinShop with a local energy minimization code in order to achieve low-energy initial configurations. We found some anomalies in the minimization code that used a large number of unnecessary iterations. Ricardo Oliva, from Juan Meza's group worked on a new, faster version of the local minimization code that is based on OPT++, an object-oriented nonlinear optimization library developed by Meza and colleagues. Because the local minimization method used takes hours to converge for a moderate-sized protein, we have been exploring new ways to substantially reduce this time. Thus, we have implemented an approach that decomposes the protein into smaller pieces and performs optimization on those pieces in parallel.

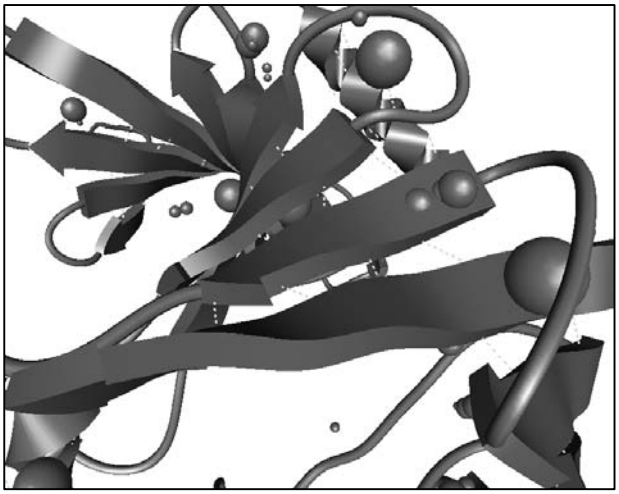

Figure 2. Atom collision and hydrogen bond rendering in ProteinShop.

Publications

O. Kreylos, N. Max, B. Hamann, S. Crivelli, and W. Bethel, "Interactive Protein Manipulation," *Proceedings of the IEEE Visualization 2003 Conference*, LBNL-52414 (March 2003).

S. Crivelli, O. Kreylos, N. Max, B. Hamann, and W. Bethel, "ProteinShop: a tool for interactive protein manipulation and steering," accepted for publication in *Journal of Computer-Aided Molecular Design*, LBNL-53731 (September 2003).

R. Oliva and S. Crivelli, "An object-oriented library for molecular dynamics energy computations," LBNL-53778 (September 2003).

New Machine Learning and Data Mining Methods for Genomics and Information Retrieval

Principal Investigators: Chris Ding

Project No.: 02014

Project Description

We propose to continue to develop new machine learning and data mining methods for discovering patterns in large datasets. The target application areas are analysis of gene expression microarray data and information retrieval.

Two areas of machine learning methods are the focus of this research. First is the feature selection, marker gene selection, for classification/prediction problems. Feature selection improves the prediction accuracy of a classifier. By finding the features most useful to characterize the problem at hand also provides insights to the problem. This problem is of immediate concern in gene expression analysis because of the large number of genes, ~5000, in a typical experiment.

Second is continuing development of the spectral graph partitioning method for data clustering, which has been shown to be effective and competitive in comparison with other leading cluster methods. The new developments will focus on extension to contingency tables, gene expression data belong to this category, and also multi-way, more than two clusters, clustering problems.

Accomplishments

How to select a small subset, marker genes, out of the thousands of genes in microarray data is important for accurate classification of phenotypes. Widely used methods typically rank genes according to their differential expressions among phenotypes and pick the top-ranked genes. Feature sets so obtained have certain redundancy and study methods to minimize it. We proposed and evaluated a minimum redundancy-maximum relevance (MRMR) feature selection framework. Genes selected via MRMR provide a more balanced coverage of the space and capture broader characteristics of phenotypes. They lead to significantly improved class predictions in extensive experiments on five gene expression data sets: NCI, Lymphoma, Lung, Leukemia and Colon. Improvements are observed consistently among four classification methods: Naïve Bayes, linear discriminant analysis, logistic regression, and support vector machines. Our marker gene selection work using an unsupervised method work using an

supervised method that does not rely on prior knowledge is published in *Bioinformatics*.

We further developed the cluster analysis framework based on scaled principal components, spectral method. The key self-aggregation feature, i.e., members of the same cluster aggregate automatically, are extended to interdependence relations between rows (genes) and columns (tissue samples) of the same data matrix (gene expressions), which can be viewed as a contingency table and represented by a bipartite graph. The new features are the three self-aggregation networks, describing the row-column, row-row, and column-column relationships, i.e., the genes self-aggregate while tissue samples aggregate at the same time. Theoretical analysis based on perturbation analysis is carried out and closed-form perturbation results are obtained.

The MinMaxCut spectral clustering method is completed via systematically generalized to multi-way clustering, with new results in cluster balance analysis, the upper-bound for the optimal clustering objective function value, which help to assess the quality of clustering results, and cluster selection methods for practical divisive hierarchical clustering. Application to Internet newsgroups demonstrates the method can clearly identify/separate both unrelated topics and related topics such as articles belonging to computer graphics, window operating systems, and electronics. We found that the key factor affecting performance is cluster balance during divisive process, and average-similarity based cluster selection is most effective because of its cluster balancing effect.

Publications

C. Ding, "Unsupervised feature selection via two-way ordering in gene expression analysis," *Bioinformatics* **19** 1259–1266 (2003).

C. Ding and H. Pang, "Minimum redundancy feature selection for gene expression data," *Proceedings of IEEE Computer Society Bioinformatics Conference,* 523–529 (August 2003) Stanford, California, LBNL-51985.

C. Ding, "Document retrieval and clustering: from principal component analysis to self-aggregation Networks," *Proceedings 9th International Workshop on Artificial Intelligence and Statistics*, January 2003, Key West, Florida, editors: C.M. Bishop and B.J. Frey.

C. Ding, "Data clustering: principal component analysis, hopfield and self-aggregation networks," *Proceedings of 16th International Joint Conference on Artificial Intelligence* (August 2003).

C. Ding, X. He, H. Zha, M. Gu, and H.D. Simon, "A MinMaxCut spectral method for data clustering and graph partitioning," LBNL-54111, submitted for publication.

Numerical Simulation of Fuel Cells

Principal Investigators: Joseph Grcar

Project No.: 02015

Project Description

The purpose of this project is to study the mathematical issues that arise in combining the most accurate models of fuel cell components and materials into a comprehensive, highly accurate computer simulation capability. The goal is to develop numerical algorithms, which will bring the state-of-the-art in fuel cell simulation to high fidelity, in order to support more detailed fundamental studies of fuel cells for scientific or engineering design purposes.

The approach is to decompose the complex electro- and thermochemical system represented by a fuel cell into its constituent physical phenomena, and then to select or develop the numerical methods that are best suited to each component and to its interaction with the other components. This will result in simulation algorithms that are highly accurate, efficient, and yet robust with respect to extreme or unusual combinations of conditions in underlying physical models.

Accomplishments

Following are general results and observations made during this project.

The work has been devoted to acquiring an understanding of the range of physical models that have been developed to simulate fuel cells. Solid oxide cells were the original focus because of their relative simplicity when compared to other fuel cell technologies. This year polymer electric fuel cells were also considered, which introduce the complexity of a hydrated membrane. Fuel cell models are an ideal example of the need for multi-scale, multi-physics computer simulations. For example, transport of reactants occurs in fluid channels and porous media, but reactions are confined to thin, catalytic layers. Both the large and fine scales are coupled: heat and electric current are produced on the fine scale, but the geometric complexity of the cell stack and fuel channels impacts production through the distribution of reactants, which may cause the local cell to operate at other than optimal temperatures or potentials.

Fuel cell models can be grouped into three types: thin film models, resistor-network models, and porous electrode models. The simplest, the thin-film models, are essentially phenomenological and treat the cell stack as circuit elements. The second, network models, add spatial parameterizations to the properties of the thin film models,

and represent the physical arrangement of the device's components through interconnected networks of simpler models. The third type of simulation, describes the cell's operation in terms of macroscopic conservation laws in the flow channels and porous membranes. The transport of reactants is modeled through the use of effective transport coefficients that take into account the volume fractions and tortuosities of the flow paths through the material. These parameters can be estimated; the chemical kinetics of many fuels are well known. As a result, these comprehensive models are the most suitable for future algorithm development.

A survey of the literature finds that computer simulations of fuel cells using comprehensive models fall into two categories: (1) one-dimensional and steady state and (2) higher dimensional and transient. The former models are of a single membrane-electrode assembly and are used either to trace current-voltage (I-V) curves under different operating conditions, or to infer parameters for the electrochemistry submodels. Parameter estimation, essentially by solving inverse problems, is crucial to model building in lieu of *in-situ* diagnostics, which are difficult to obtain because of limited access to the components of an operating cell. The higher dimensional models are necessarily transient because time-marching algorithms suggest economical splitting algorithms that allow the various physical submodels to be treated independently. Often these methods are of doubtful time accuracy, because very small time steps may be needed to faithfully reproduce dynamic behavior. The purpose of transient simulations may be simply to approach a steady state or to examine genuinely transient behavior such as start/stop transients and load changes. Two-dimensional models are either transverse or parallel to fuel channels. The three-dimensional models may be obtained by linking one- or two-dimensional components that follow flow or current paths.

At the present time it is difficult to assemble predictive models because of the incomplete understanding of many submodels. Most models focus on using hydrogen fuel in part because of uncertainty concerning catalytic reaction processes for hydrocarbons. Moreover, electrochemical processes may not be sufficiently well known in terms of the precise functional relationships needed for computer simulations. Charge-transfer reactions, described by the Butler-Volmer equation, must overcome both the thermal energy barrier of conventional reactions and an electric potential. The exchange current density term is often treated as a constant; its true value likely depends on operating conditions such as the composition of reactants and products in the reactive layer of the electrode. The primary use for comprehensive fuel cell simulations may be to examine properties of the submodels needed for predictive engineering simulations.

Publications

J. F. Grcar, "Multiscale and multiphysics numerical models of fuel cells," in preparation.

Interactive Visualization Methods for Exploration and Comparison of Multi-billion Base Pair Sequence Data

Principal Investigators: Bernd Hamann

Project No.: 03012

Project Description

This project will design and implement new visualization techniques to analyze gene sequence data. As more and more sequence data become available, and we compare massive amounts of gene sequence data from multiple species against each other, we need more powerful tools. Of specific scientific interest are those regions in sequence data that do not seem to code for genes. The function of these regions is largely unknown, but it is suspected that they may still play a role in controlling crucial processes. To interactively explore massive, i.e., multi-billion base pair data, we need more powerful visualization techniques supporting the simultaneous comparative analysis of two, and even more, sequence data sets.

A major problem faced when interactively analyzing or comparing massive amounts of sequence data is scale. Currently used line plots display a measure of sequence similarity by highly condensing large stretches of sequence regions, hundreds to thousands of base pairs, into an area of merely one millimeter width. We propose to develop innovative multi-resolution methods that will enable a scientist to visualize selected areas in sequence data at arbitrary levels of resolution—and define statistical metrics used to perform similarity analysis of aligned sequence stretches. Interactive exploration is central to this effort. A user will be able to fully control all parameters: local area(s) of interest, level of resolution, specification of metrics used to measure sequence similarity, etc.

Accomplishments

In the first year, we have developed an interactive visualization tool called "Phylo-VISTA" (short for Phylogenetic–Visualization tools for Alignment). The tool allows scientists to visually compare multi-species sequence data by using a phylogenetic tree as a guide for displaying the degree of conservation across species. The phylogenetic

relationship among species is important for building and analyzing multiple alignments; thus, visualizing sequence alignment data while taking phylogenetic trees into account presents a significant advance. Additional features of the tool include the possibility of using different resolutions for examining alignment data, and the ability to easily compare any subtree of a specific phylogenetic tree of all sequences used in an alignment dataset.

Phylo-VISTA supports interactive visual analysis of pre-aligned multi-species sequences by performing the following functions: (1) display of multiple alignments with the associated phylogenetic tree; (2) computing a measure of similarity over a user-specified window, defining a fixed number of base pairs, for arbitrarily-aligned subtrees in a phylogenetic tree; (3) visualizing the degree of sequence conservation among species by a line plot; and (4) presenting comparative data together with annotation data.

We used the successful VISTA concept as the basis for the visualization of multiple alignments along with an associated phylogenetic tree. For pairwise comparison, VISTA requires a user to select one of the sequences as abase sequence. To create a VISTA plot a fixed-sized window is moved across the alignment and the percent-identity between the base sequence and the aligned sequence is calculated in this window. The x-axis represents the base sequence, and the y-axis represents percent-identity. The alignment data is projected on the base sequence, and annotations are also presented in the plots. VISTA displays the size and location of gaps in the aligned sequence. Loss of information about the gaps in the base sequence and corresponding data of other sequences results by using one sequence as the base. For multiple alignment, VISTA produces plots for each sequence against the base sequence. One of the main limitations of such multiple-pairwise plots is that it is designed only to detect regions that are conserved in the base sequence; therefore, Phylo-VISTA uses the entire multiple alignment as a base. As a result, Phylo-VISTA is also capable of displaying location and length of gaps in all sequences. In addition, Phylo-VISTA provides annotations beyond those associated with a single base sequence. Multi-species plots allow a user to analyze desirable features in a single visualization.

For Phylo-VISTA, a similarity measure different from the one used in VISTA was developed, to make possible the comparison of more than two sequences. Currently, we use a sum of weighted pairwise similarity measures for this purpose, and we plan to consider and implement more advanced similarity measures as well.

Phylo-VISTA provides more biological information than other multi-pairwise alignment visualization tools since it allows comparison of a level of conservation among several species originated from the same internal node of the tree, not just a comparison with a reference sequence. Navigating through the phylogenetic tree allows easy identification of regions conserved among subsets of sequences within a multiple alignment. This ability to identify subclass-specific regions can highlight prime candidates for functional analysis to study differences in gene regulation among a wide range of species. (Phylo-Vista has been implemented as a Java applet that is available online.) Biologists closely collaborating with us on this effort have contributed substantially to the overall quality of the tool; they have been able to use Phylo-VISTA to verify facts concerning specific data sets.

Publications

N Shah, O. Couronne, L.A. Pennacchio, M. Brudno, S. Batzoglou, E.W. Bethel, E.M. Rubin, B. Hamann, and I. Dubchak, “Phylo-VISTA: interactive visualization of DNA multiple alignments,” to appear in *Bioinformatics*, LBNL-54135 (2003) http://www-gsd.lbl.gov/phylovista/.

N. Shah, O. Couronne, L.A. Pennacchio, M. Brudno, S. Batzoglou, E.W. Bethel, E.M. Rubin, B. Hamann and I. Dubchak, “Interactive visualization of multiple aligned DNA sequences,” *Proceedings of the 2003 UC Davis Student Workshop on Computing*, TR CSE-2003-24, 10-11, LBNL-54136 (2003).

Phylo-VISTA is available at http://www-gsd.lbl.gov/phylovista. It requires an Internet browser with Java Plug-in 1.4.2 and it is integrated into the global alignment program LAGAN at http://lagan.stanford.edu.

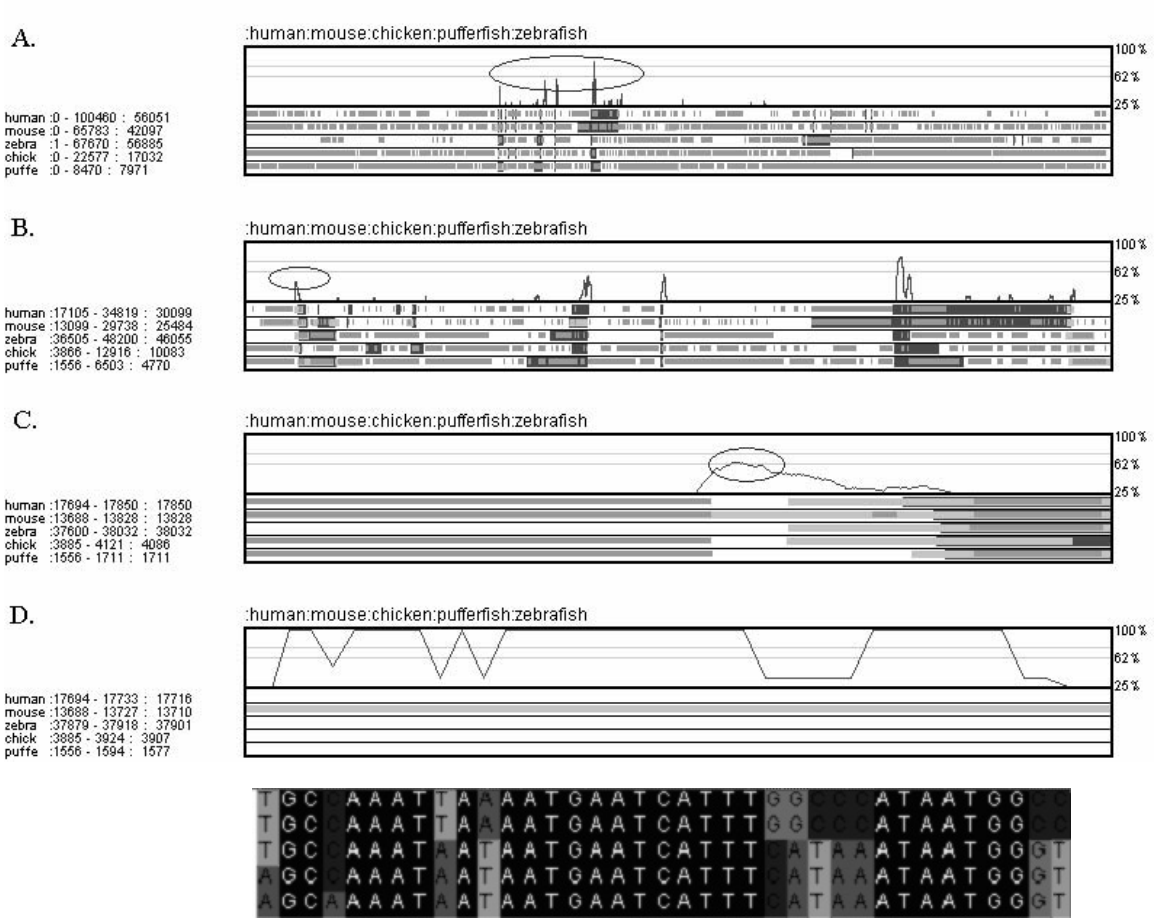

Figure 3. Multiresolution visualization of a multiple-alignment data set consisting of human, mouse, chicken, pufferfish, and zebrafish stem cell leukemia region.

Segmentation of Mammary Ductal Structure Using Geometric Methods

Principal Investigators: Ravi Malladi

Project No.: 02017

Project Description

The goal of this project is to develop image analysis algorithms for automatically detecting, segmenting, and visualizing three-dimensional tissue structure from a series of two-dimensional histological sections. This requires highly optimized segmentation algorithms, able to perform massive computations in a short period of time. Such a unique capability will have a tremendous impact in the scientific community, opening a new avenue for adding the morphological parameter to the already existing molecular and cellular investigation. We aim to use the geometric partial differential equation (PDE) methods and the level set framework to build schemes both for image registration and for segmentation of mammary gland and ductal structures

Accomplishments

The chief accomplishments are as follows:

- We have completed the task of packaging the image analysis tools into a user-friendly format. We built a visualization tool kit (VTK) based visualization framework that works in tandem with our image denoising and segmentation PDE solvers. This has been built to operate on both Red Hat Linux and Solaris platforms. We have added some new functionality to this suite of tools, namely path extraction and fly-through mechanisms.
- On the algorithms front, we have worked on and added an image pre-processing filter that has the ability to

enhance locally tubular structures, thereby increasing the accuracy of ductal structures. This is especially useful when the original slice image is noise corrupted.

- Once the global branching ductal structure is extracted, we added algorithms that can compute the shortest path between two points inside the duct. This is helpful for inspection and subsequent re-acquisition of data at the cellular resolution.

As mentioned in our previous report, we submitted a R21/R33 grant proposal to the National Institute for Biomedical Imaging and Bioengineering (NIBIB) and received a fundable score.

Publications

R.F. Gonzales, U. Adiga, A. Idica, T. Deschams, R. Malladi, and C.O. Solorzano, "Automatic segmentation of structures in normal and neoplastic mammary gland tissue sections," *Proceedings of The International Society for Optical Engineering (SPIE)* **4964** (January 2003).

R.F. Gonzales, A. Idica, T. Deschams, R. Malladi, and C.O. Solorzano, "Automatic segmentation of histological structures in mammary gland tissue sections," to appear in the *Journal of Biomedical Optics*, special issue on Woman's Health (2004).

Parallel Methods for Robust Optimization and Uncertainty Quantification

Principal Investigators: Juan Meza

Project No.: 02045

Project Description

Optimization of functions derived from the modeling and simulation of some physical process constitutes an important class of problems in many scientific applications. For these types of problems, the function evaluation is computationally expensive and dominates the total cost of the optimization problem. It is desirable that the optimal solution be robust in the sense that small changes in the model parameters or data do not generate large perturbations in the optimal solution. This research will focus on two major areas: (1) the development of parallel algorithms for robust optimization under uncertainty and (2) the development of parallel methods for uncertainty quantification in simulation models.

We propose to focus on new methods that combine the parallel direct search method and the trust-region method into a new class of algorithms called Trust-Region Parallel Direct Search (TRPDS), which takes advantage of the best properties of both algorithms. TRPDS has been shown to have rapid convergence rates typical of Newton-type methods while gaining the advantage of parallelism inherent in the parallel direct search methods. This research will extend that earlier work to increase the robustness of TRPDS through the use of interior point methods. We also propose to investigate the use of filter methods for nonlinear constraints in the setting of interior point methods. As part of the uncertainty quantification problem, we will also develop methods for model reduction and surrogate functions.

Accomplishments

Our efforts this year were concentrated on the development of new algorithmic capabilities and the application of these algorithms to new problems. A major development was an implementation of a Limited-Memory BFGS (LBFGS) algorithm for solving large-scale unconstrained optimization problems. We tested the LBFGS algorithm with all of the unconstrained test problems in the Schittkowski collection. In addition, we applied the algorithm on an energy minimization problem for a large protein (over 3000 atoms). Our implementation of LBFGS proved more robust than the code previously used by the ProteinShop team, and is now the algorithm of choice for local-minimization during protein structure prediction. As part of our collaborations with the ProteinShop team, we also developed an object-oriented library for molecular dynamics energy computations. The first energy model we implemented was the AMBER energy model from which others can be derived in an object-oriented manner. This library allows us to easily interface OPT++ with protein-folding applications such as ProteinShop, in addition to facilitating the development of new energy models.

Another major development was the implementation of a direct search method known as a generating set search (GSS) algorithm. We used several generating bases to obtain different types of direct search algorithms: compass search, box-search, and minimal-basis search. We also extended the generating set classes to include pruning of search directions, and used these classes to implement gradient-pruned direct search algorithms, called GSS1, that take advantage of first derivatives to guide the optimization process. We are currently working on developing a parallel version of the generating set search methods, which is the next step towards developing the TRGSS method. In addition, we are working on developing problem specific generating-set bases for the protein-energy minimization problem. Recent test results suggest that search directions that couple the three coordinates of each atom will yield better results than those obtained with the standard bases.

Other work involved the development of an object-oriented class for managing the collection of Schittkowski test problems for nonlinear optimization. This resulted in over 300 new test problems to validate and compare algorithms under development. We also constructed an object-oriented class to interface with Protein Data Bank files that are used to encode protein configurations.

The second component of this work involves the use of the new algorithms on real world applications. This year we developed a prototype heat-conduction parameter identification problem for a multi-material surface to validate the GSS algorithm. Our next step is to apply this framework on a parameter estimation problem that includes uncertainty quantification.

We also used our new energy computation code and the LBFGS algorithm OPT++ to solve several protein folding problems in collaboration with the Scientific Visualization group. Examining these results, we observed that during the energy minimization phase, the atoms within the protein move in small groups involving a few dozen atoms at a time. We are attempting to exploit this observation to develop new strategies for protein-structure prediction.

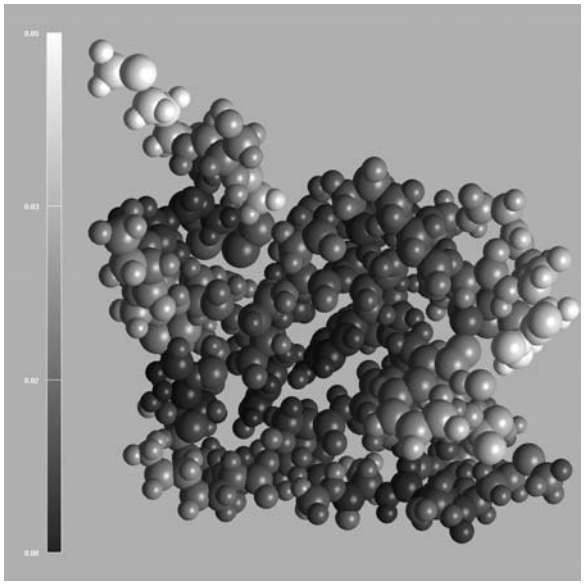

Figure 4. Minimization results for the 1e0m protein using OPT++ on the AMBER energy function. The atoms are shaded according to the magnitude of their displacement relative to a previous minimization step—the more active atoms appear in light gray.

Publications

J.C. Meza, R.A. Oliva, P.D. Hough, and P.J. Williams, "OPT++: An object-oriented toolkit for nonlinear optimization," submitted for publication in *Association for Computing Machinery* (ACM) Transactions of Mathematical Software, June 2003) LBNL 54161.

J.C. Meza, R.A. Oliva, Tapia Conference reference.

R.A. Oliva, PBD library reference, LBNL-53778

Second-order Methods for Solid-fluid Shock Coupling with Application to Martian Meteorites

Principal Investigators: Gregory Miller

Project No.: 01016

Project Description

We are developing new numerical methods to model impact problems that include multiple materials separated by complex time-dependent boundaries. Our goal is an accurate, robust solver that can be used for very large three-dimensional problems by exploiting parallelism and adaptive mesh refinement.

We are applying our new methods to impact problems on planetary surfaces. The specific scientific application we are concerned with is the mechanism by which meteorites have been sent from Mars to the Earth, presumably by impact, but without showing evidence of having experienced large shock pressures. Two qualitative models have been suggested. In one, jets emitted in an impact propel rocks from the surface—like a fire hose sweeping pebbles off pavement. In the other, an interaction between the compressive shock and zero-pressure surface boundary condition is imagined to provide large accelerations by small pressures. We plan to model realistic scenarios with sufficient fidelity in order to assess the feasibility of these proposed mechanisms.

The approach we adopt consists of three major components. First, we are developing a new numerical framework for solving multiphase dynamics on Eulerian grids, with adaptivity, and in parallel. The second step consists of constructing new hyperelastic equations of state and constitutive models. This is necessary to accurately model the response of rocks and ice to high velocity impact. Two key concerns are phase change (melting and vaporization), and fracture (breakup of a solid into rubble with no strength in tension). Third, there are adjustments to the numerical method that may improve its robustness and accuracy. This involves substantially new algorithm development.

Accomplishments

A high-order Godunov method for Eulerian solid mechanics was developed and implemented in one dimension, two dimensions, and three dimensions. The method is approximately second-order accurate with excellent shock-capturing properties. A simple hyperelastic-plastic equation of state was employed to demonstrate the method.

This high-order Eulerian method for solids was coupled to a previously-developed high-order method for fluid dynamics in a stable, conservative, and robust manner. The combined methodology uses a volume-of-fluid representation to indicate the physical extent of the various materials: solid, fluid, and/or vacuum. The volume fraction field is updated by solving appropriate two-material Riemann problems across the interface. The mass redistribution formalism of Chern and Colella is employed to address the well-known fractional cell stability issue. This combined solid-fluid shock capturing method was one of the first applications to use the Chombo software infrastructure to implement parallelism and adaptive mesh refinement.

Numerical experiments with these codes exposed two areas requiring more accurate treatment. One is the solid-solid Riemann solver, which is used inside a solid domain and across heterogeneous solid-solid material interfaces. The approach first attempted is a formally second-order accurate approximation in which the jump is resolved in eigenvectors of an approximate linear advection matrix. While second-order accurate, the solver may nevertheless compute points in the material's state space where the equation of state is non-convex or where some continuum mechanics conditions are not satisfied. To address this robustness issue, a new and numerically exact iterative Riemann solver strategy was developed and tested.

The second issue concerns a systematic error in the volume-of-fluid moving boundary approach adopted in the multiphase solver. This systematic error led to growing density deficits on the trailing edge of moving bodies and a density surplus on the leading edge of the bodies. The cause of this error was discovered to be an assumption in the construction of apertures which measure the time-integrated area fraction covered by a given material phase in fractionally-occupied Eulerian computational cells. These apertures had been computed in a symmetric fashion based largely on experience with stationary irregular boundary problems. In the moving boundary case, an upwind-biased aperture calculation removed this systematic error, significantly improving the stability and robustness of the overall method.

A third area of accomplishment is the construction of material models which embody a sub-grid-scale model of spall or cavitation. The need for such a model was discovered in very-large velocity impact calculations of 20+ kilometers per second where the impactor undergoes extremely large extensional strains on its free surface. A model in which the total deformation is decomposed into multiplicative elastic, plastic, and homogeneous dilatational parts was constructed with evolution laws motivated by existing porous rock and soil mechanics models, such as the Drucker-Prager cap model and the critical state model.

The development of a new Riemann solver strategy for solid mechanics, the diagnosis and correction of the systematic density error, and the development of new equations of state were the principal accomplishments in the third year of this project.

In the course of this work, numerous impact computations were performed with spherical impactors striking planar surface at high velocity and various impact angles. These computations have revealed a new mechanism for the ejection of meteorites from the Martian surface. Constitutive modeling is the principal area for future development.

Publications

G.H. Miller and P. Colella, "A conservative three-dimensional Eulerian method for coupled fluid-solid shock capturing," *Journal of Computational Physics* **183,** 26–82 (2002) also LBNL-50932.

G.H. Miller, "An iterative Riemann solver for systems of hyperbolic conservation laws, with application to hyperelastic solid mechanics," *Journal of Computational Physics* **193**, 198–225 (2003) also LBNL-53795.

G.H. Miller, "Minimal rotationally-invariant bases for hyperelasticity," submitted to *SIAM Journal of Applied Mathematics*.

Combinatorial Algorithms in Scientific Computing

Principal Investigators: Ali Pinar

Project No.: 02018

Project Description

Combinatorial algorithms have long played an important role in many applications of scientific computing such as sparse matrix computations and parallel computing. The growing importance of combinatorial algorithms in emerging applications like computational biology and

scientific data mining calls for development of a high performance library for combinatorial algorithms. Building such a library requires a new structure for combinatorial algorithms research that enables fast implementation of new algorithms, as well as new algorithms that are amenable for high performance computing. The objective of this project is to produce not only combinatorial solutions to some fundamental problems in scientific computing but also design a research structure for combinatorial scientific computing, which can accommodate computationally efficient libraries for a wide variety of applications and combinatorial techniques.

Discrete mathematics and combinatorial algorithms will play an increasingly important role in many Department of Energy applications with a leading role in emerging applications such as computational biology and scientific data mining, as opposed to its supportive role in the traditional applications of scientific computing. In this project we are not only seeking solutions to some fundamental combinatorial problems but also designing a research structure for combinatorial scientific computing, which can accommodate computational efficient libraries for a wide area of applications and combinatorial techniques.

Accomplishments

We follow a similar roadmap to the numerical algorithms community. First, we try to identify model problems that will serve as the interface between combinatorial algorithms and the applications that are akin to differential equations for numerical algorithms. We are also trying to identify fundamental combinatorial algorithms that might serve as building blocks for more sophisticated algorithms. Finally, we seek the kernel operations that will enable efficient implementation of the fundamental algorithms on high performance computing platforms.

Our research will lead to efficient solvers for combinatorial algorithms on high performance computing platforms, which will increase the utilization of combinatorial techniques in many DOE scientific computing applications. More importantly, the structure we are proposing for combinatorial algorithms research will impact the future of combinatorial scientific computing. This structure will promote high quality; algorithms will be implemented with well-tuned kernels and high productivity since such kernels will provide rapid implementations of new algorithms and enable researchers to concentrate only on combinatorial aspects of the problems. Following, we describe our contributions on several problems studied under this project.

Parallel computing

In many applications, distribution of the data unambiguously implies distribution of work among processors but there are exceptions where some tasks can be assigned to one of several processors without altering the total volume of communication and clever assignment of these tasks improves balance. We modeled this problem as a version of the network-flow problem and proposed two algorithms based on parametric search and augmenting paths. For a practical parallel solution we also considered numerical formulations of the problem and reduced it to the linearly-constrained optimization problem. We have recently generalized our algorithms to heterogeneous systems.

We also worked on Cartesian partitioning methods, which are preferred for particle-in-cell methods or other agent-based simulations, where geometric space is partitioned and assigned to processors. Cartesian partitions enable efficient communication among processors and easy tracking of particle- and agent-ownerships by the processors. We designed and tested efficient exact one-dimensional partitioning algorithms. We show that exact algorithms yield significant improvements in load balance over heuristics with negligible overhead. We also introduce novel algorithms that are asymptotically and runtime efficient. Our experiments on sparse matrix and direct volume rendering datasets verified that balance can be significantly improved by using exact algorithms. On average, the proposed algorithms are 100 times faster than a single sparse-matrix vector multiplication for 64-way decompositions. We conclude that exact algorithms with proposed efficient implementations can effectively replace heuristics.

Sparse matrix computations

We have previously proposed exploiting dense blocks of a sparse matrix to improve memory performance of sparse matrix-vector multiplication. To effectively exploit these dense blocks, we need algorithms to permute matrices to create more dense blocks, and algorithms to find a maximum number of non-overlapping such dense blocks in the matrix. We studied the problem of finding a maximum number of non-overlapping dense blocks of a sparse matrix.

The problem of finding sparse null-space bases is an important problem, which has applications in finite-element analysis and linearly-constrained optimization. We have developed several algorithms for finding a block-diagonal basis for a matrix. Our greedy algorithms rely on adding columns to an empty basis until the basis has full rank. While adding columns, we make sure the column increases the rank and the block-diagonal structure is affected the least. We also considered top-down approaches, where we repeatedly remove columns, so that the resulting set of columns are decomposed into two or more components, and still have full rank. Experiments showed that our algorithms can identify bases with very small blocks in many matrices.

Scientific data management

Many scientific applications require efficient storage of, and access to, large volumes of data. Typically, the data is composed of multidimensional points. One method is bitmap indexing, which is based on dividing ranges of variables into bins and locating each item in one bin. This enables storage of the information with only bits, so that we have a 1 in a bin if the entry falls into the corresponding range. For efficiency of queries, the information in one bin is stored as a bit slice. Notice that it is sufficient to store only the 1's for each slice. Moreover, for storage efficiency, these vectors can be compressed with run-length encoding. Effectiveness of run-length encoding relies on positions of the 1's in each slice so that performance increases when 1's are in consecutive positions, thus reordering tuples of the database to align 1's to consecutive positions will improve performance. We formulated the reordering problem as a version of the well-known traveling salesperson problem (TSP), and tailored TSP heuristics. Our initial experiments showed improvements of approximately 20%. We are currently investigating new techniques to improve our results and experimenting with different datasets.

Finally, for new applications of combinatorial scientific computing we are also investigating new applications of combinatorial scientific computing in areas such as computational biology, electric power systems analysis, and astrophysics.

Publications

A. Pinar, "High performance combinatorial algorithms," LBNL-53989.

V. Vassilevska and A. Pinar, "Finding dense blocks of sparse matrix," in preparation.

E. Chow, A. Pinar, and A. Pothen, "Combinatorial techniques for constructing sparse null-space bases," in preparation.

E. Chow, A. Pinar, and A. Pothen, "The nice basis problem," in preparation.

A. Pinar and B. Hendrickson, "Improving load balance by exploiting flexible assignable work," submitted to *IEEE Transactions of Parallel and Distributed Computing*.

A. Pinar and B. Hendrickson, "Interprocessor communication with limited memory," to appear in *IEEE Transactions of Parallel and Distributed Computing*.

A. Pinar and C. Aykanat, "Fast optimal load balancing algorithms for one dimensional partitioning," to appear in *Journal of Parallel and Distributed Computing.*

A. Pinar, T. Tao, and H. Ferhatosmanoglu, "Efficient indexing for scientific databases," in preparation.

Scalable Methods for Studying Collisional Breakup and Rearrangement Processes

Principal Investigators: William McCurdy and Thomas Rescigno

Project No.: 02019

Project Description

Sophisticated first-principles calculations of collisional ionization have so far been limited to electron impact on the simplest target, atomic hydrogen. By contrast, electron collisions with heavier, multi-electron atoms have been limited in terms of the level of accuracy of the underlying methodologies employed and the types of processes that have been studied. For the case of positron impact, there are currently no detailed studies of collisional ionization, even for the case of one-electron targets.

The purpose of this project is to develop scalable methods for studying collisional ionization that will be practical to apply to multi-electron targets. We will extend our studies to cover breakup in the presence of rearrangement channels, developing methods to treat collisional ionization by positron, as well as electron, impact.

Accomplishments

The *exterior complex scaling* method provides a path to the computation of wave functions from which dynamical information can be extracted without having to explicitly impose detailed scattering boundary conditions; it is, therefore, the foundation of our approach to studying collisional breakup. During this past year, we focused our efforts on carrying out the first realistic calculations using this approach on an atomic target with two active electrons. To avoid the direct solution of large systems of complex linear equations in three dimensions, we developed a time-dependent method that propagates a wavepacket on an exterior-scaled three-dimensional grid and accumulates its Fourier transform during the course of the propagation. Our studies of electron-helium ionization in the S-wave model, which were carried out on National Energy Research Scientific Computing (NERSC) Center supercomputers, are the first *ab initio* studies of a three-electron system to have been carried out beyond the frozen-core model.

Double photoionization (absorption of a single photon, followed by ejection of two electrons), like electron-impact ionization, is a sensitive measure of electron-electron correlation. It is also an active area of experimental

research at the Advanced Light Source, which prompted us to undertake theoretical calculations on this problem. Our initial efforts were carried out in collaboration with Fernando Martin, Universidad Autonoma de Madrid, who has implemented the use of B-splines in atomic calculations. We have demonstrated that B-splines are an effective basis for implementing exterior complex scaling, allowing for the correct application of outgoing-wave boundary conditions; we have carried out a successful adaptation of the B-spline approach to study double photoionization of atomic helium. Our initial efforts in this area were successful; some typical results are illustrated below.

We have also carried out a formulation of positron-molecule scattering using an extension of our complex Kohn variational method, which is the principle tool we have developed for studying electron-molecule collisions. The trial wave function in this approach is a close-coupling expansion in molecular target states and is constructed as a sum of product term involving discretized N-electron target pseudostates and single particle channel functions describing the scattered positron. We have found that the various bound-bound, bound-free, and free-free matrix elements that are needed in the construction of the Hamiltonian in this trial basis can be easily calculated in terms of the one-particle transition densities between the various target states. We have used this method to calculate both elastic and electronic excitation cross sections for H_2 and N_2. The elastic cross sections we calculated, for both molecules, are in excellent agreement with experimental measurements. The excitation cross sections for H_2 also agree well with recent measurements.

Publications

T.N. Rescigno, M. Baertschy, and C.W. McCurdy, "Resolution of phase ambiguities in electron-impact ionization amplitudes," *Physical Review A* **68**, 020701(R) (2003).

T.N. Rescigno and A.E. Orel, "Low-energy positron interactions with H_2 and N_2: a coupled-channel pseudostate approach," International Symposium on Electron-Molecule Collisions and Swarms, July 30 to August 2, 2003, Prague, Czech Republic.

C.W. McCurdy, D.A. Horner, T.N. Rescigno, and F. Martin, "Theoretical treatment of double photoionization of helium using a B-spline implementation of exterior complex scaling," submitted to *Physical Review A.*

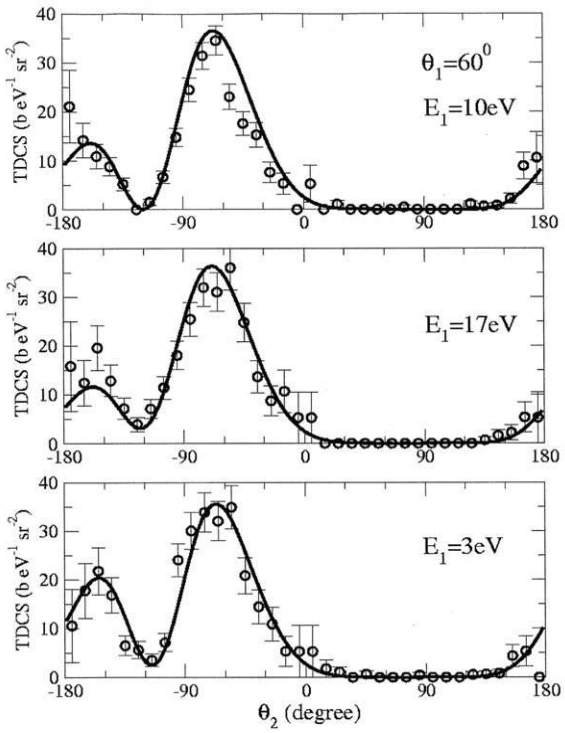

Figure 5. Triple differential cross sections for double photoionization of helium at photon energies 20 eV above threshold. The ejection angle of one electron is fixed at 60 degrees while the angle of the second electron is varied. Three different energy sharings are plotted. Present theoretical results (solid curves) are compared with experiment.

Evaluation of Computer Architecture Alternatives

Principal Investigators: Paul Hargrove and Katherine Yelick

Project No.: 03030

Project Description

The goal of this project is to evaluate the technology building blocks of high performance machines for future acquisitions at National Energy Research Scientific Computing (NERSC) Center, and across the Department of Energy (DOE), by examining both established and emerging technologies for processors, memory systems and interconnects from industry, academia and government laboratories. This work will provide insight into emerging designs and their potential effects on next-generation supercomputing architectures and the applications that run on them. It will provide a mechanism for evaluating future designs through collaboration with industry and may lead to the inclusion of specific system features in those designs.

Our approach is to use a combination of microbenchmarks, application kernel benchmarks, and performance models to measure the benefits and limitations of emerging architectural technologies. The application kernel benchmarks help identify the need for new algorithms for a given architecture, and allow us to explore an entire class of problems. The microbenchmarks isolate particular aspects of the hardware that prove to be a bottleneck, and thereby enable studies of variations on a particular hardware implementation. Finally, we will work with new and existing performance models to predict the performance on machines that do not yet exist.

Accomplishments

One technique for addressing the memory system bottleneck in conventional systems is to use a Processor-in-Memory (PIM) design for the central processing units (CPU). One of our first projects was the evaluation of two related processors that are designed to address the memory bottleneck. The first is Stanford's Imagine, a stream-based architecture that exploits fine-grained data parallelism, but allows for parallelism across an array or stream of records, rather than across a vector of scalar values. The second approach is reflected in the DIVA processor from Information Sciences Institutes, University of Southern California (ISI/USC), which uses a PIM technology combined with a conventional RISC processor extended with wide-word (SIMD-like) instructions. We have defined a set of scientific kernel benchmarks in collaboration with the ISI group, and will complete a report on the results by the end of this year. We have also explored the issue of programmability, i.e., whether the instruction sets are amenable to compilation from a high level language, focusing on a critical problem within the processors of how to move data around within a single chip. The work in this area has produced a series of papers examining the applicability of the VIRAM, Imagine, and DIVA processors to scientific kernels.

While the work identifies specific limitations of the different approaches, the overall conclusion is that they offer significant opportunities for DOE applications in both performance and power savings. However, they represent a revolutionary change in processor design with the ever-present questions about commercial viability. We plan to continue to track these, and related efforts funded by the Defense Advanced Research Projects Agency (DARPA) High Productivity Computing Systems (HPCS) initiative, while shifting our main focus to hardware that has a shorter term potential.

We have also looked at existing commercial technology as a way of identifying opportunities for improvements in future generations of these machines and others. Measurements of the single-node performance of IBM Power3 and Power4 machines (conventional cache-based superscalar SMPs) as compared to the NEC SX6 (a vector SMP) have confirmed the widely held belief that for a large class of applications, vectorization is a highly beneficial optimization when applicable. The result is that for this class of applications, the SX6 is able to sustain a much higher fraction of its peak performance than the Power architecture. However, there remain important classes of applications that are not amenable to vectorization in their current form, and thus achieve substantially better performance on the more conventional cache-based scalar machines.

The second component of our work has been on the interconnect technology, and we are examining emerging technologies, which are positioned to challenge existing interconnects used in cluster systems in the commercial marketplace. Using some benchmarking ideas developed by the Unified Parallel C (UPC) team at Berkeley Lab, we have measured some of the basic latency, bandwidth, and overhead parameters of available hardware at the lowest level. The results show peak bandwidth superior to prior off-the-shelf networks, and latencies that are comparable. The hardware expected to come to market in FY04 will match or exceed the performance of vendor-customized interconnects.

During the past year we have taken part in discussions with many high-performance computer (HPC) vendors, from established players to recent start-ups. While these meetings

are primarily geared towards informing manufacturers more clearly of the requirements of our applications, we have also been able to discuss design choices and benchmarking methodology.

Publications

B. Gaeke, P. Husbands, X. Li, L. Oliker, K. Yelick and R. Biswas, "Memory-intensive benchmarks: IRAM vs cache-based machines," International Parallel & Distributed Processing Symposium (IPDPS), LBNL-48979 (2002). http://crd.lbl.gov/~oliker/papers/ipdps02.pdf

S. Chatterji, M. Narayanan, J. Duell and L. Oliker, "Performance evaluation of two emerging media processors: VIRAM and Imagine," Workshop on Parallel and Distributed Image Processing, Video Processing, and Multimedia (PDIVM) 2003. http://crd.lbl.gov/~oliker/papers/PDIVM_2003_final.pdf

M. Narayanan, "Compiling communication access patterns for a vector processor," to appear in Master's Report, Computer Science Division, University of California, Berkeley.

G. Griem and L. Oliker, "Transitive closure on the Imagine stream processor," to appear in Fifth Workshop on Media and Stream Processors (MSP5) 2003. http://crd.lbl.gov/~oliker/papers/msp5_2003_final.pdf

G. Griem, L. Oliker, J. Shalf, and K. Yelick, "Identifying performance bottlenecks on modern microarchitectures using an adaptable probe," submitted to Third International Workshop on Performance Modeling, Evaluation, and Optimization of Parallel and Distributed Systems (PMEO-PDS) 2004. http://crd.lbl.gov/~oliker/drafts/PMEO04_submit.pdf

M. Narayanan and K. Yelick, "Generating permutation instructions from a high level description," submitted to *Programming Language Design and Implementation* (PLDI) (2004).

M. Narayanan, L. Oliker, A. Janin, P. Husbands, and X. Li, "Scientific kernels on VIRAM and Imagine media processors," In preparation, draft available: http://crd.lbl.gov/~oliker/papers/IPDPS_03.pdf

L. Oliker, J. Chame, P. Husbands, et al., "Evaluation of architectural paradigms for addressing the processor-memory gap," in preparation.

Application of Real-time PCR with Reverse Transcription for Quantification of Specific Microbial Activity in Complex Communities

Principal Investigators: Lisa Alvarez-Cohen and Terry Hazen

Project No.: 03008

Project Description

The objective of this work is to develop and apply a series of molecular techniques that can be applied to environmental samples for the concurrent quantification of: (1) the occurrence of specific dehalogenating microorganisms, (2) genes associated with the dehalogenation reaction, and (3) the expression of the dehalogenase genes. By applying these tools to laboratory enrichments and field samples, and correlating the results with measured dechlorination activity, we will be able to determine the important factors that control gene expression, evaluate whether the identified dechlorinator is a major contributor to the degradation reaction in the environment, and determine whether the functional gene is present in species other than the known degrader.

Our approach is to apply real-time polymerase chain reaction (PCR) and reverse transcription to quantify the occurrence and expression of dehalogenating species and genes in laboratory enrichments and field samples. Target nucleic acids for this approach will be 16S rDNA for species identification, tceA, an identified dehalogenation gene, and mRNA corresponding to the tceA. The molecular techniques will be applied to a series of laboratory enrichments and field samples. Specific comparisons will be made between samples from sites where lactate injection resulted in complete degradation to ethene and sites where degradation stopped at dichloroethene, with no ethene production.

Accomplishments

Over the past year we have made significant progress toward the development and application of the quantitative polymerase chain reaction (QPCR) methodology. Primers and probes for the *D. ethenogenes* 16S rDNA and the tceA gene have been optimized for use with laboratory or field samples. We are also developing a universal 16S primer/probe set that will allow us to quantify the total number of bacterial cells in mixed communities for normalization of specific genes. Initial laboratory experiments testing and calibrating the quantification of all three targets, 16S of *D. ethenogenes*, the tceA gene, and tceA mRNA, have been successful. In addition, we have applied these methods for comparison of the presence of *D. ethenogenes* and the tceA gene at two field sites that differ in ability to degrade chlorinated solvents.

The 16S and tceA genes has been quantified for both the pure culture of *D. ethenogenes* and the mixed dechlorinating culture derived from Alameda Naval Air Station (ANAS). In the pure culture, the two genes were, as expected, present in approximately equal number. The mixed community experiment extended this technique to a culture where the ratio of *D. ethenogenes* 16S rDNA and tceA is not fixed. The 16S and tceA results, normalized to the pure culture results, gave a ratio of roughly 2.5 16S genes per tceA gene. This result is consistent with the hypothesis that dechlorination in the mixed culture is carried out by two or more strains of *Dehalococcoides*, some of which use the tceA gene to catalyze the degradation of perchloroethene (PCE) to *cis*-dichloroethene (cDCE), and some of which catalyze the degradation of *cis*-DCE or vinyl chloride (VC) to ethene using genes such as the recently described vinyl chloride reductase, vcrA. Future experiments will quantify the vcrA gene number in order to further test this hypothesis. More broadly, quantitative analysis of the 16S rDNA in the mixed culture suggested that *Dehalococcoides* makes up ~15% of the culture by weight and ~40% of the culture by cell number. Previously, a combination of direct microscopy and 16S rDNA clone library results were used to estimate that 30% of the ANAS cells were *Dehalococcoides* species. Our QPCR results confirm this estimate, and validate the QPCR approach.

The expression level of the tceA gene has also been quantified as a ratio of mRNA copy number per tceA gene copy number. This ratio has been measured for both the pure *D. ethenogenes* culture and the mixed ANAS culture. Preliminary results are encouraging. The expression level of tceA mRNA was measured in the mixed culture at short intervals during a seven-day feeding cycle. While the tceA gene number changed little over the seven days, as expected, the tceA mRNA copy showed an increase of approximately one log during degradation. Further exploration of tceA regulation would be a valuable contribution to our understanding of reductive dechlorination kinetics. Quantitative results from the pure culture suggest that further calibration is required, however.

Initial experiments found tceA mRNA copy numbers that were two to three orders of magnitude lower than the tceA gene number. Several explanations for this discrepancy are being investigated, including loss of mRNA during cell lysis and nucleic acid extraction, poor reverse transcription, and poor PCR efficiency for reverse-transcribed templates as compared to purified plasmid standards. The inclusion of an internal mRNA control and mRNA standard that are processed in parallel should control for all these sources of error and will be tested during further calibration using the pure *D. ethenogenes* culture.

Finally, we have used QPCR to compare field groundwater samples from the Idaho National Environmental Engineering Laboratory (INEEL), where trichloroethene (TCE) is degraded all the way to ethene, to groundwater samples from Seal Beach, California, where PCE is degraded only as far as DCE. Large numbers of *Dehalococcoides* 16S rDNA and tceA gene copies were found at the INEEL site, while no 16S rDNA or tceA were detected at Seal Beach. In addition, the results at INEEL follow a general trend. The number of *Dehalococcoides* 16S rDNA and tceA roughly decreased with distance from the source of TCE and lactate injection, the nutrient source for the organism. In this field application, the use of QPCR to query the presence of specific organisms and functional genes was much more effective than traditional molecular techniques such as terminal restriction fragment length polymorphism (T-RFLP) or clone library construction and sequencing.

Publications

R.A. Freeborn, V. K. Bhupathiraju, S. Chauhan, K. West, R.E. Richardson, T.A. Goulet, and L. Alvarez-Cohen, "Phylogenetic analysis of a TCE-dechlorinating community enriched on alternate electron donors," in review at *Environmental Science and Technology* (2003).

J. French, A. Rossi, T. Kirk, D. Blackwelder, K. Sorenson, B. Rahm, L. Alvarez-Cohen, S. Le, M. Pound, and P. Tamashiro. 2003, "Phased *in situ* biostimulation/ bioaugmentation pilot testing in a coastal aquifer," Seventh International Symposium on *In Situ* and On-site Bioremediation, Orlando, Florida.

B. Rham, A. Fortin, V.F. Holmes, C. Wu, R. E. Richardson, and L. Alvarez-Cohen, "Application of real-time PCR to quantify reductive dechlorination of TCE," 103rd general meeting of American Society for Microbiology, Washington, D.C. 2003.

B. Rahm, V. F. Holmes, S. Chauhan, K. Sorenson, and L. Alvarez-Cohen, "Characterizing the microbial population at two sites that differ in intrinsic reductive dechlorination ability; a comparison through multiple molecular techniques," in preparation for submission to *Environmental Science and Technology*.

Microbial Controls on Metals in the Environment

Principal Investigators: Jillian Banfield

Project No.: 02020

Project Description

Microorganisms can largely control the form, distribution, mobility, and toxicity of metals in the environment. Microorganisms can increase the rates at which environmental metal pollution occurs through increasing the rate of metal sulfide dissolution or by altering the speciation of metal ions through organic complexation. Conversely, microorganisms can directly and indirectly decrease the mobility and bioavailability of metals in the environment through metal uptake and sequestration, adsorption of ions onto cellular and extracellular polymers, and by inducing precipitation of metal-containing minerals. Questions to be pursued in the final year of this project are: What can we learn about the physiology of microorganisms responsible for these processes? By what molecular pathways do microorganisms fix carbon and nitrogen and carry out the transformations central to the ecology of the system? How does the microbial community activity respond to environmental perturbation? What role does biomineral particle size play in determining the long-term fate of precipitates?

Accomplishments

We have constructed clone libraries to determine the major phylotypes in microbial communities from an acid mine drainage (AMD) system and determined how these communities vary over space and time and as a function of geochemical conditions. Our results confirm the earlier deduction that the communities have low species numbers, but the organisms are typically phylogenetically diverse (Druschel, Baker et al. GT, in review). We constructed libraries for analysis of environmental microbial community genomic DNA and put in place arrangements to sequence these libraries. We have analyzed the small insert library shotgun sequence data from one natural biofilm sample and reconstructed or partially reconstructed several genomes and partially annotated these. The results, as well as analyses funded by other grants, are reported in Tyson et al. (*Science*, in review). We have documented the fungal community in several biofilm samples using molecular methods (sequencing of the 18S rRNA and beta tubulin genes), developed fluorescence *in situ* hybridization probes to detect these organisms in biofilm samples, and

established that the organisms are active in pH < 1 solutions (Baker et al. *PNAS*, in press). We determined that a subset of the protists in the communities have an alphaproteobacterial endosymbiont [detected via the fluorescent *in situ* hybridization (FISH) using species-specific oligonucleotide probes (Baker et al. *AEM* 2003)]. We detected a new deeply branching archaeal lineage in the AMD system in the shotgun library 16S rRNA gene sequences, identified several genes in this organism, and evaluated the phylogeny of this lineage using these genes (Baker et al. work in progress).

We cultivated a *Leptospirillum ferriphilum* population closely related to the dominant member of the microbial community studied via genomic methods. We have analyzed the strain-level heterogeneity in the cultivated and natural *Leptospirillum* populations and found that it is quite high, despite the dominance of one clonal type. This result indicates that there are numerous low abundance variants closely related to the dominant strain (Lo et al. in prep.). In addition, we obtained cultures of novel archaea and were able to demonstrate that they reduce ferric iron. Thus, we have characterized the microbial populations at the physiological and molecular levels, evaluated microbial community structure at the species and strain level, and developed an understanding of correlations between geochemical conditions and microbial activity. Ongoing experiments will explore the response of communities to perturbation using gene expression data obtained via arrays that will be constructed from the community genomic sequence.

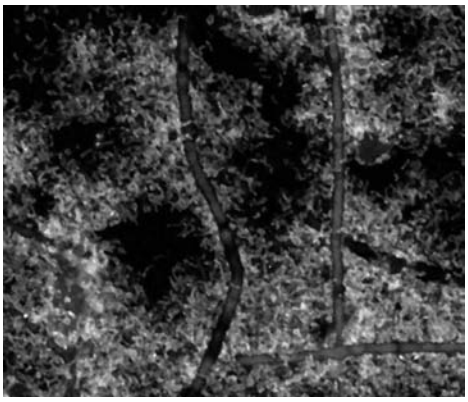

Figure 1. Confocal microscope image of an acid mine drainage biofilm. Microbial eukaryotes (fungal filaments and round protists), Leptospirillum ferriphilum-related bacteria, archae, and bacteria related to Sulfobacillus can be identified.

Publications

G.K. Druschel, B.B. Baker, T.H. Gihring, and J.F. Banfield, "Acid mine drainage biogeochemistry at Iron Mountain, California," *Geochemical Transactions*, in review.

B.J. Baker, M.A. Lutz, S.C. Dawson, P.L. Bond, and J.F. Banfield, "Multi-gene phylogenetic, rRNA probe, and cultivation-based study of metabolically active eukaryotes related to neutrophilic lineages in pH 0.8–1.4 acid mine drainage," *Proceedings of the National Academy of Science*, in press.

B.J. Baker, P.H. Hugenholtz, S.C. Dawson, and J.F. Banfield, "Circumneutral pH habitats within extremely acidophilic protists host Rickettsiales-lineage endosymbionts with an intervening sequence in their 16S rDNAs." *Applied and Environmental Microbiology* **69**, 5512–5518 (2003).

B.J. Baker and J.F. Banfield, "Microbial communities associated with acid mine drainage," *FEMS Microbiology Review* **44**, 139–152 (2003).

G.W. Tyson, J. Chapman, P. Hugenholtz, E. Allen, R.J. Ram, P. Richardson, V. Solovyev, E. Rubin, D. Rokhsar, and J.F. Banfield, "Reconstruction of genomes from a natural environment: insights into microbial community structure and metabolic networks," *Science*, in review.

I. Lo, G.W. Tyson, P. Hugenholtz, and J.F. Banfield, "Population structure of leptospirilum in an acid mine drainage microbial community," in preparation, to be submitted to *Applied and Environmental Microbiology*.

Comparative Studies Between Earth and Planetary Sciences

Principal Investigators: Gudmundur Bodvarsson

Project No.: 03004

Project Description

This project proposes to explore in greater depth specific processes that should add insights into understanding important issues such as carbon management and climate change by comparative study of bodies from other planets and moons in our solar system. These bodies, which have been frozen in the early development period of the solar system, are likely to have similar or directly analogous processes to the early Earth. Therefore, comparative studies of these bodies hold great promise in developing insights

into the global processes of Earth that are very difficult to study because of the loss of much of the early record of Earth history, due to the more highly interactive nature of atmospheric and geological processes on the Earth, and the cross-disciplinary nature of the relevant studies.

We will conduct pilot studies that are in part motivated by questions raised from discoveries from other solar system objects that can be conducted in Earth laboratories and that address on a specific level the evolution of the Earth's atmosphere and its chemistry, as well as the climate, thermal, and geological history of the Earth.

Accomplishments

Major accomplishments from the LDRD are as follows:

Planetary remote sensing of surface composition and its application to the terrestrial iron cycle

Initially, we proposed the use of remote sensing and iron isotope geochemistry to elucidate the terrestrial iron cycle. To this end, we have spent the past year analyzing the iron isotopic composition of a variety of components within the terrestrial iron cycle. The results of this work, which include analyses of river waters, pelagic clays, marine carbonates, soils, and igneous rocks, were presented at the Fall 2002 and Fall 2003 American Geophysical Union Conference in San Francisco. In short, we propose that continental weathering fractionates iron isotopically and that the isotopic signal from weathering is carried mainly in the dissolved fraction of streams. This signal is consequently passed on to the ocean where it may be recorded in marine deposits such as ferromanganese crusts.

In addition to the isotopic research, we have investigated the utility of various spaceborne platforms for achieving our remote sensing goals for this project. We have determined that Moderate Resolution Imaging Spectroradiometer (MODIS) multispectral data are ideal for examining our target region, North Africa, on a large spatial scale (250 m to 2 km spatial resolution) and at coarse spectral resolution (36 bands from 0.459 to 14.385 μm). Thus far, we have used MODIS data to identify both key dust-producing regions and control regions where the iron mineralogy can be easily determined. The next step is to use Hyperion hyperspectral reflectance data (7.65 km wide by 185 km long swaths, 30 m spatial resolution, 0.4 to 2.5 μm spectral range) to characterize the surface mineralogy in both the control and unknown regions. Overall, this approach is limited by the spatial resolution of the remote data, our ability to correct for atmospheric effects, and the fine particle grain size inherent in dusty regions. Thus far, progress has been limited by faulty atmospheric correction software. Ultimately, we feel that the unique combination of isotope geochemistry and remote sensing will increase our understanding of iron cycling at the Earth's surface.

Anisotropic waveform tomography of the Earth's mantle

The waveform tomographic methodology is based on a normal-mode formalism, which includes the effects of three-dimensional structure on body waves through the coupling across different mode branches. This allows us to include information contained in entire seismograms, and notably, extend the use of waveform tomography to wave-packets containing body wave arrivals with broadband sensitivity kernels that account both for the ray character of body waves and for the finite frequency effects which spread the sensitivity away from the ray-theoretical wave path.

Initially, this formalism was developed to invert for isotropic S velocity structure. Panning and Gung worked to extend it to the case of radial anisotropy, as described by the five Love parameters: A C F L N, and density—testing possible assumptions on relations between the parameters, to bring down the number of unknowns to two, isotropic velocity Vso and the parameter ξ, which is a measure of the difference between the velocities of vertically and horizontally polarized S waves.

This work led to two main results:

- A study of upper mantle anisotropy, in which we determined that the discrepancy in thickness of the lithosphere under cratons between different seismological studies can be explained by the presence of anisotropy, with a strong component of horizontal shear, in the depth range 200-400 kilometers, under cratons, similarly to what is found under ocean basins at shallower depth.
- A study of radial anisotropy in the deep mantle, showing that it becomes significant in the last 300 kilometers of the mantle (D-Region), with a $\delta \ln \xi > 0$, indicative of the predominance of horizontal shear, confirming the notion that D-Region is a boundary layer for convection in the mantle. $\delta \ln \xi > 0$ except in the vicinity of the two large low S velocity regions under the central Pacific and under Africa where the upwelling flow is likely to be more vertical.

Landslide Forecasting Tool

This was a collaborative project between Norman Miller at Berkeley Lab's Earth Sciences Division and William Dietrich at University of California's Department of Earth and Planetary Science to develop a web-based state-wide shallow landslide forecasting tool, to be accessed from Miller's hydro-climate and impacts research website within the Earth Sciences Division homepage. This collaboration uses the Miller program for taking climate forecasts, downscaling them and making the 72 hour MM5-based precipitation forecasts across the state. Our goal is to have an automated shallow landslide hazard warning system for

all regions in California that have landslide risk potential. Dino Bellugi, an EPS programmer working with Dietrich, made good progress towards this goal. He compiled the 30 m digital elevation dataset for of the California domain, ran our shallow slope stability model, SHALSTAB, for the entire state, and developed a demonstration data set to show how precipitation forecasts could be used to identify landslide producing storms. We are close to implementing the program and expect to have our beta version running in January 2004. We will then monitor landslide forecasts and observations to evaluate performance. If this simple coupled modeling is successful, it could become a tool of great practical value in warning communities of risk.

Publications

M.S. Fantle and D.J. Depaolo, "Iron isotope fractionation during continental weathering," submitted to *Earth and Planetary Science Letters.*

Y. Gung, M. Panning, and B. Romanowicz, "Global anisotropy and the thickness of continents," *Nature* **422**, 707–711 (2003).

M. Panning and B. Romanowicz, *Science* **303**, 351–353 (January 2004).

Coupling of Seismologic and Hydrologic Processes

Principal Investigators: Michael Manga

Project No.: 02023

Project Description

We will document the coupling of earthquakes and hydrologic processes in natural geologic systems, both in space and in time. Understanding this coupling will allow us to predict the conditions under which hydrologic changes (for example, those caused by fluid injection, fluid extraction, and/or changes in subsurface temperature) may induce seismicity. Understanding natural systems provides a baseline for interpreting observations in engineered systems. We will search for statistically significant correlations in space and time between earthquakes and hydrologic processes. Two problems will be studied: (1) earthquake triggering by natural groundwater recharge and (2) changes in streamflow following earthquakes. Observed behaviors will be interpreted with poroelastic flow models.

Accomplishments

One of the most commonly observed hydrological responses to earthquakes is an increase in streamflow. Three hypotheses for the origin of the excess streamflow have been proposed: (1) coseismic static strain, (2) consolidation or liquefaction caused by dynamic strain, and (3) enhanced permeability. These different hypotheses imply different processes for groundwater recharge and discharge in earthquake cycles. Furthermore, because the different hypotheses imply different changes in pore pressure and different locations for the pore pressure change, they also imply different scenarios for triggered seismicity. Our compilation of published studies supports hypothesis two best, though a single explanation is not required.

Because all previous studies focused on the hydrologic response to single earthquakes, we searched for streams that record streamflow responses to multiple earthquakes. We focused the analysis on Sespe Creek in southern California because its discharge changed after several earthquakes. Regardless of the sign of the static strain caused by the earthquake, flow increased. The magnitude and occurrence of changes in streamflow are best explained by consolidation of alluvial deposits. We also show that changes in streamflow cannot be caused by changes in aquifer permeability.

Changes in fluid pressure can also influence seismicity. This is well established in "engineered" settings where stress changes follow the filling of reservoirs, or where fluids are injected into the subsurface. In order to determine whether natural changes in fluid pressure can influence seismicity, we analyzed the earthquake record in the Cascade volcanic arc where large changes in fluid pressure are expected because groundwater recharge rates are high. We find a statistically significant correlation between groundwater recharge and seismicity at Mt. Hood, Oregon. The time lag of about 150 days between recharge and seismicity allows us to determine the regional hydraulic diffusivity (10^0 m^2/s) and other hydrogeologic parameters (permeability of 10^{-13} m^2, vertical matrix compressibility of 10^{-10} m^2/N). These values are comparable with those we determine independently by using coupled heat and groundwater flow models to interpret bore hole temperature data at Mt. Hood We thus conclude that hydroseismicity occurs in this region and is caused by natural groundwater recharge. This result also suggests that faults in this area are near critically-stressed. Discerning whether hydroseismicity can be induced by pore fluid-pressure changes as small as the 0.1 to 0.2 megapascal estimated during groundwater recharge, has implications for seismic risk evaluations related to reservoir impoundment, subsurface injection of waste fluids, carbon sequestration, geothermal energy exploration, and estimates of the state of stress in the crust.

In addition, by employing this approach, hydrogeologic properties such as permeability and specific storage can be estimated on a large spatial scale.

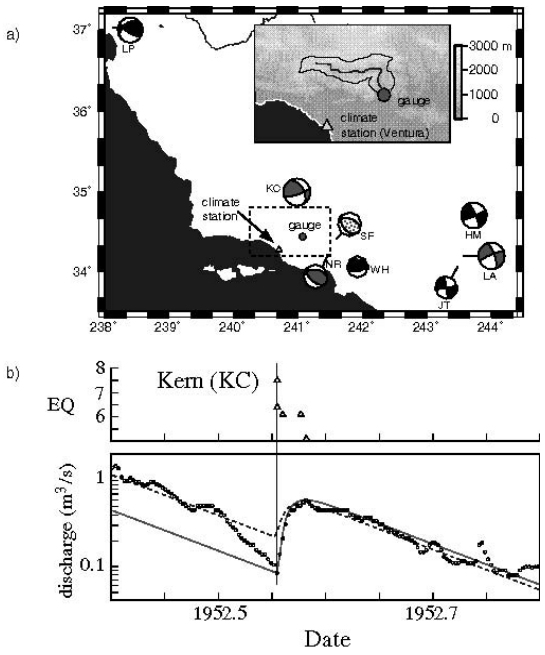

Figure 2. (a) Map of southern California showing earthquake locations and focal mechanisms. KC, SF, NR, and LA are earthquakes caused a change in streamflow in Sespe Creek. WH, JT, and HM indicate no change in flow. (b) Observed streamflow (small dark circles) and model predictions (dashed line, thin grey line) for the response to the 1952 Kern County earthquake. The model assumes the excess discharge after the earthquake was caused by consolidation of alluvial deposits. No precipitation during the time period shown.

Publications

M. Manga, E.E. Brodsky, and M. Boone (2003) Response of streamflow to multiple earthquakes and implications for the origin of postseismic discharge changes, *Geophysical Research Letters* **30**, doi:10.1029/2002GL016618.

D.R. Montgomery and M. Manga, "Streamflow and water well responses to earthquakes," *Science* **300,** *2047-2049* (2003).

M.O. Saar and M. Manga, "Seismicity induced by seasonal groundwater recharge at Mt. Hood, Oregon," *Earth and Planetary Science Letters* **214,** 605-618 (2003a).

M.O. Saar and M. Manga, "Depth dependence of permeability in the Oregon Cascades inferred from hydrogeologic, thermal, seismic, and magmatic modeling constraints," submitted to *Journal of Geophysical Research* (2003b).

Development of Monitoring Strategies for Carbon Sequestration Verification using Coupled Subsurface and Surface Layer Simulation

Principal Investigators: Curtis Oldenburg

Project No.: 02024

Project Description

The accumulation of vast quantities of injected CO_2 in geologic sequestration sites entails failure risk, i.e. risk that injected CO_2 will escape to the atmosphere, and health and environmental risk from potential seepage of CO_2 into the near-surface environment. The overall objective of this project is to use detailed coupled simulations of subsurface and atmospheric surface layer migration of CO_2 from geologic sequestration sites to predict concentration distributions under a variety of geological and atmospheric conditions. These concentration distributions will provide the basis for determining above-ground and near-surface instrumentation needs for carbon sequestration monitoring and verification, for ensuring public safety, and for minimal environmental impact.

Accomplishments

In this project, we have: (1) developed and tested a coupled subsurface–surface-layer modeling capability built on the TOUGH2 simulator called TOUGH2 for CO_2 and Air (T2CA), (2) applied the capability to simulate CO_2 concentrations in the unsaturated zone and near-surface atmospheric surface layer, (3) assessed instrumentation and monitoring technology relevant to CO_2 detection, and (4) conceived of monitoring and instrumentation strategies to discern a CO_2 leakage or seepage signal (LOSS) from background variability associated with the natural carbon cycle. Leakage is defined as migration of injected CO_2 away from the primary CO_2 storage target, while seepage is migration of injected CO_2 across a boundary such as the ground surface.

We developed T2CA, a simulator for subsurface and surface layer flow and transport of CO_2 and air, along with water, brine, and a gas tracer. The full multicomponent treatment is applied in the subsurface and surface layers and the simulation is carried out on a single grid. The domain can be three-dimensional, but the wind velocity profile must be logarithmic and unidirectional along the x-axis of the grid. Dispersion in the surface layer is modeled using standard atmospheric dispersion approaches.

We have used the new code to show that fluxes of similar magnitude to the net ecosystem exchange (NEE) result in shallow soil CO_2 concentrations that are quite high. As for surface layer mixing, application of this new capability shows that seeping CO_2 will be strongly diluted in the surface layer. Results from two-dimensional T2CA simulations for a variety of time-average winds and end-member Pasquill-Gifford (P-G) stability classes F–moderately stable, and A–extremely unstable, are shown in Figure 3. We have chosen zero background CO_2 concentrations to focus on the additional CO_2 added by seepage. In this coupled system, CO_2 migrates upward through the unsaturated zone and into the atmospheric surface layer where it is advected and dispersed. Rainfall infiltration brings some CO_2 back into the subsurface as a dissolved component in the aqueous phase. As shown in Figure 3, subsurface CO_2 concentrations are high while surface layer concentrations are very small because surface layer dispersion is effective in diluting CO_2. This simulation suggests that instrumentation and monitoring strategies in the surface layer are only likely to succeed if the flux is large and if the instrumentation is near the source region. On the other hand, the simulations show that the subsurface CO_2 concentrations can be quite high, which shows the potential advantages of CO_2 monitoring in the subsurface.

We have also carried out a review of existing instrumentation and approaches to monitoring CO_2 gas concentrations and fluxes. Gas concentration in soil gas can be measured at a point by infrared (IR) absorption at wavelengths (e.g., 4.26 μm) specific to CO_2. Concentrations in the surface layer can also be measured along a line-of-sight path as an integrated value by IR absorption. For large scale flux measurements, the IR absorption approach can be used with micrometeorological measurements to infer a net efflux of CO_2 through a large area based on theoretical considerations involving the height of measurement.

While advanced technologies exist for detecting CO_2, the challenge in geologic carbon sequestration verification is in discerning a CO_2 LOSS from the natural background variability. We have developed an integrated sampling and analysis approach that emphasizes baseline monitoring and analysis to understand the natural variability of CO_2 cycling at a site independent of CO_2 injection. From this detailed understanding, ongoing periodic monitoring and sampling with analyses of stable and radiogenic carbon isotopes, as well as land-surface and flow and transport modeling, can be carried out in a cost-effective way during and after CO_2 injection. Unexpected changes in CO_2 concentrations and carbon isotopic compositions can indicate a potential LOSS. In this case, more detailed and comprehensive monitoring, sampling, and analyses would be undertaken to confirm seepage and locate its source.

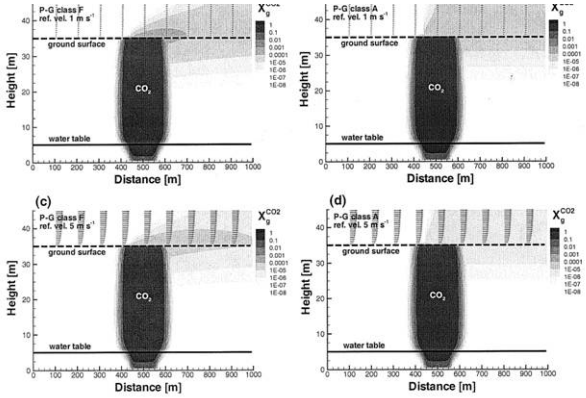

Figure 3. Simulation results showing mass fraction of CO_2 in the gas phase and gas velocity vectors for the coupled problem. (a) P-G class F, wind speed 1 m s^{-1}; (b) P-G class A, wind speed 1 m s^{-1}; (c) P-G class F, wind speed 5 m s^{-1}; (d) P-G class A, wind speed 5 m s^{-1}.

Publications

C.M. Oldenburg and A.J.A. Unger, "On leakage and seepage from geologic carbon sequestration sites: unsaturated zone attenuation," *Vadose Zone Journal* 2, 287–296 (2003a).

C.M. Oldenburg and A.J.A. Unger, "Coupled subsurface-surface layer gas transport and dispersion for geologic carbon sequestration seepage simulation," submitted to *Vadose Zone Journal* (2003).

C.M. Oldenburg, J.L. Lewicki, and R.P. Hepple, "Near-surface monitoring strategies for geologic carbon dioxide storage verification," LBNL-54089 (October 2003).

J.L. Lewicki and C.M. Oldenburg, "Integrated near-surface modeling and analysis for CO_2 storage verification," submitted to *Proceedings of the American Chemical Society, Division Fuel Chemistry* (October 2003) LBNL-54076.

Applying a Coupled Climate-land Surface Regional Model to Deduce Trends in Soil Moisture from Air Temperature Data

Principal Investigators: William Riley, Margaret Torn, Marc Fischer, John Harte, and Helen He

Project No.: 02025

Project Description

The goal of this project is to develop a modeling framework to evaluate coupling and feedbacks between the land surface and atmosphere at regional to continental scales. From extant models of ISOSLM and MM5, we have developed a fully coupled land-surface and atmosphere regional-scale model that is running at Berkeley Lab National Energy Research Scientific Computing (NERSC) Center. The coupled model allows for mechanistic treatment of the interactions between the surface energy balance and carbon exchanges via photosynthesis and predicts the net ecosystem exchange of carbon (CO_2). Understanding and being able to accurately simulate energy and mass exchanges between the land surface and atmosphere is critical to our ability to predict the long-term impacts of anthropogenic activity, which includes continued fossil fuel combustion, land use, and water-cycle changes. The development of this tool is also intended to assist other researchers who are interested in coupled interactions between atmospheric processes and carbon, energy, and water cycles.

With the coupled model we are addressing several questions: (1) Is there a discernable relationship in amplitude or phase between the diurnal temperature range (DTR) and soil moisture? (2) How will large-scale human land-use, such as harvesting and fallow fields, impact regional atmospheric processes and near-surface air temperatures, soil moisture, and soil temperature? (3) How will changes in the direct and diffuse fraction of shortwave radiation at the surface impact surface energy, water, and CO_2 exchanges? (4) Can we use large-scale estimates of CO_2 and water vapor fluxes across the planetary boundary layer to accurately infer temporally integrated net surface exchanges? (5) Can we use the ^{18}O content of atmospheric CO_2 to partition site-level measured net ecosystem carbon fluxes, and regionally, to estimate CO_2 flux spatial distributions, and can we develop a computationally efficient method to study this problem in the coupled model?

Accomplishments

We have successfully coupled MM5 and ISOLSM and have tested the model in several ways. First, we compared simulations to precipitation maps from several periods to test large-scale, continental, predictions. Second, we used data from the three-year 225 km^2 FIFE dataset to test the finer resolution results. Finally, we are currently using data from our 60 meter tower in the Atmospheric Radiation Measurement Cloud and Radiation Testbed (ARM-CART) region of Oklahoma to test the model. Overall, the new model simulates energy exchange, precipitation, near-surface air temperatures, and soil moisture and temperatures at least as well as the current land-surface model in MM5 and, importantly, provides consistent estimates of gross and net CO_2 exchanges with the atmosphere.

Using the coupled model, we investigated the response of several measures of surface climate to perturbations in soil moisture. Simulations over the ARM-CART were performed in June and August 1998. The control runs were initialized with uniform soil moisture, while the treatment runs were initialized with 80% of the control run soil moisture. For each run, predicted 2 m air temperature, surface temperature and moisture, sensible and latent heat fluxes, and cloudiness were saved for analysis of DTR and time of maximum temperature (T_m). We found that approximately 50% of the variance in DTR is explained by the combination of variance in cloudiness ~30%, soil moisture ~ 15%, and latent heat flux < 10%. The impact of soil moisture reversed between June and August. In contrast to DTR, the variance in T_m is poorly explained (10%), by the combination of these variables. Together, these results indicate that cloudiness, and not soil moisture, has a strong impact on surface air temperature over the time-scales and range of driving variables applied in these simulations.

Winter wheat harvest can have substantial impacts on surface fluxes, air temperatures, and regional climate in the Southern Great Plains ARM-CART region. We chose to study the winter wheat harvest because wheat accounts for about 20% of the ARM-CART land area. Two harvest dates, one month apart and bracketing the inter-annual range in the region were simulated and compared. Differences in latent and sensible heat fluxes, 2 m air and soil temperatures, and precipitation associated with the early harvest varied over the two-month simulation. During the first three days after harvest, midday latent heat fluxes increased substantially, and much of the near-surface soil moisture was lost via evaporation. Over the next two weeks, midday latent heat fluxes decreased as transpiration was eliminated and evaporation was sharply reduced in the harvested area. The concurrent increase in sensible heat fluxes resulted in midday air-temperature increases of about 1° C. After the second harvest, air temperature and soil moisture and temperature levels rapidly converged between the two scenarios, indicating that the system has relatively little memory of the early harvest. Changes within the

harvested areas are substantially larger than the regionally averaged results. Figure 4 shows the difference in 2 m air temperature; further, there are some edge effects. For example, latent heat fluxes increased and sensible heat fluxes decreased in areas adjacent to the harvest, because of the drier air being advected from the harvested region. Simulations of the winter wheat harvest in the ARM-CART region indicate that coherent harvesting substantially impacts regionally averaged and local surface conditions and climate.

The direct and diffuse partitioning of shortwave radiation at the surface substantially impacts net ecosystem carbon exchange (NEE). The coupled model we have developed at NERSC is ideal for addressing the impacts of global and regional changes in direct and diffuse radiation on NEE; we have applied the model to examine the impact of the 1992 Mount Pinatubo eruption on changes in carbon uptake across the continental U.S. and Canada. Our results indicate that the shift from direct to diffuse radiation resulting from the lofted aerosols produced about a 10 to 15% increase in net ecosystem carbon uptake over the several months following the eruption. The impact lessened over time, until it was indiscernible two years later. There was a concurrent smaller impact on soil respiration.

The use of the ^{18}O content of atmospheric CO_2 to partition site-level measured net ecosystem carbon fluxes, and regionally, to estimate CO_2 flux spatial distributions is a potentially powerful tool. However, numerical models used to approximate the $\delta^{18}O$ value of the soil surface CO_2 flux, δF_s are computationally expensive. We therefore developed, and successfully tested, a numerical model reduction approach (HDMR), and then used the reduced model to investigate the factors important in determining the $\delta^{18}O$ value of the soil surface CO_2 flux, δF_s. The largest changes in δF_s occur when soil water $\delta^{18}O$ gradients in the top five centimeters are large. These results indicate that recent approaches to estimating global and regional distributions of the surface $C^{18}OO$ flux are problematic, and demonstrate the importance of accurately resolving near-surface soil water $\delta^{18}O$ values. Also, the development of the HDMR approach allows for accurate and computationally affordable simulations of regional and global distributions of δF_s. We are working to include the HDMR approach in the coupled MM5-ISOLSM model.

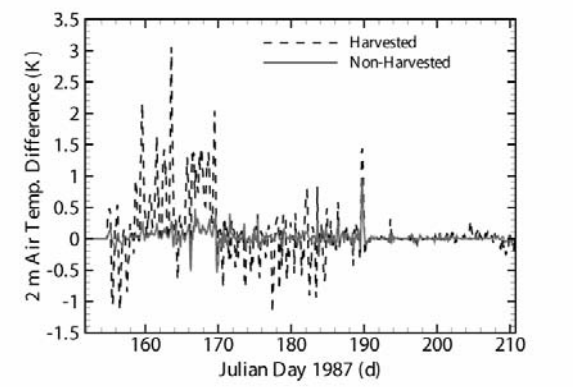

Figure 4. Midday air temperatures declined during the three days following harvest due to increased latent heat flux. Temperatures warmed following Julian Day 160 and were elevated until Julian Day 170. The subsequent air temperature decline is closely tied to an increase in precipitation in both scenarios

Publications

H.S. Cooley, W.J. Riley, M.S. Torn, and Y. He, "Agricultural practice and regional climate interactions: Investigations using a coupled land surface and atmospheric mesoscale model," to be submitted to *Journal of Geophysical Research–Atmospheres* (2004).

W.J. Riley, "Predicting the $\delta^{18}O$ value of the soil-surface CO_2 flux using a high-dimension model representation technique," to be submitted to *Geophysical Research Letters* (2004).

W.J. Riley, "Impact of the near-surface $\delta^{18}O$ value of soil water on the $\delta^{18}O$ value of the soil-surface CO_2 flux," submitted to *Geophysical Research Letters* (2004).

H.S Cooley, W.J. Riley, and M.S. Torn, "Effect of harvest on regional climate and soil moisture and temperature," Chapman Conference on Ecosystem Interactions with Land Use Change, Santa Fe, New Mexico, 2003.

H.S. Cooley, W.J. Riley, and M.S. Torn, "Interactions between land cover change and climate in a coupled regional climate model," 88th Ecological Society of America Annual Meeting, Savannah, Georgia, 2003.

W.J. Riley, H.S. Cooley, Y. He, and M.S. Torn, "Coupling MM5 with ISOLSM: Development, testing, and application," PSU/NCAR Mesoscale Modeling System Users' Workshop, Boulder, Colorado, June 10-11, 2003.

W.J. Riley and D.D. Baldocchi, "Estimating impacts of enhanced diffuse radiation on regional net ecosystem exchange: Application of a coupled meteorological and ecosystem mode," Berkeley Atmospheric Sciences Symposium, Berkeley, California, October 20, 2003

Reactivity of Nanoparticles in Natural Environments

Principal Investigators: Glenn Waychunas, Jillian Banfield, Hoi-Ying Holman, and Paul Alivisatos

Project No.: 02026

Project Description

This project is to investigate how nanoscale weathering and microbial biomineralization products impact the geochemistry of the environment. It will seed investigations into how new biological and geochemical processes combine to generate nanometer-scale particles, and the ways in which the reactivity and fate of these particles are size dependent. New knowledge will be applied to development of strategies for remediation of environments contaminated with metals sequestered within, or adsorbed onto, nanophase minerals. These efforts are also expected to yield novel approaches for the creation of new impurity-doped and composite biomaterials for other technologies.

Preliminary results from ongoing small-scale research activities at Berkeley Lab and University of California, Berkeley, have revealed unexpected behavior associated with nanophase materials, suggesting that a focused research effort dealing with nanoscale particles in complex natural systems can yield important insights into environmental processes. We will investigate the pathways for nanomineral particle formation, growth, and assembly in the presence of naturally organic compounds by several complementary and mutually supportive efforts. Banfield's group will cultivate microorganisms that induce mineral precipitation due to their utilization of inorganic species as electron acceptors ($Fe^{3+}U^{6+}$, SO_4^{2-}) or electron donors (Fe^{2+}, S^-), and characterize the products via transmission electron microscopy (TEM) and x-ray diffraction (XRD). Holman's group will investigate the impact of organic species on the size distribution and growth morphology of nanomineral particles, concentrating on the specifics of organic binding at surfaces. Waychunas' group will characterize nanomineral size distributions and surface/bulk structure, and conduct real-time studies of growth and aggregation kinetics using small angle x-ray scattering (SAXS) and x-ray absorption spectroscopy (XAS). Alivisatos' group will investigate particle morphology and phase control via manipulation of size, growth pathway and solution chemistry. Together, these approaches will ensure new insights into the fundamental physical, chemical, and biological processes that control reactions at the surfaces of essentially ubiquitous nanosized particles in natural environments.

Accomplishments

Phase transitions in ZnS nanoparticles

The surface energy, and presumably structure, of a nanoparticle influences thermodynamic stability and can permit special pathways for phase transformation and coarsening. Research has been performed on nanoparticles of ZnS, a tetrahedrally coordinated semiconductor, and also a naturally occurring nanoparticulate ZnS is a good model system because the small free energy difference between the cubic (sphalerite, the stable bulk phase below 1020° C) and hexagonal (wurtzite) phases permits investigations of phase stability at small particle size.

The kinetics of phase transitions in nanoscale ZnS were studied via x-ray diffraction, x-ray absorption spectroscopies, and high-resolution transmission electron microscopy (TEM). When ~3 nanometers ZnS nanoparticles are heated in vacuum (350° C to 750° C), sphalerite transforms to wurtzite, implying reversal in phase stability in small particles. However, there was no detectable conversion of sphalerite to wurtzite when samples were heated in air at 350° C, probably due to chemisorbed water. Coarsening of 3 nm ZnS nanoparticles in a hydrothermal (i.e. high-temperature, aqueous) environment yielded wurtzite only on the surface of primary sphalerite particles. Crystal growth of wurtzite stops when the diameter of the sphalerite-wurtzite interface reaches 20 nm. Results suggest a dependence of the activation barrier for the transformation on particle size.

Solvent and ligand effects

Solvent or ligand changes at the nanoparticle surface can drive structural transitions at room temperature. Methanol desorption and rewetting, water binding, and aggregation and disaggregation have been found to produce structural modification in nanoparticle ZnS. Reversible switching between distorted and crystalline structures can be induced by sorbing and desorbing methanol and by changing the aggregation state at room temperature. The data imply low activation energies for the transformations and indicate that nanoparticle structure is not kinetically trapped, but responsive to environmental changes. To our knowledge, these are the first surface-driven room temperature transitions observed in nanoparticles.

Coarsening behavior in nanoparticles

ZnS nanoparticles in water with no organic capping group (H_2O-ZnS) and mercaptoethanol-capped ZnS were coarsened in a hydrothermal environment. Early crystal growth of both H_2O-ZnS and mercaptoethanol-capped ZnS occurs predominantly via crystallographically-specific oriented attachment (OA). Twins and stacking faults form in the coarsened mercaptoethanol-capped ZnS whereas more complex, closely spaced twins, stacking faults, and intergrowths are characteristic of coarsened H_2O-ZnS. At

longer reaction times, diffusion-controlled growth removes surface irregularities arising from OA to yield rounded particles with complex internal structures.

Growth and characterization of α-FeOOH nanoparticles

An especially important natural nanophase material is α-FeOOH (goethite) which is present in most soils. Of particular interest is the rate of goethite surface reactions with natural or anthropogenic toxic sorbates and organic soil components and how these are affected by particle size. By a combination of heat treatments and aging, nanogoethite with very narrow size distributions, a few nm, has been synthesized. Products have been characterized with dynamic light scattering (DLS), SAXS, extended x-ray absorption fine structure (EXAFS) spectroscopy, and TEM imaging. Real time SAXS studies of growth suggest that 5 nm primary goethite particles grow by oriented attachment, while larger particles may coarsen mainly through a diffusive process. EXAFS analysis of sorption of Hg, Zn, AsO_4 and Cu suggest that the number and type of reactive surface sites change with crystallite habit and diameter.

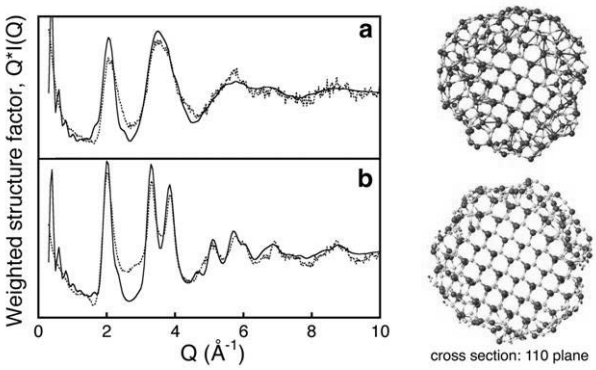

Figure 5. Wide-angle x-ray scattering (WAXS) observation of water binding. Experimental (dotted lines) WAXS Q-weighted structure factors of ZnS nanoparticles in methanol a, before and b, after water binding. Superimposed (solid lines) are the patterns predicted by molecular dynamics (MD) relaxation of a 3 nm ZnS particle a, without and b, with surface bound water. Shown on the right are views of the corresponding nanoparticle structures predicted by MD without (top) and with (bottom) surface water. Central cross-sections are given, showing the 110 plane, to better reveal the interior structure. In the absence of water ligands (top) the outer shell is severely distorted. WAXS data acquired at APS, Argonne. From Zhang, Gilbert et al. Nature, *2003.*

Publications

B. Gilbert, F. Huang, H. Zhang, and J. F. Banfield, "Surface modification of lattice dynamics in ZnS nanoparticles," *EOS Transactions, American Geophysical Union* **94** (46), Fall Meeting Supplement Abstract B11E-02, 2003.

B. Gilbert, F. Huang, H. Zhang, and J. F. Banfield, "Measurements of the internal strain and structural dynamics of ZnS nanoparticles," in preparation for submittal to *Science.*

H. Zhang, F. Huang, B. Gilbert, and J. F. Banfield, "Molecular dynamics simulations, thermodynamic analysis and experimental study of phase stability of zinc sulfide nanoparticles," *Journal of Physical Chemistry B* **107** (47), 13051 –13060 (2003).

F. Huang, H. Zhang, and J. F. Banfield, "Two-stage crystal-growth kinetics observed during hydrothermal coarsening of nanocrystalline ZnS," *Nano Letters* **3**, 373-378 (2003).

F. Huang, H. Zhang, and J. F. Banfield, "The role of oriented attachment crystal growth in hydrothermal coarsening of nanocrystalline ZnS," *Journal of Physical Chemistry B* **107**, 10470-10475 (2003).

H. Zhang, F. Huang, B. Gilbert, and J. F. Banfield, "Reversible, surface-controlled structure transformation in nanoparticles induced by aggregation-disaggregation," submitted to *Physical Review Letters.*

H. Zhang, B. Gilbert, F. Huang, and J. F. Banfield, "Water-driven structure transformation in nanoparticles at room temperature" *Nature* **424**, 1025-1029 (2003).

B. Gilbert, H. Zhang, F. Huang, Y. Ren, D. Haskel, J. C. Lang, G. Srajer, A. Jürgensen, G. A. Waychunas, and J. F. Banfield, "Analysis and simulation of nanoparticle structures observed in a surface-driven structural transformation," submitted to *Journal of Chemical Physics B.*

B. Gilbert, H. Zhang, F. Huang, M. P. Finnegan, G. A. Waychunas, and J. F. Banfield, "Special phase transformation and crystal growth pathways observed in nanoparticles," *Geochemical Transactions* **4**, 20-27 (2003).

B. Gilbert, B. H. Frazer, H. Zhang, F. Huang, J. F. Banfield, D. Haskel, J. C. Lang, G. Srajer, and G. De Stasio, "X-ray absorption spectroscopy of the cubic and hexagonal polytypes of zinc sulfide," *Physical Review B* **66**, 245205 (2002).

C.S. Kim, J.F. Banfield, and G.A. Waychunas, "Reactivity and speciation of heavy metals with nanoparticulate goethite," *EOS Transactions, American Geophysical Union* **84** (46), Fall Meeting Supplement, Abstract V51H-0380 (2003).

Environmental Energy Technologies Division

Miniaturized Systems for Particle Exposure Assessment

Principal Investigators: Michael Apte, Lara Gundel, and Anthony Hansen

Project No.: 02028

Project Description

This project is developing prototype instrumentation to advance knowledge about the relationship between exposures to particles and human health, a national research priority. At present, statistically-adequate studies of relationships between health outcomes and particle concentrations and composition are prohibited by high cost and limited capabilities of suitable instrumentation.

Using advanced sensor technology, we are prototyping the next generation of low-cost compact instrumentation for particulate matter (PM) exposure assessment. The Miniaturized System for Particle Exposure Assessment (MSPEA) will measure aerosol mass, size, and composition simultaneously.

In this project we are attempting to utilize a low-inertial particle collection mechanism that has been under-utilized in existing particle measurement technologies. The physics of this mechanism scale well with micro-electromechanical mass measuring devices such that the particle mass sensor can be integrated into very small packages—potentially to the scale of microchips.

The optical properties of the most abundant and harmful airborne particle species, i.e., diesel exhaust, environmental tobacco smoke, and wood smoke, are well understood; thus, enabling us to design simple optical probes that can differentiate between them when they are collected on a reflective or transparent surface. Advances in microelectronic light sources and detectors and fiber optics will enable us to integrate miniature optical probes into the miniature particle mass monitor.

Accomplishments

Optical particle characterization

We configured a miniature spectrometer (Ocean Optics) with a reflectance probe for continuous ultraviolet (UV) to near infrared (NIR) absorbance measurements of a quartz crystal microbalance (QCM) surface. The reflectance probe was positioned normal to the quartz crystal surface at a distance of 3 millimeters. To ensure reproducible positioning of the probe relative to the crystal surface, a miniature optical bench component was fabricated by the Design Works group of the Engineering Division to stabilize the crystal, wire, and optical probe (Figure 1a). The new fixture has three wires, in series, to increase collection efficiency. A quartz slide with high UV and NIR transmission was positioned between the heating wire and the face of the optics probe to prevent thermophoretic deposition of particles onto the probe. The slide was easier to clean than the probe surface. The probe was positioned so that its beam of light passed through the slide, past the heating wire, through the collected particle deposit to the reflective chrome surface of the quartz crystal electrode. The reflected light returned the way it came and thus passed twice through the deposited particles increasing the sensitivity of the optical measurement. The slide was farther from the heating wire than the mass-sensing crystal and, as a result, would collect less particles. However, whatever particles were collected on the quartz slide also enhanced the total light absorption.

The test fixture was exposed to environmental tobacco smoke (ETS) in our room-sized test chamber. Figure 1b shows the change of absorbance with time for blue light (450 to 480 nm) as one cigarette was smoked every four hours for 24 hours. The rate of change of the absorbance was directly proportional to the particle mass concentration measurements made by both an optical particle counter (OPC) and the MSPEA QCM-based mass sensor. The optical absorbance, OPC, and MSPEA measurements were calibrated using simultaneous measurements made with a cascade impactor quartz crystal microbalance. As expected, the ETS particles absorbed more blue (450 to 480 nm) than near infrared (696 to 725 nm) light at constant ratio. These regions are illustrated because light emitting diodes are available for these spectral regions that can be used to discriminate ETS from diesel-generated particles. Figure 1c shows 8-hour ambient PM data averaged from MSPEA and calibrated OPC sampling over three days. The estimated mass concentration eight-hour limit of detection is about 6 $\mu g\ m^{-3}$.

Thermophoretic mass collection

Theromophoretic particle collection efficiency increases with increasing temperature gradient between the heating wire and the collection surface. Measurements made with a 10 µm diameter thermocouple indicated that the temperature difference between the heating wire and the crystal surface was only 5° C in our current sensor configuration. While particle collection indeed occurred with this surprisingly small temperature gradient, our year one work with a free-standing quartz crystal indicated that the sensor's sensitivity could be greatly improved by decreasing the crystal surface temperature. A common approach to decreasing the temperature of an electrical component is to attach a heat sink, typically a finned aluminum block. However, placing a metal block in contact with the quartz crystal would dampen its vibration and substantially decrease its sensitivity to deposited mass. Heat can also be transferred via radiation and convection, although not as effectively as with as metal-to-metal conduction. When a black anodized, finned aluminum heat sink was placed within 1 millimeter of the crystal surface, opposite the surface facing the wire, the temperature gradient between the wire and the crystal increased from 5° C to 22° C. More specifically:

- *Quartz Crystal Temperature Response:* As with all piezoelectric quartz crystals, the crystals used in the MSPEA have resonant frequencies that vary with temperature. We conducted studies to overcome resulting limitations, as well as lower the sensor's limit of detection. We ultimately were able to design a new oscillator/mixing circuit.
- *Low-Power Flow Control:* We have devised and tested a low-cost, low-power flow control module for the MSPEA. Using a small lead-acid gel cell battery and a fan designed for laptop computers as an impeller and a hypodermic needle as a flow control orifice, we were able to maintain airflow through the MSPEA at 15.5 ± 0.3 cm2 min-1 for several weeks.

System Integration

Figure 1d depicts a conceptualized package for the MSPEA device.

Publications

M.G Apte, D.R. Black, L.A. Gundel, and A.D. Hansen, "Miniaturized system for particle exposure assessment," patent application submitted.

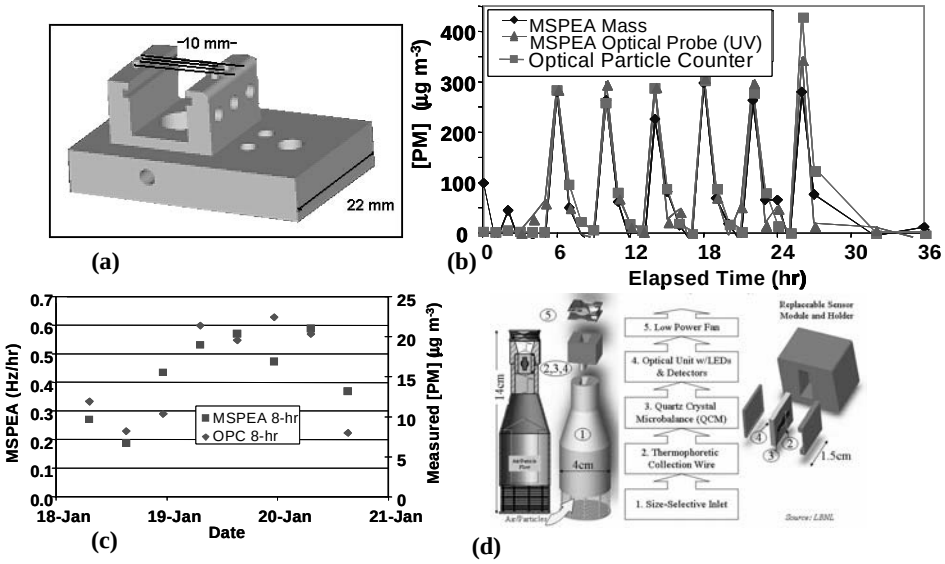

Figure 1. (a) MSPEA sensor fixture with heating wire. Components not shown include the collection crystal that rests on the posts that hold the wire, the quartz slide that is held by the notches below the wire, and the optical reflectance probe that passes through the hole centered beneath the wire. (b) Particle mass concentration measurements made by the MSPEA quartz crystal, an optical particle counter (OPC), and the rate of change of the UV light absorbance while one cigarette was smoked every four hours. (c) Response to ambient particulate matter at concentrations near limit of detection. (d) Conceptual design for integrated MSPEA system.

Determining the Light-Absorbing Properties of Aerosol Particles

Principal Investigators: Thomas Kirchstetter
Project No.: 03015

Project Description

This project is to develop a method to determine light absorbing properties of aerosol particles. Recent studies suggest that light absorption by atmospheric aerosols: (1) may be the second largest component of direct climate forcing after carbon dioxide, (2) impacts the hydrological cycle and regional climates, and (3) alters photochemical air pollution formation. Presently, limitations in analytical methods prohibit accurate determination of absorbing properties of aerosols and, thus, their realistic representation in climate models. To date, no method measures light absorption separately for the organic carbon (OC) and black carbon (BC) fractions of aerosol particles; measurements of the spectral light absorbance are scarce.

This work will develop a new method that combines two existing methods: the optical transmission method (e.g., as employed in an optical spectrometer) and the Berkeley Lab evolved gas analysis (EGA) method used for determination of aerosol carbon content. The new method will be employed in an instrument that simultaneously measures chemical and optical properties of aerosols samples to: (1) identify the different types of light absorbing carbonaceous material in aerosols, (2) measure the absorption efficiency for each type of absorbing aerosol component, and (3) determine the spectral dependence of aerosol light absorption.

It is intended that application of this method to aerosol samples collected in different fossil, biomass, and biofuel burning regions of the world will aid in determining the geographical variability in the absorbing properties of aerosols.

Accomplishments

Differences in the spectral dependence of light absorption by aerosols of different origin, including those collected in biomass burning regions and in urban areas, were demonstrated. The effect of OC on aerosol light absorbance was assessed by extracting the samples with acetone, which removed OC but left BC in tact. Sample carbon content was measured using the Berkeley Lab EGA method; light absorbance was determined by measuring light transmission through the filter-collected samples using an optical spectrometer and a newly constructed optical transmission device equipped with multiple discretely emitting diodes (MWLTI). Light absorption by aerosols produced from biomass burning exhibited enhanced wavelength dependency compared to diesel-dominated aerosols. The stronger wavelength dependence was marked by enhanced adsorption at wavelengths less than 600 nanometers, and the enhancement was largely reduced when the OC aerosol fraction was extracted. The weaker spectral dependency of the diesel aerosols was similar to that predicted using the small particle limit of the Mie equations assuming a wavelength independent refractive index—in agreement with other studies of BC optical properties. An apportionment of light absorption by the biomass smoke aerosol suggested that the OC absorbed about 50% and 25% of light at 350 nanometers and 500 nanometers, respectively.

Light transmission measurements made with backup quartz filters revealed that organic gases emitted during biomass burning adsorb to quartz filters and absorb light at wavelengths less than 400 nanometers. (A backup filter is a filter that is placed behind the filter that collects particles. The backup filter is subjected to gases, but not particles, since the front filter exhibits nearly 100% particle removal efficiency.) Therefore, light absorption at wavelengths less than 400 nanometers by particle-laden quartz filter samples may be due to collected particles and adsorbed gases. Thus, we have discovered that the same, well-known, artifact that leads to over estimated mass concentrations of particulate OC also may lead to over estimated attribution of light absorption to particulate OC, and thus it must be considered in the course of this work.

Two working prototype instruments were developed. The first is the MWLTI and the second is a single wavelength version of the instrument that is the centerpiece of this proposal: a multiple wavelength thermal-optical EGA system. The MWLTI was first designed with six light sources (LEDs) and is presently being upgraded to accommodate eleven LEDs for more complete coverage from the UV-A to the near-IR spectral regions. The detector is a silicon photodiode capable of measurement over this region. The optical EGA also employs multiple LEDs and a silicon photodiode. Optical interference filters and polished quartz rods are necessary optical components of the EGA in its present design. A ceramic sample holder that also aligns the quartz light guides was fabricated at Berkeley Lab. Initial development of the optical EGA has focused on instrument stability, signal to noise issues, and optical interference from the furnaces that are used to heat samples. At all wavelengths, optical interference filters eliminated or greatly minimized optical interference. Methods to further reduce optical interference are being considered. Low current output from the silicon photodiode detector (down to tens of nanoamps) is measured with a picoammeter. Presently a single wavelength instrument, the method of

multiple wavelength light transmission is possible only by repeated analysis of a sample. The multiple wavelength method is presently being developed.

Aerosol samples have been collected in different regions, including Nepal, Mexico City, Berkeley, and Oklahoma. Sample collection in Nepal was coordinated with SCRIPPS Institution of Oceanography in support of the Atmospheric Brown Cloud-Asia study.

Publications

T.W. Kirchstetter and T. Novakov, "On the wavelength dependence of light absorption by atmospheric aerosols," in preparation for submission to *Geophysical Research Letters.*

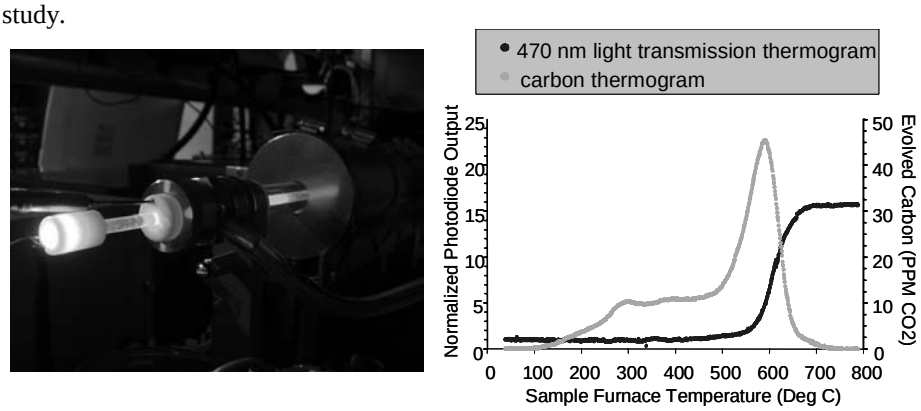

Figure 2. Prototype multiple wavelength optical evolved gas analysis apparatus (shown here with single blue wavelength capability) and plots of concurrently obtained data using this instrument: transmission of light through a filter-collected aerosol sample and thermally evolved carbon content.

Health Effects of Indoor and Outdoor Particle Concentrations, Assessed with Epidemiology

Principal Investigators: Mark Mendell

Project No.: 02029

Project Description

The scientific goals of this project are: (1) to advance scientific knowledge about the health effects of particles, by evaluating the association of respiratory symptoms with exposures to indoor and outdoor particle concentrations and by determining the protective effects of filtration systems; and (2) to evaluate the feasibility of conducting an innovative epidemiologic study to assess health effects of outdoor particles separately from those of outdoor gaseous pollutants, and also to assess the benefits of enhanced filtration in protecting a susceptible population against outdoor particles.

This study will contain two main elements. The first element focuses on analysis of a unique epidemiologic data set from 100 U.S. office buildings, to determine if respiratory symptoms are associated more strongly with indoor than with outdoor concentrations of particles, and more with fine than with coarse particles. The second element involves evaluating the feasibility of several innovative epidemiologic studies to assess health effects of indoor exposures to particles originating outdoors. These studies use differences in air filtration to isolate effects of particle and gaseous pollutant exposures and to quantify benefits of higher efficiency filtration for susceptible populations. Evaluated designs will include a large observational follow-up study of major health events, in multiple facilities with differing protection of occupants from outdoor particulate pollutants, and a smaller intervention study assessing the effects on clinically monitored health parameters of improved protection from particulate pollutants in residential buildings

Accomplishments

This project included two elements related to advancing scientific knowledge about the health effects of particles in indoor environments.

For the first element, we completed a multivariate analysis, using a large existing dataset of environmental and health data collected from 100 representative U.S. office buildings. The analysis focused on the relationships between respiratory or irritant symptoms in building occupants and indoor concentrations of particles of two sizes: aerodynamic diameters less than 2.5 μm ($PM_{2.5}$), and from 2.5 to 10 μm ($PM_{2.5-10}$). Associations of symptoms with related building factors, such as efficiency of particle filters in ventilation systems and frequency of filter change

were assessed simultaneously, along with a variety of other building and personal factors, in mixed effects multivariate logistic regression models that adjust for potential correlation among occupants in each building. Analyses showed that indoor concentrations of both particle sizes, inside and outside the study buildings, were extremely low. Concentrations of particles, inside or outside, showed suggestive, but not consistent relationships, to lower respiratory or mucous membrane symptoms among the occupants.

More specifically, there was a nonsignificant tendency for a higher prevalence of building-related lower respiratory symptoms with the top three quartiles of indoor fine particles (10 to 30% increases in symptoms, with 5.4 to 10.8 $\mu g/m^3$ of $PM_{2.5}$), but no relationship with eye, nose, or throat irritation symptoms. There was a significant 40% increase in prevalence of eye, nose, or throat irritation with the third quartile of indoor coarse particles (11 to 22 $\mu g/m^3$ of $PM_{2.5-10}$), but no increase with the highest quartile, and a nonsignificant reduction in lower respiratory symptoms in the highest quartile of coarse indoor particles. Regarding filtration efficiency, measured on the minimum efficiency reporting value (MERV) scale, analyses showed a surprising and unexplained relationship in our data. The *more* efficient the particle filtration in the HVAC systems, the greater the frequency of symptoms. For instance, for the highest two quartiles of filter efficiency, occupants were 130 to 190% more likely to report lower respiratory symptoms. A weaker relationship was evident for eye, nose, or throat irritation symptoms, with the higher two quartiles of filter efficiency associated with nonsignificant 30 to 60% increases in frequency. This set of somewhat surprising findings, summarized in Table 1, require confirmation and replication.

A draft paper of this analysis is being completed and will be submitted for publication in a peer-reviewed journal. This project helped us to demonstrate our strong capabilities in multivariate statistical analyses of epidemiologic data, providing the foundation for a research proposal to the National Institute for Occupational Safety and Health, and also for an informal proposal to the U.S. Environmental Protection Agency. Decisions on funding are pending.

For the second element, we evaluated the feasibility of four approaches to assess health effects of indoor exposures to particles originating outdoors, and chose the most promising to develop. We have completed the initial design in a projected research program to experimentally prevent selected components of the ambient pollutant mixture from entering indoor air over extended periods, and to measure associated changes in a variety of acute health effects. The research would be conducted with susceptible individuals who spend most of their time within their residences, and in climates/seasons in which windows and doors are seldom opened. We determined that the initial study in the program, using a newly developed fan/filter unit to ventilate and positively pressurize residences, would experimentally prevent entry of essentially all outdoor particles into the residences of susceptible subjects, such as elderly with respiratory or cardiovascular disease or asthmatics. The process would not significantly influence the entry of outdoor gaseous pollutants or the concentrations of indoor-generated pollutants. The initial measured health outcomes would be noninvasive indicators of lung inflammation, such as exhaled nitric oxide, potentially related to asthma. A controlled, multiple crossover experimental design would allow comparison of health effects during periods of normal particle and gas entry into each unit with periods of only gas entry. This strategy could provide new estimates of the acute effects of ambient particulate pollutants over weeks or months, independent of the effects from other pollutants that do not change systematically across the experimental conditions. It will also assess potential benefits of sheltering susceptible individuals from these pollutants. This strategy combines advantages of field studies and short-term controlled laboratory exposure studies. The current study design has been described in a draft Berkeley Lab report and provided the basis for a research proposal to the Health Effects Institute.

Risk Factors/Covariates	Mucous Membrane		Lower Respiratory	
	OR	95% CI	OR	95% CI
Fine indoor particle concentrations ($\mu g/m^3$)				
≤ 5.4	1.0	---	1.0	---
> 5.4- ≤ 7.2	1.2	0.9-1.6	1.2	0.8-1.9
> 7.2 - ≤ 10.8	1.0	0.8-1.3	1.1	0.8-1.6
> 10.8	0.9	0.7-1.2	1.3	0.9-2.2
Coarse indoor particle concentrations ($\mu g/m^3$)				
≤ 2.4	1.0	---	1.0	---
> 2.4 -≤ 3.9	1.0	0.8-1.3	1.0	0.6-1.5
> 3.9 -≤ 5.6	1.4*	1.1-1.8	0.9	0.6-1.3
> 5.6	1.1	0.8-1.4	0.7	0.4-1.0
Filter Efficiency (MERV)				
≤ 6	1.0	---	1.0	---
>6 to ≤ 7	0.9	0.7-1.3	1.3	0.8-2.0
> 7 - ≤ 12	1.3	0.9-1.8	2.9*	1.9-4.6
> 12	1.6	0.8-1.6	2.3*	1.5-3.4

* P-value < 0.05

Table 1. Adjusted odd intervals (CIs) for associations between symptom outcomes among occupants and risks related to indoor particle exposures and particulate filtration efficiency, in the EPA BASE data collected from U.S. office buildings, 1994-1998. MERV = minimum efficiency reporting value, a scale of filter efficiency that emphasizes a filter's ability to retain the hardest-to-filter particles (around 0.3 μm in diameter).

Publications

M.J. Mendell, M. Cozen, M.G. Apte, M.J. Lipsett, and W.J. Fisk, "Reducing indoor exposures to specific outdoor-generated pollutants: a proposed approach to estimating the health effects of ambient pollutants and protecting susceptible individuals," draft in preparation for Berkeley Lab report.

M.J. Mendell, M. Cozen, M.G Apte, and M Lahiff, "Particle concentrations, filter characteristics, and symptoms among office workers in 100 U.S. office buildings: analyses of the EPA BASE Data," to be submitted to *Indoor Air*.

Evaluation of Dynamic Air Quality Impacts of Distributed Generation

Principal Investigators: Robert Van Buskirk and Shaheen Tonse

Project No.: 03034

Project Description

A critical challenge for the atmospheric sciences is to understand the anthropogenic impacts on atmospheric chemistry over spatial scales ranging from the urban, to the regional, and ultimately to the global, over corresponding time scales ranging from minutes to weeks and ultimately annual trends. A similar challenge for energy policymakers is to integrate an understanding of air quality impact dynamics into the economic dynamics of energy supply and demand. The need for dynamic analysis of emissions impacts from the energy sector has substantially increased with a new focus on emerging distributed energy resources (DER).

We are building a long-term approach to perform integrated analysis of the dynamic economic, meteorological and air chemistry impacts, and effects from distributed generation and ultimately from a diversity of combustion-based emissions. Our approach explicitly integrates the economic demand/supply price dynamics with meteorology, emissions, and atmospheric chemistry dynamics for application to optimized emissions regulation. The problem is challenging due to the inherent non-linearity of the photochemistry at all spatial scales, the difficulties in simultaneously representing atmospheric fluid dynamics at different scales within a numerical model, and the complex geographic and temporal dynamics of the economics of electricity markets and distributed energy demand and supply. This project is to initiate this effort by building a modeling system that integrates component models that are the product of previous research.

Accomplishments

During the first year of this project, we have developed the basic foundation for integrated modeling of distributed generation air quality impacts:

- Meteorological modeling is performed by Mesoscale Model 5 (MM5) with runs completed for a four kilometer resolution 190x190 grid centered at 37.0ºN latitude, and 120.5ºW longitude and for a sample of periods over the year 2000 summer, focusing initially on the July 28 to August 5 episode.
- The baseline emissions inventory of Rob Harley and Linsey Marr has been acquired and converted for use in the air quality model.
- The Models-3/CMAQ modeling system is configured and has been run for the July 28 to August 5 episode for multiple cases to perform an initial examination of incremental air quality impacts.
- A distributed generation air quality policy review was conducted.
- Statistical analyses have been performed for Environmental Protection Agency (EPA) data on generation emissions contained in the eGRID database.
- Additional analyses have been performed on hourly generation emissions data from the EPA to better characterize marginal emissions from utility generation as a function of system electricity demand.
- Initial draft dynamic policy/price metrics have been formulated for characterizing incremental air quality impacts.
- An initial examination of the economic cost of agricultural pump air quality impact mitigation in the Central and San Joaquin Valleys has been performed.

Some of the very tentative findings of the investigations to date include:

- It is possible for marginal emissions intensities from utility generation to vary by up to a factor of ten between low demand and peak demand times.
- Given relatively large errors of high time resolution wind fields, characterization of air quality impacts through the simulation of statistical ensembles of episodes may be more reliable than targeted, specific simulations of particular air quality episodes.

- Incremental impacts of generation emissions on ozone concentrations have high geographic variability with near-field impacts tending to be negative for the July 28 to August 5, 2000, episode and far-field impacts tending to be positive during the daytime.
- The air quality mitigation cost of pumped groundwater in the Central and San Joaquin Valleys is likely to be of the order of $5 per acre-foot.

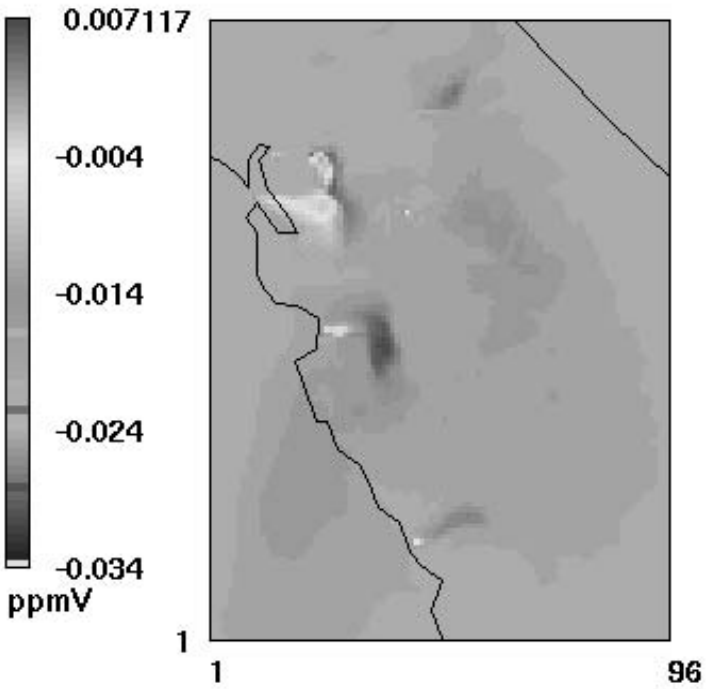

Figure 3. A simulated incremental ozone concentration impact from central power plants at 3:00 p.m. on a hot summer day on a 117x96 computational grid of California.

Genomics Division

Identification and Characterization of Conserved Noncoding Sequences Using Comparative Genomics and Transgenic Technology

Principal Investigators: Edward Rubin

Project No.: 03034

Project Description

Gene regulatory sequences embedded within 98% of the human genome are noncoding. Determining the level, the timing, and the location of gene expression is essential. Unfortunately, identification and characterization of these functional sequences has been extremely slow due to the difficulty in distinguishing them from other noncoding sequences. Thus, the goal of this project is to use comparative genomics and subsequently *in vivo* studies to discover and characterize the function of evolutionarily conserved noncoding sequences (CNS) that regulate the expression of genes.

The bacterial artificial chromosome (BAC) transgenic mouse system has been extremely informative in identifying and functionally characterizing noncoding regulatory elements. Generating stable transgenics has, however, been a slow, labor intensive, and expensive process. To sift through a large number of CNSs relatively quickly and to link these sequences to function in a high throughput manner, we will employ an alternative strategy, that of transient transgenesis.

Accomplishments

To achieve this goal, we first identified CNSs that reside in two gene deserts bracketing human DACH, a gene expressed in numerous tissues and involved in the development of brain, limbs, and sensory organs. To examine the possibility that these sequences, conserved over one billion years of parallel evolution, might represent enhancers, we explored their *in vivo* ability to drive gene expression with the use of a reporter assay system in transgenic mice. Nine elements were tested, spread over a 1530-kb region surrounding the human DACH's TATA box. Each corresponding human element was individually cloned upstream of a mouse heat shock protein 68 minimal promoter coupled to ß-galactosidase and injected in fertilized mouse oocytes. The embryos were examined at embryonic days 10 through 13 for spatial and temporal patterns of gene expression. Seven elements were shown to reproducibly drive ß-galactosidase expression in a distinctive set of tissues in transgenic mice, recapitulating several aspects of DACH endogenous expression. The demonstration that several of the enhancers characterized in this study reside in gene deserts highlights that these regions can indeed serve as reservoirs for sequence elements containing important functions.

Our strategy to use comparative genomics to identify putative regulatory elements and then determine the role of these elements in the regulation of gene expression using transient transgenesis assay has been successful.

Publications

M. Nobrega, I. Ovcharenko, V. Afzal, and E. Rubin, "Scanning human gene deserts for long-range enhancers," *Science* **302**, 413 (2003).

Biomechanics of Cell Matrix Adhesion in Normal and Malignant Mammary Epithelial Cells

Principal Investigators: Jordi Alcaraz, Mina Bissell, and Carlos Bustamante

Project No.: 03003

Project Description

Cells within a tissue are continuously exposed to signals from their local microenvironment. Depending on the nature of these signals and how they are processed, cells will divide, apoptose, or differentiate. Among the different components of the microenvironment, the extracellular matrix (ECM) plays a major role in regulating cell fate. In particular, the correct cell-ECM communication is fundamental for the regulation and maintenance of tissue structure, while a loss of this communication has been shown to be a key factor in the acquisition of a malignant phenotype. The initiation of ECM signaling involves its binding to integrins and other cell membrane receptors, depending on the affinity and avidity between ECM ligands and these cell receptors. Adhesion forces of different strengths and kinetics are expected. Although a lot of experimental work has been carried out to elucidate the biochemistry of this cell-ECM interaction, little is known about the biomechanical signals. The main goal of this interdivisional project was to determine the biomechanics of cell-ECM adhesion in normal and malignant cells using the mammary epithelial cell models available in Mina Bissell's lab and the biophysical techniques from Carlos Bustamante's lab.

Given the fact that integrins are linked to cytoskeletal filaments, which in turn provide mechanical and shape stability to the cytoplasm and to the nucleus, we hypothesized that ECM could directly signal to the nucleus through the physical molecular connections between the cell membrane, the cytoskeleton (CSK), and the nuclear envelope. Previous studies in Bissell's lab showed that the β-casein gene expression is regulated by ECM in mammary epithelial cells and is correlated with a dramatic shape change. This previous work allowed us to expand the proposed aims of characterizing cell-ECM adhesion and measuring the transmission of forces from the ECM to the interior of the cell to include determination of the effect of mechanical signals at the level of gene expression. The measurement of ECM induced forces was addressed as proposed at the single cell level using the Atomic Force Microscope (AFM) available in Bustamante's lab. In addition, we also use the more straight forward approach to study the effect of mechanical signals on β-casein expression by analyzing many cells simultaneously and by utilizing all the molecular biology techniques available for detection and quantification of gene expression. For these studies, we purchased a commercially available Flexcell System which allowed us to culture the cells on a mechanically active substrata. This technique allowed us to apply defined mechanical strain to cells cultured in the presence of ECM and to determine the effect of these mechanical signals on β-casein expression. The complexity of the performance and interpretation of these biomechanical experiments in normal cells has made us postpone the examination of the behavior of malignant cells.

Accomplishments

We had previously shown that mammary epithelial cells cultured on top of laminin-rich ECM (Matrigel) are able to express β-casein. This expression is accompanied by a dramatic shape change in which the cells take on a completely rounded morphology. In contrast, the same cells cultured on a standard plastic surface do not express β-casein and exhibit a flattened morphology. We further characterized how the ECM organizes the cytoskeleton (CSK) of these cells by measuring their mechanical properties by using atomic force microscopy and by visualizing of the actin network by immunofluorescence staining. We found that cell rounding is associated with a decrease in tensional forces, as seen in the four-fold decrease of the elastic modulus in cells cultured on top of Matrigel as opposed to cells cultured on tissue culture plastic, see Figure 1. However, the dynamic mechanical behavior of cells as measured by atomic force microscopy was similar in both conditions. This suggests that the CSK has a similar complex organization with and without ECM signaling, while ECM more directly affects the CSK elements responsible for the overall cell stiffness. The analysis of the actin cytoskeleton by fluorescence microscopy shows that cells on plastic exhibit stress-fibers; whereas, cells on top of Matrigel do not exhibit these stiff structures and the actin is mainly cortical. This ECM reorganization of the actin CSK could partially explain the decrease in tensional forces measured by AFM. The correlation between changes in morphology, tensional forces, and gene expression strongly supports the model that cell adhesion to the ECM triggers a reorganization of the CSK in mammary epithelial cells that becomes apparent through the change in cell morphology and in the cell's

internal mechanical tension. Together with the ECM-induced activation of biochemical pathways, the ECM-induced change in mechanical tension may deliver a mechanical signal to the nucleus necessary for the activation of the transcription of the β-casein gene. To further explore the validity of this model, we are currently developing an experimental approach for visualizing the activation of the β-casein gene in single living cells.

The effect of mechanical signals on β-casein expression was explored: (1) by subjecting mammary epithelial cells cultured in the presence of laminin-rich ECM to different types of strain and (2) by checking the effect of the mechanical manipulations on the levels of mRNA and intracellular and extracellular β-casein. We found that different mechanical signals had different effects on the β-casein expression. While the most dramatic effects could be detected in the levels of extracellular β-casein, we could also detect effects on the mRNA and intracellular levels. These data show that β-casein secretion can be regulated by mechanical signals and suggest that transcription and expression are also likely to be sensitive to mechanical manipulation. However, the underlying mechanisms of such mechanical regulation of gene expression are not well understood and are currently under investigation.

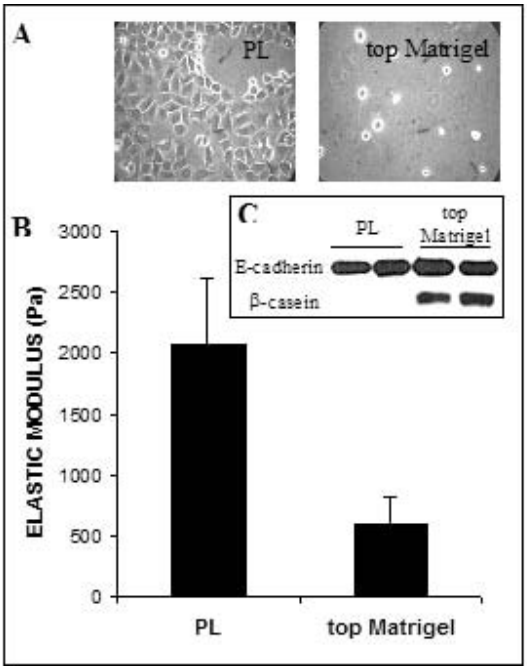

Figure 1. Relationship between (A) cell shape phase-contrast, 40X, (B) stiffness atomic force microscopy; mean ± sem, n=7 for PL, n=4 for top, β-casein expression and (C) (western blott; E-cadherin is used as a loading control in normal mammary epithelial cells cultured on plastic (PL) and on top of a laminin-rich ECM, Matrigel.

Dynamic Reorganization of Chromosome Architecture during Meiosis

Principal Investigators: Abby Dernburg

Project No.: 01024

Project Description

All sexually reproducing organisms rely on a special cell division process called meiosis to generate gametes, which contain only a haploid number of chromosomes. The central event of meiosis is a reductional division in which pairs of homologous chromosomes must segregate to different daughter nuclei. The accuracy of this unique division depends on recombination, the presumed raison d'être of the entire process, which in turn requires that each chromosome must find and pair with its appropriate homologous partner. Errors in meiosis lead to missegregation with disastrous consequences if an embryo inherits an abnormal number of chromosomes.

We will study the complex macromolecular structures that are built and disassembled during meiosis. We will harness both the molecular genetic and cytological advantages of the tiny soil-swelling nematode, *C. elegans*. This integrated approach will bridge the gap between individual gene products and large-scale meiotic structures.

The long-term goal of this project is to understand the relationship between structural elements and their function in the meiotic nucleus. In our initial experiments we will:

- Visualize and quantify the dynamic properties of meiotic chromosomes.
- Probe the role of chromosome architecture in controlling the distribution of crossovers.
- Investigate the essential role of the meiotic "pairing center" and associated proteins.

The project will integrate several technological approaches including, three-dimensional imaging, functional genomics, and genetics. We will use genetics to identify and characterize novel components of the chromosome-organizational machinery that remodels the nucleus during meiosis. Using high-resolution fluorescence imaging, we will localize molecular components at the subcellular level to learn how they contribute to nuclear modeling.

Accomplishments

Addressing the first aim, *in vivo* analysis of chromosome dynamics has been our most technically challenging goal. We are continuing to optimize ballistic transformation technology to generate transgenic *C. elegans* expressing fluorescent fusion proteins. To enhance this effort, we have also recently designed a synthetic gene to express a very rapidly-folding and pH-insensitive variant of yellow fluorescent protein known as Venus, with optimized codon usage for *C. elegans*. We are currently testing the performance of this construct in somatically-expressed fusion proteins and if it meets our expectations, we will shuttle it into our germline expression vectors. In parallel, we have developed a number of computational analysis tools for quantitative analysis of chromosome dynamics; among these is a molecular dynamic simulation approach that has led us to a new hypothesis about chromosome movement. We believe that large-scale chromosome reorganization that we observe during meiotic prophase may be driven by alterations in the surface properties, e.g. electrostatic interactions of meiotic chromatin. This unconventional model for large-scale chromosome organization predicts that essential components of meiotic chromosome pairing should undergo post-translational modification through the course of meiotic progression. We have raised polyclonal antibodies against a number of interesting candidate proteins and we are testing this idea experimentally using protein blotting methods.

The second aim is to experimentally link the regulation of meiotic crossover distribution to large-scale chromosome structure. This was our least well-defined goal at the outset because so little is understood about the molecular basis for crossover control. Work over this granting period has provided a compelling entry point to better understand this phenomenon. Specifically, we have observed that mutations that specifically perturb synapsis of a single chromosome cause a delay in the zygotene-pachytene transition and also cause an increase in recombination on the other chromosomes. This is similar, perhaps identical, to the interchromosomal effect known from genetic studies in *Drosophila*.

We are carrying out detailed recombination analysis to determine whether this global increase in recombination results from a reduction in genetic interference, as we suspect. If so, this enables us to identify molecular components responsible for crossover interference, one of the most far-reaching and poorly-understood aspects of meiotic regulation. As an important milestone in this project, we have recently identified a novel regulator of sex chromosome behavior in *C. elegans*, known as *him-8*. Mutations in this gene specifically impair synapsis and recombination of the *X* chromosome. Through mapping and sequencing of mutant alleles we have shown that this gene encodes a recently-evolved zinc-finger protein, and we are pursuing a detailed analysis of this gene's function in regulating sex chromosome organization and interactions. In addition, we have carried out an analysis of two mutations in genes that modify meiotic chromatin by adding and removing poly-ADP-ribose groups, a Poly-ADP-Ribose Polymerase (PARP) and a Poly-ADP-Ribose Glycohydrolase (PARG), respectively. We found that PARG mutations make germline nuclei extremely hypersensitive to DNA damage induced by ionizing regulation and that this sensitivity can be overtly suppressed by treatment of worms with a PARP inhibitor. However, while more PARP-inhibited worms survive following radiation treatment, these animals show very high frequencies of mutations and infertility, both of which are indicators of genomic rearrangements. This work is shedding light on the mechanisms that safeguard genome integrity during meiotic recombination, which requires the function of DNA repair enzymes and damage-sensing checkpoints.

For the third aim, one graduate student and one postdoctoral fellow are focusing on a molecular dissection of meiotic pairing center (PC) function. Carolyn Phillips' efforts have been focused on more precisely identifying the region of the *X* chromosome that contains PC function. As of a year ago, this site had been mapped to a region of about two megabases, roughly 10% of the chromosome. Through systematic physical mapping of deletions and other chromosome rearrangements, she has localized the PC to within the most distal 125 kilobases of the *X* chromosome. With this new information, we have been able to eliminate a number of candidate sequences and have become focused on a detailed analysis of this small stretch of the chromosome. In particular, we have identified an unusual repetitive element that is enriched in this region, and which also shows a distribution on the five autosomes that is consistent with a role in mediating PC function. Currently, we are working to define a functional role for this element or associated sequences in meiotic chromosome behavior by making transgenic animals that carry many extra copies of these sequences.

Needhi Bhalla is identifying *trans*-acting pairing center components. She has characterized genetic interactions between mutations that compromise PC function and other known meiotic mutations; this analysis has indicated that PC lesions dramatically sensitize worms to additional defects in chromosome structure and pairing components. This provides a very useful and efficient way to screen for these components by reverse genetics. She is also pursuing an observation reported last year that defects in synapsis are monitored by a checkpoint that triggers apoptosis. Her work has shown that cell death in response to unsynapsed chromosomes occurs in the absence of essential components of the DNA damage checkpoint, indicating the function of a distinct synapsis checkpoint. The existence of such a checkpoint has been suggested by evidence in organisms from yeast to humans but has been difficult to dissect because in most organisms; synapsis is dependent

on double-strand breaks. Because synapsis can be uncoupled from DNA breaks in *C. elegans*, we are in an excellent position to identify and characterize components of this regulatory mechanism, some of which are likely to emerge from the genome-wide screen Needhi has initiated to identify PC components by RNA interference (RNAi).

Publications

A.F. Dernburg, Meiosis Researchers Exchange Information in the Alps, Meeting Review, *Developmental Cell* **5**, 691–3.

Enabling Bioinformatic Analysis of Regulatory Information in Animal Genomes through the Systematic Determination of in vitro DNA Binding Specificities of Regulatory Proteins

Principal Investigators: Mark Biggin and Michael Eisen

Project No.: 03010

Project Description

The purpose of this project is to dramatically increase our ability to understand regulatory information encoded in genomic DNA by systematically determining the DNA binding sequence specificities of all transcription factors regulating gene expression in the early *Drosophila* embryo. These data will enable further development and deployment of bioinformatics tools we have recently developed for characterizing and understanding regulatory information in the *Drosophila* genome. The data will also allow us to create computational tools to infer transcription factor binding specificities from sequence, expression, and comparative genomics data alone, which will enable the analysis of transcriptional networks in other sequenced organisms.

We will develop a new, more extensive *in vitro* DNA binding selection method in which low, medium, and high-affinity binding sites will be selected from pools of random oligonucleotides and be identified en masse by concatemerization and high-throughput DNA sequencing. After establishing this method, we will express full-length protein and/or DNA binding domains for ~100 *Drosophila* transcription factors in bacteria—or, if necessary, insect cell-lines, purify the proteins using affinity tags, and determine *in vitro* DNA binding of all proteins. These data will be used together with genomic DNA sequence information to extend bioinformatics algorithms we recently developed to allow the first system-wide analysis of an animal transcription factor network and to decipher non-protein-coding DNA**.**

Accomplishments

Our most significant accomplishment has been to develop a reproducible protocol for preparing active, soluble proteins. Our method uses renaturation by dilution, followed by affinity purification to concentrate the protein. This has been successfully used to prepare five *Drosophila* transcription factors—hunchback, Kruppel, relish, knirps and dorsal—that were insoluble using other methods. We are hopeful that this method will be generally applicable to most proteins, which will greatly aid our future goal of analyzing up to 100 *Drosophila* factors.

We have also succeeded in establishing the proposed SELEX method, a method that can quickly and cheaply derive data for thousands of DNA binding sites. We have applied this method to study binding of one factor so far, hunchback. As we had hoped, our approach provides a significantly clearer and more detailed description of this factors DNA binding specificity than was available from the literature. We are now testing if this additional data helps predictions of functional hunchback sites in the fly genome.

We are in the process of applying these protein expression and SELEX binding assays to further proteins.

As a result of this work, we obtained a $15 million grant for five years from the National Institute of General Medical Sciences (NIGMS) to fund scale up of this project to examine binding of all *Drosophila* factors. This grant will also fund collection of additional data classes to help model transcriptional regulatory networks and learn how to decode animal genome sequences.

Structural Studies of Presenilin-1, a Membrane Protein Critical to the Onset of Alzheimer's Disease

Principal Investigators: Bing Jap

Project No.: 02030

Project Description

Defects in γ-secretase have been associated with early onset of Alzheimer's disease. It has recently been shown that four membrane protein subunits (presenilin-1, nicastrin, APH-1 and PEN-2) are necessary to form catalytically active γ-secretase. Presenilin-1 is the catalytic component of γ-secretase, which cleaves the C-terminal end of the amyloid precursor protein (APP); together with the

cleavage at the N-terminal end by β–, this process produces amyloid β fragments (Aβ), which form amyloid plaques that are characteristically present in the brain of Alzheimer's patients. This enzyme complex is a novel aspartyl protease having the catalytic active site embedded in the membrane. Mutations of presenilin-1 and/or its homologue presenilin-2 have been associated with the cause of an aggressive form of Alzheimer's disease and are potential targets for therapeutic drugs.

The aim of this project is to purify γ-secretase from HeLa cells for subsequent crystallization trials and x-ray crystallography structure determination. This involves the development of the purification protocol for γ-secretase from HeLa cell membranes and the characterization of the purified protein complex. When purified γ-secretase complexes are available, we will determine whether the four known components are the only components of the complex. Efforts outside the scope of this project will be needed to determine the molecular structure of γ-secretase. The structure should provide us with atomic details of this novel protein enzyme, yield insight into the mechanism of its proteolytic activity within the membrane, and help in the design of therapeutic drugs.

Accomplishments

Very recently, it has been shown that four membrane protein subunits (presenilin-1, nicastrin, APH-1, and PEN-2) are necessary to form catalytically active γ-secretase. It became clear that a complete understanding of the functional mechanism of γ-secretase would require that the structure of the complex be determined. Our efforts have accordingly changed from determining the structure of presenilin-1 to that of the entire complex. To this end, we have evaluated a few chromatographic columns for purifying γ-secretase from HeLa cell membranes. Our preliminary data indicates that about 0.3 milligrams of the γ-secretase protein complex can be obtained from about 100 liters of HeLa cell culture. This amount of protein is adequate for our crystallization trials utilizing recently developed microfluidic techniques that allow crystallization experiments to be performed with sample volumes on the order of ten nano-liters per crystallization condition.

We have developed a protocol for the purification of γ-secretase from HeLa cell membranes. Briefly, cell membranes isolated from HeLa cells were solubilized with FOS-CHOLINE detergent and then applied to a Q-Sepharose HP column. The bound proteins were eluted with a step gradient and fractions containing γ-secretase, as identified by Western blot with antibody against nicastrin (N1660, Sigma), and were found to elute at a salt concentration of 100 to 200 mM NaCl. These fractions were pooled and then loaded onto a lentil lectin column; the bound proteins were eluted with 200 mM alpha-mannopyranoside. The eluted fractions were pooled and concentrated, and then further purified by molecular sieve chromatography. An aliquot of the purified sample was applied to a 4 to 20% SDS-PAGE gel (Bio-Rad) and the gel was stained with Coomassie blue. The gel shows six major protein bands, five of which have molecular weights similar to the known weights of the γ-secretase components: nicastrin (~110 kDa), presenilin-1 NTF (~33 kDa), presenilin-1 CTF (~20kDa), Aph-1 (~30 kDa) and PEN-2 (~14 kDa). The identification of these five bands were confirmed by Western blot using anti-nicatrin (N1660, Sigma), anti-presenilin-1 NTF (SC-1245, Santa Cruz Biotechnology, Inc), anti-presenilin-1 CTF (MAB5232, CHEMICON), anti-PEN-2 (provided by Dr. Kim, Columbia University) and anti-APH-1 (provided by Dr. G. Yu, University of Texas, Southwestern Medical Center). In addition to these five bands, we detected an additional band (45 kDa) that is not likely associated with the product of nicastrin proteolysis, as it is not recognized by the C-terminal-end directed nicastrin antibody, since to produce the 45 kDa band would require the removal of part of the N-terminal domain of nicastrin as well as part of the C-terminal end. The 45 kDa band is also not likely to be from a full-length presenilin-1 since the band is not recognized by anti-presenilin-1 NTF and anti-presenilin-1 CTF antibodies in the Western blot. This band therefore could be an, as of yet, unidentified component of the γ-secretase complex. This additional band is currently being characterized to determine if it is indeed a previously unidentified component of the γ-secretase complex.

Identification and Analysis of Determinants of Centromere Identity in Drosophila *(CID)*

Principal Investigators: Gary Karpen

Project No.: 03032

Project Description

Chromosome replication and transmission are essential for the inheritance of genetic traits. The centromere is a chromosomal locus that serves as the key attachment site to the spindle during mitosis and meiosis. A pressing question in the centromere field today is how centromere identity is propagated from one generation to the next in multicellular eukaryotes. Elucidating the determinants of centromere identity, propagation and function requires identification of the gene products that promote centromere formation and function in *trans,* and determining how they interact with the *cis*-acting elements to perform their essential functions.

In essence, we need to understand the organization, replication, and modification of centrometric chromatin.

We propose genetic, molecular, cell biological, and biochemical experiments designed to identify and characterize gene products that promote the assembly and propagation of centromeric chromatin in *Drosophila* and to determine their properties and functions. We will also conduct experiments to elucidate the organization of centromeric proteins and chromatin and their hierarchy. Our entry point into centromeric chromatin and DNA will be a conserved histone H3-like protein (CENP-A) that localizes exclusively to functional centromeres.

Accomplishments

We have made substantial progress in identifying and studying proteins involved in determining centromere identity. By demonstrating the following key points, we have laid the groundwork for the experiments proposed for FY04:

- Overexpression of CENP-A Drosophila (CID, for Centromere IDentifier) results in ectopic localization of this protein, recruitment of other kinetochore components, and chromosome fragmentation and mis-segregation.
- Centromeric chromatin shows a distinct pattern of histone modifications.
- Biochemical and genetic methods are both valuable strategies for identifying CID-interacting factors.

CID overexpression results in recruitment of kinetochore proteins to euchromatin, and chromosome fragmentation and mis-segregation

Studies in diverse organisms have demonstrated that CENP-A proteins provide a structural and functional foundation for the kinetochore, and are necessary for the recruitment of all known kinetochore proteins. Is CENP-A also sufficient for kinetochore formation and function? We examined the consequences of overexpressing CID in *Drosophila* tissue culture cells and animals using tagged proteins. Overexpression of CID in S2 cells, embryos, and larval salivary glands and neuroblasts resulted in broad incorporation of CID into euchromatin and abnormal recruitment of outer kinetochore proteins at multiple sites on each chromosome. High levels of CID overexpression in animals resulted in 99% lethality, and the rare survivors were small and sick. These phenotypes are consistent with cell lethality during larval development. At the cellular level, larval neuroblasts and embryos with overexpressed CID exhibited a high frequency of chromosome fragments, which contained CID, as well as other missegregation phenotypes. These results suggest that functional kinetochores formed on sites of ectopic CID incorporation, resulting in individual chromatids with attachments to opposite poles, followed by fragmentation and mis-segregation. Thus, CENP-A appears to be sufficient for kinetochore formation, though it is possible that other, broadly distributed chromatin factors also contribute. These findings also have relevance to cancer biology, because they provide a direct demonstration that CENP-A overexpression and mislocalization recently observed in colon cancer cells is likely to result in missegregation and aneuploidy.

The patterns of histone H3 modification in the centromeric chromatin are distinct from both euchromatin and flanking heterochromatin

Patterns of histone tail modifications epigenetically specify functional and structural chromatin domains in eukaryotes. In most eukaryotes, centromeres are embedded in heterochromatin, which has led to the assumption that centromeric chromatin is heterochromatic. A different view is suggested by our recent studies of histone modifications in human and fly CEN regions using a chromatin fiber method and modification-specific antibodies. Our results indicate that centromeric chromatin has a histone modification pattern that is distinct from both euchromatin and heterochromatin.

The interspersion of H3 with CENP-A, and the different modification patterns of H3 within the centromeric chromatin and in flanking heterochromatin, may contribute to the three-dimensional structure of the kinetochore and centromeric cohesion. In addition, a new model for deposition of CENP-A specifically in centromeric chromatin is suggested by these observations. It is possible that the modification pattern of interspersed H3 nucleosomes and general histone modification proteins, e.g. acetyltransferases, methyltransferases, and kinases, play an important role in propagating centromere identity, rather than, or in addition to, CENP-A associated proteins.

Biochemical identification of CID-interacting proteins

The identification and analysis of proteins that interact with CENP-A will greatly enhance our understanding of the mechanisms responsible for centromere identity and structure. We have used CID antibodies and tagged constructs to identify CID-associated proteins using *in vitro* binding, complex fractionation, immunoprecipitation, and mass spectrometry. Although the biochemical screens are not yet complete, we have already identified CID binding proteins that affect CID function *in vivo*.

The CID-specific proteins identified in this pilot analysis include interesting candidates based on associations with chromatin-related functions or domains. One interesting candidate identified in this pilot study is CHD1. This protein associates with chromatin and contains a chromodomain, a motif that binds to specific histone tail modifications, as well as a helicase activity frequently found in chromatin remodeling complexes. Recent studies have shown that depletion of CHD1 inhibits replication-

independent nucleosome assembly in crude extracts from budding yeast. This result makes CHD1 a particularly attractive candidate for involvement in CID deposition since CENP-A proteins, as well as other histone variants, are incorporated into chromatin by replication-independent mechanisms.

Publications

D. Fyodorov, M.D. Blower, G.H. Karpen, and J.T. Kadonaga, "The ACF chromatin assembly factor affects transcriptional silencing and cell cycle progression," *Genes and Development* **18** (2) (2004), in press.

B.A. Sullivan and G.H. Karpen, "Centromeric chromatin displays a pattern of histone modifications that is different from both euchromatin and heterochromatin," submitted to *Nature Genetics*.

M.D. Blower, T. Daigle, T. Kaufman, and G.H. Karpen, "CENP-A mutations in *Drosophila* cause an early mitotic delay that involves a component of the spindle assembly checkpoint," in preparation, to be submitted to the *Public Library of Science* (PLOS)

M.D. Blower and G.H. Karpen, "Chromatin assembly factors are necessary for both H3 and *Drosophila* CID/CENP-A nuclear import, and associate with newly synthesized and chromatin-incorporated H3 and CID," in preparation, to be submitted to *Current Biology*.

S.E. Erhardt, M.D. Blower, P. Heun, A. Skora, and G.H. Karpen, "Overexpressed CID is incorporated into euchromatin and is sufficient for ectopic kinetochore formation and function," in preparation, to be submitted to *Science.*

Systems Biology: Biological Input-Output Devices

Principal Investigators: I. Saira Mian

Project No.: 02031

Project Description

Biological systems surpass current silicon-based technologies in areas such as sensor fusion, pattern recognition, adaptability and information storage, retrieval, processing, and related tasks. Irrespective of the level of resolution at which it is viewed, a molecular, (sub)cellular, multicellular, or higher level system transforms internal and external inputs to yield outputs that maintain homeostasis or ensure a smooth transition to a new state. The common feature is large numbers of potentially unreliable parts interconnected in unknown, irregular, and time-varying ways cooperating to generate a coherent and unified response.

Biological systems are *in vivo* input-output devices with the capacity to perform parallel and distributed computing in a robust, reliable, secure, error- and fault-tolerant manner. Enhanced knowledge of the means by which this complex task is solved provides an opportunity to control existing devices, fashion novel devices for designed purposes, and create fundamentally new information systems and technologies.

The aims of this project are the development and application of mathematical, statistical, and computational methods for investigating input-output devices. The two complementary approaches being employed to realize these goals are data-driven modeling and conceptual modeling.

Accomplishments

Statistical modeling of biomedical corpora: mining the Caenorhabditis *Genetic Center Bibliography*

The statistical modeling of biomedical corpora could yield integrated, coarse-to-fine views of biological phenomena complementary to discoveries made by genome-scale data analysis. We have demonstrated the potential of such modeling by examining the 5,225 free-text items in the *Caenorhabditis* Genetic Center (CGC) Bibliography. Items in this biomedical text corpus are modeled using the Latent Dirichlet Allocation (LDA) model, a hierarchical Bayesian model which represents a document as a random mixture over latent topics and characterizes each topic by a distribution over words.

We have shown how corpus-, document-, and word-level LDA parameters can be combined with labels from the gene ontology to enhance the explanatory value of the CGC LDA model, and illustrated this approach via a retrospective study of known nematode gerontogenes. A novel pairwise document similarity measure based on the posterior distribution on the topic simplex was used to search the CGC database for "homologs" of a "query" document discussing the life span-modifying *clk-2* gene. New hypotheses about the role of *clk-2* were formulated by interrogating *clk-2* document homologs and the topics most likely to have generated words in them. Like graphical models for genetic, genomic, and other types of biological data, LDA provides a method for extracting unanticipated insights and generating predictions amenable to subsequent experimental validation.

Robust sparse hyperplane classifiers: application to uncertain molecular profiling data

Molecular profiling can generate abundance measurements for thousands of transcripts, proteins, metabolites, or other species (features) in, for example, normal and tumor tissue samples (data points). Given such two-class, high-dimensional data, sparse hyperplanes are successful statistical algorithms for classifying data points into one of two categories (classification and prediction) and defining a small subset of discriminatory features (relevant feature identification). However, this and other extant classification methods address implicitly the issue of observed data being a combination of underlying signals and noise. Recently, robust optimization has emerged as a powerful framework for handling uncertain data explicitly.

We have exploited ideas from the field of robust optimization to develop robust sparse hyperplanes, i.e., classification and relevant feature identification algorithms that are resilient to variation in the data. Specifically, each data point is associated with an explicit data uncertainty model in the form of an ellipsoid parameterized by a center and covariance matrix. The task of learning a robust sparse hyperplane from such data is formulated as a Second Order Cone Program (SOCP). Gaussian and distribution-free data uncertainty models are shown to yield SOCPs that are equivalent to the SOCP based on ellipsoidal uncertainty. We have demonstrated the real-world utility of robust sparse hyperplanes via retrospective analysis of breast cancer-related transcript profiles. Data-dependant heuristics were used to compute the parameters of each ellipoidal data uncertainty model. The generalization performance of a specific implementation, designated robust Liknon, is better than its nominal counterpart.

Publications

L.R. Grate and I.S. Mian, "Small-sized discriminatory feature sets," in preparation, *Genome Biology* (2003).

C. Bhattacharyya, L.R. Grate, M.I. Jordan, L. El Ghaoui, and I.S. Mian, "Robust sparse hyperplane classifiers: application to uncertain molecular profiling data," in preparation, *Journal of Computational Biology* (2003).

D.M. Blei, K. Franks, M.I. Jordan, and I.S. Mian, "Statistical modeling of biomedical corpora: mining the *Caenorhabditis*," Genetic Center Bibliography, submitted, *Genome Biology* (2003).

R.B. Calder, J.D. Garza, R. Beems, H. van Steeg, J. Hoeijmakers, P.H.M. Lohman, I.S. Mian, and J. Vijg, "A Mouse Phenotype Analysis System: application in studying symptoms of accelerated aging in DNA repair defective mice," in preparation, *Genome Biology* (2003).

A.V. Loguinov, I.S. Mian, and C.D. Vulpe, "Exploratory differential gene expression analysis in microarray experiments with no or limited replication," in press, *Genome Biology* (2003).

E.A. Worthey, A. Schnaufer, I.S. Mian, K. Stuart, and R. Salavati, "Comparative analysis of editosome proteins in trypanosomatids," *Nucleic Acids Research* **31**, 6392–6408 (2003).

M.J. Bissell, A. Rizki, and I.S. Mian, "Tissue architecture: the ultimate regulator of breast function," in press, *Current Opinions in Cell Biology* (2003).

N.F. Lue, Y.-C. Lin, and I.S. Mian, "A conserved telomerase motif within the catalytic domain of TERT is specifically required for repeat addition processivity," *Molecular and Cellular Biology* **23**, 8440–8449 (2003).

L. Chen, L. Lee, B.A. Kudlow, H.G. Dos Santos, O. Sletvold, Y. Shafeghati, E.G. Botha, A. Garg, N.B. Hanson, G.M. Martin, I.S. Mian, B.K. Kennedy, and J. Oshima, "LMNA mutations in atypical Werner's syndrome," *The Lancet* **362**, 440–445 (2003).

D. Bosoy, Y. Peng, I.S. Mian and N.F. Lue, "Conserved N-terminal motifs of telomerase reverse transcriptase required for ribonucleoprotein assembly," *Journal of Biological Chemistry* **278**, 3882–3890 (2003).

L.R. Grate, C. Bhattacharyya, M.I. Jordan, and I.S. Mian, "Integrated analysis of profiling and sequence data," *Mechanisms of Ageing and Development* **124**, 109–114 (2003).

C. Bhattacharyya, L.R. Grate, A. Rizki, D.C. Radisky, F.J. Molina, M.I. Jordan, M.J. Bissell, and I.S. Mian, "Simultaneous relevant feature identification and classification in high-dimensional spaces: application to molecular profiling data," *Signal Processing* **83**, 729–743 (2003).

Characterization of Adult Stem Cell Involvement in Mammary Gland Development

Principal Investigators: Carlos Ortiz de Solórzano

Project No.: 03024

Project Description

Our goal is to identify the three dimensional location and distribution of adult stem cells (ASCs) in the murine mammary gland, and establish a model of ASC involvement in mammary gland development, which may help us establish their potential role as targets for neoplastic transformation. Namely, we aim to describe the involvement of epithelial ASCs in the development of the mammary gland. We then want to know whether partially differentiated bone marrow adult stem cells can undergo trans- or de-differentiation and participate in the development of the mammary gland. We want to look at these dynamic processes *in vivo* using low or nil-morbidity, noninvasive imaging methods.

Since there is a lack of good markers for native ASC detection, we will perform same-species transplantation of labeled ASCs and look at the activity of those foreign-labeled cells in their new environment. To accomplish this, we will use an existing computer-assisted, three-dimensional microscopy system to measure the location and distribution of transplanted green fluorescent protein (GFP) labeled ASCs (both from the mammary gland and bone marrow) in recapitulated mammary glands. Since ASC activity is dynamic and may involve migration from the locus of transplantation, we will complement our initial *in vitro* studies with *in vivo* detection of GFP-ASC activity using intra-vital microscopy and whole body detection of GFP emissions.

Accomplishments

In the first year of this project, we achieved a number of milestones:

- *Breeding protocol:* We produced all the animals required for the experiments, wild type c57bl and FVBs as well as GFP transgenic c57bl in house.
- *Fixation Protocol:* We tested different methods to determine the optimum fixation method for the GFP mammary gland tissue.
- *Cell culture:* We stained our cultures with keratin to control the purity of the cultures, we have more than 95% of epithelial cells. We also controlled that the GFP was maintained in the cells in culture doing a simple fixation and Dapi staining.

Transplant experiments

- *Tissue transplant:* All four second and third glands of two GFP animals were minced into small tissue organoids and implanted in six three-week old wild-type animals (three fresh tissue, three frozen tissue). Sections will be examined to see if all the cells of the transplants express the GFP.
- *Cell transplant:* We used12 GFP and 12 wild type animals to make purified primary epithelial cell cultures that were re-implanted into cleared fat pads of wild-type animals at different concentration in order to determine if the entire mammary gland can be the result of a single stem cell.
- *Bone marrow transplant*: We started a collaboration with Dr. Greenberger, University of Pittsburgh Medical Center, whose lab does routine bone marrow cells extractions. He will send us frozen GFP bone marrow cells of males in mid-January.

Label Retaining Cell experiments

- *BrdU* in vivo *labeling, animal sampling, and tissue collection:* A group of nine animals (wildtype FVB female mice) were implanted with bromodeoxyuridine (BrdU)-filled osmotic pumps at three weeks of age. The pumps deliver BrdU at a constant rate of 0.5µl/hr. After two weeks, the pumps were removed from all the animals and tissue collection done on euthanized animals at two, seven, and nine weeks. The fourth mammary glands of these animals will be used to look at the distribution of label retaining cells across the mammary gland and to study the microenvironment of these cells.
- *BrdU staining:* Using frozen tissue belonging to the second and third mammary glands, we developed a protocol for immunofluorescence staining of BrdU-labeled cells in (thin) frozen tissue sections. Similarly, using formalin-fixed, paraffin-embedded tissue from second and third mammary glands, we put together a protocol for immunofluorescence staining of BrdU-labeled cells in (thin) paraffin-embedded tissue sections.
- *Tissue reconstruction and spatial analysis:* We have worked on the improvement of the whole-gland three-dimensional reconstructions rendered by our system. Also, tools have been developed for the two-dimensional spatial analysis of the distribution of the LRCs, as well as to study the relationship between the LRCs and the different types of cells in their close neighborhood.

Materials Sciences Division

Interactive Hybrid Materials for the Construction of Cell-based Biosensors

Principal Investigators: Carolyn Bertozzi, Matthew Francis, Jay Groves, and Tony Tomsia

Project No.: 03002

Project Description

The integration of biological components into a synthetic device environment is a major frontier in the design of microscale and nanoscale devices. Living cells possess many capabilities that are desirable in a device context, such as multi-enzyme metabolic conversions that are useful for environmental bioremediation, energy harvesting, and industrial fermentation. Living cells can also amplify and transduce signals in response to detection of soluble analytes and thereby could function in biosensing devices. To achieve this, molecular control of the interface between the biological molecule or cell and the surrounding material is paramount.

The majority of intercellular communication events occur between proteins and oligosaccharides that are positioned on cell surfaces by lipophilic domains that extend into the plasma membrane. These molecules comprise a diverse collection of receptors and ligands that serve to anchor the cell to appropriate growth locations, receive communication from adjacent cells and soluble signaling molecules, and send information regarding the polypeptide synthesis occurring within. Through a variety of complex mechanisms, these molecules serve to relay environmental information to the cell interior, ultimately resulting in gene regulation and thus control of cellular behavior. In order to establish connections between this communication system and inanimate substrates, an intervening surface that can mimic these phenomena in a controlled and dynamic fashion is likely to be required. The focus of this project is to develop a common molecular platform that can be used to interface living cells with synthetic materials in an interactive manner and to study the response of cells to their support material. The studies will provide essential information for the successful incorporation of cells into device structures.

Accomplishments

Supported lipid bilayers have been chosen as the central material for these studies because they closely, and perhaps uniquely, mimic the two-dimensional fluid reaction environment corresponding to the surface of another cell. In order to communicate with cells in an optimal fashion, we must be able to decorate these bilayers with a variety of receptors and ligands that can interact with their surface molecules. As such, much of the focus during the first cycle of funding for this project has involved the development of the synthetic techniques to prepare these hybrid materials and new characterization methods for study. The progress to date and future experiments in each of these areas is detailed below.

Decorating lipid bilayer surfaces with mucin mimics

Mucins are an important class of large glycoproteins found at cell surfaces and in secretions. The rigid, extended conformations of the proteins, caused by the array of sugar groups bound to the peptide backbone, makes them structurally important in presenting epitopes outside a cell's glycocalyx, for example; it prevents other cells from adhering. Studies of the physical behaviors of mucins at membranes have been limited by the inability to synthesize such large glycoproteins. In this year of the project, Bertozzi and coworkers developed a methodology to synthesize mimics of mucin in which these same sugar groups were attached to an artificial polymer backbone. The mimics show the same rigid, extended structure as native mucin. Moreover, the mimic allows attachment of chemical groups that are amenable to binding to lipid bilayers, so that membrane-bound mucin can be studied, see Figure 1. In the last year, Groves and coworkers have incorporated fluorescently labeled mucin mimics into lipid bilayers. Using fluorescence interference contrast microscopy, in which interference between the light of a fluorophore and its reflection from a silicon surface provides nanometer-scale topographic information, we studied the orientation of mucin mimics bound by a C18 tail to a planar lipid bilayer. Preliminary results suggest that individual mucin mimics support themselves "upright," jutting out from the lipid bilayer. We plan to extend these studies to determine the role of density, binding strength, and the presence of other proteins on the behavior of mucin in the hopes of better understanding the mechanics of these and other cell-surface molecules.

Development of new chemistries for protein-surface conjugation

In the past year, Francis and coworkers have developed a new reaction for selective modification of proteins at

disulfide sites using ruthenium carbene chemistry. The new reaction allows the selective modification of proteins with lipid functionalities for immobilization in supported bilayers. The technique will permit the attachment of proteins to supported bilayers to serve as interfaces with cells and other biomaterials. These are ongoing studies at present. A second chemical transformation was also developed for specific modification of proteins at solvent-accessible tyrosine residues. The transformation provides an alternative mode of site-specific protein modification.

Transcript profiling of cells attached to synthetic substrates: a new approach for quantifying biocompatibility

A major concern in the development of new interfacial chemistries for bridging biological and non-biological materials is their effect on living cells. To address this at a molecular level, Bertozzi and coworkers studied the effects of cell attachment to synthetic materials on global gene expression patterns. Two substrates were analyzed, polystyrene and a collagen matrix that mimics the natural extracellular matrix *in vivo*. Transcripts were quantified using the Affymetrix gene chip; several statistical differences were identified. These included transcripts encoding oxidative stress proteins and pro-inflammatory growth factors. The results suggest that cells grown on an artificial, non-biomimetic surface undergo stress responses not experienced by cells grown on a biomimetic surface. This approach will be used to evaluate the biological approximation of new surface coatings designed in the Groves and Francis labs for interfacing cells with materials.

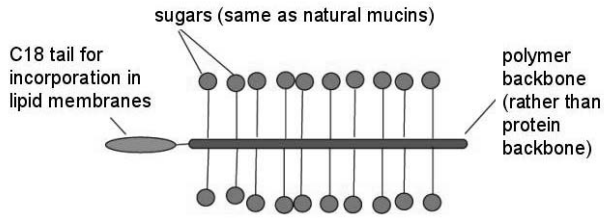

Figure 1. Architecture of mucin mimics studies in supported bilayers.

Publications

C.M. Klapperich and C.R. Bertozzi, "Global gene expression patterns of cells attached to a tissue engineering scaffold," *Biomaterials*, in press.

G.S. Lee, Y. Shin, I. Choi, H. Hahn, and C.R. Bertozzi, "Design and synthesis of mucin glycodomain mimics," to be submitted to *Journal of the American Chemical Society*.

New Femtosecond Spectroscopies of Structural Dynamics: IR Pump X-ray Probe Experiments

Principal Investigators: Andrea Cavalleri and Robert Schoenlein

Project No.: 03007

Project Description

The main goal of the project is the development and demonstration of new time-resolved experiments in which mid-infrared pulses are used to initiate large-amplitude atomic motions in the electronic ground state. The ensuing electronic, magnetic, and atomic structural changes are measured using visible, infrared or x-ray pulses. These experiments are particularly significant for materials where electronic, magnetic, and optical properties are strongly susceptible to rearrangements in the structural degrees of freedom, and where subtle changes in local structure may result in large modulation of the electronic density of states (e.g. transition-metal oxides).

Early proof of principle experiments will rely on mid-infrared-pump [using a mid-infrared optical parametric amplifier (OPA)] and optical probe geometries (absorption, reflectivity, dicroism at visible wavelengths) in the femtosecond timescale. The ultimate goal will be to use femtosecond x-ray spectroscopy [extended x-ray absorption fine structure (EXAFS), near edge x-ray absorption fine structure (NEXAFS), magnetic circular dichroism (MCD) or photoemission).

Accomplishments

The project was originally proposed for two-years; it was funded for the first year. Nonetheless, sufficient accomplishments were achieved with year one funding that will enable further progress with follow-on support.

- Infrared-OPA technology has been obtained in the laboratory, with fs radiation that is continuously tunable from the visible to 24 μm. A suitable postdoctoral scientist was also identified and recruited.
- Progress has been made at beamline 5.3.1 of the ALS in the development of femtosecond NEXAFS diagnostics in Vanadium Dioxide, where an optically driven insulator-to-metal transition has been identified and measured in the picosecond timescale. We expect to be able to measure electronic dynamics through femtosecond NEXAFS spectroscopy in the near future.

With future support, an infrared pump/visible probe experiment will be conducted in the coming year, with a

demonstration of the possibility of modulating of electronic structure (e.g. metal insulator transition) via excitation of an infrared active vibration in VO_2 both in bulk and nanorods. The demonstration of an optical pump/NEXAFS probe experiment on the femtosecond timescale at beamline 5.3.1 is also planned. The medium term plan will entail the demonstration and scientific application of infrared-pump/NEXAFS-EXAFS probe experiment at the ALS.

Publications

A.Cavalleri, H.H. Chong, Th. Dekorsy, J.C. Kieffer, and R.W. Schoenlein, "Structural bottleneck in the photo-induced insulator-to-metal transition in VO2", submitted to *Physical Review Letters.*

A. Cavalleri, H.H. Chong, S. Fourmaux, T.E. Glover, P. Heimann, J.C. Kieffer, H, Padmore, and R.W. Schoenlein "Picosecond soft x-ray absorption measurement of the photo-induced insulator-to-metal transition in VO_2," submitted to *Physical Review B.*

Self-assembling Arrays of Nanocrystals Templated by Cytoskeletal Proteins

Principal Investigators: Matthew Francis

Project No.: 02034

Project Description

Actin is a remarkably versatile structural protein, serving both as a major component of the cytoskeleton and as the central scaffold of the muscle contractile apparatus. The utility of actin as a structural building block arises from its ability to form helical polymers that maintain their rigidity over lengths in excess of 10 μm [in comparison, double stranded deoxyribonucleic acid (DNA)] displays this property for only ca. 50 nanometers). Since these filaments are readily produced *in vitro* when the protein monomers are placed under the proper concentration, salt, and temperature conditions, modified actin subunits could provide a new method for arranging attached materials into periodic linear arrays through self-assembly. It is anticipated that these arrays could serve as useful components of optical devices and could be used to prepare nanoscale circuits after the subsequent deposition of additional metals.

To this end, this project focuses on: (1) the design of a modular coupling strategy for the attachment of inorganic materials to protein surfaces, (2) the synthesis of water-soluble, uncharged nanocrystals with the appropriate functional sites for protein attachment, (3) the synthesis of actin conjugates modified in specific locations that do not interfere with self-assembly, (4) polymerization of the resulting conjugates into linear arrays, and (5) deposition of elemental silver along the template strands to yield metallic nanoscale conductors.

Accomplishments

Research efforts during the past year have focused on the attachment of functional components to the surface of actin monomers. As this protein readily assembles into fibers that are ten nanometers in diameter, see Figure 2a, this protein could serve as a versatile scaffold for the construction of nanoscale wire-like materials. In particular, this work has focused on the attachment of inorganic nanocrystals, with the ultimate goal of forming highly-regular linear arrays of conducting and semiconducting particles.

In order to secure the protein building blocks, a series of in-house protocols have been developed for the efficient isolation of highly-pure actin from rabbit muscle tissue. The optimized procedures utilize a combination of size exclusion chromatography (SEC) and ion-exchange chromatography to remove undesired proteins and the small amount of cross-linked actin that is present in natural samples. The isolation protocols reported in the literature remove these contaminants less thoroughly, thus hampering the interpretation of polymerization experiments carried out with material obtained in such a manner.

Following the isolation of the protein monomers, we have developed a modular strategy to attach virtually any chemical functionality to the building blocks. A poly(ethylene)glycol spacing moiety was appended with a ketone functional group and an iodoacetamide for protein attachment. A procedure was then developed for the highly site-selective alkylation of cysteine 374 on the actin surface using this molecule, thus incorporating the ketone group in a specific location on the protein surface, see Figure 2b. As proteins do not possess ketones in the naturally occurring amino acid side chains, this site supplies a unique functional handle for further bioconjugation. Liquid chromatography/mass spectrometry (LC/MS) analysis of the modified protein revealed highly pure and homogeneous material.

With the modified actin in hand, we next evaluated its competency for self-assembly. Although several previously reported modifications severely or completely inhibited the polymerization capabilities of the protein, it was found that the ketone-modified actin polymerized at rates that were qualitatively similar to that of the wild-type protein. Thus, we now have the modifiable core protein component to form the self-assembling scaffolds.

We next synthesized functional components that can be attached to the individual monomers. It was found that the monomers can be functionalized with alkoxyamines, affording stable oxime linkages, as well as with hydrazides. This was carried out on pre-polymerized actin fibers and on actin monomers that were later polymerized. In both cases, fibers displaying the new functional groups at 5.5 nanometer intervals were obtained, see Figure 2c.

A substantial portion of this research area has involved the preparation of water-soluble gold and cadmium sulfide (CdS) nanoparticles that can be attached to the ketone-labeled actin monomers. Because actin polymerization is extremely sensitive to the overall charge state of the protein monomers, it was critically important that cationic and anionic stabilizers were not used to passivate the nanocrystal surfaces. Instead, we have generated 0.8 nanometer gold nanocrystals possessing alkoxyamine-containing phosphines on their surface, see Figure 2d. This functional group lends water solubility and can be conjugated to the ketones directly. In related experiments, we have prepared two nanometer CdS nanoparticle surfaces passivated with *p*-aminothiophenol derivatives. Although these particles are not themselves water soluble, through the use of cosolvents we are hopeful that they can be attached to the actin ketones through oxime formation. Once attached, the high charge of the protein, -14 at neutral pH, will enhance the solubility of the particles. In the case of both nanocrystal types, conjugation experiments are in progress, and the assembly behavior of the conjugates is being monitored by transmission electron microscopy (TEM).

In related research, we have also modified a natural product, cytochalasin B, which is known to bind to one end of growing actin fibers. After isolating and characterizing the natural product analog, its ability to bind actin fibers was confirmed through polymerization assays. Ongoing experiments have involved the attachment of this compound to inorganic particles as a means to grow the actin fibers to material surfaces.

As a result of these studies, a promising new scaffold for the construction of self-assembling linear material has emerged. All of the key building blocks have been prepared and our modular design will allow rapid optimization of the components as polymerization studies unfold. Once these studies are complete, the further elaboration of these scaffolds into nanoscale electronic and optical materials will be pursued.

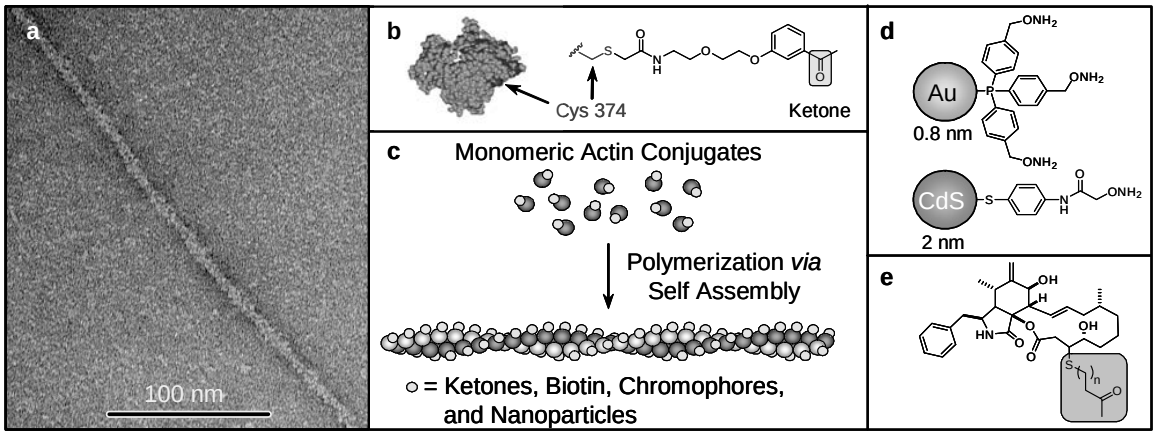

Figure 2. Preparation of functionalized self-assembling fibers. (a) Actin monomers readily polymerize into fibers that are microns in length and 10 nanometers in diameter. (b) Chemistry has been developed to modify Cys 374, allowing the attachment of a ketone functional group in a specific location on each protein monomer. (c) Upon polymerization, components attached to the ketone are displayed along the fibers with a periodicity of 5.5 nanometers. (d) New water soluble gold and cadmium sulfide nanoparticles have been prepared for attachment to the ketones on the fibers. Note that multiple copies of the organic functionality extend from the surface of each nanocrystal. (e) A modified cytochalasin B analog will be used to attach electrodes and other functionality to the growing ends of the fibers.

High Spatial and Energy Resolution Electron Energy Loss: Spectroscopy for Nanoscale Materials Applications

Principal Investigators: Nigel Browning and Christian Kisielowski

Project No.: 03005

Project Description

The purpose of this program is to develop the capability to obtain electron energy loss spectra (EELS) in a scanning transmission electron microscope (STEM) with a spatial resolution of ~0.13 nanometers and an energy resolution of ~0.2 eV. Such capabilities will be used to investigate the atomic scale electronic structure of interfaces, defects, and nanoscale materials systems. Through such analyses, a direct measurement of properties such as band-offset, cohesive energy, vacancy clustering, and segregation, and the formation of defect/interface states can be achieved. These properties are critical in determining the performance of nanoscale electronic, optical, magnetic, and chemical materials systems; their quantification is the first step in the design of optimized device structures.

The ultimate aim of this research is to integrate the high spatial resolution and high-energy resolution capabilities of the new STEM that was installed in the National Center for Electron Microscopy (NCEM) in April 2003. Although this instrument has demonstrated a spatial resolution approaching 0.13 nanometers, the integration of the monochromator, the first of its kind in the U.S., will permit high-energy resolution EELS to be obtained; it requires the optimization of the electron-optical coupling in all sections of the instrument to enhance both stability and sensitivity. This optimization will be achieved by targeting specific materials issues where high spatial and energy resolution are essential: defects in GaN and precipitates in MgB_2.

Accomplishments

Two students were employed with this funding to develop these applications. During the initial period, when the instrument at NCEM was being installed, tested, and made available to users, these students worked on the development of the techniques at the University of Illinois at Chicago (UIC). In addition, the students developed samples at UIC, which were used to test the instrument in the factory, prior to shipment to NCEM, and after installation. This proactive approach to optimizing both the STEM techniques and the instrument significantly reduced the installation time at NCEM and made an instrument capable of delivering state-of-the-art results rapidly available to the general community.

To develop the ability to achieve high spatial and energy resolution spectroscopy, this one-year project focused on two materials systems, GaN and MgB_2. In the case of GaN, the analysis that was performed enabled the first direct atomic scale experimental observations of oxygen segregation to dislocation cores in GaN to be obtained. The amount of oxygen present in each of three distinct types of screw dislocation core (open, closed and decorated with pinholes) was found to depend on the evolution and structure of the core and thus gives rise to a varying concentration of localized states in the band-gap. Furthermore, contrary to previous theoretical predictions, the substitution of oxygen for nitrogen was observed to extend over many monolayers for the open core, indicating that the presence of localized electronic states in the band-gap may be more extensive than previously thought for this type of structure.

The second area of study concerned MgB_2, and in particular, the effect of coherent oxide precipitates on the local transport properties. Mg (B,O) nanostructured precipitates in bulk MgB_2 are thought to behave as fluxpinning centers increasing the critical current J_C without decreasing the transition temperature T_C. Possible candidates for these $Mg_2B_3O_x$ nanostructures, observed experimentally in bulk MgB_2 by Z-contrast imaging and electron energy loss spectroscopy in the STEM, were studied by first-principles calculations. The electronic structures, phonon modes, and electron phonon coupling parameters were calculated for two oxygen-ordered MgB_2 compounds of composition Mg_2B_3O and $Mg_2B_3O_2$ (that agreed with the images), and compared with those of MgB_2. The density of states for both $Mg_2B_3O_x$ structures show a very good agreement with experimental electron energy loss spectra, indicating that they are excellent candidates to explain the observed coherent oxygen precipitates. Of particular importance for the development of the spectroscopic methods is that this agreement between experiment and theory could only be verified using the 0.2 eV resolution spectra from the monochromated microscope.

The two samples described above (and the students working on the research projects) played a large role in the testing of the STEM prior to installation at NCEM. Based on the test results, the installation parameters, and expected performance of the microscope were defined. The installation of the microscope at NCEM began in April 2003; development continued until acceptance of the instrument. The testing experiments were crucial in assisting the rapid installation and optimization of this advanced and unique instrument.

Although there has been a rapid advancement in the installation and operation of the microscope, further work with follow-on funding is required to optimize the performance for wide-spread materials science applications.

Publications

I. Arslan and N. D. Browning, "The role of oxygen at screw dislocations in GaN," *Physical Review Letters* **91**, 165501 (2003).

I. Arslan, S. Ogut, P. D. Nellist, and N. D. Browning, "Comparison of simulation methods for electronic structure calculations with experimental electron energy loss spectra," *Micron* **34**, 255-260 (2003).

R. F. Klie, I. Arslan, and N. D. Browning, "Atomic resolution EELS," submitted to *Journal of Electron Spectroscopy.*

J. Idrobo, S. Ogut, T. Yidirim, and N. D. Browning, "The electronic and superconducting properties of oxygen ordered precipitates in MgB2," submitted to *Physical Review Letters.*

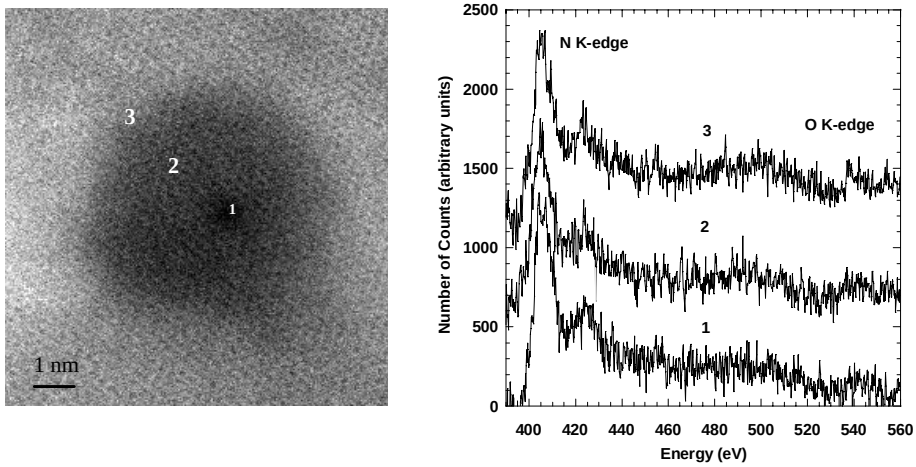

Figure 3. (a) Image of a filled nanopipe (dislocation decorated with pinholes), or filled screw dislocation that is ~9 nm in diameter. The darker contrast in the center of the nanopipe signifies a thinner region of material that filled in the nanopipe at a later stage of growth. The positions for the EELS analysis are marked on the image. (b) The corresponding nitrogen and oxygen K-edges. The spectra from positions 1 and 2 do not show an oxygen signal that is quantifiable above the noise, but the signal from position 3 does show a distinct peak at the characteristic oxygen core-loss energy, indicating that some oxygen is still bonded at the edge of the nanopipe even though GaN has filled in the rest of the core.

Modeling Quantum Coherence and Transport in Nanoscale Spin, Charge, and Flux Devices

Principal Investigators: Joel Moore

Project No.: 03017

Project Description

This project will start a new theoretical research effort in nanoscale devices and quantum coherence. Problems to be studied include the creation and control of quantum entanglement in systems with coupled degrees of freedom, and the electronic and mechanical properties of single-molecule and single-electron transistors. One primary scientific goal is to find a theoretical explanation for recent experimental results indicating that vibrational excitations strongly influence transport in single-molecule transistors. Another goal is to understand causes of decoherence in coupled spin and flux devices for quantum computing.

Successful theoretical modeling of nanoscale electronic devices will eventually require a combination of analytical techniques and *ab initio* computational methods. This combination has proved very useful in traditional semiconductor electronics. Molecular electronics are at an early stage, and for some devices there is not even a qualitative understanding of their properties. The majority of the proposed research will be analytical and aimed at developing and studying basic models for experiments that are not yet understood. Specific methods include the Keldysh and Landauer descriptions of nonequilibrium transport and the Caldeira-Leggett approach to dissipative systems. Once testable models are developed, it may be desirable to refine these models using high-performance computation.

Accomplishments

The main results in the first year of this project are a theory of anomalous phonon effects in subresonant and resonant transport through single-molecule devices, and a study of entanglement dynamics in coupled superconducting devices. The first set of results was motivated by a number of experiments on single-molecule transport: experiments saw unexpectedly strong phonon signatures in some cases but no phonon effects in others. We now understand that higher phonon harmonics are strongly damped in the "subresonant" regime, when the molecular level is only virtually occupied, while higher harmonics can be quite strong in the resonant regime, when the molecular level's mean occupation is of order unity. We also studied a "pumped" regime where transport electrons passing through a molecule generate a nonthermal distribution of phonon states. Some of the predictions may be confirmed in experiments currently underway at Bell Labs and elsewhere.

The second set of results concerns the behavior of "entanglement" in superconducting devices: entanglement is a measure of how quantum-mechanical the correlations in a system are, and entanglement is the essential ingredient for exponentially fast quantum computing. Our motivation was twofold: to understand the basic question of how an entangled quantum-mechanical state evolves into a product state in the presence of dissipation and the applied question of how entanglement, and hence quantum information processing, can survive in a dissipative environment. Some celebrated theoretical work of Leggett and others in the 1980s led to a picture of how a single two-state system moves under dissipation from a quantum superposition to a classical mixed state. Our results answer the analogous question of how a bipartite system moves toward a product state: we were able to show that the rate of entanglement decay is 2/log 2 times faster under some circumstances, than the rate of single qubit decoherence and to develop a numerical analysis for the entanglement dynamics in more general parameters.

The specific system considered was made up of two coupled superconducting qubits like those studied experimentally in the Clarke group at Berkeley Lab. By numerical integration of the Bloch-Redfield equations, or analytic solution in a few simplified cases, we were able to get a general understanding of entanglement evolution in this system. Perhaps the most surprising result is that often fidelity decays without entanglement: that is, the quantum state evolves under dissipation to a different entangled state well before losing its entanglement entirely.

The other directions of research are understanding the restoration of superconductivity after it has been destroyed by an ultrafast optical pulse and developing new numerical methods for many-body problems based on using entanglement as a metric for efficient coding of quantum states. We believe that these numerical methods may lead to improved analysis of a broad class of problems that are currently numerically intractable.

Publications

V. Aji, J.E. Moore, and C.M. Varma, "Higher harmonics of electronic-vibrational coupling in sub-resonant and resonant transport in a single-molecule device," accepted for publication in *International Journal of Nanoscience* (2003).

V. Aji and J.E. Moore, "Dynamics of entanglement in two coupled qubits," submitted to *Physical Review A* (2003). http://xxx.lanl.gov/cond-mat/0312145

J. E. Moore and D.-H. Lee, "Geometric effects on T-breaking in p+ip and d+id superconductors," submitted to *Physical Review B* (2003). http://xxx.lanl.gov/cond-mat/0309717

Chemical Dynamics under Reaction Conditions

Principal Investigators: D. Frank Ogletree and Miquel Salmeron

Project No.: 03018

Project Description

High pressure surface reaction mechanisms can be fundamentally different from those at ultrahigh vacuum. For example, NO dissociates on Rh(111) at low coverage but adsorbs intact at high pressures due to steric barriers to decomposition. Scanning tunneling microscopy (STM) studies of CO and NO coadsorbed on Rh(111) at Torr pressures revealed different, more closely packed adsorption structures with lower adsorption energies than those found in UHV. High pressure STM studies of CO oxidation on Pt(110) showed that the surface morphology changes dynamically as a function of reactant pressures, and that the reaction rates are strongly correlated with surface morphology.

We are investigating the electronic structure and chemical composition of catalyst surfaces and the energetics of catalytic reactions *in situ* under realistic conditions of pressure and temperature. Thanks to our recent development of a unique High Pressure Photoemission Spectrometer (HPPES) at Berkeley Lab, these studies are now possible. The prototype HPPES instrument has been operating at beamline 9.3.2 of the Advanced Light Source (ALS); the second generation instrument, with enhanced energy resolution, sample preparation and characterization

facilities, was recently commissioned at the new Molecular Environmental Sciences beamline 11.0.2. In a recent collaborative study with a group from the Fritz Haber Institute, we investigated the partial oxidation of methanol on copper oxide using our HPPES for *in situ* characterization of the catalyst and confirmed that the activity was related to a sub-oxide species that exists only under reaction conditions.

Accomplishments

Three different surface reactions have been investigated by HPPES over the one year of this project. The site-selective displacement of CO by NO on Rh(111) was investigated under conditions similar to the STM studies mentioned above. The surface composition of salt crystals and solutions in equilibrium with water vapor has been studied as part of a joint project with Professor J. C. Hemminger of the University of California (UC) at Irvine. The surface composition of atmospheric salt particles can have important consequences for atmospheric chemistry. A new investigation is focused on the oxidation and reduction of the Pd(111) surface as a function of oxygen gas pressure and surface temperature is now underway.

The first real experiments have been carried out on the second generation HPPES system. It is now possible to transfer samples between a preparation/characterization chamber and the high-pressure analysis chamber. Samples can be heated, cooled, and cleaned by ion sputtering or a low-energy flux of atomic or ionic species. Sample condition can be verified by low energy electron diffraction (LEED) and Auger spectroscopy. In the analysis chamber, the x-ray polarization and the angle of incidence on the sample can be varied. The sample can also be translated parallel to its surface plane to control beam damage from the high x-ray flux. The new beamline together with the new electron energy analyzer are capable of high resolution. Test measurements on the oxygen *2p* line of molecular oxygen easily resolved the vibrationally-excited fine-structure, with a measured peak width of only 96 milli-electronvolts.

Initial results on Pd oxidation show a dynamic dependence on gas pressure. A series of Pd valence-band photoemission Pd were recorded at room temperature as O_2 pressure was first increased from 0.001 to 40 Pa then decreased again to 10^{-6} Pa. A continuous evolution of the Pd valence-band structure was observed as pressure increased. These changes were partly reversed as oxygen pressure decreased. Although the surface remained partly oxidized, the Pd electronic structure during exposure to 40 Pa of oxygen was different from that found after the oxygen was evacuated.

The surface composition of several salts, KBr, NaCl, in equilibrium with water vapor has been investigated using the prototype HPPES system. There is clear evidence for changes in the surface composition of the saturated salt solution produced at a relative humidity above the deliquescence point. There is additional evidence for humidity-dependent changes below the deliquescence point, but the interpretation is complicated by x-ray beam damage, which is difficult to control in the prototype system. This problem has important implications for environmental chemistry; we are preparing a joint proposal with UC Irvine and Pacific Northwest National Laboratory (PNNL) to continue this work.

The investigation of CO/NO co-adsorption on Rh(111) has been completed. Both CO and NO can adsorb at two different sites on Rh(111), the top and hollow sites, as shown in Figure 4. High-resolution x-ray photoemission spectroscopy (XPS) in the carbon region can resolve the two CO populations. When a small amount of NO is added to the gas mixture, the hollow-site CO concentration drops rapidly while the top-site population changes only slightly. Even in a pure NO atmosphere, a significant top-site CO concentration persists for hours and it is necessary to increase the substrate temperature to completely displace CO within a few minutes. These observations give insights into the energetics of CO and NO adsorption on this important automotive emission-control catalyst.

Publications

F.G. Requejo, E.L.D. Hebenstreit, D.F. Ogletree, and M. Salmeron, "Bridging the pressure gap: *in situ* XPS study of site competition of CO and NO on Rh(111) in equilibrium with the gas phase," submitted to *Journal of the American Chemical Society*.

S. Ghosal, F.G. Requejo, D.F. Ogletree, M. Salmeron, and J. Hemminger, "The effect of water vapor on the surface composition of alkali halides: from dry solid to solution," American Vacuum Society 50th International Symposium & Exhibition, November 2–7, 2003, Baltimore, Maryland.

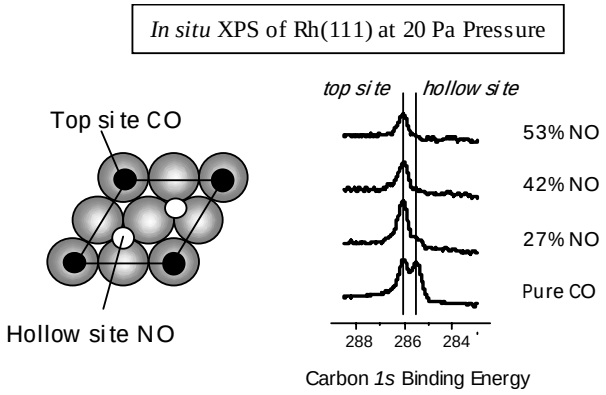

*Figure 4. Photoemission spectrum showing the changes in surface composition of Rh(111) as the CO/NO pressure ratio is changed. The C*1s *line, shown at right, has two components: the higher binding-energy component corresponds to CO adsorbed in top sites, indicated by black circles in the schematic at left, and the lower binding-energy component corresponds to CO in hollow sites, indicated by white circles in the schematic. When the gas mixture is changed from 100% CO to 73% CO:27% NO, very few CO molecules are displaced from top sites, while 80% of CO molecules are displaced from hollow sites. This site-dependent adsorption affinity offers insights into the reaction mechanisms.*

Nanoscale Electronic Phase Separation: A New Paradigm for Complex Electronic Materials

Principal Investigators: Dung-Hai Lee and Joseph Orenstein

Project No.: 02033

Project Description

This project is designed to explore the issues of nanoscale electronic phase separation (nano-EPS) as a fundamental element in the physics of complex electronic materials and to study its relation to application-relevant properties. An understanding of nano-EPS will also lead to new strategies for design of strongly correlated electronic materials with pre-determined application-relevant properties. Our approach will combine made-to-requirement materials, powerful characterization, and new theoretical tools to establish a link between nano-EPS physics and macroscopic properties in complex electronic matter.

High-resolution studies will be carried out on various complex electronic materials to directly observe nano-EPS and to study its phenomenology. Transport measurements using terrahertz (THz) spectroscopy will be performed on the same materials as studied by scanning tunneling microscopy (STM). The parallel combination of tunneling and optical measurements will act synergistically to characterize nano-EPS in these complex materials.

Accomplishments

The major accomplishments in this project were the development and application of two experimental tools for probing the dynamics of quasiparticles in cuprate superconductors, as well as theoretical tools for understanding these dynamics. The first tool is Fourier transform spectroscopy of maps of the local electronic density of states (LDOS) obtained by STM. Spectroscopy with atomic scale resolution was enabled by an ultra-low vibration environment. The stability of the system permitted mapping of the LDOS with atomic resolution and position registry throughout a large area, several hundred angstroms on a side. In our first application, the STM probed the surfaces of the cuprate superconductor [$Bi_2Sr_2CaCu_2O_{8+\delta}$ (BSCCO)], which were cleaved at low temperature and in high vacuum. The LDOS maps revealed enormous variation in both the amplitude and shape of the superconducting gap as a function of position on the sample surface. The gap magnitude varies by 50% with a change in position of only a few tens of angstroms. The extent of spatial inhomogeneity was entirely unanticipated, despite extensive characterization of these materials with other spectroscopic techniques.

When examined superficially, the patterns of inhomogeneity appeared to be random in nature. However, motivated by theoretical work by members of our team, the LDOS maps were investigated by Fourier transform analysis. The Fourier analysis revealed that the variation of LDOS at each energy results from the superposition of ripples with well-defined wavelength and orientation in real space. The wavevector of the ripples changes, or disperses, systematically with energy. Again relying on theoretical insights developed during this project, the shape of the Fermi contour and the variation of the gap energy along it were determined from the dispersion relations. Ultimately, we were able to construct a comprehensive model that explains all the main features revealed in the momentum space maps. This work also stimulated members of our group to develop new theoretical approaches to the transition from the Mott insulating state to the superconducting state. Using these approaches they were able to find an explicit model that exhibits a Mott insulating ground state without any symmetry breaking, proving that the long-sought featureless Mott insulator can indeed exist in nature. The work also led to the understanding that there

are two basic types of Mott insulator, one of which can support electronic inhomogeneity and one of which cannot.

The second experimental tool was the development of a femtosecond laser-based technique capable of direct measurement of quasiparticle propagation. This tool is critical in understanding the extent to which the inhomogeneity revealed by STM affects the dynamics of quasiparticles. In the new technique, two ultrashort laser pulses incident on a sample create a standing wave of intensity, generating a periodic variation in the density of quasiparticles just below the superconductor's surface, see Figure 5. Because the index of refraction at the surface depends on the local quasiparticle density, the surface of the superconductor becomes a diffraction grating. The amplitude of the grating, and hence the crest to trough variation in quasiparticle density, can be measured by a probe beam arriving at the sample after a variable delay time on the order of picoseconds. Following its creation, the grating decays due to the combined effects of recombination, in which quasiparticles reform superconducting Cooper pairs, and diffusion. By adjusting the angle between the two pulses that create the quasiparticles, gratings with spatial periods between two and five microns were made. Analysis of the decay rate of the grating as a function of the spatial period allowed the effects of recombination and diffusion to be separated. Our team found diffusion coefficients of 20, or 24 cm^2/s in the superconductor $YBa_2Cu_3O_{6.5}$ (depending on orientation with respect to the crystal axes) and a recombination lifetime that reached 100 picoseconds at low quasiparticle density. Together these parameters imply a quasiparticle diffusion length of approximately 400 nanometers, which is remarkably large for high-energy quasiparticles. Most importantly, the same diffusion coefficient found in homogeneous crystals of $YBa_2Cu_3O_{6.5}$ were found in BSCCO as well, suggesting that the motion of photogenerated quasiparticles is remarkably insensitive to the extent of gap inhomogeneity.

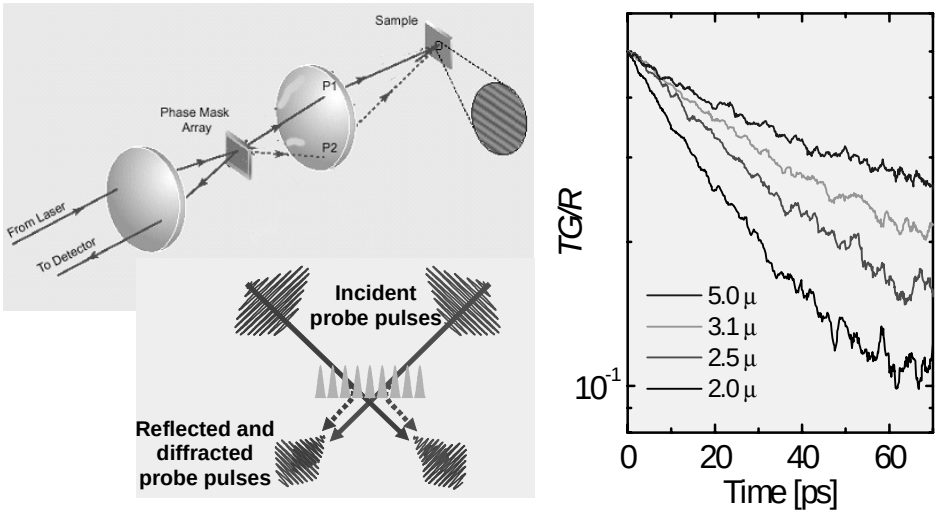

Figure 5. ***Experimental procedure****. (Left figure) Pump pulses are split by a phase mask into two pulses, P1 and P2, which arrive together at a sample of YBCO cooled to 5 °K. Their interference creates a spatially periodic variation in the concentration of photogenerated quasiparticles. Because the index of refraction depends on the quasiparticle density, a transient diffraction grating is formed. A delayed pair of probe pulses detects the grating (lower figure, beams shown in transmission for clarity). Each probe beam is split by the grating into reflected (large amplitude) and diffracted (small amplitude) beams. The decay of the diffracted amplitude with increasing probe delay gives the lifetime of the grating.*

Decay in time *(Right figure) of the quasiparticle grating amplitude for different values of the grating period between 2 and 5 microns. TG is the peak-to-trough amplitude and R is the average grating amplitude. Their ratio (TG/R) decays with time as quasiparticle diffusion depletes the grating crests and fills in the troughs. Analysis of the decay rate of TG/R as a function of period yields the quasiparticle diffusion coefficient and recombination lifetime.*

Publications

K. McElroy, R.W. Simmonds, J.E. Hoffman, D.-H. Lee, J. Orenstein, H. Eisaki, S. Uchida, and J.C. Davis, "Relating atomic-scale electronic phenomena to wave-like quasiparticle states in $Bi_2Sr_2CaCu_2O_{8+\delta}$," *Nature,* **422,** 522 (2003).

J. Orenstein, "Optical conductivity of a superfluid density wave," *Physica C: Superconductivity* **390,** 243 (2003).

N. Gedik, J. Orenstein, R. Liang, D.A. Bonn, and W.N. Hardy, "Propagation of nonequilibrium quasiparticles in a high-Tc superconductor," *Science* **300**, 1410 (2003).

N. Gedik, J. Orenstein, R. Liang, D.A. Bonn, and W.N. Hardy, "Transient gratings formed by nonequilibrium quasiparticles in YBCO6.5," *Journal of Superconductivity: Incorporating Novel Magnetism* **17,** 117 (2004).

N. Gedik, J. Orenstein, R. Liang, D.A. Bonn, and W.N. Hardy, "Non-equilibrium quasiparticle dynamics in single crystals of YBCO Ortho II," to appear in *Physica C*.

N. Gedik, J. Orenstein, R. Liang, D.A. Bonn, W.N. Hardy, "Single-quasiparticle stability and quasiparticle-pair decay in $YBa_2Cu_3O_{6.5}$ (Ortho II)," submitted to *Physical Review B*, available as arXiv:cond-mat/0309121.

Q.-H. Wang and D.-H. Lee, "Quasiparticle scattering interference in high temperature superconductors," *Physical Review B* **67**, 20511 (2003).

D.-H. Lee, "Inhomogeneity in doped Mott insulator," *J. Low Temp. Phys.* **131**, 181 (2003).

D.-H. Lee and S. A. Kivelson, "Two classes of Mott insulator," *Physical Review B* **67**, 24506 (2003).

D.-H. Lee and J.M. Leinaas, "Mott insulators without symmetry breaking", submitted to *Physical Review Letters.*

X.J. Zhou et al, "Quasiparticle scattering in underdoped (La2-xSrx)CuO4 superconductors," submitted to *Physical Review Letters.*

Photoemission Study of Magnetic Quantum Well Interaction

Principal Investigators: Zi Qiang Qiu

Project No.: 02036

Project Description

Quantum well (QW) states are now well recognized as a general property that plays the key role in generating spin dependent phenomena in magnetic nanostructures. In the last few years, it has been shown that the formation of QW states is responsible for oscillatory magnetic coupling and giant magnetoresistance. At the current stage, most effort has been focused on the understanding of a single QW system and its relation to the magnetic interlayer coupling. In this project, we go beyond the single QW to investigate the coupling of QW states from different layers, and then the new magnetic properties in these nanostructures. Electronic states of the QW structures will be measured using angle resolved photoemission spectroscopy (ARPES) at beamline 7.0.1.2 at the Advanced Light Source (ALS) and magnetic properties will be measured using the Photo-Electron Emission Microscope (PEEM) at beamline 7.3.1.1. Then the direct connection between the magnetic behaviors and the electronic confinement will be established in magnetic nanostructures.

Accomplishments

QW states in copper thin films grown on Co/Cu(001) were studied using ARPES. For the normal photoemission, QW states from both lower and higher energy bands relative to the vacuum level were measured, and explained by phase accumulation method (PAM). QW states from the lower band were studied in details as a function of the in-plane momentum. We found that the QW states dispersion depends on the copper film thickness. From the experimental data, we deduced the quantized perpendicular momentum and the energy as a function of in-plane momentum. Our results show that the in-plane effective mass can not be obtained by a simple parabolic fitting.

Magnetic phase transitions in coupled magnetic sandwiches of Cu/Co/Cu/Ni/Cu(100) and Cu/Co/Fe/Ni/Cu(100) are investigated by PEEM. Element-specific magnetic domains are taken at room temperature to reveal the critical thickness at which the magnetic phase transition occurs. The results show that a coupled magnetic sandwich undergoes three types of magnetic phase transitions depending on the two ferromagnetic films' thickness. A phase diagram is constructed and explained in the process of constructing Monte Carlo simulations, which corroborate the experimental results.

Publications

Y.Z. Wu, C.Y. Won, E. Rotenberg, H.W. Zhao, F. Toyoma, N.V. Smith, and Z.Q. Qiu, "Dispersion of quantum well states in Cu/Co/Cu(001)," *Physical Review B* **66**, 245418 (2002).

Y. Z. Wu, C. Won, H.W. Zhao, and Z.Q. Qiu, "SMOKE study of Co thin films grown on double curved Cu(001)," *Physical Review B* **67**, 094409 (2003).

C. Won, Y.Z. Wu, N. Kurahashi, K.T. Law, H.W. Zhao, A. Scholl, A. Doran, and Z.Q. Qiu, "Evidence of the oscillatory magnetic anisotropy in Ni/Co/Ni/Cu(100) ," *Physical Review B* **67**, 174425 (2003).

J.M. An, D. Raczkowski, Y.Z. Wu, C.Y. Won, L.W. Wang, A. Canning, M.A. Van Hove, E. Rotenberg, and Z.Q. Qiu, "Quantization condition of quantum-well states in Cu/Co(100)," *Physical Review B* **68**, 045419 (2003).

C. Won, Y.Z. Wu, H.W. Zhao, A. Scholl, A. Doran, and Z.Q. Qiu, "Effect of the interlayer coupling on the Ni spin reorientation in Ni/Fe/Co/Cu(100) ," *Physical Review B* **68**, 052404 (2003).

C. Won, Y.Z. Wu, A. Scholl, A. Doran, N. Kurahashi, H.W. Zhao, and Z.Q. Qiu, "Magnetic phase transition in Co/Cu/Ni/Cu(100) and Co/Fe/Ni/Cu(100) ," *Physical Review Letters* **91**, 147202 (2003).

A MEMS "Test Kit" for Structure—Mechanical Property Relationships at the Nanoscale

Principal Investigators: Eric Stach, Robert Ritchie, and Ulrich Dahmen

Project No.: 03026

Project Description

The explosion of research in nanostructured materials has led to a critical need for mechanical property determination. Our goal was the creation of a "Test Kit" of micromachines for determining the mechanical properties of nanomaterials coupled with real time observations of microstructural response at the nanoscale. Specifically, we had planned to:

- Standardize testing methods for *in-situ* transmission electron microscopy mechanical testing of thin films and nanostructured materials.
- Develop infrastructure and expertise in the area of mechanical testing of nanomaterials to meet the needs of the nanoscience community, both at Berkeley Lab's Molecular Foundry and the broader scientific community through the National Center for Electron Microscopy's (NCEM) user facility.

The proposed method was the modification of the existing microelectromechanical system (MEMS) mechanical testing machines so that they may be operated within the objective lens region of both transmission and scanning electron and ion microscopes at NCEM. This offers the unprecedented ability to observe in real time the physical links between microstructural response and mechanical properties of materials at the nanoscale. This will permit unparalleled *in situ* characterization of structural micromechanisms at these dimensions. The approach will be to standardize the different machines so that they may all be operated on the same platform. This will allow us to utilize the different imaging capabilities of the electron microscopes at NCEM to look at both surface and internal structure at ultrahigh resolutions during mechanical deformation.

Accomplishments

As a primarily experimental project, the first tasks undertaken were the design and building of the experimental apparatus to permit the operation of MEMSs inside the electron microscope. There are several fundamental challenges associated with this experimental method, namely: the small space within the microscope, the need to make relatively high voltage, low noise interconnects to the devices, and to address basic questions regarding whether or not the devices would function properly under the electron beam current and whether or not simultaneous imaging would be possible during actuation.

We first approached this problem by building a simple system for NCEM's scanning electron microscope. This microscope has the advantage of having a larger sample chamber, easier electrical access, and smaller electron beam current for answering the questions outlined above. A simple sample stage—based on a common testing solution used in the electronics industry—was fabricated. Following this, two relatively widely accepted MEMS-based micromechanical testing devices were used to determine the feasibility of the approach. The first of these—an electrostatically actuated resonating fatigue testing structure—is shown operating *in-situ* in Figure 6 a. From this image it is apparent that very high quality images of the sample surfaces can be obtained even during actuation. A second device—an on-chip wear structure obtained from the Sandia MEMS reliability group—is shown in two different stages of the actuation process as Figure 6b and 6c. Again, one can see that it is possible to run these devices in the microscope concomitant with the acquisition of high quality images.

Following these "proof of principle" experiments, we embarked upon the design and building of stages for actuation in NCEM's DualBeam Focused Ion Beam/Scanning Electron Microscope system, which allows higher contrast images, along with section and micromanipulation capabilities, and the 300 kV *in situ* Transmission Electron Microscope (TEM) for imaging of

the internal structure of the sample. The apparatus for the FIB/SEM was completed by the termination of this project, and the design for the TEM—a significantly more challenging task due to the small volume (20 mm^2) of the microscope chamber—was begun.

Continuation funding for this project was not approved. Nonetheless, we feel that several important questions were answered regarding the feasibility of this type of experimentation and several initial observations regarding the mechanisms of fatigue and wear in these systems were obtained. Based on our firm belief in the unique insight that can be obtained from this experimental approach and the importance of this particular area of study, we will be incorporating this work into our upcoming renewal for DOE core funding in the area of High Performance Metals and Semiconductors in the Materials Science Division's Center for Advanced Materials.

Publications

D.H. Alsem, E.A. Stach, C.L. Muhlstein, M.T. Dugger, and R.O. Ritchie, "Combining on-chip testing and electron microscopy to obtain a mechanistic understanding of fatigue and wear in microelectromechanical systems," oral presentation at the Minerals, Metals, and Materials Society (TMS) 2004, Annual Meeting.

D.H. Alsem, E.A. Stach, C.L. Muhlstein, M.T. Dugger, and R.O. Ritchie, "Combining on-chip testing and electron microscopy to obtain a mechanistic understanding of fatigue and wear in microelectromechanical systems," oral presentation at the Materials Research Society Spring 2004 meeting.

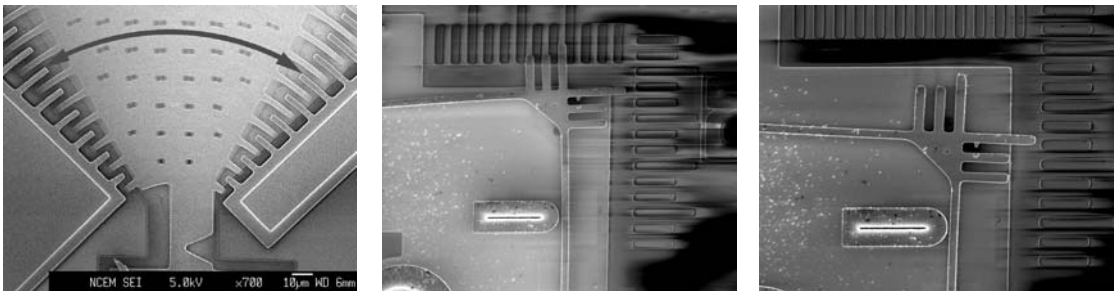

(a) ***(b)*** ***(c)***

Figure 6. (a) Scanning electron micrograph of an electrostatically actuated fatigue structure resonating during in situ *imaging in the TEM (b-c) two higher resolution images of an electrostatically actuated wear structure showing that real time imaging is feasible.*

All Nitride, Full Solar Spectrum Photovoltaics

Principal Investigators: Wladyslaw Walukiewicz, Joel Ager, Eugene Haller, and William Schaff (Cornell University)

Project No.: 03029

Project Description

We have recently discovered that the bandgap range of the $In_{1-x}Ga_xN$ ternary alloy system extends over a very wide energy range from 0.7 to 3.4 electron volts and thus provides a near-perfect match to the solar energy spectrum. This creates the opportunity to synthesize material with any band gap within the solar spectrum and to design and fabricate new multijunction solar cells that will realize the theoretically predicted ultimate efficiency of this design. We anticipate at least a two-fold increase of the efficiency of the solar cells based on the $In_{1-x}Ga_xN$ alloy system compared with the maximum efficiency of about 30% in currently available multijunction cells, which are constrained to use materials with non-optimal bandgaps. An additional and very important advantage of the proposed material system is its thermal stability and radiation hardness that would uniquely qualify $In_{1-x}Ga_xN$ based solar cells for applications in harsh environments (radiation, space, and military).

We determined a number of critical properties of $In_{1-x}Ga_xN$ alloys that are relevant for using this system in super high efficiency multijunction solar cells. We focused on the properties of the newly discovered low-band gap In-rich alloys synthesized by molecular beam epitaxy by William Schaff's group at Cornell University. The crystal growth was optimized to reduce the dislocation density and the level of unintentional doping. We concentrated on measuring the properties of the conduction band and on evaluating the radiation hardness of the material. We also attempted to achieve p-type doping and evaluated candidates for forming heterojunctions. Results have been useful in developing designs for maximum efficiency multijunction cells for terrestrial as well as space applications.

Accomplishments

We have undertaken a systematic study of InN and In-rich group III-nitride alloys, utilizing films grown by molecular beam epitaxy (MBE) by our collaborators at Cornell University. As shown in Figure 7, we have used optical absorption, photoluminescence, and photomodulated reflection data to demonstrate unequivocally that the direct band gap of InN is only 0.7 eV as opposed to the formerly accepted value of 2 eV. This finding has remarkable consequences for the understanding of the electronic structure of all group III-nitride alloys. We showed that the small band gap and the strong interaction between the conduction and the valence band in InN leads to a highly non-parabolic dispersion relation for the conduction band and to an energy dependent electron effective mass, which varies from $0.07m_0$ in intrinsic InN to $0.26m_0$ for an electron concentration $n = 10^{21}$ cm^{-3}. Owing to the Burstein-Moss shift, the absorption edge shifts from 0.7 eV in intrinsic InN with n in the range of 10^{18} cm^{-3} to above 2 eV for $n = 10^{21}$ cm^{-3}. This result nicely explains the origin of the apparent large band gaps previously observed in polycrystalline InN films synthesized by sputtering and other methods.

In light of our new understanding of InN we have systematically evaluated the composition dependence of the band gap of all group III-nitride alloys with an emphasis on In-rich $In_{1-x}Ga_xN$ alloys. The alloy bandgaps in InGaN, AlGaN, and AlInN can now be described in a consistent manner by relatively small bowing parameters which scale with the energy gap difference between the constituent compounds. Our work shows that the direct energy gap in group III-nitride alloys can be continuously changed from the near infrared in InN to deep ultraviolet in AlN. This unprecedented energy gap range creates opportunities for new applications. For example, the band gaps of $In_{1-x}Ga_xN$ alloys provide a nearly perfect match to the solar spectrum, raising the interesting possibility of using these alloys for high efficiency multijunction solar cells. Since the space is the primary place for utilizing such cells the radiation hardness is critical. As an initial test of the radiation resistance of the InN-GaN system, a series of InN and $In_{1-x}Ga_xN$ films was exposed to 2 MeV proton doses of up to $4x10^{14}$ cm^{-2}. It was observed that the photoluminescence (PL) intensity, which is sensitive to the minority carrier lifetime, was reduced by a maximum of a factor of ten at the highest dose (PL from GaAs decreased by a factor of 1000 at this dose). Given that proton irradiation at much smaller doses (ca. 10^{12} cm^{-2}) have been observed to reduce the power conversion efficiency of GaAs cells by 50%, these results suggest that the optoelectronic properties of InN and InGaN are much less affected by radiation damage.

Two significant challenges in developing practical optoelectronic devices in this alloy system are achieving efficient carrier transport (majority and minority) and establishing p-type doping. We showed that the room temperature electron (majority carrier) mobility in MBE-grown InN is at least 2/3 that of the theoretical limit. This shows that the electrical quality of the MBE material is very high. We have assessed the feasibility of achieving p-type doping in InN and In-rich $In_{1-x}Ga_xN$; if the concentration of unintentional donors can be reduced sufficiently, this should be achievable, although electron accumulation at surfaces and interfaces may be an issue. We also evaluated candidates for forming heterojunctions to p-type materials. There are a number of candidates in the Cu-III-VI_2 chalcopyrites that are promising.

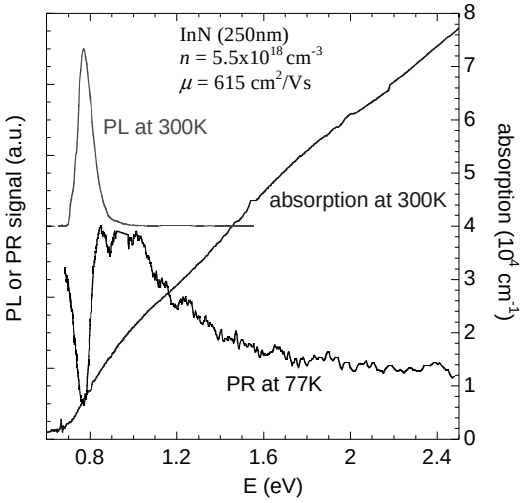

Figure 7. Absorption, photoluminescence (PL) and photomodulated reflectivity (PR) spectra demonstrating the 0.7 eV direct gap of InN.

Publications

J. Wu, W. Walukiewicz, K.M. Yu, J.W. Ager, S.X. Li, E.E. Haller, H. Lu, and W.J. Schaff, "Universal bandgap bowing in group-III nitride alloys," *Solid State Communications* **127**, 411 (2003).

J. Wu, W. Walukiewicz, W. Shan, K.M. Yu, J.W. Ager III, S. X. Li, E.E. Haller, Hai Lu, and W. J. Schaff, "Temperature dependence of the fundamental bandgap of InN," *Journal of Applied Physics* **94**, 4457 (2003).

J. Wu, W. Walukiewicz, K.M. Yu, W. Shan, J.W. Ager III, E.E. Haller, H. Lu, and W. J. Schaff, W.K. Metzger, S.R. Kurtz, and J.F. Geisz, "Superior radiation resistance of $In_{1-x}Ga_xN$ alloys: a full-solar-spectrum photovoltaic material system," *Journal of Applied Physics*, **94**, 6477 (2003).

J. Wu, W. Walukiewicz, K.M. Yu, J.W. Ager III, E.E. Haller, H. Lu, and W. J. Schaff, "Narrow bandgap group-III nitride alloys," *physica status solidi* (b), 240, 412, (2003).

S.X. Li, J. Wu, W. Walukiewicz, W. Shan, E.E. Haller, H. Lu, and W.J. Schaff, "Hydrostatic pressure dependence of the fundamental bandgap of InN and In-rich group III-nitride alloys," *Applied Physics Letters* **83**, in press 2003.

W. Walukiewicz, K.M. Yu, J. Wu, H. Lu, and W. J. Schaff "Environmental resilient, full solar spectrum group III-nitride based high efficiency multijunction photovoltaic devices," LBNL Patent Application IB-1827P.

Fabrication and In Situ *TEM Study of Nanocontacts in Embedded Nanophase Systems*

Principal Investigators: Xiao-Feng Zhang, Peidong Yang, and Peggy Hou

Project No.: 03031

Project Description

The goal of this project is to investigate nanoscale hetero-contacts that are anticipated to be a major focus as nanotechnology advances from synthesizing nanophases to interconnecting nanocomponents. A computer chip in the future may contain billions of permanent nanocontacts that are extremely important to the performance and reliability of devices. However, there is a severe lack of information on how the atomic bonding at nanocontacts will be developed and how the nanocontacts will behave under active application environments. We propose to study oxide/metal and semiconductor/metal nanocontacts using atomic resolution, *in situ* transmission electron microscopy (TEM). Through the study, fundamental knowledge of the formation and stability of bonding and structural evolution in dynamic situations that mimic application environments will be acquired. The project also emphasizes the development of advanced nanofabrication techniques that produce nanocontacts suitable for structural and analytical characterizations using TEM.

Nanocontacts with point and line geometries will be fabricated and studied. Vertically grown Si or Ge nanowires on Si substrates will be embedded in epoxy and to form point nanocontacts with a metal film. Oxide nanowires will be coated with nanometer-thick metal layers to form one-dimensional hetero-contacts. Both systems allow the study of size effects on structure and property of the nanocontacts. *In situ* TEM characterizations will be carried out at elevated temperatures or with applied electric current flow to provide crucial information on the response of the nanocontacts to external fields.

Accomplishments

Realizing that one-dimensional, line contacts are one of the most important components in nanodevices, high priority was given to their fabrication and characterization. In preparation of the line nanocontacts for *in-situ* TEM study, a new method was developed which allows direct TEM observation of the fabricated samples without further modification that could introduce impurities. In this method, oxide nanoribbons are first produced using a chemical method. These ribbons are tens of micrometers long, less than 20 nanometers thick and the minimum width is between 15 and 40 nanometers. Hetero-structural, one-dimensional contacts of truly nanometer dimensions are formed by depositing a metal layer onto the narrow edge of the ribbons, and the sample is immediately ready for TEM investigation. SnO_2 and ZnO nanoribbon templates have been produced, on which Cu, Al, Ni, and Au metal lines were deposited. Intensive TEM analyses were performed along the hetero-interface with the interface line perpendicular to the electron beam.

Two examples of line nanocontacts are shown in Figure 8. The interface is always seen to be smooth, abrupt, and without secondary phase. While the metal coating in most of the one-dimensional metal/oxide nanocontact systems showed a polycrystalline structure, Cu lines on SnO_2 produced both single and polycrystalline structures, depending on the orientation of the template surface. Thermal stability of the Cu/SnO_2 line nanocontacts was examined in a high spatial resolution transmission electron microscope equipped with a double-tilt, *in situ* heating stage. The firmly bonded interface and the different thermal expansions between Cu and SnO_2 caused elastic bending of the bilayer nanobeams upon heating, but the nanocontacts remained to be structurally stable up to 200°C in the microscope vacuum. This elastic bending behavior was completely reversible during thermal cycling if the Cu was single crystalline and the elastic bending could be precisely fitted to models developed for micro cantilever beams. At about 300 to 350°C, minor undulation was seen on the top surface of the Cu lines, implying activation of atomic diffusion. Debonding occurred at the Cu/SnO_2 interface above 400°C, giving rise to islands of Cu separated by nanometer sized gaps. The rate of boundary receding at the edge of the Cu islands shows an initial linear relationship with time, indicating surface diffusion controlled kinetics. The equilibrium shape of the Cu islands should be dictated by the surface and interface energies of the Cu and SnO_2. Alloying between Cu and SnO_2 did not happen until about 700°C.

In order to perform *in situ* bias TEM study on the one-dimensional line nanocontacts, a TEM bias holder has been designed and fabricated by the National Center for Electron Microscopy at Berkeley Lab. The bilayer nanoribbons can be placed to make connection between two metal feet in the

holder which are connected with an external d.c. source-measure unit with a measurement sensitivity of 10^{-14} A and 10^{-5} V. The effect of d.c. current on structure of Cu/SnO_2 and Cu/Si one-dimensional nanocontacts are under study.

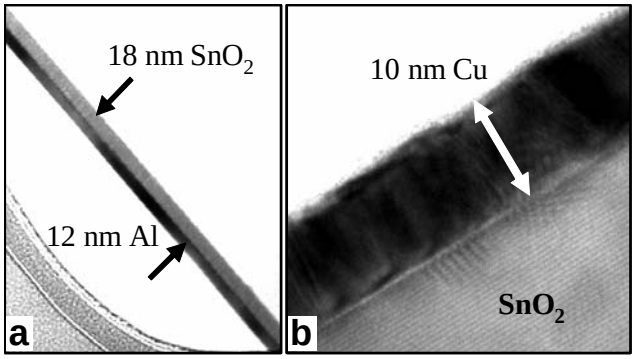

Figure 8: (a) Al/SnO_2 one-dimensional nanocontact. (b) 10 nanometers-thick single crystalline Cu layer bonded with a SnO_2 nanoribbon template.

Publications

M. Law, T. KuyKendall, P. Yang, and X.F. Zhang, "The thermomechanical behavior of bilayer nanocantilevers," *Proceedings of 2003 Materials Research Society (MRS) Spring Meeting,* April 2003.

X.F. Zhang, M. Law, R. Yu, T. KuyKendall, and P. Yang, "Structure of Cu/SnO_2 nanoscale line contacts," in preparation.

X.F. Zhang, M. Law, R. Yu, T. KuyKendall, and P. Yang, "*In-situ* heating TEM study of nanoscale Cu/SnO_2 bilayer ribbons," in preparation.

M. Law, X.F. Zhang, T. KuyKendall, J.R. McKinney, and P. Yang, "The bending behavior of bilayer nanocantilevers," in preparation.

Nuclear Science Division

Effective Field Theory and Few-nucleon Systems

Principal Investigators: Paulo Bedaque

Project No.: 02039

Project Description

The goal of this project is to extend the effective field theory methods recently developed for the two-nucleon sector to systems involving three or more particles, including bulk matter. Our aim is to develop model independent, rigorous, and precise calculations of processes involving electroweak currents on triton-3He.

More specifically, we plan to perform a third-order calculation of the triton decay that can then be applied to determine the short distance contribution needed for a 1% level calculation of neutrino-deuteron break up, relevant for Sudbury Neutrino Observatory (SNO) and proton-proton fusion, fundamental for solar models.

Due to the similarities between the physics of the low-energy nucleon-nucleon interaction and that of some atomic species we will examine applications to the physics of atomic traps, especially close to a Feshbach resonance.

Accomplishments

The kind of fine tuning that is the hallmark of nucleon-nucleon interactions, and forms the backbone of the effective field theory approach we investigate, also occurs in other nuclear systems in higher partial waves. As an example, there is a resonance in the neutron ^{4}He scattering very close to threshold. We extend our formalism to these situations with an eye towards the application of our methods to halo nuclei. The power counting near a resonance in an arbitrary partial wave was established and we are presently applying it to the simplest three-body halo nucleus, ^{6}HE.

The effective theory approach to superfluid systems led us to recognize a new important degree of freedom at super-nuclear densities that had not been considered before. It is believed that at densities around twice the nuclear density, neutrons form Cooper pairs in a p-wave. The formation of this condensate breaks rotational symmetry and leads to the existence of Goldstone bosons. These Goldstone bosons, being massless, dominate the transport properties of neutron matter at small temperatures. They also couple to neutrinos; collisions among them can produce neutrino emission at a rate that is not suppressed by Boltzman factors. By simple arguments one can see that this process is proportional to T^9, where T is the temperature. Our estimate of the proportionality constant indicates that this process is the dominant cooling mechanism for a range of temperatures. It will probably not be a significant mechanism of cooling of neutron stars since Cooper pair formation that dominates close to the critical temperature can occur at all times in some shell inside the star.

Pairing between fermionic systems can occur in a variety of physical systems, ranging from nuclear and quark matter to atomic traps. In particular, the creation of paired fermionic states in atomic traps achieved this year raised a lot of interest in the problem. Since in BCS theory pairing occurs between particles with equal and opposite momenta, it is unclear what would be the ground state of a system with two species of particles with different Fermi momenta. In the last year two exotic alternatives appeared in the literature, one involving deformed Fermi surfaces and the other where a “hole” in momentum space is created to accommodate pairing with different densities. We argued that those states are unstable against the formation of an inhomogeneous state, mixed state, composed of two phases: a BCS phase with equal densities for the two species and a normal phase with very asymmetric densities. We also argued that the creation of these asymmetrical, inhomogeneous states could be used for the experimental detection of fermion superfluidity in atomic traps, an outstanding problem in the field, by imaging the two species separately and looking for the bubbles of the BCS phase inside the normal phase. We are also discussing the inclusion of Coulomb effects necessary to determine whether this mixed phase is likely to occur in quark matter in neutron stars.

The connection between nuclear physics and quantum chromodynamics (QCD) has been a long term goal of the field. Effective Field Theory methods, such as the ones we are developing, are an essential ingredient in this program. One reason is that the quark masses in the current simulations are larger than in the real world; therefore, a rigorous way of extrapolating nuclear observables as a function of the quark masses can provide the link between feasible simulations and realistic physics. We realized that the interaction between a Λ and a nucleon would be the least dependent on the quark masses. They are also important for the physics of hypernuclei and very poorly known experimentally. The extension of the nuclear effective theory to include the hyperon is straightforward and we provide the dependence of the effective range

parameters of Λ-nucleon scattering not only as a function of the quark masses but also for separate dependence on the sea and valence quark masses, which are useful for extrapolations from partially quenched simulations.

Publications

P.F. Bedaque, H.W. Hammer, and U. van Kolck, "Narrow resonances in effective field theory," *Physics Letters B* **569,** 159–167 (2003).

P.F. Bedaque, G. Rupak, and M.J. Savage, "Goldstone bosons in the 3P(2) superfluid phase of neutron matter and neutrino emission," nucl-th/0305032, May 2003, to be published in *Physical Review C*.

P.F. Bedaque, H. Caldas, and G. Rupak, "Phase separation in asymmetrical fermion superfluids," cond-mat/0306694 , June 2003, to be published in *Physics Review Letters*.

S.R. Beane, P.F. Bedaque, A. Parreno, and M.J. Savage, "Exploring hyperons and hypernuclei with lattice QCD," nucl-th/0311027, submitted to *Physical Review C*, (November 2003).

P.F. Bedaque, A. Bulgac, and G. Rupak, "Quantum corrections to dilute bose liquids," *Physical Review A* **68**, 033606 (2003).

P.F. Bedaque, G. Rupak, H.W. Griesshammer, *and* H.W. Hammer, *"Low-energy expansion in the three-body system to all orders and the triton channel," Nuclear Physics A* ***714***, 589–610 (2003).

Design of Digital Signal Processing Electronics for High-resolution Solid State Detectors

Principal Investigators: I-Yang Lee

Project No.: 01032

Project Description

This project was carried out to initiate the development of digital electronics and associated data processing software for future high-resolution radiation detectors, such as the Gamma-Ray Energy Tracking Array (GRETA) project led by the Nuclear Science division of Berkeley Lab. The goal of this project is to design, manufacture, and test an 8-channel, 100 MHz analog to digital converter (ADC) board to: (1) instrument the GRETA module prototype array and (2) serve as a basis for a more complex 40-channel ADC board required for the full GRETA array. The board also meets the specifications for a general-purpose digital signal processing board for the low-energy nuclear physics community outlined at the digital electronics workshop held at Argonne National Laboratory in 2001.

Unlike commercially available ADC boards, specialized real-time signal processing is required on the board itself to perform real time data reduction, implement the complex trigger logic that the system requires, and emulate the required elements of traditional analog systems. This board requires very high readout rates due to both the high detector counting rates, 20 kilohertz, and the large amount of data produced per gamma-ray interaction, 100 bytes.

The board itself is designed around eight commercial 100 megahertz pipeline ADC chips whose data streams are fed into a single Virtex 2 Field Programmable Gate Array (FPGA) which is responsible for all on board processing. This state of the art FPGA also contains internal memory buffers that are employed to allow for up to 10μs of latency for more flexible trigger configurations. The FPGA provides eight leading edge discriminators for triggering and eight constant fraction discriminators for amplitude independent signal timing. The energy of each signal is determined by application of a trapezoidal filter to the incoming signal. An adjustable window is also generated allowing one to extract only the part of the signal required for subsequent signal decomposition thus eliminating extraneous data early in the data acquisition process. Data is sent to the acquisition computer through a standard VERSA Module Eurocard (VME) bus allowing the card to be used in the wider low-energy nuclear physics community as well as the GRETA project.

Accomplishments

We have completed the prototyping and production of a digital signal processing board for highly segmented HPGe detectors to be employed in gamma-ray tracking arrays such as GRETA. Activities this year included the comprehensive testing of a digitizer board produced last year and the design and construction of a second prototype that addressed shortcomings in the initial board found during testing.

The noise level of the board was measured to be $\pm$ 1 bit, which is essentially the noise level of the pipelined ADC chip that was employed. This demonstrated effective isolation of the digital and analog stages of the board even in the presence of data transfers over the VME backplane. The board threshold was shown to be below 20 kilo-electronvolt with a dynamic range of 5 mega-electronvolt.

Initial tests of the digital signal processing board with pulsers and sources showed the energy resolution to be poorer then equivalent analog systems. This problem was

traced to two causes. The primary reason for the degraded energy resolution was found to be a problem in the front-end variable gain amplifier employed by the board. Fixing the gain of this stage during the test improved energy resolution to a level comparable with analog systems. The second problem, which was previously understood, was the lack of a pole-zero corrector in the energy algorithm implemented on the board. When the correction was applied offline an energy resolution of 2.3 kilo-electronvolt at 1.3 mega-electronvolt was achieved which is competitive with analog systems.

The energy spectrum obtained is shown in the Figure 1. An algorithm for a pole/zero corrector and its VHDL was developed this year. VHDL stands for VHSIC (Very High Speed Integrated Circuits) Hardware Description Language, implementation.

With sources, the board achieved rates of several thousand counts per second, including associated signal traces, and was only limited by the network interface of the embedded processor used for data acquisition. This throughput, facilitated by the windowing algorithm employed on the board that extracts only relevant parts of the signal trace, meets the requirements for performing tests with tracking detectors. Other tests carried out included the global timing and board synchronization system and the board's three triggering modes.

The three digitizer boards were also used in an in-beam test with the GRETA prototype 2 detector; they were found to be very stable and met the required resolution and data rate requirements.

Following the testing procedure a redesign of the board was carried out to add several new features and address problems found during the testing procedure. The variable gain amplifier was replaced by a two-way switchable, fixed-gain amplifier. A mechanism to program the FPGA over the VME backplane was developed and implemented allowing easier experimentation with new algorithms on the digitizer board. Also, the DC-DC converters that were previously mounted on an external power supply board are now mounted on the digitizer board itself making the system much easier to use.

In summary, the eight-channel boards developed and produced during this project were found to meet the needs for testing gamma-ray tracking detectors and will serve as the basis of the 10-channel signal processing board for the GRETA detector array. Prototype boards were sent this year to Oak Ridge National Laboratory (ORNL) and National Superconducting Cyclotron Laboratory (NSCL) at Michigan State University for testing and evaluation for use in future projects. New funding has been obtained from DOE in FY04 and we are producing 15 signal processing boards for use in the testing of the Gretina prototype detector.

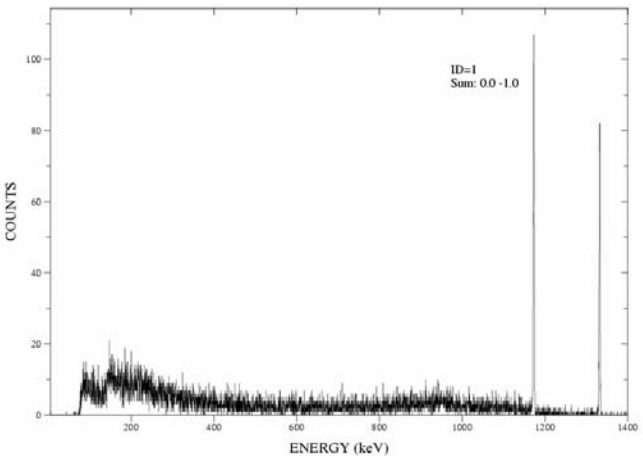

Figure 1. Energy spectrum obtained from a ^{60}Co source from the prototype signal processing board following an offline pole-zero correction.

Publications

I-Yang Lee, "Gretina, a gamma ray energy tracking array," Radioactive Nuclear Beams 6, Argonne, Illinois, 2003.

S. Zimmerman, "Front-end digital signal processing for Majorana," Majorana Collaboration Meeting, Seattle, Washington, 2003.

M. Cromaz, "The GRETA prototype ADC board," Workshop on Experimental Equipment for RIA, Oak Ridge, Tennessee, 2003.

Concepts for a Premier Stable Beam Capability for Low Energy Nuclear Physics

Principal Investigators: Daniela Leitner, I-Yang Lee, and Stuart Freedman

Project No.: 03016

Project Description

Our goal is to initiate and develop the technical plan for creating a world-class stable ion beam accelerator capable of accelerating essentially all elements and providing high intensity light and heavy mass ion beams with precise timing capabilities. First, we will explore the feasibility and cost effectiveness of a major reconstruction of the 88-Inch Cyclotron to determine whether an upgrade would provide essential new accelerator capabilities for meeting the needs of the low energy nuclear physics community during the next decade. A key element is to find possibilities to

enhance the capabilities of the accelerator with respect to true maximum and minimum final energy as well as the ion beam intensities. Then, we will evaluate alternative concepts to determine if: a new cyclotron or a superconducting linac should be sited at the 88-Inch Cyclotron complex or another Berkeley Lab site. These detailed analyses will result in a list of parameters and requirements, conceptual beam optics, and preliminary engineering layouts. Then, we will evaluate the results of the initial research and refine the overall plan.

Accomplishments

This project focused on the development of a technical plan to substantially upgrade the 88-Inch Cyclotron vacuum system. The upgrade would greatly expand the capabilities of the accelerator especially in the low energy range and overall increase the ion beam intensity for heavy ions. The results of this engineering study are documented in detail in the LBNL report LBID-2492.

The results were accomplished in a stepwise approach.

First, we have derived a detail ProE three-dimensional, computer aided design (CAD) model of the cyclotron from the original prints that included all documented and undocumented upgrades and changes. The effort was focused on the components critical for the proposed vacuum upgrade. We drafted 127 drawings in ProE for this project. In addition, the modeling focused on the documentation of all iron parts and the electromagnetic coils. This information will be essential during the upgrade to model the magnetic field. To maintain the performance of the cyclotron, it is critical to preserve the magnetic field configuration as closely as possible. Therefore, the magnetic modeling will be an important tool during the construction and the re-commissioning phases. As an example, Figure 2 shows the assembly drawing of the 88-Inch Cyclotron accelerator. The three-dimensional model proved to be very useful for this study and was used extensively. Initially the model was used to understand the original design and construction of the 88-Inch Cyclotron. It also helped to establish a procedure and timeline to disassemble and reassemble the cyclotron. In addition, the ANSYS models for the finite element analyses (FEA) were extracted from these ProE drawings.

As the next step the FEA with ANSYS was conducted to understand the cause of the vacuum dependence on the magnetic field in the cyclotron. The magnetic and vacuum loads on the seal region as well as the Dee tank and resonator tank were modeled with FEA. The results from the FEA were verified with measurements of displacements of the magnetic poles. They conclusively explain the observed correlation between the magnetic field and the vacuum and establish the displacement of the magnetic iron poles due to magnetic force as the cause of vacuum leak in the Dee tank.

Based on the results of the FEA study, new vacuum seal concepts were developed and designed. The new design replaces the original, leaking, metal seal with a welded joint. Due to the strong forces, a very careful design of the weldment is necessary. The proposed solution consists of a combination of a vacuum weld and a structural weld.

In addition, the new design replaces the remaining wire and corner seals of the Dee tank with one continuous seal, which will reduce the complexity of the assembly and will further enhance the vacuum performance. Finally, a new vacuum-pumping scheme was developed that replaces the existing diffusion pumps with a turbo- and cryo-pump combination. The combination of these enhancements will establish an operating pressure of the accelerator in the high 10^{-8} Torr, which is more than an order of magnitude better than the currently achievable vacuum pressure.

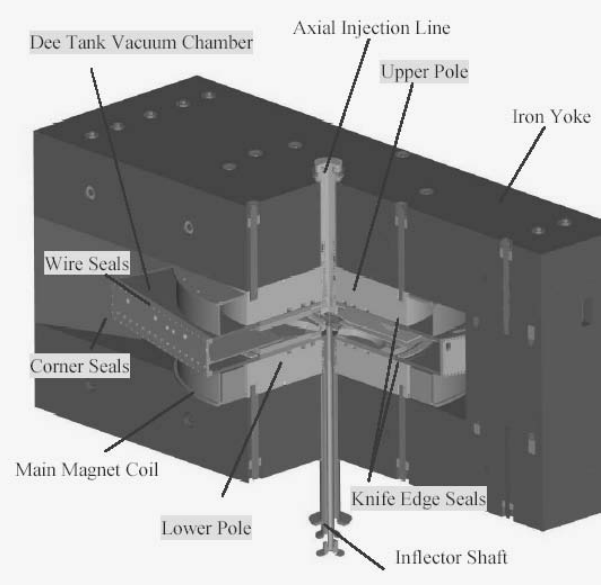

Figure 2. Three-dimensional CAD rendering of the 88-Inch Cyclotron. The hardware components forming the Dee tank are highlighted.

Publications

A.S. Ladran, Y. Minamihara, and D. Leitner "The 88-Inch Cyclotron vacuum upgrade," LBID-2492.

Detector Research and Development for Low Energy Solar Neutrino Detectors

Principal Investigators: Kevin Lesko

Project No.: 02047

Project Description

The last year witnessed many significant discoveries in the field of neutrino oscillations and neutrino properties. The results from the Sudbury Neutrino Observatory (SNO) Neutral Current Measurements both in pure D_2O and with D_2O plus NaCl continued to refine both the mixing angle (θ_{12}) and isolated the Δm^2 solution to the solar neutrino problem. When combined with other solar neutrino experimental results (Cl, Ga, and H_2O) the SNO results yield a single solution in parameter space. This solution is significant in that it consistently identifies the large mixing angle (LMA) as the only remaining solution to the solar neutrino problem, it requires the existence of matter-affects at the ~5-σ level to explain the level of suppression in SNO and the other experiments, and θ_{12} is significantly determined (at the > 5 σ level) to be non-maximal in contrast with atmospheric neutrinos. When combined with KamLAND's first results the earlier solar neutrino experiments identified two regions in the LMA, the so-called LMA-I and LMA-II as potential solutions of the Solar Neutrino Problem. SNO's refined NaCl measurement uniquely identified at greater than 99.7% confidence level that only the LMA-I solution remains and provides KamLAND with well-defined predictions for its future spectral measurements. Fortunately, the LMA-I solution should provide a noticeable spectral distortion to facilitate the precise determination of Δm^2.

These results (SNO's and KamLAND's) have refocused the discussion in the neutrino community. Future experiments involving solar neutrinos have well-determined and challenging goals. The use of well-calibrated solar proton-proton (pp) neutrinos enables the most precise determination of θ_{12} envisioned in the coming decades. It will permit detailed testing of solar models at a level approximately ten times more detailed than currently possible. Direct tests for sterile neutrinos in the solar neutrino flux can be attempted, again with an increase in sensitivity of an order of magnitude. Finally, searches for neutrino magnetic moments can be mounted using the energy-dependence of neutrino elastic scattering

Accomplishments

The efforts this year focused on three principal detector aspects: (1) preliminary engineering design, (2) identification of appropriate shielding materials, and (3) researching ancillary detection schemes for super-fluid helium. These efforts were conducted in close collaboration with the Brown University group of Lanou and Seidel.

The preliminary engineering design was produced, shown in Figure 3. This design includes all the major detector design elements and advanced earlier schematics by including detector material limitations, with the aim of providing detailed input for underground installation.

One of the major elements of the detector, not yet well-defined, is the first level of radioactive shielding. This shield provides a dead layer between the sensitive superfluid helium and cryostat. We assisted the Brown group in performing neutron activation analysis to identify potential materials for this shield. Graphite, in particular, was pursued as a likely shielding material.

The development of the engineering model has stimulated research into a variety of ancillary and independent detection techniques, compatible with the superfluid media that can potentially enhance the detection of elastically scattered neutrinos.

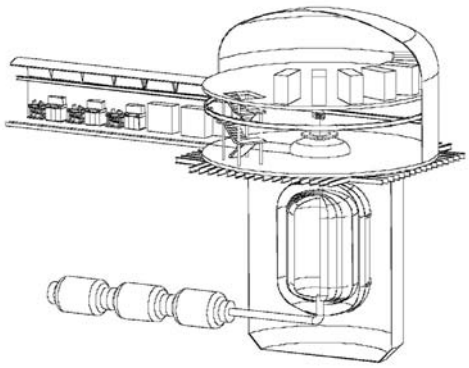

Figure 3. Engineering model of a 20 tonne superfluid helium detector for the detection p-p solar neutrinos.

Publications

H. Eguchi, Y.H. Huang, Y.H. Kim, R.E. Lanou, H.J. Maris, A.N. Mocharnuck, G.M. Seidel, B. Sethumadhavan, and W. Yao, with collaboration on engineering and computation on simulations: K.T. Lesko and A.W. Poon, "HERON, Detection of pp and ^{7}Be solar neutrino elastic scattering in superfluid helium," 4th International Workshop on Solar Neutrinos, May 19–21, 2003, APC, Paris France. Lanou et al. http://cdfinfo.in2p3.fr/LowNu2003/

H. Eguchi, Y.H. Huang, Y.H. Kim, R.E. Lanou, H.J. Maris, A.N. Mocharnuck, G.M. Seidel, B. Sethumadhavan, and W. Yao, with collaboration on engineering and computation on simulations: K.T. Lesko and A.W. Poon, "Update on HERON, Detection of pp and ^{7}Be solar neutrino elastic scattering in superfluid helium," presentation at 8th International Conference on Topics in Astroparticle and Underground Physics, September, 2003, Seattle WA. Lanou et al. http://int.phys.washington.edu/taup2003/

Research on a Next Generation Vertex Detector

Principal Investigators: Howard Wieman, Fred Bieser, Stuart Kleinfelder, and Howard Matis

Project No.: 02048

Project Description

This project will develop an improved vertex detector technology suitable for next generation experiments at the Relativistic Heavy Ion Collider (RHIC) at Brookhaven National Laboratory, heavy ions at the Large Hadron Collider (LHC) at CERN, and Next Linear Collider (NLC) at Stanford Linear Acclerator Center (SLAC). There is tremendous interest in high energy heavy ion physics, including the Solenoidal Tracker (STAR) at RHIC, as well as RHIC's PHENIX and PHOBOS collaborations in installing new thin, high-resolution vertex detectors to measure open charm through detection of D mesons. We are developing a recently demonstrated technology, active pixel sensors (APS) in standard complementary metal-oxide semiconductor (CMOS), which could be the most effective solution for meeting the vertex detector requirements at future high-energy colliders. There are several demanding technical issues, electronic and mechanical, that must be solved before practical detectors can be made using this new technology.

We start with the demonstration that minimum ionizing particles can be detected with APS constructed in standard CMOS technology. We will address a number of design issues in order to move this promising demonstration of APS into a practical detector system design. Methods for on-detector-chip data zero suppression and readout will be developed. Issues of mechanical support and electronic interconnection of multiple chips into a detector structure will be investigated. The appealing aspect of the CMOS approach is the opportunity to combine detector and readout functions on a single chip using the latest readily available commercial integrated circuit technology.

Accomplishments

To advance this work, we are collaborating with the LEPSI/IRes Laboratory in Strasbourg, France. We will strongly benefit from their unique experience as pioneers of the APS application to the detection of charged particles. They have given us one of their large (2x2 centimeters) MIMOSA 5 chips, which will allow us to investigate the issues associated with reading out 1M pixel chips. Furthermore, in the spring of 2004, LEPSI/IRes Laboratory will provide us with 5 to 10 of these MIMOSA 5 chips so that we can construct a full scale ladder prototype, hence addressing large-scale data acquisition issues as well as mechanical issues.

We have worked on improving the APS efficiency without compromising the noise rejection performances. We have produced a new chip, see Figure 4, with 16 different test structures. The noise on the single diode structure has been reduced from 17 electrons with our previous chip to 10 electrons. We have tested photo-gate structures, which prevent the electron from spreading over many pixels by very significantly increasing the charge collection area. We have successfully demonstrated that such photo-gates successfully collect charge. However, the transfer time required for moving electrons from the photo-gate to the drain appears to be very long, several milliseconds. Such long transfer time is not understood. Trapping effects have been investigated using state-of-the-art PISCES simulation and found to be small. In order to understand what is happening we intend to use an electron microscope, which will allow us to know where the electrons are generated, and thus track their path from creation to collection.

We have also investigated ways to speed up the readout time without compromising the power budget. The LEPSI/IRes group has designed a line driver that would match our goal. We are also investigating whether some data reduction could be done by a "piggy back" chip directly bounded to the APS chip. The power consumption can also be limited by reducing the amount of data that needs to be read out. We are considering increasing the pixel size from 20 to 30 millimeters. We have also designed an active pixel reset chip, which shows promising reset noise reduction performances.

The results of these investigations show that a fluence of about $2x10^{12}$ protons/cm^2 reduces the signal by a factor of two while the noise increases by 25%. This radiation dose is large compared to typical dosages at a heavy ion collider. We have shown that radiation damage is partially recovered after keeping the chip six months at room temperature or annealing it at 100°C for 24 hours.

We have investigated mechanical issues. A kapton-silicon structure has been built by bonding the silicon chips to Flex pc. The kapton-silicon structure was then successfully glued to a support ladder constructed from two 3-millimeter thick unidirectional carbon fibers offset by 20 degrees. This ladder has a natural twist, which we are currently trying to eliminate, and is vacuum coated to control carbon dust issues. We have determined a fundamental frequency of 135 Hertz for the structure. Vibration tests are underway for the ladder exposed to airflow.

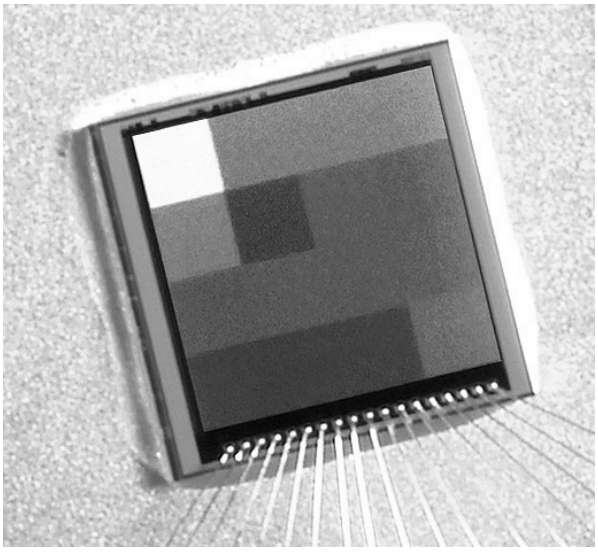

Figure 4: Photograph of AP-3. There are 16 different configurations. The sector labeling starts at the lower left corner with sector 1 and proceeds to the right. Sector 5 is just above sector 1. Sector 1 is a photodiode circuit, while sectors 5 and 6 are photogate circuits. Sector 13 is the clamp circuit.

Publications

H. S. Matis, F. Bieser, Y. Chen, R. Gareus, S. Kleinfelder, M. Oldenburg, F. Retiere, H. G. Ritter, S. E. Wurzel, H. Wieman, and E. Yamamoto, "Using an APS sensor in a vertex detector," *Proceedings of the Vertex 2003 Conference*, to be published in *Nuclear Instruments and Methods* in *Physics Research A.*

S. Kleinfelder, F. Bieser, Y. Chen, R. Gareus, H.S. Matis, M. Oldenburg, F. Retiere, H.G. Ritter, H. Wieman, and E. Yamamoto, "Novel pixel structures for vertex detectors," Nuclear Science Symposium, 2003, *Conference Record of the 2003 IEEE*, in press (2003).

H.S. Matis, F. Bieser, S. Kleinfelder, G. Rai, F. Retiere, H.G. Ritter, K. Singh, S.E. Wurzel, H. Wieman, and E. Yamamoto, "Charged particle detection using a CMOS active pixel sensor," *IEEE Transactions on Nuclear Science* **50** 4, 1020–1025 (August 2003).

H.S. Matis, F. Bieser, S. Kleinfelder, G. Rai, F. Retiere, H.G. Ritter, K. Singh, S.E. Wurzell, H. Wieman, and E. Yamamoto, "A CMOS active pixel sensor for charged particle detection," Nuclear Science Symposium, 2002. *Conference Record of the 2002 IEEE*.

S. Kleinfelder, H. Bichsel, F. Bieser, H.S. Matis, G. Rai, F. Retiere, H. Wieman, and E. Yamamoto, "Integrated x-ray and charged particle active pixel CMOS sensor arrays using an epitaxial silicon sensitive region," *Proceedings of the SPIE, Hard X-ray and Gamma Ray Detector Physics IV* **4784**, 208–217 (July 2002).

Physical Biosciences Division

Understanding the Agrobacterium Tumefaciens *T-DNA Transporter: A Type IV Secretion System*

Principal Investigators: Susan Bailey

Project No.: 03001

Project Description

The long-term goal of this project is to understand the mechanism for DNA transfer from the pathogen *Agrobacterium tumefaciens* to the nucleus of host cells using a type IV secretion system. The apparatus of the secretion system is a multicomponent complex comprising eleven proteins, which together span the inner and outer bacterial membranes, plus additional proteins required for DNA processing and for nuclear import into the host cell.

This project will investigate proteins required for virulence in *Agrobacterium tumefaciens* using an integrated biochemical and biophysical approach to characterize structures of the component proteins and their functional interactions. Specific aims are to: (1) over-express selected *Agrobacterium* virulence proteins in E-coli; (2) investigate protein:protein and protein:DNA complex formation of these proteins; and (3) initiate crystallization trials of all stable proteins and complexes.

Accomplishments

The virB operon of *Agrobacterium tumefaciens* comprises eleven proteins, of which seven were targeted for overexpression: VirB1, VirB4, VirB5, and VirB8–VirB11. Proteins VirB7–VirB10 are expected to interact and include proteins that form channel complexes and appear to be involved in protein and DNA secretion. Co-expression of the very small VirB7 with VirB9 is planned for the future, as yeast 2-hybrid models and other results predict a strong complex B9:B7 complex. VirB6 is an integral membrane protein with six transmembrane helices, and no attempt will be made to express this protein at this stage. Expression systems were established for all the targeted VirB proteins; however, in all cases the initial constructs resulted in expression of insoluble protein. Refolding of the insoluble proteins has currently been attempted for three of these proteins: VirB8, VirB9 and VirB10, using a variety of methods and conditions. Although some conditions appeared initially promising we were unable to achieve large scale refolding. In collaboration with Professor Pat Zambryski, University of California Berkeley, Plant and Microbial Sciences Department, alternative constructs were made for these three proteins, all of which are essential for virulence, with the results described.

Three different constructs of Virb8 have been overexpressed comprising residues 60–237, 77–237, and 92–237. Residues 1–56 are predicted as a signal peptide and transmembrane helix. All the recombinant proteins were produced in inclusion bodies when expressed at 37º C. The first two constructs were also insoluble when grown at lower temperatures. Refolding the protein was attempted using a variety of conditions and showed some initial promise, but the results were not consistently reproducible. The third construct produces significant quantities of soluble protein when expressed at 16º C (Figure 1a), and the conditions for soluble production have been optimized. Soluble VirB8 protein has been purified and the pure protein used for characterization. Sodium dodecyl sulfate and native gels suggest the protein may be a tetramer (Figure 1b), however, initial results from x-ray solution scattering suggest a smaller complex, perhaps a dimer. The protein appears to be very stable and crystallization trials and investigation of secondary structure using circular dichroism (CD) have started with the purified protein.

Wildtype VirB9 has 293 amino acids and residues 1–21 are a predicted signal peptide. The protein is predicted to form a heterodimer with virB7. Two constructs have been overexpressed: B9a is residues 22–293 and B9b is residues 33–293. B9a overexpresses abundantly but is very insoluble. Construct B9b showed only slight overexpression of virB9. Refolding trials have not been successful. Wildtype VirB10 has 377 amino acids with no signal peptide. Two constructs have been made comprising residues 48–377 and 175–377. Both constructs express abundant amounts of insoluble protein at 37º C and much lower amounts of insoluble protein at 20º C. Extensive refolding trials using the larger construct show some promise using CD as a tool to investigate folding.

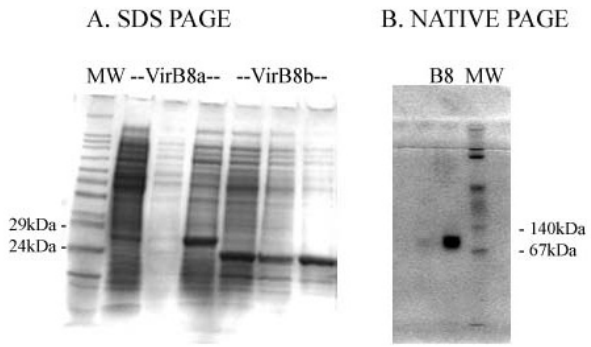

Figure 1. (a) SDS PAGE gel showing pattern of overexpression of constructs VirB8a, residues 77–237, and VirB8b, residues 92–237: for each construct the first lane is the soluble protein fraction, the second lane is the soluble protein binding to a nickel resin, and the third lane is the insoluble protein fraction. VirB8b monomers have an apparent molecular weight of around 24kDa (b) native gel showing approximate molecular weight of VirB8b as 80–100kDa.

Publications

D.V. Ward, P.C. Zambryski, J.G. Grossmann, and S. Bailey, "Characterization of the soluble domain of the virulence protein virB8 from *Agrobacterium tumefaciens*," manuscript in preparation.

Microscopic Imaging in High-throughput Screening for Crystals of the Bacterial Ribosome

Principal Investigators: Jamie Cate

Project No.: 03006

Project Description

The goal of this project is to develop microscopic imaging tools to facilitate screening for crystals of the bacterial ribosome in different functional states in a high-throughput manner. Liquid-handling robotics are increasing the number of crystallization trials we are presently conducting in the laboratory; yet, we have not been able to adequately document and quantify the results of crystallization trials in a systematic way. As the number of crystallization trials increase and the volume of each trial shrinks, it will be critical to automate the imaging of each experiment as a function of time. The tools developed in this work will be widely applicable to the structural study of many other supramolecular complexes at the center of key biological processes.

We propose to integrate a high-magnification light microscope, an *x-y* stage and *z* focus, standardized crystallization arrays, and a charge coupled device (CCD) camera to automate the microscopic imaging of crystallization trials as a function of time. We will explore the usefulness of the ultraviolet absorption of RNA and proteins as a means to detect crystals. In addition, we will exploit the fluorescence of tagged ligands bound to crystals to quantify binding in the crystals *in situ*. Finally, we will identify lighting geometries and wavelength ranges that enhance the birefringence of microcrystalline macromolecule samples, in order to readily capture the birefringence in the recorded CCD images.

Accomplishments

We proposed to integrate a high-magnification light microscope, an *x-y* stage and *z* focus, standardized crystallization arrays or microfluidics devices, and a CCD camera to automate the microscopic imaging of crystallization trials as a function of time. During the course of experiments, we identified automation parameters that will be easier to control and others that will be difficult.

We have identified promising lighting geometries and wavelength ranges to enhance the birefringence of microcrystalline macromolecule samples, in order to readily capture the birefringence in recorded digital images. We have found that the best platform for detecting birefringence does not include any molded plastic in the light path. For example, the newly available Fluidigm microfluidics chips are extremely well suited for detection of birefringence, whereas, all of the commercially available 96-well crystallization plates have severe problems in terms of birefringence detection. Further experiments to evaluate 96-well plates are in progress for FY2004.

We have also tested a number of microscope layouts and found a geometry that will allow us to conduct several types of observations on a given crystallization trial. The geometry will allow us to look at samples by transmission lighting and back lighting. The former will allow us to detect sample shapes, as well as birefringence and ultraviolet absorption. The latter will permit us to exploit sample fluorescence. For example, we are testing the fluorescence of tagged ligands as a means to detect and quantify ligand binding to ribosomes in crystals *in situ*. We are presently building the microscope and testing it with different crystallization trials.

In most crystallization trials of supramolecular complexes, we need to use 4° C for the experiments. We have not been able to identify a satisfactory way to introduce a cold stage into the microscope. None of the possible enclosure geometries would be simultaneously compatible with the

microfluidics chip, the lighting geometries we wish to use, a motorized *x-y* stage, and a stable temperature of 4° C. In particular, we are concerned about long-term exposure of the electronics to the cold and damp environment of a cold room. We have, therefore, decided to proceed with a modular microscope design that will allow us to remove sensitive components from the cold room when they are not in use. Two modules that will be detachable from the microscope are a manual *x-y* stage and a digital camera.

Molecular Recognition and Protein/Protein Interactions in Signal Transduction

Principal Investigators: Thomas Earnest and Randy Moon (Howard Hughes Medical Institute, University of Washington) collaborator

Project No.: 01034

Project Description

The interactions of proteins with other proteins, ribonucleic acid (RNA), or deoxyribonucleic acid (DNA) give rise to a great number of molecular and cellular functions. As genomic sequencing projects produce large numbers of protein products, the need to characterize these samples in terms of their function becomes of great importance. With the gene sequence analogous to an alphabet (and the protein sequence a translation to a different alphabet), proteins are the "words" of biology with specific or multiple functions (meanings). The interactions of these molecules in complexes, either stable or transiently in response to a signal, are the sentences that describe some biological function or set of functions. Thus, a comprehensive understanding of biological processes involves the knowledge of not only which proteins and their structures are involved but also the way they interact with one another.

The production of proteins and protein complexes is of fundamental importance in the understanding of how molecular structure leads to cellular function. Although it is difficult to identify and isolate many of these complexes, this process can be optimized by parallel insertion of many constructs into numerous expression vectors in *E. coli* and baculovirus-infected insect cell lines. Creation of appropriate diversity for these constructs and a fast assay is critical to the sufficient exploration of condition space necessary for success. We have developed a procedure for parallelizing attempts to achieve higher levels of expression by making several constructs with differing lengths and end residues on the N- and C-terminals utilizing green fluorescent protein as a fusion protein at the C-terminal of the protein of interest as a marker for expression and solubility. This method has been used to screen constructs, tagged and untagged, to more rapidly determine which constructs, or pairs of binding-partner proteins, are more likely to be successful when used for purification, crystallization, and structure determination.

The adaptation of this method to automated high-throughput instrumentation will produce the ability to more rapidly and successfully produce large amounts of soluble protein complexes and molecular machines for structural, functional, and imaging studies.

Accomplishments

As discussed in last year's report, when full-length proteins or protein complexes do not express well, it is often necessary to try expressing the domains which make up the proteins as separate constructs. Furthermore, since many proteins can only exist solubly in complex with binding partners (as in the cell), it is often exceedingly difficult to obtain large amounts of soluble protein in many cases, requiring the discovery and co-expression of the partner protein(s). This is a time consuming process since constructs that are very similar, differing in length by only one to ten amino acids at either end, can behave very differently. It is important to explore multiple parameters to increase the chances of finding constructs that express well.

Using the described domain boundaries and hydropathy plots as guides we choose three forward primers for each of the domains. All of the constructs which fluoresce gave high yields of soluble protein. Members of the Wnt pathway (CtBP, CBP/beta-catenin) have been extensively subjected to two-hybrid screening and coexpression, purification, crystallization trials and the correlation of fluorescence with over-expression of soluble protein has been high. In particular in the Wnt pathway, constructs of the large, multidomain signaling protein, disheveled, have been successfully screened and optimized for overexpression and solubility

We have developed this methodology with a focus toward high-throughput of production of proteins and protein complexes and recently taken steps toward automating and parallelizing this process. This is clearly important as many proteins will require binding partners to maintain solubility for purification and crystallization. Thus these developments will benefit structural proteomics efforts that seek to understand cellular function through structural studies of biomolecular complexes and their localization in the cell.

Publications

A. Sali, R. Glaeser, T. Earnest, W. Baumeister, "From words to literature in structural proteomics," *Nature* **422**, 216–225 (2003).

Allosteric Mechanisms in Protein Kinases

Principal Investigators: John Kuriyan

Project No.: 02040

Project Description

Crucial to the proper functioning of the cell is an elaborate control mechanism that interprets signals from the environment and then makes decisions controlling cell structure, transcription, and replication. My laboratory is studying the molecular mechanisms underlying these systems by focusing on the proteins involved in transducing signals generated by cell surface receptors. In the past, this work has been driven primarily by x-ray crystallographic analysis of three-dimensional protein structures, a crucial first step in developing molecular mechanisms. This project is aimed at initiating studies in new directions that will combine biophysical analysis of protein function with the generation of mutations aimed at probing particular aspects of function.

The primary focus is on tyrosine kinases related to the protein coded by the Src oncogene, such as the c-Src and c-Abl tyrosine kinases. The members of this family of tyrosine kinases are controlled by tyrosine phosphorylation at two distinct sites that have opposing actions on the catalytic activity of the protein. The key to understanding how these proteins work is to figure out how the dynamics of a centrally located loop within the kinase, known as the activation loop, is altered by various modifications, such as phosphorylation. The activation loop is a feature that is common to all Ser/Thr and tyrosine-specific kinases, although each kinase has a distinctive mechanism of control. Our project involves the application of NMR methodology to map the dynamics of residues located within the activation of the Src and Abl kinases, and to compare and contrast these data with those obtained for a Ser/Thr-specific kinase, p21-activated kinase (PAK). This information will be correlated with the results of molecular dynamics simulations and mutagenesis on these proteins.

Accomplishments

The past year has seen significant advances in our attempts to produce nuclear magnetic resonance (NMR) quality samples of two classes of protein kinases. For the Ser/Thr-specific protein kinases, the example we have chosen to work on is the p21-activated protein kinase (PAK kinase). For the tyrosine kinases, we have chosen to focus on two closely related kinases: the Src and Abl tyrosine kinases. For all of these systems we are limiting our studies to the catalytic domain (kinase domain), since these proteins are too big for realistic analysis by NMR.

For successful NMR experiments we have to overcome two challenges. First, we have to produce the protein using a method that makes isotope labeling economically viable. This effectively rules out insect cell or mammalian cell culture systems. This is a significant problem, particularly for the tyrosine kinases, since these proteins are normally expressed robustly only by using animal cell culture systems. Much of our effort in the past year has been focused on developing and/or optimizing *E. coli* or *in vitro* expression systems. Once expression systems are developed the next challenge to overcome is to find conditions where the proteins can be maintained in solution without aggregation at very high concentrations. This is an area that is very poorly explored for protein kinases, and much of our development effort is concentrated on this problem.

For the PAK kinases there are two main methods which we have used to produce protein, the first method being bacterial expression of a catalytically inactive version of the PAK2 kinase domain. While bacterial expression of this kinase domain has been demonstrated previously in our laboratory and in other laboratories, we needed to boost expression levels substantially in order to make the system cost effective for producing isotopically labeled protein. By extensively testing a variety of media and growth conditions, the yield of purified protein has been increased approximately ten-fold, from ~4 to 5mg/L to over 40mg/L in minimal media.

The second method being pursued for the PAK kinases is *in vitro* translation. Both the catalytically active and the catalytically inactive versions of the PAK2 kinase domain have been expressed in "cell-free" systems. The yield of purified protein has been optimized to the levels where this is now in the feasible range for NMR (1 to 2 mg/mL yield). The success of this method enables us to label the kinase at specific amino acids to aid in sequential assignments. Also, currently, *in vitro* expression remains the only method for producing the active kinase, for which a reasonable yield is also obtained for labeling experiments (0.5mg/mL). The active form of the kinase cannot be expressed in bacterial cells, presumably because it kills the bacteria.

To obtain the best spectra possible, we have also been working towards optimizing the buffers used in NMR experiments. So far we have succeeded in finding a buffer in which the catalytically inactive construct is soluble for weeks at room temperature. We are also currently trying different additives in the hopes of stabilizing the protein at higher temperatures.

At present our work on the Src and Abl kinases is focused on developing *in vitro* refolding procedures to obtain these proteins at high yields from bacterial expression systems. Both kinase domains are produced as insoluble pellets when expressed in bacteria. We have successfully developed refolding protocols to obtain highly active protein with acceptable yields. Preliminary NMR characterization of the purified kinases is currently underway.

This work is in collaboration with David Wemmer.

Structure and Functional Characterization of Heme Protein Sensors

Principal Investigators: Michael Marletta

Project No.: 02041

Project Description

Biological sensors occupy an essential biological niche in the study of prokaryotic organisms to complex animals. Evolution builds in the required specificity and sensitivity necessary for function. In some cases a molecular level understanding has emerged but we are far from fully appreciating the wide variations in sensor design.

Nitric oxide (NO) signaling is a particularly interesting example. Critical functions for this toxic, free-diffusible diatomic gas are now well established, including key roles in cellular signaling and as the host response to infection. In cellular signaling NO is biosynthesized by the constitutive isoforms of the enzyme nitric oxide synthase (NOS). Calcium and calmodulin (CaM) strictly control the activity of these enzymes. This activation is transient and highly regulated in order to avoid toxicity associated with the nonspecific chemical reactivity of NO. A highly specific and sensitive NO receptor is expected, given the toxicity of NO, and this is indeed the case in the form of the soluble isoform of guanylate cyclase (sGC). After activation by NO, this enzyme converts guanosine triphosphate (GTP) to cyclic guanosine monophosphate (cGMP) and pyrophosphate. Cyclic guanosine monophosphate subsequently brings about tissue-specific physiological responses such as blood vessel dilation via relaxation of vascular smooth muscle. Soluble guanylate cyclase is a heterodimeric protein composed of α- and β-subunits. The β-subunit contains a five-coordinate, ferrous protoprophyrin IX heme that serves to bind NO. Once bound, sGC is activated about 400-fold over basal activity.

Spectroscopic methods in combination with domain expression (residues 1 to 385 of the β-subunit) and mutational analysis have been used to extensively characterize the heme environment in sGC. This environment has evolved to have several critical pieces that allow it to serve in the capacity noted above. Most notably, the heme in sGC does not bind oxygen. Since the concentration of O_2 would dwarf that of NO in the target cell, this lack of binding of O_2 is critical for NO to operate in an aerobic environment while using a porphyrin receptor. In addition, sGC and the heme domain construct bind NO with exceptionally fast on-rates, also permitting NO to function at very low cellular concentrations.

We have become interested in whether heme-binding cyclases exist in organisms like *C. elegans*. Our extensive characterization of the heme environment and catalytic activity has allowed us to predict similar heme binding motifs from genome sequence information. Sequence analyses of the *C. elegans* genome showed that it contains seven β-type subunits. There are no predicted α-subunits. This is a surprise given that all mammalian soluble cyclases characterized to date are α/β heterodimers. Even more interesting is that the sequence analyses place five of the *C. elegans* putative cyclases closest to the β2-subunit. Homologues to the *C. elegans* putative cyclases can be found in *D. melanogaster* as well. The conclusion from our sequence analyses is that the worm and fly putative β2-subunit cyclases will bind heme.

In this project, we will continue to explore the nature of these predicted cyclases from *C. elegans* and attempt to answer long-term questions about the function of these proteins, extend our sequence comparisons to the globins in order to define the molecular determinates of oxygen sensors vs. NO sensors, truncate our β1(1–385) heme domain and attempt to solve the structure by nuclear magnetic resonance (NMR) and develop a construct to express β1(1–385) with α1(1–400).

Accomplishments

Using residues 1–194 of the soluble guanylate cyclase β1 subunit, a search of the sequence databases has generated some remarkable hits, sequences identity ranging from 40% to 12% and including a conserved histidine ligand to the heme. Predicted heme domains were found in the following facultative aerobes: *Nostoc punctiforme, Caulobacter cresentus, Vibrio cholerae, Vibrio vulnificus, Microbulbifer*

degradans, Shewanella putrefaciens, Shewanella oneidensis, Legionaella pneumophilia, and *Colwellia sp. 34H*. The predicted open reading frame's (orf) encoded proteins of ~200 amino acids. In all cases these predicted proteins were present in histidine kinase-containing operons. We have cloned several of these predicted heme domains and they express highly and behave like the mammalian NO sensors. The kinase from *Shewanella* has also been cloned. Results support our hypothesis that the heme domain sensor (HDS) and kinase are part of a two-component signaling system. NO, derived from the use of NO_3^- as an electron acceptor, serves as a signal for anaerobic growth to turn on the expression of genes that help in growth under reduced oxygen tension. Hits were also obtained from the following strict anaerobes: *Clostridium botulinumA, Clostridium acetobutylium, Clostridium tetani, Desulfovibrio desulfuricans* and the thermophile, *Thermoanaerobacter tengcogensis.* In these organisms, the heme sensor is predicted to be an O_2 sensor. We have cloned, expressed and purified the heme domain from *T. tengcogensis* (residues 1–188) and it does bind O_2 and it crystallized and with the Kuriyan group, we have obtained a structure. The structure shows a unique H-bond to the bound O_2 using a tyrosine hydroxyl group. This tyrosine residue is absent in all the HDSs that do not bind O_2. The HDS from *Legionaella pneumophilia* has a phenylalanine in that position. Mutation of the Phe to Tyr in this HDS converted it to an O_2 binder. This adds very strong support to the conclusion that the molecular engineering to exclude O_2 binding is in fact an off-rate phenomenon and O_2 as a ligand requires an H-bond to slow this off-rate down. Progress has been made with understanding these domains in *C. elegans*. Again through cloning and characterization, we find that the predicted heme domains appear to be O_2 sensors, in this case functioning to control cyclic GMP levels by O_2 binding to a unique cyclase.

Therefore, we conclude that a highly conserved domain of about 200 amino acids has evolved to function as a HDS for ligands such as NO and O_2. It is likely that the overall three-dimensional fold will be unique and the hypotheses regarding function will be related to the organism and the protein. For example, in sGC this domain is attached to the β-subunit where it functions to trap NO and through a conformational change, activate the enzyme. In facultative aerobes, our hypothesis to be tested is: as O_2 levels decrease, these organisms use NO_3^- as an electron acceptor. All of these organisms have predicted nitrate and nitrite reductases that would lead to the formation of NO. We hypothesize that this NO then serves as a signal to the organism and leads to transcriptional up-regulation of genes required for low O_2 tension/anaerobic growth. In obligate anaerobes, we hypothesize that the fusion of the HDS to an MCP is O_2 sensing protein that leads to a chemotaxis response, moving the organism away from O_2.

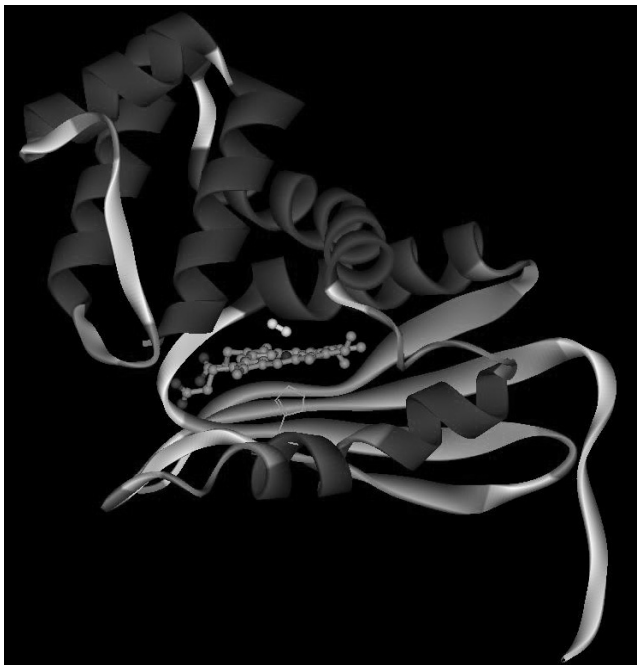

Figure 2. Structure of the heme domain from Thermoanaerobacter tengcogensis. *Ferrous-oxy complex is shown. The protein is a unique fold for a hemoprotein and clearly shows a key H-bond to the bound O_2.*

Publications

P. Pellicena, D.S. Karow, E.M. Boon, S. Huang, J. Kuriyan, and M.A. Marletta, "A structural basis for nitric oxide and oxygen ligand discrimination in hemoprotein sensors," submitted to *Nature*.

D.S. Karow, D. Pan, P. Pellicena, A. Presley, R.A. Mathies, J. Kuriyan, and M.A. Marletta, "Spectroscopic characterization of the sGC-like heme domains from *Vibrio cholerae* and *Thermoanaerobacter tengcongensis*," submitted to *Biochemistry*.

Development of Techniques for Structural Analysis of Large, Multi-subunit Eukaryotic Transcription Complexes

Principal Investigators: Gerry McDermott

Project No.: 02042

Project Description

The path from gene to protein begins with transcription of deoxyribonucleic acid (DNA) to ribonucleic acid (RNA). In eukaryotes, transcription is performed by RNA Polymerase II (Pol II), a large multi-subunit macromolecular complex. Initiation and control of Pol II activity also requires up to forty additional proteins working in concert. The majority of these proteins are involved in the formation of a pre-initiation complex. Formation of the pre-initiation complex begins when TBP, the TATA box binding protein, binds to a specific DNA sequence upstream of the gene to be transcribed. Once this occurs, a number of transcription factors (TFs) assemble together with Pol II to form a large protein-DNA complex. This complex is capable of basal levels of transcription. Complete regulation of transcription is governed by additional proteins, for example activators, that bind to specific DNA sequences, and interact with the pre-initiation complex, in particular the multi-subunit complex TFIID.

Structural information is now available on some components of the transcription machinery. Recently, the x-ray crystallographic structure of Pol II was determined to atomic resolution. However, clarifying a large body of experimental work and understanding transcription at the molecular level requires high resolution structural information on TFIID and other multi-subunit complexes.

The aim of this project is to develop techniques for the crystallization and structure determination of large multi-subunit transcription complexes.

Accomplishments

High-resolution structural information on large macromolecular complexes is now essential if we are to fully explain many fundamental processes such as the transcription of DNA to protein. Unfortunately, unlike relatively low molecular weight individual macromolecules, it is not possible to over-express these mega-Dalton sized complexes or to over-express their component molecules individually and subsequently combine them into a functional complex. Therefore, structural studies must be undertaken using small amounts of available, endogenous material. This LDRD provided funding to develop techniques to isolate, purify, and initiate crystallization trials on several macromolecular complexes, in particular TFIID, one of the central components involved in forming the transcription pre-initiation complex.

Considerable progress was made towards achieving the goals of the project. Significant amounts of TFIID, and other smaller sub-complexes were purified in the Tjian laboratory. Crystallization trials were initiated using the nanoliter scale techniques developed for use with a Cartesian crystallization robot. These trials yielded numerous crystals—all of which were screened for diffraction on the Howard Hughes Medical Institute (HHMI) beamlines at the Advanced Light Source. Unfortunately, it was discovered that physical properties of these complexes induced a large percentage of false positives, i.e. salt crystals, when using this technique. As a consequence, work was initiated to adopt microfluidic technologies for the most recent crystallization experiments. A significant number of Fluidigm crystallization chips were purchased and used. This approach yielded considerably fewer false positives; several of the crystallization conditions obtained are now being optimized with a view to obtaining good quality crystals.

The results attained during the funding period are now being used, in part, as the basis for an upcoming National Institutes of Health (NIH) P01 program project proposal.

Conformation and Reaction Dynamics at the Single Molecule Level

Principal Investigators: Haw Yang

Project No.: 02049

Project Description

This research project seeks to develop single-molecule spectroscopic techniques for advancements in the design and application of single-molecule assays. The emerging picture of inferring biomolecule functionality from its three-dimensional structure is incomplete without a fundamental understanding of the microscopic dynamics. The capability of single-molecule spectroscopy offers a unique means to bridge the gap between the static structure and the dynamic functionality.

We will focus on developing single-molecule spectroscopic techniques to take the leadership in the design and application of single-molecule assays. The emerging picture of inferring biomolecule functionality from its three-dimensional structure is incomplete without a fundamental understanding of the microscopic dynamics. The capability of single-molecule spectroscopy offers a unique means to bridge the gap between the static structure and the dynamic functionality. It is the goal of this project to develop strategies that will allow, at the single-molecule level, a quantitative description of the dynamics and mechanisms that underlie a complex biological system.

Accomplishments

Concept Development

Time-resolved single molecule fluorescence measurements may be used to probe the conformational dynamics of biological macromolecules. The best time resolution in such techniques will only be achieved by measuring the arrival times of individual photons at the detector. New analysis methods are needed to take advantage of this capability. We have developed a general approach to the estimation of molecular parameters based on individual photon arrival times. We begin by quantifying the amount of information present in the noisy single-molecule trajectory by calculating the Fisher information. Based on the information-theoretical considerations, we have derived the basic equations relating time resolution and measurement uncertainty. We have also constructed maximum likelihood estimators that extract the maximal information out of the available data. Taking advantage of these estimators to optimally analyze single molecule data, we have developed a data analysis algorithm, which extracts the maximal information out of the data acquired. This method accounts and corrects for background photons and cross-talk, and can scale to an arbitrary number of channels. The concept developed in this research project is general and can be easily applied to other observables in single-molecule imaging and spectroscopy.

Advanced Time-Resolved Single-Molecule Spectrometer

Applying the maximum-information concept, we were able to obtain high-resolution trajectories, both in time and in distance, from individual biological macromolecules. An example is displayed in Figure 3, which shows a donor-acceptor (AlexaFluor-555/AlexaFluor-647) distance time trajectory of poly-proline-8. The boxes along the trajectory represent time and distance uncertainties (one standard deviation) of the measurement. The mean distance is ~45 Å, in excellent agreement with computer simulations (~45 Å) using molecular mechanics force fields. This proof-of-principle experiment demonstrates the power of the maximum information algorithm in practical experimental settings.

Single-Molecule Dynamics of Adenylate Kinase from E. Coli

We are currently developing single-molecule assays for studies of the adenylate kinase (AK) enzyme using the newly developed spectroscopic methods. AK maintains the energy balance in a cell and serves as a prototypical system for detailed dynamic studies of structure-function relationship. We have successfully purified and characterized mutated AK from *E. coli* suitable for fluorescence resonance energy transfer (FRET) pair dual labeling and for His_6-NTA immobilization to coverslip. Experiments on the single-molecule level are under way.

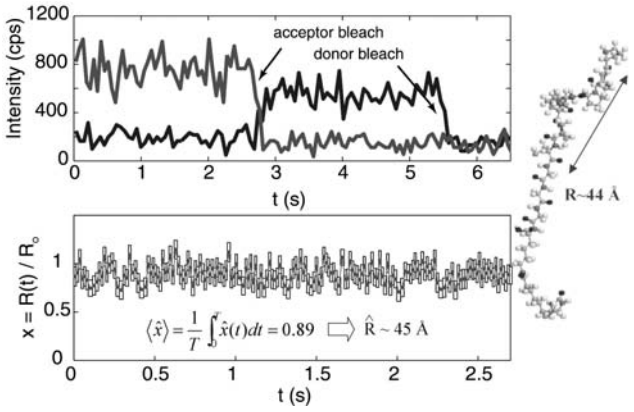

Figure 3. (Top) Donor (darker line) and acceptor (lighter line) intensities as a function of time from a single $(pro)_8$ molecule. (Bottom) Maximum-information analysis of the same trajectory reveals a donor-acceptor distance of 45 Å, in excellent agreement with molecular dynamics simulated results shown on the right.

Publications

L. P. Watkins and H. Yang, "Maximum information analysis of dynamic single-molecule fluorescence measurements," submitted to *Biophysical Journal*.

Physics Division

Future Experiments in Neutrino Physics

Principal Investigators: Stuart Freedman and Jesse Goldman

Project No.: 03033

Project Description

Our understanding of the neutrino world has changed dramatically in the past two years. Recent experiments have confirmed earlier evidence that the three types of neutrinos mix; that is, they change into one another. According to the predictions from the Standard Model, neutrinos/anti-neutrinos are without mass. Contrary to this, over the past two years, solar neutrino experiments at the SNO and Super-K detectors implied that the ghostlike snippets of matter/anti-matter do possess enough mass to enable them to oscillate and change flavor over a distance. Kamioka Liquid Scintillator Anti-Neutrino Detector (KamLAND) is the first experiment to observe the neutrino properties responsible for solar neutrino flavor changes from a terrestrial source, the reactors in Japan's nuclear power plants.

We propose to carry out a series of studies to investigate in detail the properties of the neutrinos and define the next-generation experiments to better understand the neutrino sector. The proposed work will focus on three promising areas that build on Berkeley Lab's work in KamLAND and underground at Kamioka making use of special experience of postdoc fellow, Jesse Goldman.

- A solar program with KamLAND is not presently funded in either Japan or the U.S. We will help in understanding the technical issues related to a solar ^{7}Be experiment with KamLAND. This experiment should provide better constraints on $\sin^2(2\theta)$ than is possible with reactor experiments.
- KamLAND, located in a mine cavern beneath the mountains of Japan's main island of Honshu near the city of Toyama, is the largest low-energy anti-neutrino detector ever built. KamLAND consists of a 13 meter (43 foot) diameter weather balloon filled with about a kiloton of liquid scintillator, a chemical soup that emits flashes of light when an incoming anti-neutrino collides with a proton. These light flashes are detected by a surrounding array of 1,879 photomultiplier light sensors, which convert the flashes into electronic signals that computers can analyze. The photomultipliers are attached to the inner surface of an 18-meter diameter stainless steel sphere; they are separated from the weather balloon by a buffering bath of inert oil and water, which helps suppress interference from background radiation. Data obtained with this detector indicates that the scintillator has very low contamination of uranium, thorium, and potassium. The detector should be capable of detecting low energy solar neutrinos if the levels of radioactive krypton and lead are reduced. The case for a solar phase of the experiment will be based on the feasibility of this purification process.
- We will participate in a study of possible opportunities for small underground experiments at Kamioka or other laboratories. Under present consideration is a measurement of positronium decaying to nothing: a test of theories with extra dimensions. This rather modest experiment should be carried out underground to avoid cosmic ray backgrounds.

Accomplishments

Two potential tasks were described in the original proposal.

First, investigations of the feasibility of a continuation of KamLAND into a solar neutrino phase are positive. Analysis of KamLAND data carried out by Goldman and his colleagues indicate that the level of uranium, thorium, and potassium in the KamLAND liquid scintillator is low enough to make the detection of low energy solar neutrinos feasible. Analysis of the data also indicates that the level of contamination by ^{85}K and ^{210}Pb is too high by orders of magnitude. Krypton-85 with its ten-year half life is ubiquitous because it is a product of nuclear fuel processing. Studies of methods to reduce this contamination were initiated by our colleagues in the U.S. and Japan. It appears that it will be possible to achieve the required factor of 10^6 reduction. The purification method is simple; pure gas, nitrogen or helium, is bubbled through the scintiallator. Helium is preferred because of its purity but there is some danger of adverse effect on the KamLAND scintillators. Methods for reduction ^{210}Pb are still under development. The required reduction is 10^4 to 10^5. Several techniques are being investigated. The most hopeful schemes exploit lead exchange with clean samples of lead salts. Continued analysis of the data from the ongoing experiment is being exploited to study the level of other contaminants of interest including carbon-11 and carbon-14.

Second, an extensive study of possible underground experiments at the Kamioka mine has lead to a possible search for magnetic monopoles with KamLAND. This work has become part of a senior thesis project. Goldman and Freedman are supervising the research.

Publications

K. Eguchi et al. (KamLAND Collaboration), "First results from KamLAND: evidence for reactor anti-neutrino disappearance," *Physical Review Letters* **90**, 021802 (2003), LBNL-5193.

Modeling of High Energy Physics Detectors

Principal Investigators: Ian Hinchcliffe

Project No.: 01037

Project Description

Monte Carlo simulation of detectors is a valuable tool for understanding the capabilities of the detector components and for planning strategies for using the detectors to reveal new physics processes. One crucial component will be the integration of the inner detectors into the A Toroidal LHC ApparatuS (ATLAS) simulation and reconstruction. Two components of the inner detector, the pixels and silicon strip detectors, are being partially constructed at Berkeley Lab. A common framework describing the geometry of the system is essential. This will help us to understand how the inner detector can be used in the search for new physics signatures.

The new object oriented simulation tool, GEANT-4, has recently become available. Validation of the models underlying this tool is essential. This validation needs to take place well in advance of the tool's actual use. GEANT-4 has important applications outside high energy and nuclear physics, which include medical, accelerator, and space physics studies. This proposal will undertake a detailed comparison of the predictions of GEANT-4 with a system, the ATLAS pixel test beam, where data are available. This will enable validation and refinement of the underlying physics models in GEANT-4. Detailed comparisons of the predictions of GEANT-4 with actual data are required. Comparison will be made with test-beam data to be obtained at CERN in the future. A GEANT-4 model of the ATLAS pixel test beam will be made and will be integrated into the ATLAS software framework. Results from this will be used for a detailed validation of GEANT-4. The results will be used to adjust the underlying GEANT-4 model.

Accomplishments

Work was completed on the first implementation of the atlas pixel and silicon detector system using the GEANT-4 simulation package. A complete geometry description of the system was provided using native GEANT-4 geometry classes. Conversion of the GEANT-4 energy deposits into simulated detector signals was also provided. This implementation served as a test bed and a prototype for the full description of the ATLAS detector GEANT-4. Included was the means of storing the output in a new format provided by the LHC Computing Grid Project (LCG) group. This was one of the first tests of this storage technology in the ATLAS experiment. In addition, a separate geometry description was tested that enables the description to be exported both to simulation and reconstruction software packages. This ensures consistency of the entire simulation and reconstruction software chain.

This work has led to the prompt deployment of the new object-oriented simulation framework for the ATLAS detector. Testing and validation are now beginning on this new system, which is expected to enter production in time for the next ATLAS data challenges scheduled to begin in March 2004. The schedule is tight and the research and development work done under the auspices of this LDRD project was vital to ensuring that the old, unmaintainable simulation package can finally be phased out.

POLARBEAR: An Experiment to Measure Polarization Anisotropy in the CMB

Principal Investigators: Adrian Lee and Helmuth Spieler

Project No.: 01038

Project Description

This project will conduct research and development in support of a new experiment to measure cosmic microwave background (CMB) polarization. The new experiment, called POLARization of the Background millimEter bAckground Radiation (POLARBEAR) combines the proven Millimeter Anisotropy eXperiment Imaging Array (MAXIMA) telescope and observation strategies with a new detector technology based on superconducting transition-edge sensors (TES).

The cosmic microwave background is proving to be a peerless laboratory for cosmology and fundamental physics. Recently, measurements of the spatial temperature anisotropy by MAXIMA and Balloon Observations of Millimetric Extragalactic Radiation and Geophysics (BOOMERANG) have given strong support to inflationary models with a density close to critical. We have also been able to measure the density of baryons and cold dark matter and the spectral index of the primordial power spectrum. Perhaps the most exciting promise of polarization measurements lies in their ability to probe the inflationary epoch, i.e. as early as 10^{-38} seconds after the Big Bang. Gravity waves produced at these early times propagate forward and produce structure in the photon-baryon fluid at the surface of last scattering, observable by its signature in the polarization of the CMB. Detection and characterization of this polarization will require a large leap in experimental capability. The key new technology for POLARBEAR is the large-format array of voltage-biased superconducting bolometers that are based on a superconducting film biased in mid-transition. Several tasks will be performed to examine the technical details of such a detector.

Accomplishments

Detection and characterization of the B-mode (gravity wave) CMB polarization signal will require a breakthrough in experimental capability.

We will use a new telescope that we have designed during this project. Last year's report gives some of the technical considerations we addressed. The design of the telescope is very important given the low level of signals. The off-axis response of the telescope must be very low to avoid spurious signals from nearby objects. Also, any induced spurious polarization and rotation of polarization must be kept to a very low level. We have developed an optical configuration that achieves all these goals simultaneously.

The key new technology, POLARBEAR, is the large-format array of superconducting TES bolometers that uses a superconducting film biased in mid-transition. Compared to detectors in current use, the detectors have a higher sensitivity, better linearity, and can be fabricated into large arrays with standard optical lithography. We were the first group to publish measurements showing the advantages of such sensors for bolometric operation. In addition to the development of the sensors, we are also working on novel methods to integrate the functions of optical coupling, bandwidth definition, and readout onto a single substrate—all of which will facilitate larger arrays, and hence, overall sensitivity.

In FY03, we have fleshed out the general design of the receiver. We have demonstrated the needed performance of the pulse tube cryocooler. We are the first group to demonstrate that this type of cryocooler does not adversely affect detector operation.

We have recently completed fabrication of a second round of antenna-coupled bolometer prototypes. Planar antennas for coupling to the telescope, microwave band-defining filters, and bolometers are integrated onto a single substrate. We have performed preliminary tests on the first round of detectors. These tests, along with simulations, have suggested modifications for the second round. These new chips will be tested this spring.

We have finalized the optical design for the POLARBEAR telescope. We will use a novel off-axis telescope that uses an optical fold to null spurious induced polarization.

Publications

H.T. Tran, "Polarization comparison between on-axis and off-axis dual reflector telescopes: Zemax and Grasp8 simulations," *New Astronomy Reviews* **47**, Issues 11-12, 1091-1096 (December 2003).

Cross-Divisional

Microscopic Theory of Protein Surface: Structure, Response, and Design

Principal Investigators: Phillip Geissler

Project No.: 03035

Project Description

This project is to construct a microscopic theory of heteropolymer surface that sheds light on the interfacial structure and function of proteins. It will address whether removal of hydrophobic residues from the molecular surface expected for generic solvated polymers that undergo a sharp thermodynamic freezing, i.e. folding, transitions; and whether sequences of model hetero-polymers will be selected such that native structure is sensitive to local perturbations at the surface, as in allosteric proteins. Answers to these questions may provide insight into detailed mechanisms of molecular evolution.

The project will develop and examine schematic coarse-grained models of proteins that should capture generic relationships between surface fluctuations and molecular structure. To study the behavior of these models, analytical tools such as replica mean field theory, will be extensively borrowed from the theory of spin glasses, which exhibit similar mathematical complications due to quenched disorder. Theoretical predictions will be tested by numerical simulation of related models and by comparison with statistics of known protein structures.

Accomplishments

This project was started late in FY03, so effort went into initial planning of the research, hiring appropriate graduate students, and purchasing necessary equipment and materials. Funding in FY03 was spent largely on obtaining hardware and software necessary to perform calculations described in the proposal. Purchased equipment included 32-node dual processor Linux cluster that will provide state-of-the-art computational power for the project. Assembling and installing this parallel computer required significant support from university technicians. Progress on the actual scientific goals has begun early in FY04.

Development of a Neutral Molecule Synchrotron Storage Ring

Principal Investigators: Harvey Gould and Hiroshi Nishimura

Project No.: 01010

Project Description

Our goal is to determine the feasibility and practicality of constructing molecular synchrotrons to store, slow, and cool neutral polar molecules in a way that makes it easy to use them in novel experiments, including the formation of molecular Bose-Einstein condensates.

Laser slowing, cooling, and trapping, have not been effective for molecules because the closely spaced, vibrational and rotational, levels prevent efficient cycling transitions. This makes it possible to apply accelerator and specifically synchrotron physics and technology to polar molecules. Molecular synchrotrons have the potential to be the first widely applicable and effective method to store, slow, and cool molecules in vacuum.

Static and dynamic traps have been considered for trapping molecules. The molecular synchrotron is effectively a dynamic (rf) two-dimensional trap. It has fewer constraints than a three-dimensional trap or a static trap. A molecular synchrotron's beam energy is independent of temperature and can be varied over several orders of magnitude. It preserves a beam geometry for experiments, can have field-free regions, and can be scaled to accept molecules with large kinetic energies. It is well suited for evaporative cooling of the molecules. It may be possible to use a ring as an accumulator to increase the stored intensity.

Accomplishments

Using calculations and mathematical modeling, we have demonstrated the feasibility of constructing a synchrotron storage ring for neutral polar molecules in strong-field seeking states. This effectively solves the problem of rotational relaxation losses and allows polar molecules to be stored in their lowest rotational state opening the way to evaporative cooling.

To make the ring compact, we slow the molecules to 30 meters/second in a decelerator array. The storage ring

itself is a mere 10 meter circumference. It has eight-fold symmetry with each octet containing two 22.5 degree bend elements plus focusing triplets at each end and a single buncher.

The results of our study show that it is feasible to construct a molecular synchrotron storage ring that will capture large numbers of molecules in multiple bunches, maintain the bunches, store the molecules for longer than 15 seconds, and vary their kinetic energy. The acceptance of the storage ring and decelerator scale with their size, with allowance for non-linearities, and the voltage limits of large electrode gaps. The storage ring and decelerator modeled are matched and are of a size that is typical for laboratory apparatus. The particular example we studied may stimulate interest in specific features of such a facility from which exact specifications would emerge and be pursued in its own design study.

Publications

H. Nishimura, G. Lambertson, J.G. Kalnins, and H. Gould, "Feasibility of a synchrotron storage ring for neutral polar molecules," *Review of Scientific Instruments* **74**, 3271 (2003).

Investigation of Charge Transfer in Organic Electronics Using Ultrafast Spectroscopy and Targeted Synthesis

Principal Investigators: Charles Harris, John Arnold, John Kerr, and Stephen Johnson

Project No.: 02010

Project Description

This project will investigate the dynamics and mechanisms of charge transfers at interfaces in organic electronic devices. Organic light emitting diodes (LEDs), organic photovoltaic cells, and organic electronic devices such as field-effect transistors (FETs), and memory are examples of such devices that are causing excitement. More mature fields, such as electrodeposition and lithium batteries, continue to require fundamental understanding to realize their potential. In all of these applications, progress is hindered by a lack of fundamental understanding of the interfacial charge transport processes. It is the goal of this research proposal to focus a unique combination of capabilities upon this critical bottleneck area and to take leadership in the analysis and design of interfacial structures that lead to the development of robust and efficient long-lived devices that will play a major role in meeting the nation's energy efficiency goals for the future.

Three major components of the research are envisioned:

- Application of ultrafast, femtosecond, spectroscopy techniques to organic-cathode interfaces for small molecule and polymer LEDs and to organic photovoltaic systems that utilize fullerenes, photo-sensitizers, and conducting polymers. This phase will develop the full potential of ultrafast spectral techniques to model interfaces relevant to practical devices.
- Synthesis of appropriate new molecules to facilitate the interfacial analyses and to provide relevant structure-function information.
- Construction and testing of devices that incorporate the new interfacial structures based on designs derived from the spectral analysis and structure-function relationships.

This approach not only diagnoses failure mechanisms but also leads to solutions that yield practical devices.

Accomplishments

In FY03 we made significant progress synthesizing novel molecules, studying charge injection in monolayer films with two-photon photoemission (2PPE), and building working organic light emitting diode (OLED) devices.

Synthesis

We (Kerr) have synthesized a variety of new molecules, including nine 9-dimethylfluorene monomers and dimers, nine 9-dihexylfluorene monomers, and nine 9-dipropylfluorene monomers. These molecules have allowed the Harris lab to study trends in the electronic behavior of interfacial electrons as a function of the electronic structure, e.g. the difference of conjugation length between monomers and dimers as well as side chain substitution from methyl through hexyl side chains.

Devices

We have optimized our techniques for building organic light emitting diodes of blue emitting polyfluorenes, which will allow us to compare the performance of real devices with the 2PPE spectroscopic measurements. These devices perform comparably with state of the art devices; studies of their physical and chemical degradation pathways are underway.

Ultrafast Spectroscopy

We (Harris) have examined electron injection at model cathode interfaces with 2PPE experiments of a variety of adsorbates. Highlights of this research include:

- Tris-quinolinolato aluminum (Alq_3) forms disordered multilayers on Ag (111), that do not support image potential states (IPS). This is probably due to polycrystalline domains of different morphologies that do not wet the clean silver (Ag) surface. These domains scatter electrons very rapidly <10 femtoseconds.
- We grew anthracene films on Ag(111) in one and two monolayer thicknesses, as well as a much thicker multilayer. In one and two monolayers, the IPS are drawn into the layer, as shown by the very short IPS lifetimes, 10 and 20 femtoseconds respectively, though the lifetimes of the IPS are longer than simple dielectric continuum models would predict. For thin films, one and two monolayers, the IPS electrons are delocalized at all times; though, preliminary measurements suggest that the IPS may localize in the thick films.
- Fluorene monomers with methyl or no alkyl substituents grow well-ordered monolayers that show IPS states with very short lifetimes. The side chains have a pronounced effect on the 2PPE spectra. We believe this is due to changes in the layer morphology. The nine 9-dihexylfluorene layers are disrupted by the longer hexyl chains and do not order; therefore, no IPS are observable.
- Preliminary experiments of C_{60}/Ag(111) are underway to measure the localized electron's size and test several theories which predict the electron to be the size of a one unit cell in two-dimensional systems.
- We have further supported a theoretical connection between the momentum dependent photoemisison signal and the spatial extent of a localized electron. Wavepacket simulations of a particle traveling in a model potential reveal that the relationship between the measured width of the momentum distribution and the spatial extent of the electron is not destroyed by a localizing potential of the experimentally relevant order of magnitude. Thus, this estimate is robust to final state effects.

In the year ahead, we will extend the 2PPE studies to electron injection in longer chain aromatics and fluorenes, whose properties can be more closely connected to the performance of real devices. Using these insights, we will design, synthesize, and test novel devices. In particular, we will investigate the role of LiF and CsF as a spacer layer on the device cathode.

Publications

I. Bezel, K.J. Gaffney, S. Garrett-Roe, S.H. Liu, A.D. Miller, P. Szymanski, and C.B. Harris, "Measurement and dynamics of the spatial extent of an electron localized at a metal/dielectric interface," *Journal of Chemical Physics*, in press.

P.T. Snee, S. Garrett-Roe, and C.B. Harris, "Dynamics of an excess electron at metal/polar interfaces," *Journal of Physical Chemistry B*, in press.

"Ex situ" *and "Remote" Molecular Imaging and Spectroscopy*

Principal Investigators: Alex Pines, John Clarke, David Wemmer, Jeff Reimer, Steven Gourlay, GianLuca Sabbi, Ernest Majer, and Thomas Budinger

Project No.: 03020

Project Description

We plan to develop a new interdisciplinary program to take nuclear magnetic resonance/magnetic resonance imaging (NMR/MRI) into exciting new territory by implementing novel, seemingly impossible, methods and devices of *ex situ* and remote detection, with applications over distance scales from nanometers to meters. This will allow enhanced, noninvasive, even surreptitious, scanning detection that ranges over the investigation of materials and surfaces, porous systems relevant to earth sciences, well-logging, fluid flow, multiplexed screening, and assays of target molecules, functional molecular imaging of metabolites and brain function, and an approach to objects and subjects relevant to counterterrorism.

We plan to develop and implement: (1) a new generation of *ex situ*, one-sided superconducting magnets possessing external tunable "sweet spots" for inside-out standoff NMR/MRI; (2) *ex situ* magnetic resonance theory, multidimensional pulse sequences, and detection systems and consoles for high-resolution images and spectra in the presence of field gradients; (3) new NMR/MRI techniques, whereby, a sample is dosed and encoded so as to reconstruct molecular images and spectra of the sample and contents. Our goal is to provide a proof of principle of the applicability of the *ex situ* and remote NMR/MRI methodology and instrumentation to a variety of systems, from materials and earth sciences to biomedicine and counterterrorism.

Accomplishments

The goal of our interdisciplinary research team is to expand the potential, sensitivity, and specificity of NMR and MRI technologies by initiating novel, seemingly impossible, methods and devices of *ex situ* and remote detection, with applications over distances from nanometers to meters. During this year, a lot of progress was made in several areas.

One-side ex situ *magnets*

We have recovered chemical shift information correlated to three-dimensional images in the presence of a one-dimensional inhomogeneous static magnetic field on a sample to generate separate water and oil signals in rocks. These results are preliminary but promising in the light of real *ex situ* in the field exploration currently under way and the development of an NMR/MRI-based industrial sensor. Construction is completed on the development and implementation of a new generation of one-sided *ex situ* magnets as well as devices for rotation of the magnetic field. This is an exciting venture, allowing the observation of sharp spectra for immobile objects or subjects. New superconducting magnets possessing external tunable "sweet spots" for inside-out standoff NMR/MRI will make possible a truly portable incarnation of our high resolution NMR in inhomogeneous fields outside the radiofrequency coil published recently in *Science*.

Hand-held magnetic resonance spectroscopy, imaging, and elastography sensor

Our efforts are concentrated on imaging and acquiring chemical shift information in a simulated *ex situ* environment. A set of proof-of-principle imaging and spectroscopy experiments were performed inside a superconductive magnet while an imaging gradient along one dimension, *x*, was constantly applied to simulate an inherent inhomogeneity and while the *y* and *z* gradients were controlled. A conical radiofrequency (rf) coil geometry was employed to create an inhomogeneous rf field along the same direction. These experiments yielded satisfactory results. We are presently engaged in a second set of experiments that employ more sophisticated phantoms, such as multiple cylinders of differing liquid samples. In addition, we are designing the next simulation of a true *ex situ* experiment. In this new design, the sample will be spatially and spectroscopically imaged outside of the rf coil, and with a home-built *x*,*y* gradient set that will be used in a true *ex situ* experiment. A surface coil will be used to provide an inhomogeneous rf field along *z*.

Magnet resonance theory

Work is continuing on the development and implementation of magnetic resonance theory, multidimensional pulse sequences, and consoles for high-resolution *ex situ* images and spectra in the presence of field gradients and rotation. With small powerful scanning magnets, images and spectra will be resolvable at distances up to centimeters in the initial magnet/spectrometer designs and sequences. Micro- and nanoscale detection of surfaces is necessarily *ex situ* and occurs with inhomogeneous magnetic fields. The *ex situ* methodology will be scaled down so as to investigate the possibility of producing resolved images and spectra of micro- and nanosystems with high-sensitivity optical detection.

Knowledge about pore structure and fluid flow is critical for gas and oil exploration, for hydrology and remediation technologies. By subjecting fluid containing porous rock to different physical fields, we can measure induced changes in fluid mobility, rock permeability, and porosity. Work was done to compare anticipated *ex situ* fields to current lab and field technology to determine if successful resolution and penetration could be achieved. It is hoped that comparisons of pore structure involved in fluid transport obtained from NMR/MRI can help to evaluate tortuosity, an important but elusive parameter in Biot's theory for porous rocks to evaluate contributions of diffusion and surface reflexivity into NMR decay. The first remotely detected two-dimensional Xe-129 NMR image of channel pores, one millimeter inner diameter, was obtained. A conventional void space image would be challenging due to the low concentration of gas in porous media, requiring time-intensive signal averaging. This remote experiment, consisting of 128x128 phase encoding steps and 256 points in the direct dimension, was acquired in less than two hours.

Engineering xenon binding sites into proteins

The characterization of binding sites that change affinity and/or shift in CheY has been essentially completed. Experiments are being done to determine the affinity of the modified protein for ligand, and to map the xenon binding site. Some further work has been done on preparation for derivatizing maltose binding protein with a cage for xenon. A resynthesis on ~1 gram scale is nearly complete, this material will allow us much more flexibility in executing experiments for combinatorial assaying as well as molecular imaging *in vitro* and *in vivo* using functionalized xenon sensors targeted for molecular recognition.

Coupling of NMR/MRI encoding with remote detection has enhanced the sensitive reconstruction of spectra and images in porous materials and soft matter in our experiments, encoding occurs in situ but detection and

reconstruction proceed remotely with sensitivity enhanced by many orders of magnitude. Several new sensors have been tested and are now being coupled with remote detection at high sensitivity. Several modalities of signal detection, beyond traditional Faraday coil induction are well under way for this project.

New generation SQUID detectors

One research area to date has pursued the development and implementation of a new generation of room-temperature access mobile Superconducting QUantum Interface Device (SQUID) detectors for low-frequency flux detection of samples both *ex situ* and for remote reconstruction of images and spectra using thermally prepolarized systems encoded laser-polarized gases. This opens the way to MRI without the need for big superconducting magnets, and the technology has recently been licensed for combined magnetoencephalography (MEG)/MRI instrumentation. Recent results make this modality of high-sensitivity detection an exciting reality in magnetic fields ranging from microtesla to hundreds of millitesla, with applications from materials to biomedicine.

A further research focus has centered on the coupling of remote NMR/MRI techniques, whereby a sample is dosed and encoded with a fluid which is withdrawn and detected remotely at high concentration with high sensitivity SQUID and laser detection so as to reconstruct molecular images and spectra of the sample and contents. In a SQUID MRI experiment performed in low field with linewidths approaching the lifetime limit, relatively high spatial resolution was achieved with modest magnetic field gradients which dispersed the NMR signal over only a narrow band. Consequently, the NMR transients were detected with high signal to noise ratio (SNR) in a relatively short MRI acquisition time. Images of various materials were obtained with good resolution in the absence of a high magnetic field. This methodology opens the door to the development of inexpensive MRI applications for imaging of joints and extremities and breast cancer screening where the T1 contract would be an essential feature.

Magic-Angle Rotating Field (BoMAS) Spectrometer

Though the concept of rotating a magnetic field around an object instead of spinning the sample in a magnetic field has been mentioned in the past, no feasible design has been proposed until this project. Two basic ideas underpin the current design: First, the use of the Halbach permanent magnet allows us to create a field orthogonal to an electromagnetic solenoid field. By adjusting the currents in the solenoid to give a resulting field of 54.7 degrees and then rotating the Halbach cylinder, a rotating field of 54.7 degrees is created. Secondly, low rotation speeds in the range of 40 hertz have been shown to provide good spectral resolution comparable to the usual 1 to 4 kilohertz speeds by judicious use of pulse sequence protocols which suppress side bands. The design shown below has been implemented in an almost assembled prototype where the sample size will be a mouse brain. The field will be 0.7 Tesla at 40 hertz.

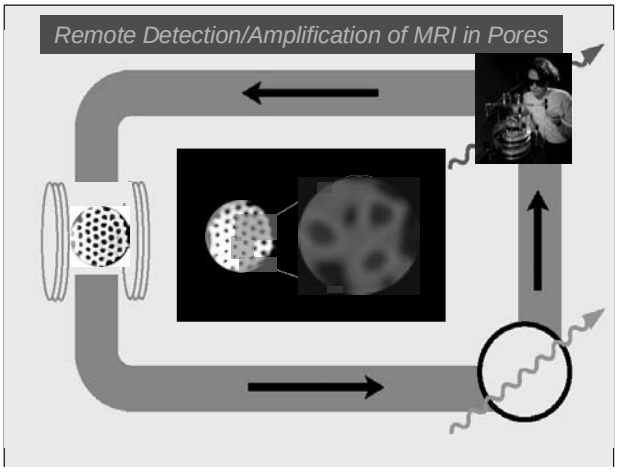

Figure 1. Remote detection with amplification of NMR and MRI in porous materials. Laser-polarized xenon gas is injected into the tubular pores, shown in the photograph, encoded for NMR and MRI images and spectra, and then withdrawn for remote detection of the pure gas with high signal/noise ratio. The spectra and images can be reconstructed from the remotely detected signals, in this case showing 100 micrometer resolution of the pores, a difficult objective with direct imaging

Publications

A. Moule, M. Spence, S-I Han, J. Seeley, K. Pierce, S. Saxena, and A. Pines, "Amplification of xenon NMR and MRI by remote detection," *Procedures of the National Academy* **100** (16), 9122–9127 (2003).

D. Sakellariou, C.A. Meriles, R.W. Martin, and A. Pines, "High-resolution NMR of anisotropic samples with spinning away from the magic angle," *Chemical Physics Letters* **377,** 333–339 (2003).

C.A. Meriles, D. Sakellariou, and A. Pines, "Broadband phase modulation by adiabatic pulses," *Journal of Magnetic Resonance* **164,** 177–181 (2003). Cover Article.

S. Rubin, L. Seok-Yong, E.J. Ruiz, A. Pines, and D. Wemmer, "Detection and characterization of xenon binding sites in proteins by ^{129}Xe NMR spectroscopy," *Journal of Molecular Biology*, **322,** 425–440 (2002).

R. McDermott, A.H.Trabesinger, M. Muëck, E.L. Hahn, A. Pines, and J. Clarke, "Liquid-state NMR and scalar couplings in microtesla magnetic fields," *Science*, **295,** 2247–2249 (2002).

Manuscripts in press

A. Trabesinger, R. McDermott, M. Muëck, E. Hahn, J. Clarke, and A. Pines, "SQUID detected liquid state NMR in microtesla fields", *Journal of Physical Chemistry*, in press–cover article (January 2004).

T.J. Lowery, S. Rubin, E. J. Ruiz, M. Spence, N. Wissinger, P. Schultz, A. Pines, and D. Wemmer, "Applications of laser-polarized ^{129}Xe NMR to biomolecular assays," *Magnetic Resonance Imaging*, in press (2003).

J. Seeley, S. Han, and A. Pines, "Remotely detected high-field MRI of porous samples," *Journal of Magnetic Resonance*, in press.

Manuscripts submitted or in preparation

R. McDermott, N. Kelso, S.-K. Lee, M. Mossle, M. Muëck, W. Myers, B. ten Haken, H.C. Seton, A.H. Trabesinger,
A. Pines, and J. Clarke, "SQUID-detected magnetic resonance imaging in microtesla magnetic fields," submitted to *Nature*.

C. Meriles, D. Sakellariou, A. Moule, M. Goldman, T. Budinger, and A. Pines, "High-resolution nuclear magnetic resonance of static samples by rotation of the magnetic field," submitted to *Physical Review Letters*.

V. Demas, C. Meriles, D. Sakellariou, S. Han, J. Reimer, and A. Pines "3D phase encoded chemical shift MRI in the presence of inhomogeneous fields," submitted to *Journal of Magnetic Resonance*.

S-I Han, K. Pierce, and A. Pines, "Gas flow visualization by laser-polarized ^{129}Xe MRI," submitted to *Science*.

Posters

V. Demas, C. Meriles, D. Sakellariou, S.Han, J. Reimer, and A. Pines, "An approach to MR spectroscopy and imaging in permanently inhomogeneous magnetic fields," poster presented at the 7th International Conference on Magnetic Resonance Microscopy, Snowbird, Utah, October 2003.

S.I. Han, "Amplification of xenon NMR and MRI by remote detection," talk presented at the 7th International Conference on Magnetic Resonance Microscopy, Snowbird, Utah, October 2003.

K. Pierce, S.I. Han, and A. Pines "Visualization of complex gas dynamics by laser-polarized ^{129}Xe NMR," poster presented at the 7th International Conference on Magnetic Resonance Microscopy, Snowbird, Utah, October 2003.

E.J. Ruiz, T. Lowery, S. Rubin, N. Winsinger, T. Wu, P. Schultz, D. Wemmer, and A. Pines, "NMR development of functionalized ^{129}Xe as a biosensor," poster presented at the 45th Rocky Mountain Conference, Denver, Colorado, October 6, 2003.

R. Martin, D. Sakellariou, C. Meriles, R. Jachmann, and A. Pines, "Hardware design and applications for high-field switched angle spinning experiments," poster presented at the 3rd annual Alpine Conference on Solid State NMR, Chamonix, France, September 14–18, 2003.

D. Sakellariou, C. Meriles, R. Martin, A. Moule, M. Goldman, and A. Pines, "NMR in rotating magnetic fields: magic angle field spinning," poster presented at the 3rd annual Alpine Conference on Solid-State NMR, Chamonix, France, September 14–18, 2003.

C. Meriles, D. Sakellariou, H. Heise, A. Moule, and A. Pines, "Approach to high-resolution *ex situ* NMR," poster presented at the Gordon Conference, Newport Rhode Island, June 15 20, 2003, and at the 10th Chianti Workshop, Nuclear and Electron, Chianti, Italy, May 25–30, 2003.

J. Seeley, "Remote detection of ^{129}xenon in porous materials and solutions," International Symposium on Xenon NMR of Materials, LaColle-sur-Loup, France, May 29–June 1, 2003.

C. Meriles, D. Sakellariou, and A. Pines, "Towards *ex situ* high resolution NMR spectroscopy: recent advances and future possibilities," poster presented at the Gordon Conference, Newport Rhode Island, June 15-20, 2003 and at the 10th Chianti Workshop Nuclear and Electron, Chianti, Italy, May 25 to 30, 2003.

T.J. Lowery, S. Rubin, E. J. Ruiz, M. Spence, N. Wissinger, P. Schultz, A. Pines, and D. Wemmer, "Applications of laser-polarized ^{129}Xe NMR to biomolecular assays," Magnetic Resonance Imaging, talk presented at the International School of Magnetic Resonance and Brain Function, Course I – New NMR Strategies, Erice, Sicily, April 6–11, 2003.

S. Rubin, E.J. Ruiz, A. Pines, and D. Wemmer, "Applications of Laser-Polarized Xenon NMR in Biomolecular Assays," poster presented at 44th Experimental NMR conference (ENC), Savannah, Georgia, April 2003.

Acronyms and Abbreviations

A

ADC	analog to digital converter
AF	antiferromagnetism
AFM	atomic force microscopy
AFRD	Accelerator and Fusion Research Division
ALS	Advanced Light Source
AMD	acid mine drainage
ANL	Argonne National Laboratory
APS	Advanced Photon Source
ARPES	angle resolved photoemission spectroscopy
ASC	adult stem cells
ATLAS	A Toroidal LHC ApparatuS

B

BAC	bacterial artificial chromosome
BNL	Brookhaven National Laboratory
BNCT	Boron Neutron Capture Therapy

C

CAD	computer aided design
CCD	charge-coupled device
CD	circular dichroism
CERN	European Laboratory for Particle Physics near Geneva, Switzerland
CH	Chemical Sciences Division
CHD	coronary heart disease
CMB	cosmic microwave background
CMOS	complementary metal-oxide semiconductor
CMR	colossal magnetoresistive
CNS	conserved noncoding sequences
COG	clusters of orthologous groups
CPU	central processing unit
CS	Computing Sciences
CSK	cytoskeleton
CSR	coherent synchrotron radiation
cw	continuous wave
CXDI	coherent x-ray diffraction imaging

D

DOD	Department of Defense
DOE	Department of Energy
DRAM	dynamic random access memory
DTR	diurnal temperature range

E

ECEs	electron cloud effects
ECM	extracellular matrix
ED	Engineering Division
EDS	energy dispersion spectroscopy
EELS	energy loss spectra
EETD	Environmental Energy Technologies Division
EM	electromagnetic
EPA	Environmental Protection Agency
EPR	electron paramagnetic resonance
ESA	European Space Agency
ESD	Earth Sciences Division
EUV	extreme ultraviolet
EXAFS	extended x-ray absorption fine structure

F

FEA	finite element analyses
FEL	free-electron lasers
FETs	field-effect transistor
FISH	fluorescence *in situ* hybridization
FNAL	Fermi National Accelerator Laboratory
FPGA	field programmable gate array
FRET	fluorescence-resonance-energy transfer
fs	femtosecond
FTIR	Fourier transform infrared spectroscopy
FY	fiscal year

G

GFP	green fluorescent protein
GRETA	Gamma-Ray Energy Tracking Array
GUI	graphical user interface

H

HDL	high density lipoprotein
HDS	heme domain sensor
HEP	High Energy Physics
HHMI	Howard Hughes Medical Institute
HIF	heavy ion fusion
HPC	high-performance computer
HPPES	high-pressure photoelectron spectroscopy
HPSS	high performance storage system
HRV	human rhinovirus

I

ir	infrared
ICT	integrating current transformer
INEEL	Idaho National Environmental Engineering Laboratory

J

JGI	Joint Genome Institute
JPL	Jet Propulsion Laboratory
JPR	Josephson plasma resonance

K

KamLAND	The Kamioka Liquid-scintillator Neutrino Detector
KeK	High Energy Accelerator Research Organization, Japan

L

l'OASIS	laser Optics and Acceleration Systems Integrated Studies
LANL	Los Alamos National Laboratory
LaS	laser absorption spectrometer
LBNL	Ernest Orlando Lawrence Berkeley National Laboratory
LC/MS	liquid chromatography/mass spectrometry
LDL	low density lipoprotein
LDA	local density approximation
LDRD	Laboratory Directed Research and Development
LEDs	light emitting diodes
LEED	low energy electron diffraction
LHC	Large Hadron Collider, CERN
LMA	large mixing angle
LP	lipoprotein
LSD	Life Sciences Division

M

MAXIMA	Millimeter Anisotropy eXperiment IMaging Array
MBE	molecular beam epitaxy
MCD	magnetic circular dichroism
MCF	Macromolecular Crystallography Facility, ALS
MEMS	micro-electro-mechanical systems
MES	molecular environmental science
MPI	message passing interface
MRI	magnetic resonance imaging
MS	mass spectrometry
MSD	Materials Sciences Division

N

NASA	National Aeronautics and Space Administration
NCAR	National Center for Atmospheric Research
NCEM	National Center for Electron Microscopy
NEMS	nanoelectromechanical systems
NERSC	National Energy Research Scientific Computing
NEXAFS	near-edge x-ray adsorption fine structure
NFL	non-Fermi liquid
NIH	National Institutes of Health
NIR	near infrared
NLC	Next Linear Collider
NMR	nuclear magnetic resonance
NOAA	National Oceanic Atmospheric Administration
NQR	nuclear quadrupole resonance
NRF	nonlinear response functions
NSCL	National Superconducting Cyclotron Laboratory at Michigan State University
NSD	Nuclear Science Division
NSF	National Science Foundation

O

OC	organic carbon
OPA	optical parametric amplifier
OPC	optical particle counter
ORF	open reading frame
ORNL	Oak Ridge National Laboratory

P

PAK	p21-activated kinase
PAM	phase accumulation method
PARG	poly-adp-ribose glycohydrolase
PARP	poly-adp-ribose polymerase
PBD	Physical Biosciences Division
PCB	printed circuit boards
PCR	polymerase chain reaction
PD	Physics Division
PDE	partial differential equation
PDF	pair-distribution function
PDSF	Parallel Distributed Systems Facility
PEEM	photo-electron emission microscope
PET	positron emission tomography
PI	principal investigator
PIM	processor-in-memory
PL	photoluminescence
PM	particulate matter
PMT	photomultiplier tube
PNNL	Pacific Northwest National Laboratory
pp	proton-proton

Q

QCD	quantum chromodynamics
QPCR	quantitative polymerase chain reaction
QW	quantum well

R

RCM	regional climate model
rf	radio frequency
RHEED	reflection high energy electron diffraction
RHIC	Relativistic Heavy Ion Collider, Brookhaven National Laboratory
RNA	ribonucleic acid

S

SAXS	small-angle x-ray scattering
SC	Office of Science, DOE
SCOP	structural classification of proteins
SEM	scanning electron microscope
SET	single electron transistors
SLAC	Stanford Linear Accelerator Center
SLIM	structured light-imaging microscope
SM	superconducting magnets
SNAP	SuperNova/Acceleration Probe
SNO	Sudbury Neutrino Observatory
SNR	supernova remnants
SOI	silicon on insulator
SQC	solid state quantum computer
SQUID	superconducting quantum interference device
SSRL	Stanford Synchrotron Radiation Laboratory
STAR	Solenoidal Tracker at RHIC
STEM	scanning transmission electron microscope
STM	scanning tunneling microscope or microscopy
STXM	scanning transmission x-ray microscope
SXH	soft x-ray holography
SXRD	scanning x-ray diffraction
SXRF	synchrotron x-ray fluorescence

T

TCR	T-cell receptors
TEAM	transmission electron aberration corrected microscope
TEM	transmission electron microscope
TF	transcription factors
tRNA	transfer RNA

U

UC	University of California
UHV	ultra-high vacuum
USBR	U.S. Bureau of Reclamation
UV	ultraviolet

V

VC	vinyl chloride
VOC	volatile organic compound
VSOM	visual servoing optical microscopy

W

WAXS	wide-angle x-ray scattering
WWTP	waste water treatment plant

XYZ

XAFS	x-ray absorption fine structure
XANES	x-ray absorption near-edge structure spectroscopy
XAS	x-ray absorption spectroscopy
XFH	x-ray fluorescence holography
XPS	x-ray photoemission spectroscopy
XRD	x-ray diffraction